SYNTHESIS OF 1,2,4-TRIAZOLE DERIVATIVES BY CYCLIZATION OF O,S-DIETHYL AROYLIMIDOTHIOCARBONATES WITH HYDRAZINES AND COMPUTATIONAL EVALUATION OF THEIR ANTIFUNGAL ACTIVITY

MANUEL ESTEBAN GUSTIN VILLOTA

Universidad de Nariño
Facultad de Ciencias Exactas y Naturales
Programa de Química
San Juan de Pasto
2021

SYNTHESIS OF 1,2,4-TRIAZOLE DERIVATIVES BY CYCLIZATION OF O,S-DIETHYL AROYLIMIDOTHIOCARBONATES WITH HYDRAZINES AND COMPUTATIONAL EVALUATION OF THEIR ANTIFUNGAL ACTIVITY

MANUEL ESTEBAN GUSTIN VILLOTA

Research work presented as a partial requirement to obtain the degree of chemist

Advisors:
CESAR AUGUSTO MUJICA MARTINEZ
Doctor en Ciencias Naturales

SILVIA DEL TRANSITO CRUZ SÁNCHEZ Doctora en Ciencias Químicas

Co-advisors: HENRY EDGARDO INSUASTY INSUASTY Doctor en Ciencias Químicas

EDITH MARIELA BURBANO ROSERO Doctora en Ciencias

Universidad de Nariño
Facultad de Ciencias Exactas y Naturales
Programa de Química
San Juan De Pasto
2021

"Las ideas y conclusiones aportadas en el siguiente trabajo de grado son responsabilidad exclusiva del autor".

Artículo 1º del Acuerdo No. 324 del 11 de octubre de 1966, emanado por el Honorable Consejo Directivo de la Universidad de Nariño.

| ACCEPTATION NO |
|------------------------------|
| |
| |
| |
| |
| |
| Cesar Augusto Mujica Mart |
| Silvia del Transito Cruz Sán |
| Advis |
| Henry Edgardo Insuasty Insu |
| Edith Mariela Burbano Ro |
| Co-advi |
| |
| |
| Revie |

San Juan de Pasto, may 19th, 2021



ACUERDO N° 071 DE 2021 (20 de Mayo)

Por el cual se concede la distinción de Laureado

EL CONSEJO DE LA FACULTAD DE CIENCIAS EXACTAS Y NATURALES DE LA UNIVERSIDAD DE NARIÑO, en uso de sus atribuciones reglamentarías y estatuarias y,

CONSIDERANDO

Que mediante Acuerdo No. 077 del 10 de diciembre de 2019 el Consejo Superior estableció y unificó la normatividad de los trabajos de grado de pregrado de la Universidad de Nariño, definiendo en su artículo 16, el reconocimiento de distinciones aplicable para las modalidades de investigación e interacción social, según la siguiente escala: Trabajo de grado Meritorio: de 90 a 99 puntos, Trabajo de grado Laureado: 100 puntos;

Que en el referido Acuerdo en su Artículo 17, se establece: "Los Consejos de Facultad otorgarán las distinciones referidas en el artículo anterior, previa presentación de la proposición correspondiente por parte de los Comités Curriculares y de Investigaciones, en la cual se adjunte un informe por parte de cada uno de los jurados evaluadores que justifique la distinción correspondiente";

Que mediante Acuerdo No. 045 de 7 de mayo de 2015 este Organismo estableció la reglamentación para presentación de proyectos y trabajos de grado, para los estudiantes del Programa de Química como requisito parcial para la obtención del título profesional de Químico;

Que el estudiante MANUEL ESTEBAN GUSTIN VILLOTA, sustentó su trabajo de grado aprobado en la modalidad investigación denominado "SYNTHESIS OF 1,2,4-TRIAZOLE DERIVATIVES BY CYCLIZATION OF O,S-DIETHYL AROYLIMIDOTHIOCARBONATES WITH HYDRAZINES AND COMPUTATIONAL EVALUATION OF THEIR ANTIFUNGAL ACTIVITY", el día 19 de mayo de 2021, a las 11:00 horas vía teleconferencia en Aula zoom asignada por la Universidad de Nariño, siguiendo todos los procedimientos estatutarios y académicos exigidos por la Universidad de Nariño;

Que el Trabajo de Grado se desarrolló bajo la dirección de los docentes Cesar Augusto Mujica Martínez y Silvia Cruz Sánchez, adscritos al Departamento de Química de la Universidad de Nariño, y la codirección de los docentes Henry Insuasty y Edith Mariela Burbano Rosero, adscritos a los Departamentos de Química y Biología de la Universidad de Nariño, respectivamente;

Que los jurados evaluadores del trabajo de Grado en mención fueron los profesionales **LUIS** ÁNGEL POLINDARA GARCÍA, profesor tiempo completo del Instituto de Química de la Universidad Autónoma de México y **EMERSON ALONSO RENGIFO CARPINTERO**, profesor tiempo completo Departamento de Química Universidad del Cauca, quienes emitieron una calificación total del trabajo de grado **de 100 sobre 100 puntos**, como consta en el Acta de sustentación de Trabajo de Grado Número 009 de fecha 19 de mayo de 2021;









Universidad de Nariño FACULTAD DE CIENCIAS EXACTAS Y NATURALES

el artículo 16º de Acuerdo 077 de diciembre 10 de 2019 "El reconocimiento de distinciones aplica para las modalidades de investigación e interacción social según la siguiente escala – Trabajo de grado Meritorio: de 90 a 99 puntos. – Trabajo de grado Laureado: 100 puntos";

Que, dada la calificación de 100 puntos, el trabajo de grado cumple con el puntaje para alcanzar la distinción de "Laureado", por lo cual cada uno de los jurados evaluadores remitió informe escrito con las justificaciones correspondientes para dicho merecimiento;

Que el profesional **LUIS ÁNGEL POLINDARA GARCÍA**, sustenta que el trabajo de grado debe ser reconocido como LAUREADO, justificando que:

"El trabajo escrito en idioma inglés, resaltó de manera excelente el desarrollo de diversos triazoles y su caracterización mediante diferentes técnicas espectroscópicas y espectrométricas, así como un estudio de QSAR enfocado en propiedades antimicóticas. El trabajo presentó claridad en la redacción, así como una amplia revisión de los antecedentes respecto a la síntesis de dichos análogos, en donde resalta la pertinencia de la bibliografía citada por el alumno, además de una adecuada discusión de resultados y conclusiones.

El trabajo computacional que se realizó cumple con altos estándares dentro de la química computacional, por lo que sus resultados podrían tener un impacto muy positivo en el desarrollo de nuevos antimicóticos de relevancia para el combate a enfermedades de interés global. Respecto a la defensa realizadas por el alumno, considero que fue excelente, ya que logró responder adecuadamente todas las preguntas realizadas por el comité evaluador.

El alumno demostró un amplio dominio de la parte sintética, así como de la parte computacional. Por lo anterior, considero que la tesis en mención, merece la distinción de LAUREADA."

Que el profesional **EMERSON ALONSO RENGIFO CARPINTERO**, presentó informe justificando que:

"En primer lugar, el trabajo escrito es de excelente calidad, destacándose el hecho de haber sido escrito en su totalidad en el idioma Ingles con una excelente gramática, lo cual le da una mayor proyección internacional al trabajo. Las secciones establecidas como Resumen, Introducción, Objetivos, estado del arte, están muy bien soportadas en la literatura, así como en la metodología planteada, la cual es coherente en todas sus etapas.

Los resultados obtenidos son importantes, claros y contundentes, tanto en el ámbito de la Química Orgánica, como en la Fisicoquímica. Muestra dominio de la parte experimental, así como en la parte teórica computacional, lo que representa un complemento interesante en la formación del estudiante. Las conclusiones son pertinentes y están en acuerdo con los resultados obtenidos.











Adicionalmente, en la sustentación oral, el estudiante realizó un uso adecuado de las diapositivas y mostró un dominio completo, realizando una excelente defensa del trabajo de investigación. Es claro que el estudiante, tiene un entendimiento de los detalles experimentales y teóricos y los alcances de la investigación que realizó.

En general, es un excelente trabajo que podría incluso ser un trabajo de una maestría."

Que el Comité Curricular y de Investigaciones del Departamento de Química mediante proposición Nº010 de 20 de mayo de 2021 y después de evaluar el concepto de los asesores, consideró que la distinción de LAUREADA se ajusta a las normas;

Que este organismo considera viable la petición y;

ACUERDA:

- Artículo 1°. Otorgar la distinción de honor como LAUREADO al Trabajo de Grado en la modalidad investigación denominado "SYNTHESIS OF 1,2,4-TRIAZOLE DERIVATIVES BY CYCLIZATION OF O,S-DIETHYL AROYLIMIDOTHIOCARBONATES WITH HYDRAZINES AND COMPUTATIONAL EVALUATION OF THEIR ANTIFUNGAL ACTIVITY.", desarrollado por el estudiante MANUEL ESTEBAN GUSTIN VILLOTA, bajo la dirección de los docentes Cesar Augusto Mujica Martínez y Silvia Cruz Sánchez, adscritos al Departamento de Química de la Universidad de Nariño, y la codirección de los docentes Henry Insuasty y Edith Mariela Burbano Rosero, adscritos a los Departamentos de Química y Biología de la Universidad de Nariño, respectivamente, según la parte motiva de la presente Proposición.
- Artículo 2°. Ocara, el Departamento Química, y la Secretaria Académica de la Facultad y Facultad de Ciencias Exactas y Naturales anotarán lo de su cargo.

COMUNIQUESE Y CUMPLASE.

San Juan de Pasto, 20 de mayo de 2021.

Proyectó: Paola Salazar





DEDICATION

To almighty God, who is my guide in every cycle of my life, because he has blessed me infinitely and given me strength in every moment of doubt and difficulty.

To my parents, my brother, and my grandparents, who are the engines of my life and my greatest inspiration, for cultivated me not only as a person and but also as a persistent, responsible, and committed professional.

ACKNOWLEDGMENTS

Personal acknowledgments

To my parents, because their teaching and support were important during the development of my career and research work.

To my girlfriend Isabella for being my life-partner and my unconditional support, her advices during my work allowed me to overcome my weaknesses and to strengthen my skills and abilities.

To "la GIFBANDA", my colleagues from GIFBA: Santiago, Carlos, Miguel, Elena, Fausto, and Dr. Cesar, not only because their contributions to my research, which were indisputably very important, but also, for sharing with me pleasant moments full of laughter.

Academic acknowledgments

My deep acknowledge to my advisor Dr. Cesar Augusto Mujica, for his constant support in my research, dedicating every day his effort to strengthen its content, likewise, for his constant effort to strengthen my investigative qualities.

To my advisor Dr. Silvia Cruz Sanchez, for her advices and suggestions in the development of my research work, her experience was valuable to improve my abilities in the laboratory and to improve and consolidate my knowledge in organic chemistry.

To my co-advisor Dr. Henry Edgardo Insuasty, for his constant engagement with my research work; his knowledge in organic chemistry strengthened my interest in this field.

To my co-advisor Dr. Edith Mariela Burbano, for their commitment and motivation for the research that allowed to strengthen the interdisciplinary nature of this work. To my colleague Santiago Burbano, for his contributions and commitment in the development of the research project.

To Andres Hidalgo, for his support in the first stage of my investigation and to Natalia Delgado, for her help in the measurement of the spectra at the UNAM laboratories (Mexico).

To my teachers in the Department of Chemistry, because thanks to their teachings I had a background as a professional in Chemistry.

To Dr. Luis Ángel Polindara García of the Instituto de Química of the Universidad Nacional Autónoma de México (UNAM) for supporting the spectroscopic characterization of the products obtained.

To Vicerretoría de Investigaciones e Interacción Social (VIIS, former VIPRI) from the Universidad de Nariño, for the financial support to project 1713, approved by Agreement No 098 of September 25th 2018, which funded this research work. Finally, to the reviewers of this work, for their observations and suggestions that help to improve this work.

ABSTRACT

The heterocyclic compounds and, specially, those having an azole core exhibit a wide range of biological activities, being the antifungal activity of particular relevance. Since the 80s, commercial antifungal drugs have in their structures the 1,2,4-triazole core and their evolution has been an important focus of investigation due to the constant limitations such as drug resistance, adverse effects, and poor pharmacokinetics. These have motivated the design of synthetic methodologies to obtain new triazoles with promising antifungal potential and, in many cases, the search of new active compounds using quantitative structure-activity relationship techniques, which, help to predict the most promising compounds reducing the experimentation time and the economic spending derived from the synthetic process.

The GICH-UN research group standardized a methodology to synthetize 1,3,5substituted-1,2,4-triazoles by cyclization of hydrazines with X,S-diethyl aroylimidothiocarbonates, which are relevant intermediates in the synthesis of several heterocyclic compounds. In this work, the versatility of this methodology is further explored by synthesizing eight triazoles with different substituents, four compounds of which are obtained for the first time. Considering different reactants, it was found that the chemical space expanded by this methodology is huge. With the purpose to predict the antifungal potential of these systems a quantitative structure-activity relationship study was carried out and mathematical models were designed for the reported antifungal activities of a series of piperazine-substituted-1,2,4-triazoles against Candida albicans, Candida parapsilosis, Candida tropicalis, Cryptococcus neoformans, Trichophyton rubrum, Fosecaea compacta, and Microsporum gypseum. Among the triazoles that can be obtained using the synthetic methodology, several structural modifications were evaluated finding the substituents that provide the best antifungal activity. These triazole derivatives are T-3b-SCF₃, as the most active against *Candida albicans*, *Cryptococcus neoformans*, Trichophyton rubrum, and Microsporum gypseum; T-16b-SC₁ as the most active against Candida Parapsilosis, and T-17a-OH as the most active against Candida tropicalis and Fosecaea compacta.

KEY WORDS: 1,3,5-substituted-1,2,4-triazoles, X,S-diethyl aroylimidothiocarbonates, antifungal drugs, quantitative structure-activity relationship, molecular descriptors.

RESUMEN

Los compuestos heterocíclicos, especialmente los que tienen un núcleo azólico presentan diversas actividades biológicas, siendo la actividad antifúngica de particular relevancia. Desde los 80s, los fármacos antifúngicos comerciales tienen en su estructura el núcleo de 1,2,4-triazol y su evolución ha sido un importante foco de investigación debido a las constantes limitaciones como fármaco resistencia, efectos adversos y pobre farmacocinética. Esto ha motivado el diseño de metodologías sintéticas para obtener nuevos triazoles con prometedor potencial antifúngico, y en muchos casos, la búsqueda de nuevos compuestos activos utilizando técnicas basadas en relaciones cuantitativas estructura-actividad, que permiten predecir los compuestos más prometedores reduciendo el tiempo de experimentación y el gasto económico derivado del proceso sintético.

El grupo de investigación GICH-UN estandarizó una metodología para sintetizar 1,2,4-triazoles-1,3,5-sustituidos por ciclación de hidracinas con aroilimidotiocarbonatos de X,S-dietilo; precursores relevantes en la síntesis de compuestos heterocíclicos. En este trabajo, se exploró la versatilidad de esta metodología al sintetizar ocho 1,2,4-triazoles con diferentes sustituyentes, de los cuales, cuatro compuestos fueron obtenidos por primera vez. Al considerar diferentes reactivos, se encuentra que el espacio químico expandido por esta metodología es adecuado. Con el fin de predecir el potencial antifúngico de estos sistemas se realizó un estudio de relaciones cuantitativas estructura-actividad y se diseñaron modelos matemáticos para las actividades antifúngicas reportadas para una serie de 1,2,4-triazoles sustituidos con piperazina contra Candida albicans, Candida parapsilosis, Candida tropicalis, Cryptococcus neoformans, Trichophyton rubrum, Fosecaea compacta y Microsporum gypseum. Entre los triazoles que pueden ser obtenidos usando la metodología sintética, se evaluaron varias modificaciones estructurales encontrando los sustituyentes que proporcionan mejor actividad. Estos triazoles son T-3b-SCF3 como el más activo frente a Candida albicans, Cryptococcus neoformans, Trichophyton rubrum y Microsporum gypseum, T-16b-SC₁ como el más activo contra Candida parapsilosis y T-17a-OH como el más activo frente a Candida tropicalis y Fosecaea compacta.

PALABRAS CLAVES: 1,2,4-triazoles-1,3,5-sustituidos, aroilimidotiocarbonatos de X,S-dietilo, fármacos antifúngicos, relaciones cuantitativas estructura-actividad, descriptores moleculares.

TABLE OF CONTENTS

| 1 | | | DUCTIONTIVES | |
|---|-------------------|-----|---|-----|
| _ | 2.1 2.2 | Gei | neral objectiveecific objectives | .26 |
| 3 | STA | ATE | -OF-THE-ART | .27 |
| | 3.1 | The | e biological importance of heterocyclic compounds | .27 |
| | 3.1 3.1 3.1 | .2 | Commercial drugs containing heterocycles | .29 |
| | 3.2 3.3 | | nthetic methodologies toward 1,3,5-substitued-1,2,4-triazoles x,S-dialkyl aroylimidothiocarbonates | |
| | 3.3 3.3 | .2 | Synthesis of X,S-dialkyl aroylimidothiocarbonates | |
| | 3.3 | • | 1,2,4-triazole derivatives from X,S-diethyl aroylimidothiocarbonates | |
| | 3.4 | Qua | antitative structure-activity relationships | .47 |
| | 3.4 3.4 3.4 | .2 | General characteristics of QSAR methods Application and importance of QSAR | .49 |
| 4 | RE | SUL | TS AND DISCUSSION | .51 |
| | 4.1 | Syr | nthesis and characterization of target products | .51 |
| | 4.1 4.1 | | Synthesis and characterization of X-ethyl aroylimidothiocarbamates. Synthesis and characterization of X,S-diethyl aroylimidothiocarbona | |
| | 4.1 | .3 | Synthesis and characterization of 1,2,4-triazoles | _ |
| | 4.2 | QS | AR study of the antifungal activity of 1,2,4-triazoles | .79 |
| | 4.2 4.2 | | Building the QSAR models Antifungal activity of the 1,2,4-triazole derivatives obtained in this wo | ork |
| | 4.2 | .3 | Aliphatic chain effect on the antifungal activity of 1.2.4-triazoles1 | |

| | | | Effect of additional modifications on the antifungal activity of 1,2,4- | 104 |
|----|------|-------|---|-----|
| 5 | MAT | ΓER | IALS AND METHODS | 110 |
| ; | 5.1 | Syn | thesis of intermediates and products | 110 |
| | 5.1. | 1 | General process for the synthesis of the X-ethyl | |
| | aroy | /limi | dothiocarbamate1 | 10 |
| | 5.1. | 2 | General process for the synthesis of the X,S-diethyl | |
| | aroy | /limi | dothiocarbonates | 111 |
| | | | General process for the synthesis of the 1,2,4-triazole derivatives $$ | |
| ; | 5.2 | QS | AR study of the antifungal activity | 115 |
| 6 | CON | NCL | USIONS | 116 |
| 7 | REC | COM | MENDATIONS | 118 |
| 8 | PRO | DDU | ICTS | 120 |
| 9 | REF | ER | ENCES | 121 |
| 10 |) AI | PPE | NDIX | 130 |

LIST OF FIGURES

| Figure 1. Triazole rings isomers and their tautomeric structures2 |
|---|
| Figure 2. Evolution of antifungal drugs2 |
| Figure 3. Nucleophilic and electrophilic centers of hydrazines and X,S-diethy |
| aroylimidodithiocarbonates, respectively. |
| Figure 4. Typical heterocyclic compounds used in commercial drugs2 |
| Figure 5. Examples of commercial drugs containing azoles in their structure2 |
| Figure 6. Structure of antifungal drugs with an imidazole ring3 |
| Figure 7. Structure of antifungal drugs with a triazole ring |
| Figure 8. Interaction of azoles with the cytochrome P450 14 _{DM} enzyme3 |
| Figure 9. Novel 1,2,4-triazole derivatives with promising antifungal activity3 |
| Figure 10. Synthetic routes for several heterocyclic compounds from X,S-dialky |
| aroylimidothiocarbonates4 |
| Figure 11. Nomenclature of the 1,3,5-substituted-1,2,4-triazoles used through th |
| document4 |
| Figure 12. General process to develop QSAR models4 |
| Figure 13. QSAR studies of antifungal activity of 1,2,4-triazole derivatives5 |
| Figure 14. High-resolution DART+ mass spectrum of compound 58h5 |
| Figure 15. FT-IR spectrum of compound 58h5 |
| Figure 16. ¹ H NMR (300 MHz, CDCl ₃) spectrum of compound 58h5 |
| Figure 17. ¹³ C NMR (75 MHz, CDCl ₃) spectrum of compound 58h5 |
| Figure 18. High-resolution DART+ mass spectrum of compound 59h5 |
| Figure 19. FT-IR spectrum of compound 59h6 |
| Figure 20. ¹³ H NMR (300 MHz, CDCl ₃) spectrum of compound 59h6 |
| Figure 21. ¹³ C NMR (top) and DEPT-135 (bottom) spectra (75 MHz, CDCl ₃) of |
| compound 59h |
| Figure 22. TLC monitoring of the reaction resulting in compound T-3b-OC26 |
| Figure 23. High-resolution DART+ mass spectrum of compound T-3b-OC26 |
| Figure 24. FT-IR spectrum of compound T-3b-OC ₂ 6 |
| Figure 25. ¹ H NMR spectrum (700 MHz, CDCl ₃) of compound T-3b-OC ₂ 6 |
| Figure 26. ¹³ C NMR (top) and DEPT-190 (bottom) spectra (175 MHz, CDCl ₃) of |
| compound T-3b-OC ₂ 7 |
| Figure 27. Two-dimensional HSQC spectrum (CDCl ₃) of compound T-3b-OC ₂ 7 |
| Figure 28. HMBC spectrum (CDCl ₃) of compound T-3b-OC ₂ |
| Figure 29. 1,3,5-substituted-1,2,4-triazole derivatives that are synthetically viable |
| using the GICH-UN methodology7 |
| Figure 30. Gibbs energy differences between 2-R ₁ and 1-R ₁ isomers of 1,2,4 |
| triazoles |
| Figure 31. 1,2,4-triazole derivatives with a 4-(4-substituted-phenyl) piperazine sid |
| chain used for the OSAR study |

| Figure 32. Comparison of R^2_{adj} (C. ALB, C. PAR, C. TRO, T. RUB, and F. COM) and |
|--|
| R ² (C. NEO and M. GYP) for the different computational methods91 |
| Figure 33. Antifungal activity of R = 2,4-dichlorophenyl triazoles96 |
| Figure 34. Antifungal activity of 3,5-dimethylphenyl- and 4-chlorophenyl-substituted |
| triazoles97 |
| Figure 35. Antifungal activity of methoxyphenyl triazoles against C. TRO and F. |
| COM98 |
| Figure 36. Predicted antifungal activity for the triazoles synthesized in this |
| investigation99 |
| Figure 37. Effect of the alkyl chain length (R') on the antifungal activity of piperazine- |
| substituted 1,2,4-triazoles101 |
| Figure 38. 1,3,5-substituted-1,2,4-triazoles with different X-alkyl chains102 |
| Figure 39. Effect of X-alkyl chains of 1,3,5-substituted-1,2,4-triazoles on the |
| antifungal activity against C. ALB, C. PAR. C. NEO, T. RUB, and M. GYP103 |
| Figure 40. Effect of X-alkyl chains of 1,3,5-substituted-1,2,4-triazoles on the |
| antifungal activity against C. TRO and F. COM104 |
| Figure 41. 1,3,5-substituted-1,2,4-triazoles with different halogenated substituents |
| in R and R ₂ position105 |
| Figure 42. Effect of additional R ₂ and R substitutions in 1,3,5-substituted-1,2,4- |
| triazoles on the antifungal activity against C. ALB, C. PAR, C. NEO, T. RUB. and M. |
| GYP106 |
| Figure 43. Effect of additional R2 and R substitutions in 1,3,5-substituted-1,2,4- |
| triazoles on the antifungal activity against C. TRO and F. COM107 |
| Figure 44. Effect of the distance between the triazole and the substituted-benzene |
| on the antifungal activity of the best 1,3,5-substituted-1,2,4-triazoles found108 |
| Figure 45. Proposed geometry for the interaction between the most active 1,3,5- |
| substituted-1,2,4-triazoles with the active site of the CYP51 enzyme109 |

LIST OF SCHEMES

| Scheme 1. Biosynthesis of fungal ergosterol | .33 |
|--|-------------|
| Scheme 2. Step reaction catalyzed by CYP51 | |
| Scheme 3. Solid phase synthesis of tri-substituted 3-alkylamino-1,2,4-triazoles. Scheme 4. Synthesis of 1,2,4-triazole C-nucleosides | |
| Scheme 5. Synthesis of 1,3,5-trisubstituted 1,2,4-triazoles from reaction carboxylic acids, primary amidines, and monosubstituted hydrazines | |
| Scheme 6. Synthesis of novel 1,3,5-trisubstituted-1,2,4-triazoles using nitrilimin | |
| Scheme 7. Synthesis of O,S-diethyl phenylimidothiocarbonate 59a and Sdimethyl phenylimidodithiocarbonate 61a | S,S- 41 |
| Scheme 8. Synthesis of X,S-diethyl aroyliminothiocarbonates by the GICH-UN Scheme 9. Synthesis of 1,3,5-triazines using S,S-dimethyl aroylimidothiocarbona precursors. | ates |
| Scheme 10. Interaction between O,S-diethyl heteroaroylimidothiocarbonates a S,S-diethyl heteroaroylimidodithiocarbonates with 5-amino-3-phenyl-1 <i>H</i> -1,2 | and 2,4- |
| riazole as a method for obtaining triazolotriazines | .45 |
| Scheme 12. Synthesis of a 1,2,4-triazole starting from a S,S-dimerarylimidodithiocarbonate and phenylhydrazine. | .45 |
| Scheme 13. Synthesis of 1,2,4-triazoles by cyclization of hydrazines with O,S-die aroylimidothiocarbonates or S,S-diethyl aroylimidodithiocarbonates | .46 |
| Scheme 14. Step 1: Synthesis of the X-ethyl aroylimidothiocarbamates of this wo | .51 |
| Scheme 15. Step 2: Synthesis of the X,S-diethyl aroylimidothiocarbonates of twork | this |
| Scheme 16. Step 3: Synthesis of the 1,2,4-triazole derivatives of this work | |
| aroylimidothiocarbonates with hydrazines | |
| 17 Scheme 19. Proposed X-alkyl and X-aryl aroylimidotiocarbamates1 | |
| Scheme 20 . Proposed synthesis of 5-(2,4-dichlorobenzyl)-3-ethoxy-1-substitut 1,2,4-triazoles using the 2-(2,4-dichlorophenyl)acetyl chloride as precursor1 | ted- |
| Scheme 21. Proposed synthesis of 1,2,4-oxadiazole derivatives by cyclization | n of |
| X,S-diethyl aroylimidothiocarbonates and hydroxylamine1 | 119 |

LIST OF TABLES

LIST OF APPENDIX

| Figure A1. ¹ H NMR (300 MHz, CDCl ₃) spectrum of compound T-3a-OC ₂ 130 |
|--|
| Figure A2. ¹³ C NMR (75 MHz, CDCl ₃) spectrum of compound T-3a-OC ₂ 130 |
| Figure A3. FT-IR spectrum of compound T-3a-OC213 |
| Figure A4. High-resolution DART+ mass spectrum of compound T-3a-OC ₂ 13 |
| Figure A5. ¹ H NMR (300 MHz, CDCl ₃) spectrum of compound T-4a-OC ₂ 132 |
| Figure A6. ¹³ C NMR (175 MHz, CDCl ₃) spectrum of compound T-4a-OC ₂ 132 |
| Figure A7. Low-resolution DART+ mass spectrum of compound T-4a-OC ₂ 133 |
| Figure A8. FT-IR spectrum of compound T-4a-OC2133 |
| Figure A9. ¹ H NMR (700 MHz, CDCl ₃) spectrum of compound T-4b-OC ₂ 13 ⁴ |
| Figure A10. ¹³ C NMR (175 MHz, CDCl ₃) spectrum of compound T-4b-OC ₂ 13 ⁴ |
| Figure A11. FT-IR spectrum of compound T-4b-OC2135 |
| Figure A12. High-resolution DART+ mass spectrum of compound T-4b-OC2 135 |
| Figure A13. ¹ H NMR (400 MHz, DMSO-d ₆) spectrum of compound T-1a-SC ₂ 136 |
| Figure A14. FT-IR spectrum of compound T-1a-SC2136 |
| Figure A15. ¹ H NMR (700 MHz, CDCl ₃) spectrum of compound T-1b-SC ₂ 137 |
| Figure A16. ¹³ C NMR (175 MHz, CDCl ₃) spectrum of compound T-1b-SC ₂ 137 |
| Figure A17. FT-IR spectrum of compound T-1b-SC2138 |
| Figure A18. High-resolution DART+ mass spectrum of compound T-1b-SC2138 |
| Figure A19. ¹ H NMR (300 MHz, CDCl ₃) spectrum of compound T-1a-OC ₂ 139 |
| Figure A20. ¹³ C NMR (75 MHz, CDCl ₃) spectrum of compound T-1a-OC ₂ 139 |
| Figure A21. FT-IR spectrum of compound T-1a-OC ₂ 140 |
| Figure A22. High-resolution DART+ mass spectrum of compound T-1a-OC2 140 |
| Figure A23. ¹ H NMR (300 MHz, CDCl ₃) spectrum of compound T-1b-OC ₂ 14 ² |
| Figure A24. FT-IR spectrum of compound T-1b-OC ₂ 14 |
| Figure A25. High-resolution DART+ mass spectrum of compound T-1b-OC2 142 |
| Figure A26. HMBC spectrum of compound T-3b-OC ₂ , couplings of CH carbons in |
| the aromatic region143 |
| Table A1. Carbon NBO charges of O,S-diethyl aroylimidothiocarbonates144 |
| Table A1. Carbon NBO charges of 0,3-detrily aroyllimidothiocarbonates. 142 Table A2. Nitrogen NBO charges for the most active 1,3,5-substituted-1,2,4- |
| triazoles |
| Table A3. Molecular descriptors of piperazine-substituted-1,2,4-triazoles with the |
| AM1 semiempirical method145 |
| Table A4. Molecular descriptors of piperazine-substituted-1,2,4-triazoles with the |
| ONIOM (CAM-B3LYP/6-31++G(d,p):AM1) method |
| Table A5 . Molecular descriptors of piperazine-substituted-1,2,4-triazoles with the |
| CAM-B3LYP/6-31++G(d,p) DFT method |

GLOSSARY

COMPUTATIONAL METHODS: Mathematical approximations implemented computationally to solve the Schrödinger equation in order to determine chemical and physical properties of a molecular system.

HETEROCYCLIC COMPOUND: Cyclic organic compounds with at least one atom other than carbon, with nitrogen, oxygen, sulfur, and phosphorus being the most common heteroatoms.

MINIMAL INHIBITORY CONCENTRATION: The minimal concentration of a biological active compound capable of inhibit the proliferation of a microorganism.

QUANTITATIVE STRUCTURE-ACTIVITY RELATIONSHIP: Methodology used in medical chemistry as well as in other fields of chemistry in which the chemical structure of a compound is related to its biological activity, thus, it is possible to rationalize the activity with molecular descriptors and make predictions over other similar chemical systems.

TRIAZOLE RING: Heterocyclic five-members ring possessing three nitrogen atoms in its structure. Two isomers can be described: 1,2,4-triazole and 1,2,3-triazole, According with the location of nitrogen atoms.

X,S-DIETHYL AROYLIMIDOTHIOCARBONATE: An organic compound containing an iminoster group and an amidic group. These compounds are considered important intermediates in the synthesis of heterocyclic compound through substitution-condensation reactions.

ABBREVIATIONS AND ACRONYMS

AM1 Austin Model 1
Asuper Superficial area

Bz Benzyl (or phenyl acetyl) substituent

C. ALB Candida albicans

C. NEO Cryptococcus neoformansC. PAR Candida parapsiolosisC. TRO Candida tropicalis

CYP51 Cytocrome P-51 enzyme
DART Direct analysis in real time

ΔH_{hydrat} Hydration energy

DEPT Distortionless Enhancement by Polarization Transfer

DFT Density functional theory

D Dipolar moment

DMF *N,N*-Dimethylformamide

EA Electronic affinity
Etherm Thermal Energy

Et Ethyl

F. COM Fonsecaea compacta

G Gibbs energy

HMBC Heteronuclear Multiple Bond Correlation HRMS High Resolution Mass Spectrometry

HSQC Heteronuclear Single Quantum Coherence IC₈₀ 80 percent of minimal inhibitory concentration

IP Ionization potential

LogP logarithm of the partition coefficient *n*-octanol–water

M. GYP Microsporum gypseum

M Molecular mass ppm Parts per million

QSAR Quantitative structure-activity relationship

S Entropy R Refractivity

TLC Thin layer chromatography

T. RUB Trichophyton rubrum

Volume lpha Polarizability

 μ electronic potential

 η Hardness δ Softness

 ω electrophilicity index

1 INTRODUCTION

This investigation focuses on compounds containing the triazole ring, which is a 5-membered ring with three nitrogen atoms. Two isomeric forms are known, the 1,2,3-triazole and the 1,2,4-triazole (Figure 1). The former is also known as osotriazole, vicinal-triazole, or *v*-triazole, while the latter is also known as isomeric symmetrical or s-triazole. Each isomer exists in two tautomeric forms as shown in Figure 1, but an additional form is possible according to the substitution pattern. For the specific case of 1,2,4-triazoles, the tautomeric forms 1*H* 3 and 4*H* 4 are found. Triazoles are captivating due their broad biological properties as antiviral, anti-VIH, anticancer, antibacterial, antitumor, among other activities; and its use as commercial medicine for the treatment of both, superficial and invasive fungal diseases. Therefore, this research area could have an important impact in the development of novel compounds with promising antifungal activity.

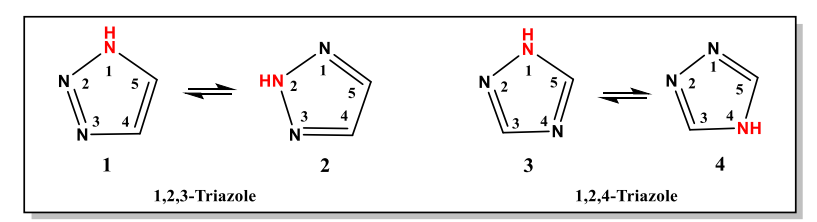


Figure 1. triazole ring isomers and their tautomeric structures. Adapted from reference 1.

The development of pharmacological compounds for the treatment of fungal diseases began in the early 1960s with the use of amphotericin B⁷ and other

¹ BENSON, Frederic; SAVELL, Walter. The Chemistry of the Vicinal Triazoles. Chem Rev. 1950; 46(1): 1-68.

² ZHOU, Loughu *at al.* Synthesis and antiviral activities of 1,2,3-triazole functionalized thymidines: 1,3-dipolar cycloaddition for efficient regioselective diversity generation. *Antivir Chem Chemother*. 2005; **16**(6): 375-83.

³ ALVARES, Rosa *et al.* 1,2,3-Triazole-[2,5-Bis-O-(tert-butyldimethylsilyl)-beta-D-ribofuranosyl]-3'-spiro-5"-(4"-amino-1",2"-oxathiole 2",2"-dioxide) (TSAO) Analogs: Synthesis and Anti-HIV-1 Activity. *J Med Chem.* 1994; **37**(24): 4185-94.

⁴ POKHODYLO, Nazariy *et al.* Synthesis of 1,2,3-Triazole Derivatives and Evaluation of their Anticancer Activity. *Sci Pharm.* 2013; **81**(3): 663-76.

⁵ GOPALRAO, Vikas *et al.* Green synthesis and evaluation of 5-(4-aminophenyl)-4-aryl-4*H*-1,2,4-triazole-3-thiol derivatives. *Iran J Pharm Sci.* 2017; **13**(2): 37-50

⁶ AL-SOUD, Yassen *et al.* Synthesis, antitumor and antiviral properties of some 1,2,4-triazole derivatives, *II Farmaco*. 2004; **59**(10): 775-83.

⁷ BARRATT, Gillian et al. Optimizing efficacy of Amphotericin B through nanomodification, *Int J Nanomedicine*. 2007; **2**(3): 301-13.

compounds as iodinated trichlorophenol haloprogin,⁸ but it was in the late 60s that the first publications related to azolic compounds with antifungal activity were reported. The first reporteed pharmacological active compounds had the imidazole ring in their structure, for example: Clotrimazole, Miconazole, and Ketoconazole⁹. Some years later, in decade of 80s, the imidazole ring was replaced by the triazol ring due to the reduced minimal concentration necessary to inhibit the growth of some fungi. Among the important compounds of this type are Fluconazole, Itraconazole, Voriconazole, and Posaconazole.¹⁰ Figure 2 briefly summarizes the historical development of antifungal drugs.

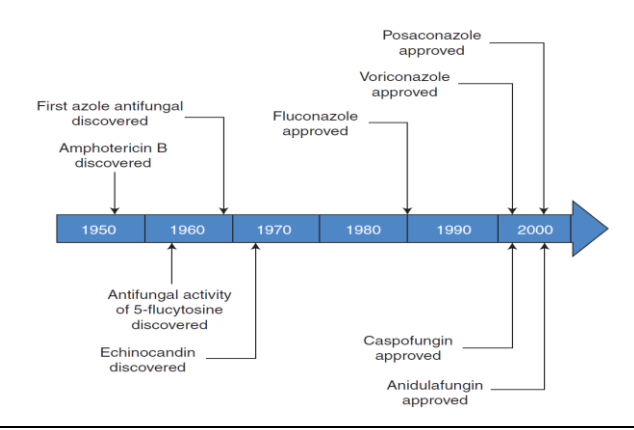


Figure 2. Evolution of antifungal drugs. Taken from reference 9.

However, different problems have appeared as drug resistance, side effects, and interaction with other drugs, ¹¹ which motivates the synthesis of new triazole derivatives as well as the development of novel synthetic methodologies to obtain them, like cyclization reactions between electrophilic and nucleophilic compounds. Some important electrophilic precursors in the synthesis of different heterocyclic compound are the S,S-diethyl and O,S-diethyl aroylimidothiocarbonates which have two electrophilic centers: the carbon of the imino ester portion and the carbon of the carbonyl group¹² (Figure 3). On the other hand, hydrazine derivatives are suitable nucleophilic compounds. Accordingly, the interaction of both allowed the synthesis of 1,3,5-sustituted-1,2,4-triazoles¹³ and therefore, this reaction promises to be

⁹ NETH, Jeniel *et al.* Antifungal agents: Spectrum of activity, pharmacology, and clinical indications. *Infect Dis Clin North Am.* 2016; **30**(1): 51-83.

⁸ SMITH, Edgar. History of antifungal, *J Am Acad Dermatol.* 1990; **23(**4): 776-78.

¹⁰ SAAG, Michael *et al.* Azole antifungal agents: emphasis on new triazoles. *Antimicrob Agents Chemother*. 1988; **32**(1): 1-8.

¹¹ PFALLER, Michael. Antifungal Drug Resistance: Mechanisms, Epidemiology, and Consequences for Treatment. *Am J Med*, 2012; **125**(1): 3-13.

¹² LAGOS, Yolanda; CHECA, Camilo. Evaluación de las interacciones del 5-amino-1-fenil-3-metilpirazol con los isotiocianatos de aroilo con los aroiliminoditiocarbonatos de S,S-dietilo. Trabajo de grado en Química, Universidad de Nariño, 2005

¹³ HIDALGO, Andres. Síntesis de nuevos 1,2,4-triazoles por reacción de aroilimidotiocarbonatos de O, S-dietilo o aroilimidoditiocarbonatos de S,S-dietilo con hidrazinas. Trabajo de grado en Química, Universidad de Nariño, 2017.

versatile and useful to synthetize a considerable number of triazole derivatives with different substituents in the electrophilic and/or nucleophilic moiety.

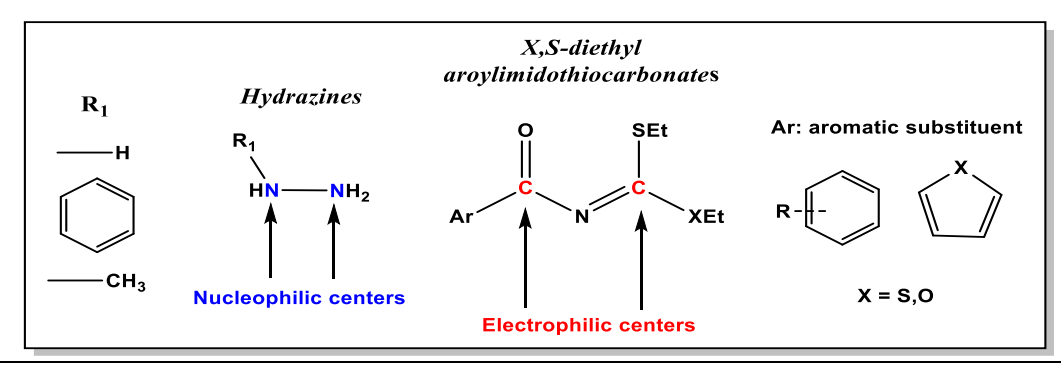


Figure 3. Nucleophilic and electrophilic centers of hydrazines and X,S-diethyl aroylimidodithiocarbonates, respectively. Source: This investigation.

Additionally, it is possible to use computational tools to predict the biological activity of a compound. One of these is the quantitative structure-activity relationship (QSAR) where the biological activity of a compound is related to its physicochemical, electronic, or structural properties using a mathematical model.¹⁴ With this model, the activity of similar compounds can be predicted, which can be advantageous because a smaller number of biological essays can be devised, only with those compounds exhibiting an important activity and therefore saving time and resources. This investigation evaluates the versatility of a methodology for the synthesis of 1,2,4-triazole derivatives using hidrazines and aroylimidothiocarbonates standardized by the Grupo de Investigación en Compuestos Heterocíclicos (GICH-UN). 13 Also, the antifungal activity of these and related derivatives was computationally evaluated against different fungal species through mathematical models designed and adjusted from a series of compounds with a common 1,2,4triazole core¹⁵ for which experimental data on their antifungal activity exist. Several modifications of the molecular structure of the triazole derivatives were proposed to determine the systems with the highest antifungal activity.

This work is organized as follows: in the *state-of-the-art* an exhaustive review about the biological importance of azole compounds is made, mainly, for the treatment of fungal diseases, explaining its mechanism of action and the limitations associated to the traditional drugs. These limitations are be key to motivate the research in different synthetic methodologies of new azole derivatives with promising antifungal activity using different precursors, among these, the X,S-diethyl aroylimidothiocarbonates, which will be extensively discussed, focusing on synthetic

¹⁴ DUDEK, Arkadiusz *et al.* Computational methods in developing Quantitative Structure-Activity Relationships (QSAR): A Review. *Comb Chem & High Through Scree*. 2006; **9**(3): 213-228.

¹⁵ XU, Jianming *et al.* Design, synthesis and antifungal activities of novel 1,2,4-triazole derivatives. *Eur J Med Chem.* 2011; **46**: 3142-3148.

strategies and applications. Then, the general aspects of QSAR techniques, as a predictive method to find new active compounds, are introduced. The *results and discussion* chapter is divided in two sections: first, the description of synthetic process, where the characterization of intermediates and final triazole products, as well as a computational study of the cyclization reaction involved in the final step is described; and second, the QSAR study, where mathematical models are designed and, subsequently, used to theoretically evaluate the antifungal activity of 1,3,5-substituted-1,2,4-triazoles obtained in this work and their structural modifications aiming to maximized their antifungal potential. Generalities are presented in *materials and methods*. Finally, based on the obtained results, *conclusions* and *recommendations* are given.

2 OBJECTIVES

2.1 General objective

Synthesize 1,2,4-triazole derivatives by cyclization between O,S-diethyl aroylimidothiocarbonates and hydrazines and evaluate their antifungal potential by QSAR techniques.

2.2 Specific objectives

- Synthesize 1,2,4-triazoles by cyclization between O,S-diethyl aroylimidothiocarbonates and hydrazines.
- Characterize intermediates and final products by spectrometric (MS) and spectroscopic (FTIR, ¹H-NMR, ¹³C-NMR) methods.
- Evaluate the antifungal activity of the synthesized 1,2,4-triazoles by QSAR techniques.

3 STATE-OF-THE-ART

In this chapter, the importance of heterocyclic compounds in the pharmacological field is discussed, specifically, triazole compounds, which are mainly used as antifungals. Also, the limitations of the traditional drugs will be described, which have led to the development of new methodologies for the synthesis of 1,2,4-triazolic systems by several research groups. Among these, the GICH-UN has used X,S-diethylaroylimidothiocarbonates as precursors for the synthesis of different heterocyclic compounds, including 1,2,4-triazoles. Finally, the generalities of the QSAR methodology and its application to predict antifungal activity will be discussed.

3.1 The biological importance of heterocyclic compounds

The first topic to review is about the importance of heterocyclic systems in several medical treatments and commercial drugs, focusing on the antimitotic activity of azole compounds, the history, action mechanism, limitations, and novel studies.

3.1.1 Commercial drugs containing heterocycles

Heterocyclic compounds have been studied in different fields like medicine and chemistry. It is known that biomolecules such as enzymes, vitamins, and nucleic acids have heterocyclic cores in their structure and, for this reason, many drugs used in medical treatments have incorporated these cores as active compounds (Figure 4). For example, drugs containing the 1,4-benzodiazepine moiety are mostly used for the treatment of anxiety, but they are also useful in treating several other conditions like central nervous system disorders. Benzodiazepines are positive allosteric modulator molecules that increase the activity of the γ -aminobutyric acid, which is used by nerves to communicate with each another; the most common drug is **Lorazepam 5** which is used as tranquilizer¹⁶. However, benzodiazepines, are not the only typical active compounds in the treatment of central nervous system diseases, the neuroamine transmitter serotonin **Sumatriptan 6**, which possesses the indole core, is also used in antidepressants, antipsychotics and anxiolytics

27

¹⁶ KHAM, Iram *et al.* 1,4-Benzodiazepine: an overview of biological properties. *Sci Rev Chem Commun.* 2015; **5**(1): 13-20.

treatment.^{17,18} **Atorvastatin 7**, one of the best-selling drugs of the last few years, is an example of a competitive HMG-CoA-reductase inhibitor belonging to the 7-substituted 3,5-dihydroxyheptanoic acid family¹⁷ which containing a pentasubstituted pyrrole ring as core. **Mometasone 8** is one drug that contains a furan ring. It is a moderately potent glucocorticoid used for the treatment of inflammatory skin disorders, asthma, and allergic rhinitis. Another pharmaceutical compound which contains the furan group is **Ranitidine 9** that is commonly used in patients with gastric ulcer¹⁷. These are some examples of typical drugs, but there are many other active compounds with different applications. Typically, to identify biologically active molecules, large collections of chemical compounds, either synthetic or derived from natural products, are tested by means of high performance pharmacological screening¹⁹ and computational methodologies based on QSAR.¹⁴

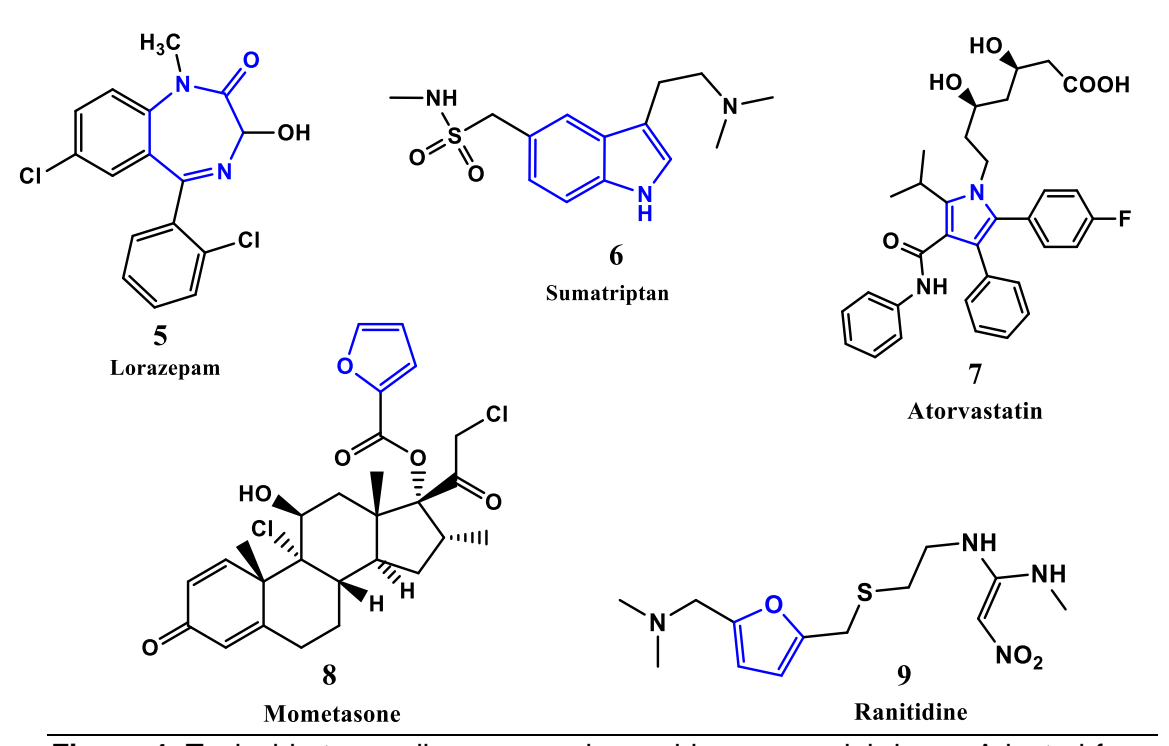


Figure 4. Typical heterocyclic compounds used in commercial drugs. Adapted from references 16, 17, and 18.

-

¹⁷ BAUMANN, Marcos *et al.* An overview of the key routes to the best-selling 5-membered ring heterocyclic pharmaceuticals, *Beilstein J Org Chem.* 2011; **7**: 442–495.

¹⁸ MARTINS, Pedro *et al.* Heterocyclic Anticancer Compounds: Recent Advances and the Paradigm Shift towards the Use of Nanomedicine's Tool Box, *Molecules*. 2015; **20**(9): 16852-16891.

¹⁹ DIAZ, Emilio et al. Industrialization of the screening process. Eur Pharm Reviews. 2004; 9: 74-77.

3.1.2 Biological activity of azole compounds

The azoles are a large family of five-membered heterocyclics containing, for example, two nitrogen atoms in the case of imidazoles and three in the case of triazoles, which have been used as active compounds in different drugs (Figure 5). The 1,2,3-triazole is used, for example, in **Rufinamide 10**, a drug for the treatment of epilepsy ²⁰. The tetrazole core has been used in **Valsartan 11**, an angiotensin II antagonist which helps to control blood pressure²¹. However, the most important reports about the use of azole compounds as commercial drugs are their use as antifungal agents, mainly, imidazole and 1,2,4-triazole derivatives.

Figure 5. Examples of commercial drugs containing azoles in their structure. Adapted from references 20 and 21.

3.1.3 Antifungal activity of azole compounds

3.1.3.1 Development and evolution of azole drugs

The synthesis of antifungal agents for the pharmaceutical industry began in the 20th century and since then, the design of new molecules to fight against fungal infections has not stopped. In order to focus on the specific scope of this project, a review will be made of the most general aspects of the evolution of antifungal medications based on azoles, which have a common enzymatic action.

In the early 60s, the commercially available antifungal to treat systematic fungal infections was amphotericin B, but it showed to be nephrotoxic with chronic renal failure occurring in 44% of patients receiving it, also generating hypokalemia and

²⁰ WHELESS, James; VASQUEZ, Blanca. Rufinamide: A novel broad-spectrum antiepileptic drug. *Epilepsy Curr.* 2010; **10**(1): 1-6.

²¹ KAUSHIK, Manu; MOHIUDDIN, Syed. Clinical utility of valsartan in treatment of children and adolescents with high blood pressure. *Adol Heal Med and Therap.* 2011; **2**: 97-103.

renal acidosis.²² The unfortunate adverse effects associated with this drug promoted investigations on new compounds, in 1969, the first publications related to azole compounds with antifungal activity were reported, highlighting two compounds **Clotrimazole 12** and **Miconazole 13** (Figure 6), whose common characteristic is to contain the imidazole ring as responsible for the biological activity. However, they differ in the distance from the heterocyclic to the asymmetric carbon.²³ **Ketoconazole 14** is a derivative of Miconazole and became the first chemical compound with sufficient oral bioavailability for the treatment of deep fungal infections. The novel structural feature of **Ketoconazole** was the incorporation of a dioxolane ring in the asymmetric carbon (Figure 6).²⁴

Figure 6. Structure of antifungal drugs with an imidazole ring. Adapted from reference 23.

In the 80s, new changes were introduced in the structure of these molecules: the imidazole ring was changed to the triazole ring and the chlorine of the benzene ring attached to the asymmetric carbon was replaced by fluorine, both modifications are related to a greater specificity for the enzyme of the fungus and lower toxicity for the humans²³, this compounds were denominated as *first-generation triazoles* (Figure 7). Thus, the first description of **Itrazonazole 15**, that was given in 1984, evidenced the change of the imidazole ring to triazole; while **Fluconazole 16**, that appeared near 1990, exhibited both modifications, with an additional hydroxyl group included in the asymmetric carbon²³. Both drugs continue to be widely used for the treatment of superficial and invasive fungal infections. However, clinical limitations were demonstrated early in relation to their spectrum of activity, thus, to overcome these limitations, several analogues have been developed. These new generation triazole antifungal drugs were called *second-generation triazoles*²⁵ (Figure 7). The substitution of one triazole ring in Fluconazole by a pyrimidine and the addition of a

30

²² PEYTON, Lee et al. Triazole antifungal: A review. Drugs Today. 2015; 51(12): 705-718.

²³ SADABA, Belen *et al.* Relación entre estructura y función de los azoles. *Rev Esp Quimioterap.* 2014; **17**(1): 71-78.

²⁴ ARAGON, Martin et al. Antimicóticos dermatológicos. Farmacia Profesional. 2014; 18(7), 38-48.

²⁵ CORRADO, Girmenia *et al.* New-generation triazole antifungal drugs: review of the Phase II and III trials. *Clin Invest.* 2011; **1**(11): 1577-1594.

methyl group allowed the synthesis of **Voriconazole 17,**²⁶ the first example of a second-generation triazole, which significantly reduced the IC₅₀ against some fungal species like *Aspergillus fumigatus*. The IC₅₀ is the half maximal inhibitory concentration and represents the concentration of a drug that is required for 50% inhibition *in vitro*²⁷. Also, in the 21st century, an important structural change was made to Itrazonazole, where the triazolone alkylated chain was extended and hydroxylated, giving rise to a new compound called **Posaconazole 18** with improved activity.^{23,28} Finally, **Ravuconazole 19** which is another derivative of fluconazole developed by Bristol-Myers Squibb, represents the most current second-generation triazole. Ravuconazole has a broader antifungal spectrum than Fluconazole and Itraconazole, particularly against *Candida krusei* and *Cryptococcus neoformans*.²⁸

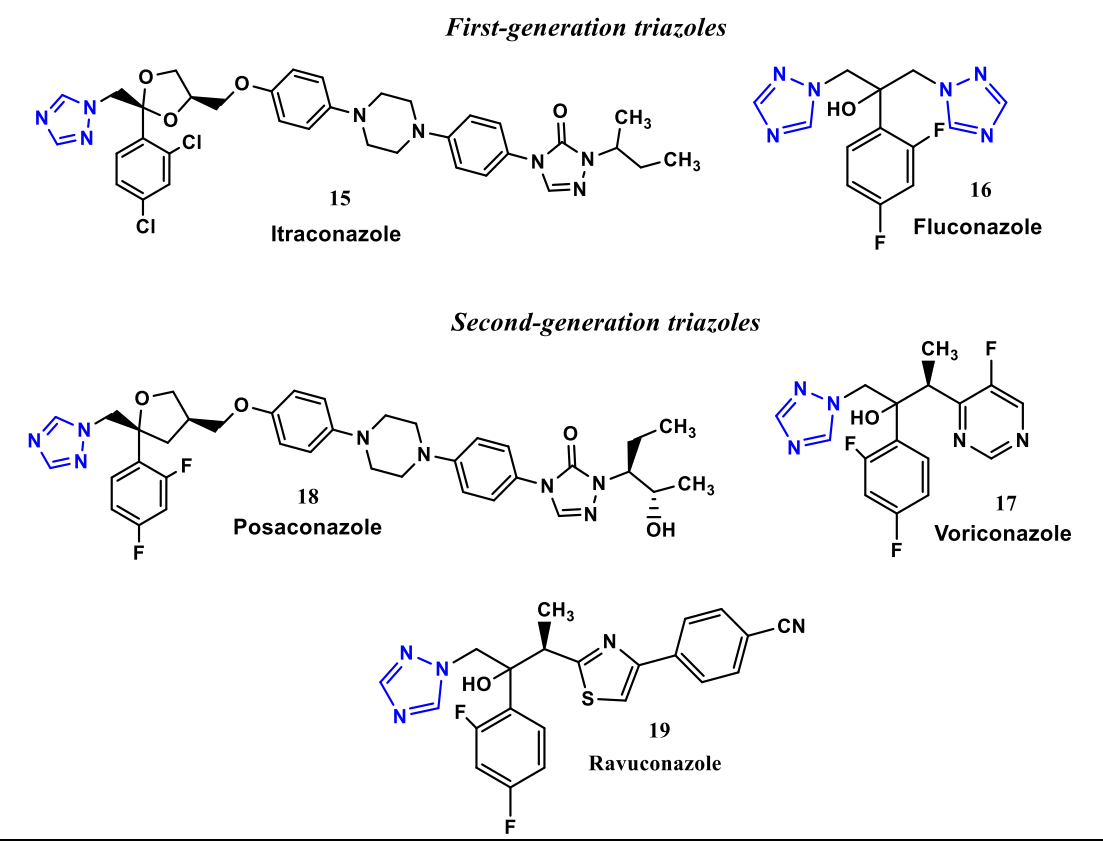


Figure 7. Structure of antifungal drugs with a triazole ring. Adapted from references 23 and 28.

²⁶ HERBRECHT, Raoul. Voriconazole: Therapeutic review of a new azole antifungal. *Expert Rev Anti-infect Ther.* 2004; **2**(4): 485-497.

31

_

²⁷ CALDWELL, Gary et al. The IC₅₀ Concept Revisited. Curr Top Med Chem. 2012; **12**(11): 1282-1290

²⁸ MAERTENS, Jan. History of the development of azole derivative. Clin Microbiol Infect. 2004; **10**(1): 1-10

3.1.3.2 Enzymatic action of azoles

The mechanism of action of triazoles and, in general, compounds containing an azole ring consists in inhibiting the biosynthesis of fungal ergosterol 31 which is generated from lanosterol 22 (Scheme 1). The inhibition mechanism of azoles is common. 22,23,29,30,31 these compounds inhibit the activity of the enzyme cytochrome P450 14_{DM}, also called lanosterol 14-α-demethylase or CYP51 of the fungus. This enzyme catalyzes the elimination of the 14-methyl group (C-32) of lanosterol 22 or its metabolites 23, 24. This enzymatic system is present in almost all living organisms and its function is the synthesis of ergosterol in the case of fungi and cholesterol in the case of mammals²³.

Demethylation catalyzed by CYP51 is a three-step reaction, each requiring one molecule of O2 and two molecules of NADPH (Scheme 2). First, methyl group (C-32) is converted to 14α -hydroxymethyl **32**, then to 14α -carboxyaldehyde **33**, and, finally, this group is released as formic acid with the introduction of a double bond between carbons 14 and 15 at the sterol core 34²². This double bond is reduced later by a $^{14}\Delta$ reductase²⁹ to generate other intermediates as zymosterol **30.**

²⁹ WHEAT, Joe et al, Hypothesis on the Mechanism of Resistance to Fluconazole in Histoplasma capsulatum, Antimicrob agents chemother. 1997; 41(2): 410-414.

³⁰ GHANNOUM, Mahmoud; RICE, Louis. Antifungal Agents: Mode of Action, Mechanisms of Resistance, and Correlation of These Mechanisms with Bacterial Resistance, Clin Microbiol Rev. 1999; 12(4): 501-517.

³¹ WEETE, John. Mechanism of Fungal Growth Suppression by Inhibitors of Ergosterol Biosynthesis. En: Ecology and Metabolism of Plant Lipids. FULLER, G.; NES W. D. Eds, Chapter 17, 1987: 268-265.

Scheme 1. Biosynthesis of fungal ergosterol **31**. Adapted from references 22, 23, 29, 30, and 31.

Scheme 2. Step reaction catalyzed by CYP51. Adapted from reference 22.

The azoles have a mechanism of competitive inhibition and their action is carried out in the first step of the mono-oxygenation reaction (Scheme 2). The isoenzyme has a heme group in its structure, which is a co-factor involved in the redox processes³². The heme group is accessible through a long channel where there are also hydrophobic amino acids that recognize lanosterol **22** or azoles allowing the entry of one to exclude the other. The azoles bind to the cytochrome P450 14_{DM} in three places (Figure 8): 1) to the iron atom of the heme group through one nitrogen atom; 2) to a substrate binding site through the difluorophenyl (or dichlorophenyl) group, here, the fluorine atoms can form H-bonds with the residue Glycine; and, 3) the lateral side chains, although they are not determinant for the antifungal activity, form hydrophobic and Van der Waals interactions with amino acids in the entrance channel³³ and play an important role in conditioning the physicochemical properties of the molecule, helping to reduce side effects and improving pharmacological characteristics.²³

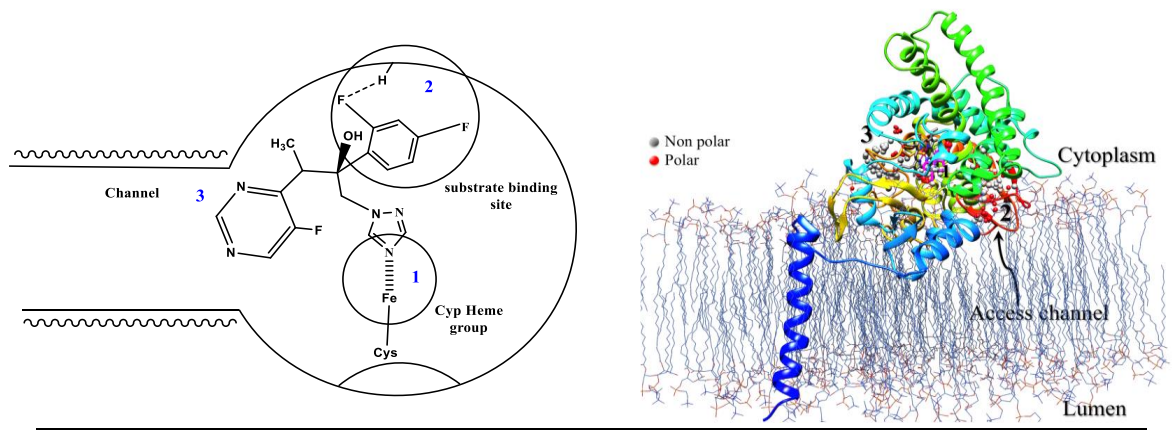


Figure 8. Interaction of azoles with the cytochrome P450 14_{DM} enzyme. Adapted from references 23 and 32.

Experimental evidence proved the activity of the azoles with the accumulation of 14-methylated products as oburicol **23**, obtusifolione **24**, and 4,14-dimethylzymosterol **27**^{22,29} and other genetic studies in which Geber *et al*²⁹ cloned the structural genes encoding the CYP51. Ergosterol serves as a bioregulator of the membrane fluidity and, consequently, of the membrane integrity in fungal cells. The cell membrane requires sterols without methyl groups; inhibition of 14α -demethylase leads to depletion of ergosterol and accumulation of methylated sterol precursors resulting in the formation of a plasma membrane with altered structure and function which could lead to inhibition of cell growth (fungistatic action) or its death (fungicidal action).³⁰

³² EGBUTA, Chinaza *et al.* Mechanism of Inhibition of Estrogen Biosynthesis by Azole Fungicides. *Endocrinology.* 2014;**155**(2): 4622-4628

³³ YU, Shichong *et al.* Triazole derivatives with improved in vitro antifungal activity over azole drugs. *Drug Des Devel Ther.* 2014; **8**: 383-390.

34

Generally, triazoles are fungistatic; only Voriconazole and Itraconazole are considered fungicidal.²²

3.1.3.3 Limitations of azole antifungals

Despite the constant advances in the chemistry of antifungal compounds and their high tolerability, currently research on new antifungals has become a focus of interest of many pharmaceutical industries and researchers due to the limitations presented by many typical antifungals. These limitations are mainly due to three facts: side effects, drug resistance, and poor pharmacokinetics²².

Drug resistance is the main problem to mention. Two types of drug resistance have been demonstrated experimentally and both are related to genetic mutations on the CYP51 enzyme. First, amino acid substitutions in the drug target which inhibit drug binding are a common azole-resistance mechanism, this substitution occurs near the heme-binding site. In *Aspergillus fumigatus*, target site alterations are the most reported resistance mechanism, with over 30 CYP51 mutations identified.³⁴ The second type of drug-resistance is the overexpression of CYP51 which is common among azole-resistant clinical isolates of *Candida glabrata, Candida parapsilosis, Candida tropicalis*, and *Candida krusei*. This contributes directly to resistance because an increase in abundance of the target enzyme requires more drug for inhibition and this reduces susceptibility.³⁴

There are a series of side effects that can cause health problems, for example, Voriconazole can produce visual disturbances, hepatic abnormalities, and skin reactions;²⁶ Fluconazole can cause rashes, nausea, and digestive abnormalities among other side effects;²³ Itraconazole generates dizziness, headache, and gastrointestinal disturbances; Posaconazole can cause skin irritation and sensibility; and even Ravuconazole, a very recent antifungal, can produce urinary incontinence and diarrhea.²²

About the pharmacokinetic effects, some antifungals as Ketoconazole and Itraconazole should only be administered with food to ensure adequate bioavailability since absorption of the azole antifungal is impaired by high gastric pH. Furthermore, antacids and sucralfate interfere with the absorption of Ketoconazole. Newer oral antifungals are slowly eliminated. Azoles are also associated with pronounced drug interactions, for example, Ketoconazole, Itraconazole, and Fluconazole influence the cyclosporin metabolism.³⁵

³⁴ COWEN, Leah et al. Mechanisms of Antifungal Drug Resistance, *Cold Spring Harb Perspect Med.* 2017; **5**(7):

³⁵ SCHDFER-KORTING, Monika. Pharmacokinetic Optimization of Oral Antifungal Therapy. *Clin Pharmacokinet*. 1993; **25** (4): 329-341.

3.1.3.4 Novel antifungal 1,2,4-triazoles

Several authors have reported *in vitro* antifungal activity of novel 1,2,4-triazoles derivatives, this, with the purpose of overcome the limitations of the traditional drugs. Some relevant studies are described below.

1,2,4-triazoles derivatives with a 4-(4-phenylsubstituted)-piperazine side chain **35** (Figure 9A) with a similar chemical structure to Fluconazole were developed by Xu et al and their activity against Candida albicans, Candida paropsilosis, Candida tropicalis, Cryptococcus neoformans, Aspergillus fumigatus, Trichophyton rubrum, and Microsporum gypseum was evaluated¹⁵. The results indicate antifungal activities comparable to Ketoconazole and Voriconazole and better than Fluconazole and Itraconazole. Due to the important results obtained in their investigation, these compounds were taken as reference for the QSAR study that will be discussed in detail in the next chapter.

On the other hand, Begihalli *et al* designed new 1,2,4-triazoles which were coordinated to cobalt (II), nickel (II), and copper (II) obtaining metallic complexes **36** (Figure 9B) that were evaluated against the bacteria *Escherichia coli*, *Staphylococcus aureus*, *Streptococcus pyogenes*, *Pseudomonas aeruginosa*, and *Salmonella Typhi* and the fungi *Aspergillus niger*, *Aspergillus flavus*, and *Cladosporium sp.*³⁶ In all cases, the compounds exhibited antibacterial and antifungal activity, but were less effective than Gentamicin and Fluconazole used as standards, respectively.

More recently, 1,2,4-triazol analogues of Voriconazole **37** (Figure 9C) were synthesized by Wu *et al*³⁷ and evaluated against several fungi, with some of them exhibiting better activities than Fluconazole. Besides, molecular docking studies demonstrated that some of these compounds possessed superior affinity (than Fluconazole) with the target enzyme (CYP51) by strong hydrogen bond from a morpholine ring.

³⁷ WU, Junqi *et al.* Molecular docking, design, synthesis and antifungal activity study of novel triazole derivatives. *Eur J Med Chem.* 2018; **143**: 1840-1846.

36

³⁶ BAGIHALLI, Gangadhar *at al.* Synthesis, spectral characterization, in vitro antibacterial, antifungal and cytotoxic activities of Co(II), Ni(II) and Cu(II) complexes with 1,2,4-triazole Schiff bases. *Eur J Med Chem.* 2008; **43**: 2639- 2649.

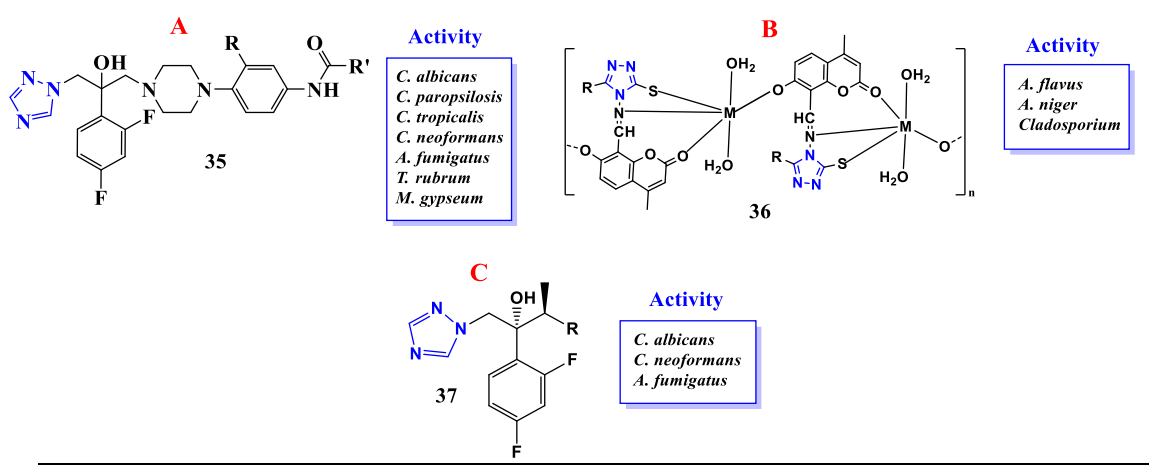


Figure 9. Novel 1,2,4-triazole derivatives with promising antifungal activity. Adapted from references 15, 36, and 37.

The cited examples indicate that currently, a lot of effort is aimed to obtain new triazole derivatives that could exhibit broader biological activities, not only to expand the spectrum of possible compounds with pharmacological importance but also to overcome the deficiencies of current drugs. Therefore, investigations in this field are a priority due to the urgent need for new compounds with antimicrobial activity.

3.2 Synthetic methodologies toward 1,3,5-substitued-1,2,4-triazoles

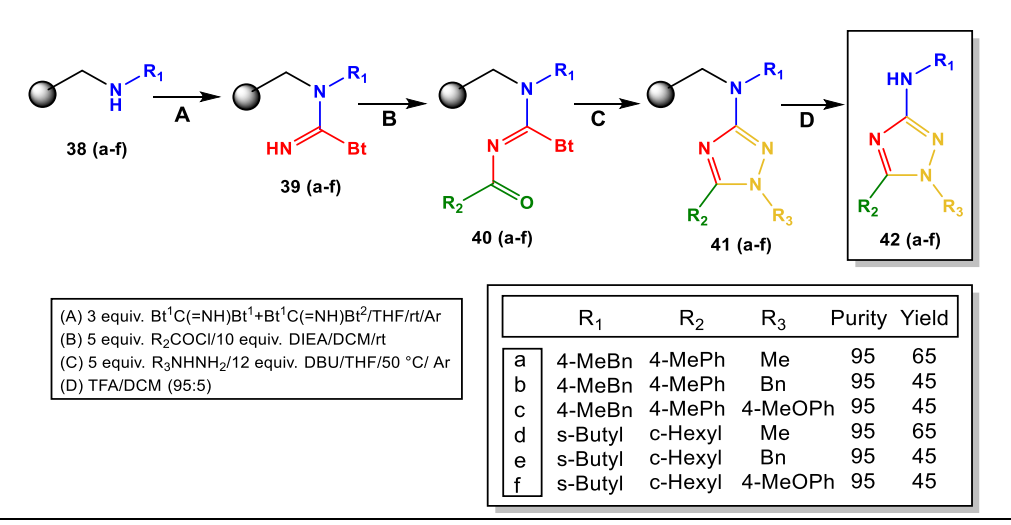
The limitations of traditional antifungals and the progress of heterocyclic chemistry have been a motivation for researchers who venture into new synthetic routes to obtain new compounds, so, the need to have compounds with improved antimycotic activity has led to the development of new synthetic methodologies to obtain triazolic compounds analogous to traditional drugs by different structural modifications. For this reason, a review of some methods used for the synthesis of 1,2,4-triazoles will be made, and specifically, of 1,3,5-trisubstitued systems which are similar to the compounds synthesized in this investigation.

The solid phase synthesis of non-sequential molecules such as heterocyclic compounds, in particular, 1,2,4-triazole derivatives has been widely studied, especially in the last years, because this synthetic technique has been intricately linked to combinatorial chemistry. The importance of solid phase synthesis is based on the use of a minimum amount of organic solvent and its contribution to green chemistry, especially in terms of atomic economy. To cite a related study, Makara *et al*³⁸ carried out the solid phase synthesis of tri-substituted 3-alkylamino-1,2,4-triazoles **42 (a-f)** (Scheme 3). The synthesis of triazoles was carried out using a

37

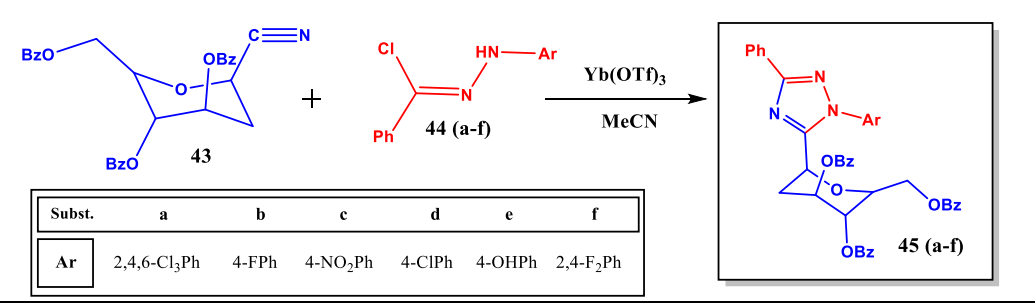
³⁸ MAKARA, Gergely. Solid-phase synthesis of 3-alkylamino-1,2,4-triazoles. *Org Lett.* 2002; **4**(10): 1751-1754

cyclization between immobilized *N*-acyl-1*H*-benzotriazole-1-carboximidamides **40** (a-f) and hydrazines, affording the products with high purity in acceptable yield.



Scheme 3. Solid phase synthesis of tri-substituted 3-alkylamino-1,2,4-triazoles. Adapted from reference 38.

Al-Masoudi *et al*³⁹ developed a methodology which included treatment of the glycosyl nitrile **43** and the hydrazonyl chlorides **44 (a-f)** in the presence of a catalytic amounts of ytterbium (III) triflate in refluxing acetonitrile to afford the 1,2,4-triazole C-nucleosides **45 (a-f)** in 58-74% yield (Scheme 4). The advantages of this method include the facile experimental procedure, catalyst reuse, easy work-up, and the use of reflux temperature.



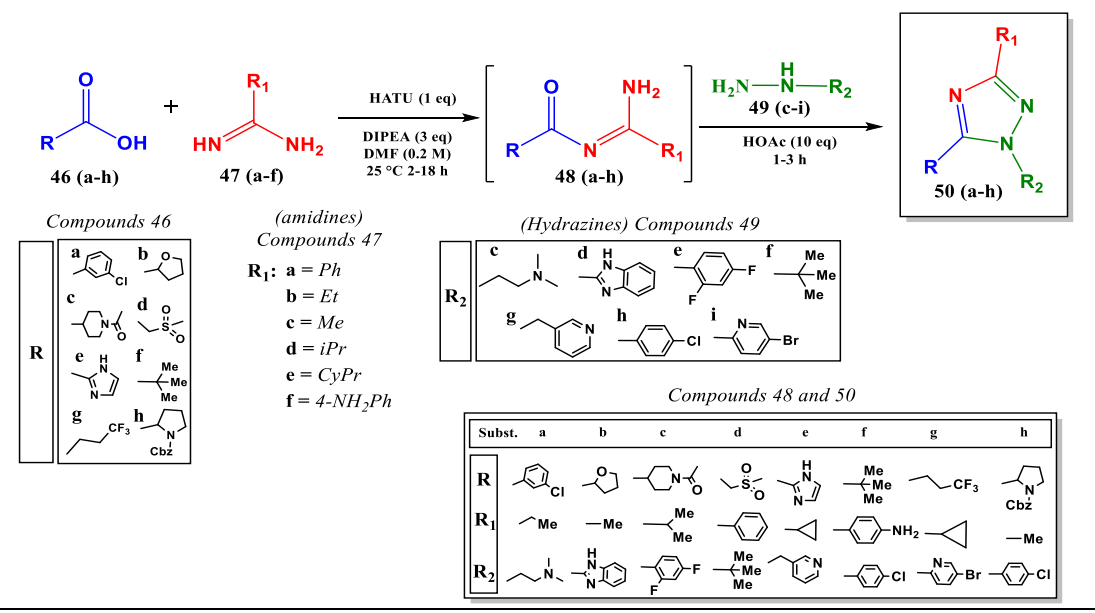
Scheme 4. Synthesis of 1,2,4-triazole C-nucleosides. Adapted from reference 39.

Castanedo *et al*⁴⁰ designed a general method for the synthesis of 1,3,5-trisubstituted 1,2,4-triazoles **50** (a-h) from reaction of carboxylic acids **46** (a-h), primary amidines

³⁹ AL-MASOUDI, Najim et al. synthesis of 1,2,4-triazole c-nucleosides from hydrazonyl chlorides and nitriles, *Nucleos Nucleot Nucl.* 2007; **26**: 37-43.

⁴⁰ CASTANEDO, Georette et al. Rapid Synthesis of 1,3,5-Substituted 1,2,4-Triazoles from Carboxylic Acids, Amidines, and Hydrazines. *J Org Chem.* 2011; **76**: 1177-1179.

47 (a-f), and monosubstituted hydrazines **49 (c-i)** (Scheme 5). This highly regioselective one-pot process provides rapid access to highly diverse triazoles and allows greater diversity at the 5-position in comparison with other methodologies.

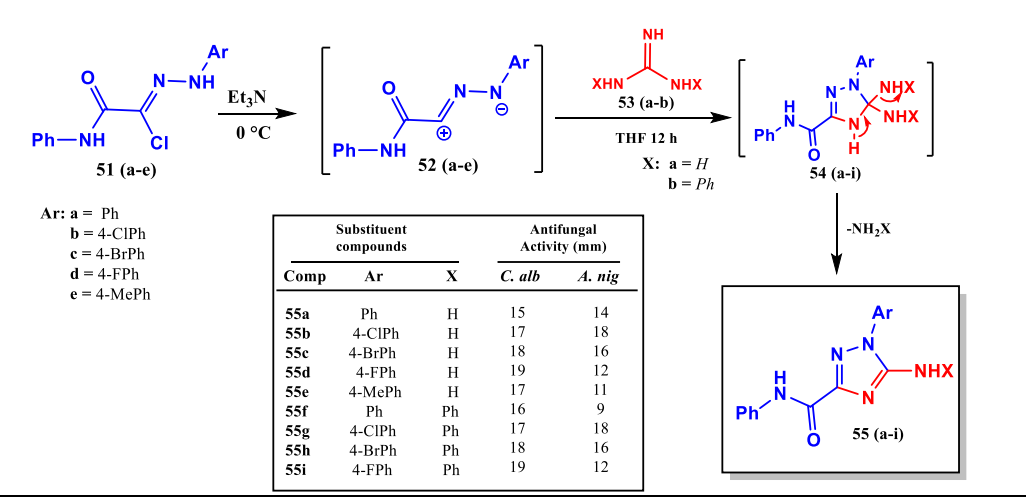


Scheme 5. Synthesis of 1,3,5-trisubstituted 1,2,4-triazoles from reaction of carboxylic acids, primary amidines, and monosubstituted hydrazines. Adapted from reference 40.

Dalloul⁴¹ reported a synthetic methodology to obtain novel 1,3,5-trisubstituted-1,2,4-triazoles **55** (a-i) by 1,3-dipolar cycloaddition of C-phenyl amino-carbonyl-*N*-arylnitrilimines **51** (a-e) with guanidines derivatives **53** (a-b). This process take place via the formation of 5,5-diamino-1,2,4-triazoles **54** (a-i) through nucleophilic addition of the electron pair of the imino group of guanidine followed by the cyclization at the imine carbon (Scheme 6). Final compounds exhibited antifungal activity against *C. albicans* and *A. niger*.

-

⁴¹ DALLOUL, Hany. Heterocyclic synthesis using nitrilimines: Part 19. Synthesis of novel 1,3,5-trisubstituted-1,2,4-triazoles. *Arab J Chem.* 2014; **7**(5): 604-608.



Scheme 6. Synthesis of novel 1,3,5-trisubstituted-1,2,4-triazoles using nitrilimines. Adapted from reference 41.

In general, the routes use two mechanisms, either condensation between an electrophile and a nucleophile or 1,3- dipolar cycloaddition as shown. In this investigation, a route based on the first mechanism is used. The intermediates synthetized with this purpose are the X,S-diethyl aroyilimidothiocarbonates, which are interesting compounds due to its versatility in heterocyclic chemistry. In the next section, their synthesis and applications are discussed.

3.3 The X,S-dialkyl aroylimidothiocarbonates

As mentioned before, there are a considerable number of methodologies for the synthesis of 1,2,4-triazole derivatives. However, it is of interest for this project to obtain 1,2,4-triazoles using O,S-diethyl aroylimidothiocarbonates and S,S-diethyl aroylimidodithiocarbonates as precursors. These carbonates have been widely studied by the GICH-UN owing to their versatility in interacting with compounds that have an amino group like hydrazines and urea to obtain five and six membered heterocyclic compounds such as triazoles and triazines, respectively. 13,42

The reactivity of these compounds is due specifically to the presence of two electrophilic centers which are susceptible to nucleophilic attacks (Figure 3): the carbon of the imino ester portion and the carbon of the carbonyl group, with the former being more susceptible than the latter to the attack of a nucleophilic agent. Generally, the imino ester group is susceptible to substitution reaction, detaching an alkylthiol; while the carbonyl group to condensation reaction.

⁴² CASTRO, Edison; SANCHEZ, Edison. *Evaluación de las interacciones entre las 4,5-diamino-6-pirimidonas y los aroil y heteroiliminotiocarbonatos de O,S-dietilo*. Trabajo de grado en Química, Universidad de Nariño, 2008.

40

The synthetic methodology to obtain them has several advantages like short reaction time, high yield, the use of room temperature conditions, and the fact that this process do not use expensive catalysts.

3.3.1 Synthesis of X,S-dialkyl aroylimidothiocarbonates

The synthesis of O,S-diethyl phenylimidothiocarbonate **59a** was reported by Dixon in 1899. Likewise, the synthesis of S,S-dimethyl phenylimidodithiocarbonate **61a** was carried out too and later standardized by Nash *et al* in 1969, using benzoyl isothiocyanate **57a** as precursor and methyl iodide as methylating agent of the S-methylphenylimidotiocarbamate intermediate **60a** (Scheme 7). 12,42

Scheme 7. Synthesis of O,S-diethyl phenylimidothiocarbonate **59a** and S,S-dimethyl phenylimidodithiocarbonate **61a**. Adapted from reference **12**.

More recently, Checa and Lagos¹² (GICH-UN) reported the optimization of a methodology for obtaining S,S-diethyl aroylimidodithiocarbonates 63 (a-c) in two stages (Scheme 8). First, the preparation of the S-ethyl aroylthiocarbamates 62 (ac) starting from the reaction between aroyl chlorides 56 (a-c) and potassium thiocyanate; then, the subsequent reaction with ethanethiol in acetonitrile; finally, the ethylation of the carbamates 62 (a-c) with ethyl bromide instead of ethyl iodide in presence of NaH in DMF, to produced the respective S,S-diethyl aroylimidodithiocarbonate 63 (a-c). The S,S-diethyl nitrophenylimidodithiocarbonate was also synthetized by the same authors starting with 4-nitrobenzoyl chloride under the same conditions. 12

Based on this work, Castro and Sanchez⁴² reported the synthesis of O,S-diethyl aroylimidothiocarbonates **59** (a-c) and O,S-diethyl heteroaryl-amidothiocarbonates **59** (f-g) following the same methodology but using ethanol instead of ethanethiol in

the second step (Scheme 8). Likewise, Estrada⁴³ synthesized O,S-diethyl heteroaroylimidothiocarbonates **59** (**d-e**) under the same conditions.

Scheme 8. Synthesis of X,S-diethyl aroyliminothiocarbonates by the GICH-UN. Adapted from references 12, 42, and 43.

3.3.2 X,S-dialkylimidothiocarbonates as precursors of heterocyclic compounds

The chemical and structural properties of the aroylimidotiocarbonates have allowed their use as precursor in the synthesis of the different heterocyclic compounds as summarized in Figure 10. 12,13,42,44,45,46,47

 $^{^{43}}$ ESTRADA, Sandra. Síntesis de nuevas 4-heteroarilpirazolo[1,5- α]-1,3,5-triazinas por reacción entre heteroaroiliminotiocarbonatos de O,S-dietilo y 5-amino-3-aril-1*H*-pirazoles. Trabajo de grado en Química, Universidad de Nariño, 2009.

⁴⁴ INSUASTY, Henry *et al.* Solvent-free microwave-assisted synthesis of novel 4-hetarylpyrazolo[1,5- α][1,3,5] triazines. *J Heterocyclic Chem.* 2012; **49**; 1339-1345.

⁴⁵ INSUASTY, Henry *et al.* Three practical approaches for the synthesis of 4,7-dihetarylpyrazolo[1,5- α]-1,3,5-triazinas. *Tetrahedron.* 2012; **68:** 9384-9390.

⁴⁶ INSUASTY, Henry *et al.* Regioselective synthesis of novel 4-aryl-2-ethylthio-7-methylpyrazolo[1,5- α]-1,3,5-triazinas. *Tetrahedron Lett.* 2006; **47**: 5441-5443.

⁴⁷ RESTREPO, Vanessa. Evaluación de la interacción entre los heteroilimidotiocarbonatos de O,S-dietilo y el 5amino-3-fenil-1H-1,2,4-triazol como método de obtención de nuevas triazolotriazinas. Trabajo de grado en Química, Universidad de Nariño, 2012.

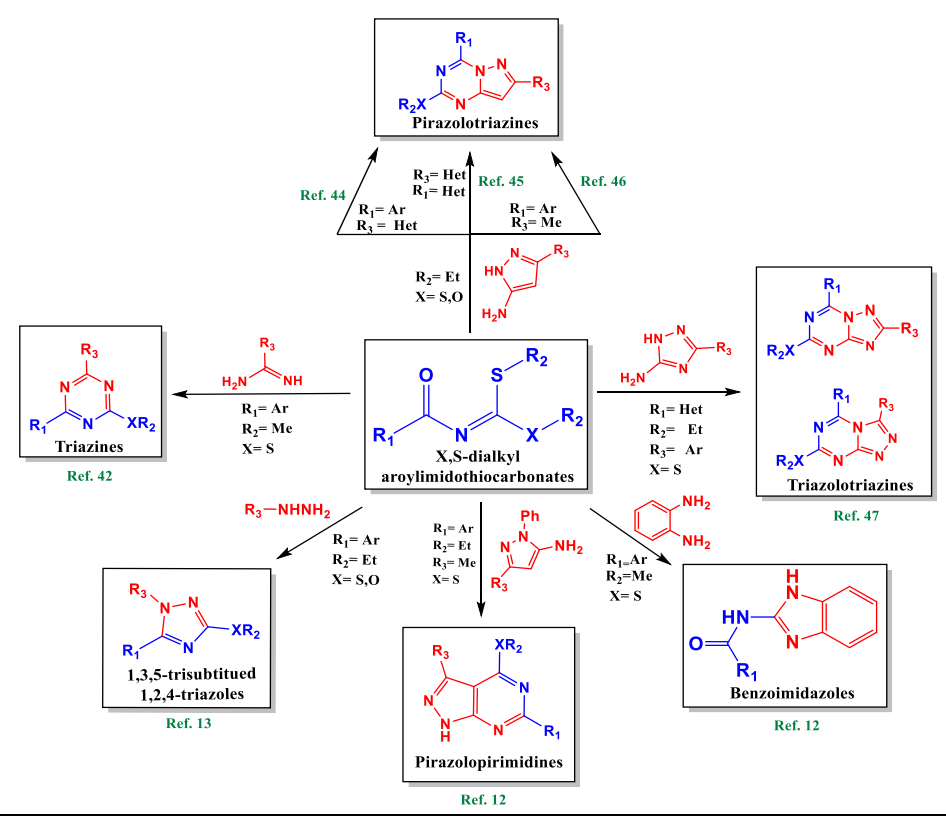
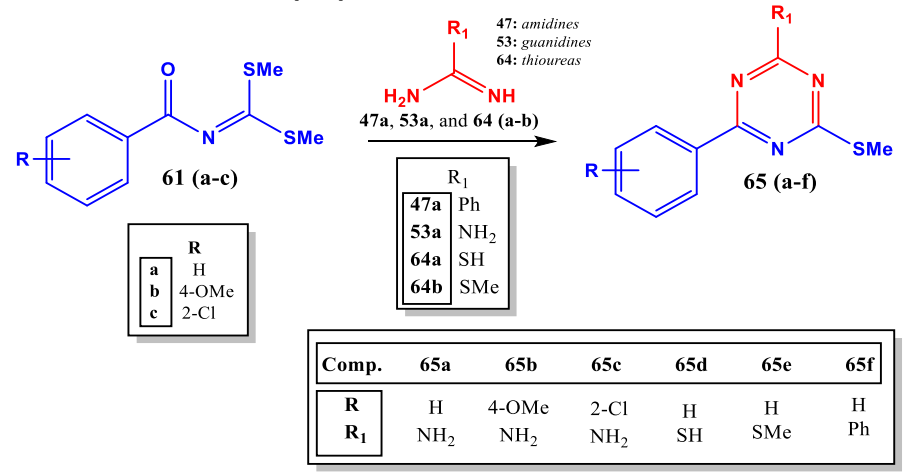


Figure 10. Synthetic routes for several heterocyclic compounds from \overline{X} ,S-dialkyl aroylimidothiocarbonates. Source: This investigation, using information from references 12, 13, 42, 44, 45, 46, and 47.

Scheme 9 shows that the *S*,*S*-dimethyl aroylimidodithiocarbonates **61 (a-c)** react with benzamidine **47a**, guanidine **53a**, and also with thioureas **64 (a-b)** to generate substituted 1,3,5-triazines **65 (a-f).**⁴²



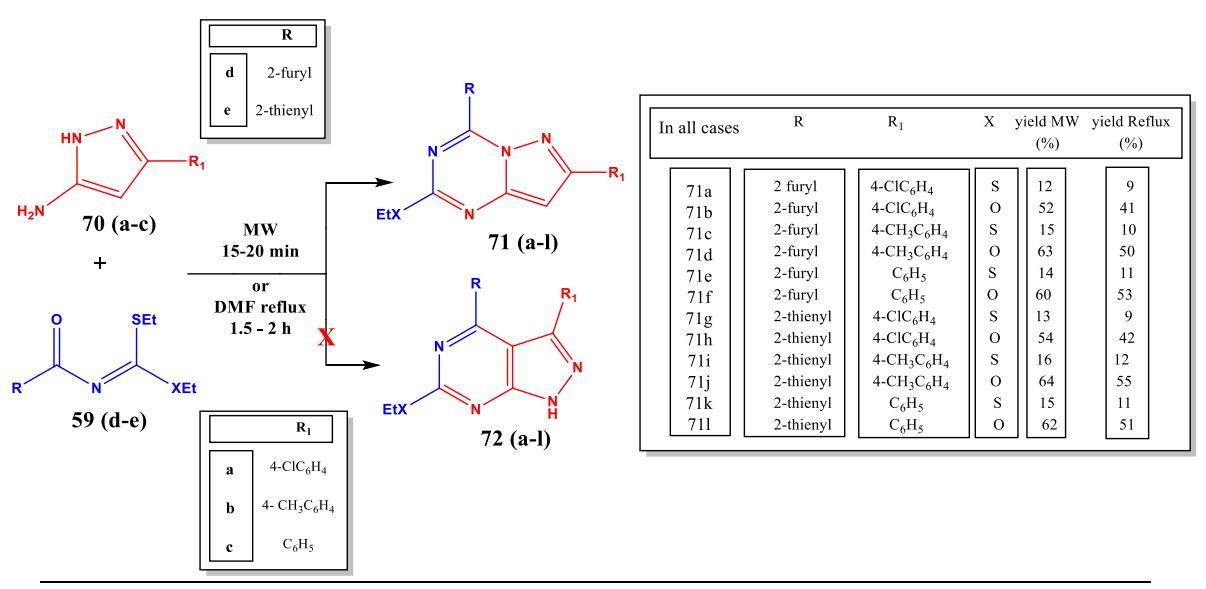
Scheme 9. Synthesis of 1,3,5-triazines using S,S-dimethyl aroylimidothiocarbonates as precursors. Adapted from reference 42.

The interactions of carbonates with similar structures but different nucleophiles have been evaluated as a synthetic route to obtain heterocyclic compounds by the GICH-UN. In particular, Restrepo⁴⁷ evaluated the interaction between O,S-diethyl heteroarylamidothiocarbonates **59** (d-e) and S,S-diethyl heteroaroyliminodithiocarbonates **63** (d-e) with 5-amino-3-phenyl-1*H*-1,2,4-triazole **66** as a method to obtain the triazolotriazines **67** (a-b), **68** (a-b), and **69** (a-b) (Scheme 10).

Scheme 10. Interaction between O,S-diethyl heteroaroylimidothiocarbonates and S,S-diethyl heteroaroylimidodithiocarbonates with 5-amino-3-phenyl-1*H*-1,2,4-triazole as a method for obtaining triazolotriazines. Adapted from reference 47.

Similary, Insuasty *et al*⁴⁴ reported the synthesis of a series of novel 4-heteroaryl substituted pyrazolo[1,5- α][1,3,5]triazines **71 (a-I)** under solvent-free conditions by microwave assisted reaction between O,S-diethyl heteroarylimidothiocarbonates **59 (d-e)** and 5-amino-3-aryl-1*H*-pyrazoles **70 (a-c)** (Scheme 11). Comparison of the reactions mediated by microwave irradiation and by conventional heating in solution of DMF indicated that both procedures afforded the same products, but the first technique required shorter reaction times and gave higher yields than the second one. This procedure led to the formation of mixtures of two new pyrazolotriazine derivatives in a 1:4 ratio depending on the leaving group ethanol or ethanethiol of the carbonate in the cyclization reaction, respectively. The spectroscopic analysis

indicated that the products were the 4-heteroaryl substituted pyrazolo[1,5- α][1,3,5]triazines **71** (a-I) and not the pyrazolo[3,4- α]pyrimidines **72** (a-I).



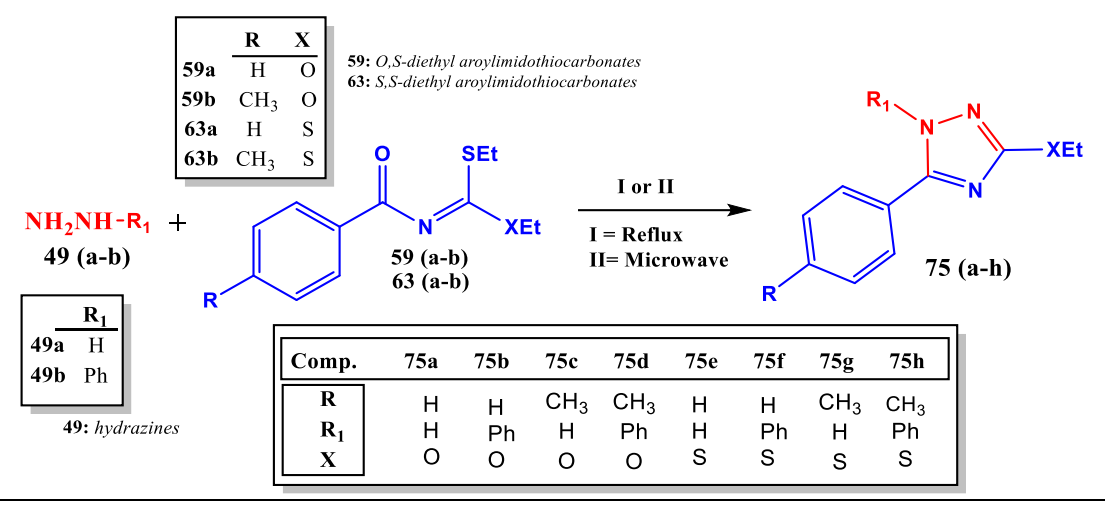
Scheme 11. Synthesis of 4-heteroaryl substituted pyrazolo[1,5- α][1,3,5]triazines. Adapted from reference 44.

3.3.3 1,2,4-triazole derivatives from X,S-diethyl aroylimidothiocarbonates

1,2,4-triazoles can also be obtained from carbonates by cyclization with hydrazines. This reaction exhibits high selectivity because of the two possible isomers shown in Scheme 12, only the 1,5-diphenyl-3-methylthio-1,2,4-triazole **73** is obtained, which indicates that the amino group of the phenylhydrazine **49b** reacts first with the iminoester [-N=C(SMe)₂] portion of the carbonate **61a** and not with the amidic carbonyl group.

Scheme 12. Synthesis of a 1,2,4-triazole starting from a S,S-dimethyl aroylimidodithiocarbonate and phenylhydrazine. Adapted from reference 13.

Hidalgo¹³ reported the synthesis of the 1,2,4-triazoles **75 (a-h)** by cyclization of the X,S-diethyl aroyliminothiocarbonates **59 (a-b)** and **63 (a-b)** with the hydrazines **49 (a-b)** using two methodologies: 1) reflux in ethanol and 2) microwave (Scheme 13). Similar results are obtained in both cases with reaction yields between 45 and 90%. The conditions with microwave methodology were standardized.



Scheme 13. Synthesis of 1,2,4-triazoles by cyclization of hydrazines with O,S-diethyl aroylimidothiocarbonates or S,S-diethyl aroylimidodithiocarbonates. Adapted from reference 13.

As the structure of 1,2,4-triazoles studied in this investigation includes or is similar to the general structure of compounds reported by Hidalgo **75 (a-h)** and due to the large number of derivatives evaluated in this work, a new nomenclature in the form **T-RR**₁-**XR**₂ was designed to specify them and to improve the understanding through the document. Figure 11 shows the generalities of the new nomenclature in detail.

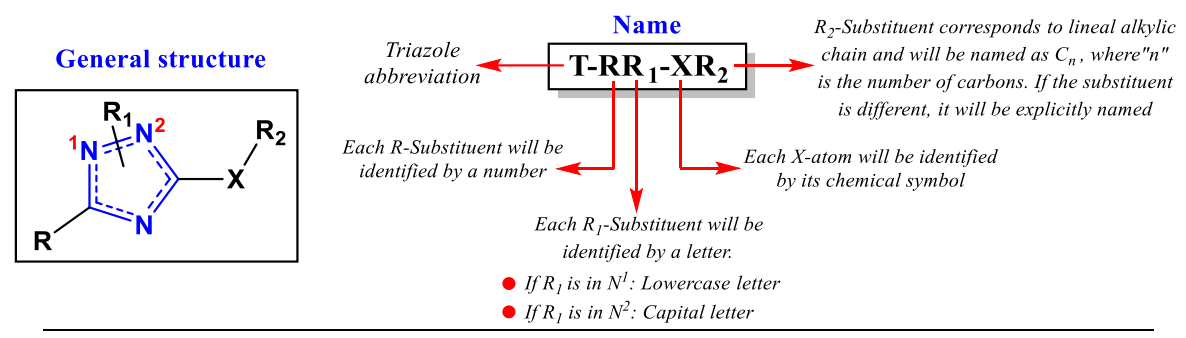


Figure 11. Nomenclature of the 1,3,5-substituted-1,2,4-triazoles used through the document. Source: this investigation.

In this way, it is possible to re-name the systems previously mentioned in this section. Table 1 shows the corresponding equivalences.

Table 1. Equivalent names of 1,3,5-substituted-1,2,4-triazoles using the new nomenclature designed. Source: this investigation.

| R | H ₃ C | | R ₁ | $ \begin{array}{c cccc} & & & & \\ & & & \\ \hline & & & \\ & & & \\ \hline & & & \\ & & & & \\ \hline & & & \\ \hline & & & & \\$ | X | X = 0 $X = S$ | R ₂ | $C_1 = H_3C - \frac{1}{5}$ $C_2 = H_3CH_2C - \frac{1}{5}$ |
|-----------------|------------------|----------------------|----------------|--|---|----------------------|----------------|---|
| Assigned number | | New nomenclature | | Assigned number | | New nomenclature | | |
| 73 | | T-1b-SC₁ | | 75d | | T-2b-OC ₂ | | |
| 74 | | T-1B-SC₁ | | 75e | | T-1a-SC₂ | | |
| 75a | | T-1a-OC ₂ | | 75f | | T-1b-SC ₂ | | |
| 75b | | T-1b-OC ₂ | | 75g | | T-2a-SC₂ | | |
| 75c | | T-2a-OC ₂ | | 75h | | T-2b-SC ₂ | | |

3.4 Quantitative structure-activity relationships

The prediction of the antifungal activity of the 1,2,4-triazoles synthetized in this investigation was made through mathematical models based on quantitative structure-activity relationships (QSAR). For this reason, in this section the main characteristics about QSAR, the importance and the applications of this methodology in pharmacology, and some QSAR studies of the antifungal activity of triazoles will be described.

3.4.1 General characteristics of QSAR methods

QSAR is a technique based on the general principle of medicinal chemistry which affirms that the biological activity of a compound is related to its molecular structure or properties, so, molecules with similar structure or similar properties might have similar biological activities. The information about the molecular structure is quantitatively encoded on molecular descriptors, which mathematically represent some intrinsic molecular properties and can be obtained from experiments or theoretical calculations. However, the set of descriptors is not unique and therefore, a large set should be determined. The final purpose is to obtain a QSAR model that provides a mathematical relationship between descriptors and the biological activity of known compounds that can be used to predict the activity of other compounds.⁴⁸ The general procedure when doing QSAR studies relies on three major steps:

⁴⁸ MYINT, Kyaw; XIE, Xiang. Recent Advances in Fragment-Based QSAR and Multi-Dimensional QSAR Methods. *Int J Mol Sci.* 2010; **11**(10): 3846-3866.

First step: Generation of molecular descriptors. The structure of the molecules cannot be directly used for creating structure-activity models, for this reason, it is necessary to extract the information with the help of computational tools. Various rationally designed molecular descriptors quantify different chemical properties in terms of physicochemical, quantum-chemical, geometrical, and topological features¹⁴. Usually, it is necessary a previous geometry optimization of the molecule with the purpose to obtain a stable structure at the minimum of the potential energy surface. The QSAR techniques can be classified by the type of descriptors used, so, in the 2D-QSAR the descriptors share a common property of being independent from the 3D orientation of the compound while 3D-QSAR use 3D grid of points around the molecule and each point having properties associated with it, such as electron density or electrostatic potential⁴⁹.

Second step: selection of relevant descriptors. Even though many descriptors can be calculated with computational tools, only some of them are able to describe the biological activity. Therefore, the selection of appropriate descriptors should consider, for example, the principle of independence among descriptors and that their number cannot be larger than the number of molecules. In general, the methods to select the descriptors can be grouped as 'filtering methods', in which descriptors are excluded prior to the building of the models based in the inter-descriptor correlation, and 'wrapper methods', which operate in conjunction with a mapping algorithm and the choice of best subset of descriptors is guided by the error of the mapping algorithm such as the validation or regression parameter.^{14,50}

Thirst step: mapping and building the mathematical models. Once the relevant molecular descriptors are calculated and selected, the activity can now be written as a function of the descriptors¹⁴. This process involves two sub-stages; the mathematical adjustment of function through regression parameters and the validation of models that determine their predictive character.^{50,51}

Figure 12 summarizes the general process to develop QSAR models.

⁴⁹ YOUNG, David. Computational Drug Design. Jhon Wiley & Sons; 2009.

⁵⁰ PUZYN, Tomasz; LESZCZYNSKI, Jerzy; CRONIN, Mark. Recent Advances in QSAR Studies: Methods and Applications. Vol. 8. Springer; 2010.

⁵¹ VEERASAMY, Ravichandran *et al.* Validation of QSAR Models - Strategies and Importance. *Int J Drug Discov.* 2011; **2**(3): 511-519.

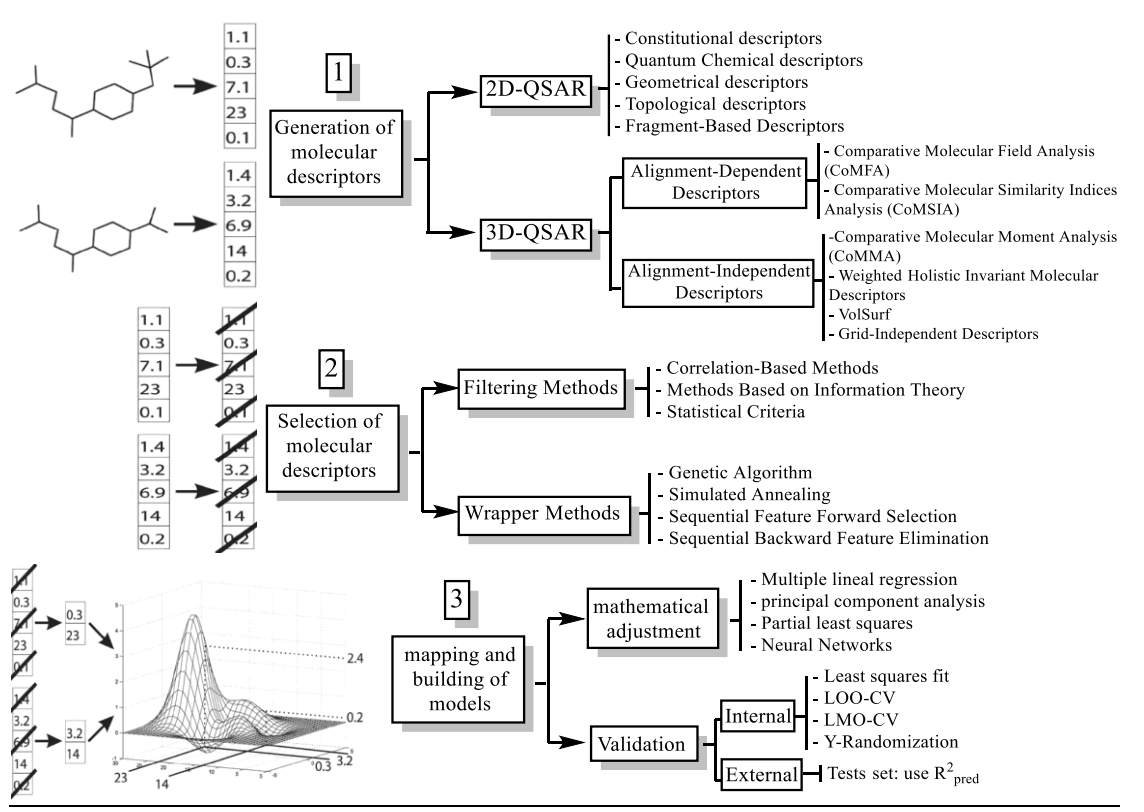


Figure 12. General process to develop QSAR models. Source: This investigation, using information from references 14 and 51.

3.4.2 Application and importance of QSAR

QSAR methods are not only used to rationalize the activity of a compound in terms of its molecular properties, on the contrary, the principal objective of QSAR is to generate models with predictive character,⁵⁰ for this, these techniques have been useful as a complementary methodology to the high throughput screening and combinatorial chemistry in drug discovery.¹⁴ In this way, the virtual filtering and screening allows to reduce the number of compounds tested experimentally by theoretically predicting their biological activity, which, among others, helps to reduce the cost and the time of drug development.⁵⁰

3.4.3 QSAR studies of the antifungal activity of 1,2,4-triazole derivatives

Many investigations have been carried out to find predictive models about different biological activities of triazole derivatives;^{52,53,54} however, only a couple related with the antifungal activity will be mentioned because of the goals of this work. Wei *et al*⁵⁵ carried out the synthesis and QSAR study of novel 1,2,4-triazole compounds containing the thioamide group **76**, for which a correlation between fungicidal activities and the energy difference between the frontier molecular orbitals HOMO and LUMO and the molecular volume was found (Figure 13A). On other hand, Nowaczyk and Modzelewska published a QSAR study⁵⁶ of the activity against yeast and filamentous fungi of triazolic fungicide agents containing a quinazolinone ring **77**; a correlation between both antifungal activities and physicochemical parameters such as the logarithm of the *n*-octanol/water partition coefficient, the polarizability, and the molar refractivity was established using multiple linear regression (Figure 13B).

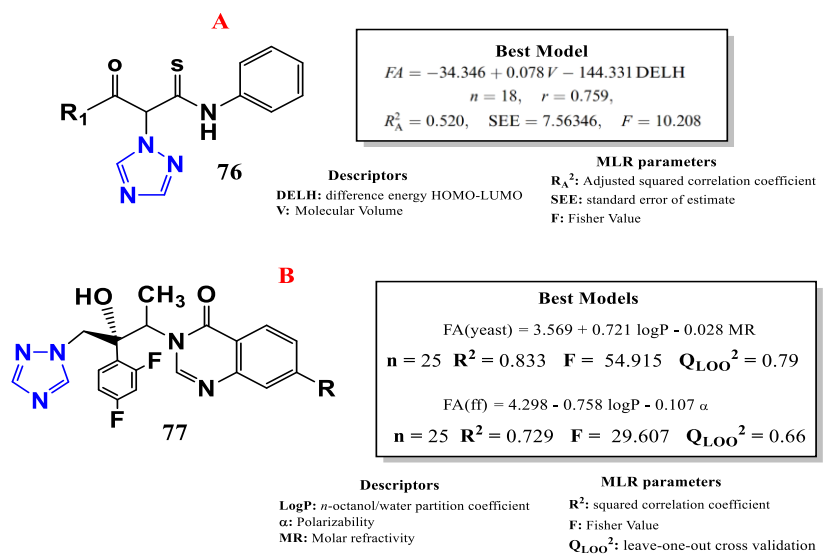


Figure 13. QSAR studies of antifungal activity of 1,2,4-triazole derivatives. Adapted from references 55 and 56.

⁵² DIMOVA, Vesna; PERIŠIĆ-JANJIĆ, Nada. QSAR study by 1,2,4-triazoles using several physicochemical descriptors. *Maced J Chem Chem Eng.* 2009; **28**(1): 79-89.

⁵³ POKURI, Sateesh *et al.* Insights on the Antioxidant Potential of 1, 2, 4-Triazoles: Synthesis, Screening & QSAR Studies. *Current Drug Metabolism.* 2014; **15**(4): 389-397.

⁵⁴ GRAMATICA, Paola *et al.* QSAR Modeling is not "Push a Button and Find a Correlation": A Case Study of Toxicity of (Benzo-)triazoles on Algae. *Mol. Inf.* 2012; **31**: 817-835.

⁵⁵ WEI, Quing-Li *at al.* Synthesis and QSAR studies of novel triazole compounds containing thioamide as potential antifungal agents. *Bio Med Chem.* 2006; **14**(21): 7146-7153.

⁵⁶ NOWACZYK, Alicja; MODZELEWSKA-BANACHIEWICZ, Bożena. QSAR studies of a number of triazoles antifungal alcohols. *Cent Eur J Chem.* 2010; 8(2): 440-447.

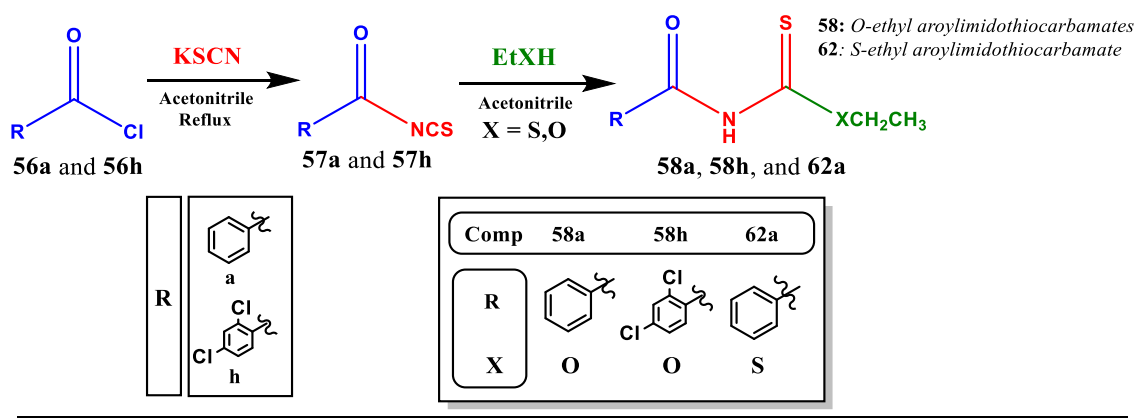
4 RESULTS AND DISCUSSION

4.1 Synthesis and characterization of target products

In this section, the description of the synthetic procedure will be carried out. Also, the spectroscopic and spectrometric characterization of intermediates and products will be described.

4.1.1 Synthesis and characterization of X-ethyl aroylimidothiocarbamates

The synthesis of the aroylimidothiocarbamate intermediates was carried out following the synthetic methodology standardized by the GICH-UN (Scheme 14). The benzoyl chlorides **56a** and **56h** react with the potassium thiocyanate through nucleophilic substitution of the halogen on the acyl group to generate the isothiocinate intermediate **57a** and **57h** on reflux conditions. Then, ethanol or ethanethiol is added to produce the O-ethyl aroylimidotiocarbamates **58a** and **58h** and the S-ethyl aroylimidotiocarbamate **62a** by nucleophilic attack of the alcohol to the carbon of the NCS group.



Scheme 14. Step 1: Synthesis of the X-ethyl aroylimidothiocarbamates of this work. Source: This investigation.

The carbamates **58a** and **62a** have been reported previously by the GICH-UN. 12,42 The physical characteristics and chromatography (TLC) of the synthesized compounds are compared with the reported standards in Table 2, as well as reaction

times and yields. On other hand, the O-Ethyl(2,4-dichlorobenzoyl)imidotiocarbamate **58h** is a new compound that is synthetized in this investigation for the first time.

The parameters observed in Table 2 indicate that the intermediate carbamates have similar melting points and retardation factors in comparison with those reported in the literature. Likewise, were obtained with high yield and high purity as can be seen in the chromatographic plates. The products can be purified by recrystallization from hexane but generally these are recovered without impurities after crystallization in ice.

Table 2. Physicochemical parameters of the synthesized X-ethyl aroylimidothiocarbamates and comparison with the reported compounds by the GICH-UN.^{12,42} Source: This investigation.

| Compound | 58a | 62a | 58h |
|--|----------------------|--------------|----------------|
| TLC plates 1. Product obtained in this investigation 2. Reported standard by the GICH-UN Mobile phase Hexane:ethyl acetate (6:4) | 1 2 | 1 2 | 1 |
| Obtained melting point (°C) | 70 – 72 | 78 – 80 | 88 – 90 |
| Reported melting point (°C) | 70 – 72 | 81 – 83 | |
| Physical appearance | light green solid | yellow solid | white solid |
| Yield (%) | 96 | 95 | 96 |
| Reaction time (h) | 20 | 24 | 24 |

The compound **58h** was synthetized using the same conditions as other carbamates reported by the GICH-UN.¹² However, the synthetic methodology to obtain the carbamates requires reaction times within the range of 20 to 26 hours, for this reason, different assays were carried out at different reaction times: 20, 22, 24, and 26 h in order to obtain the highest yield. As Table 3 shows, for compound **58h**, the optimal reaction time was 24 hours (yield: 96%), longer times are not relevant in the yield. The purification of the compound was carried out by recrystallization of hexane which is the same solvent used for the purification of other carbamates.

Table 3. Determination of the optimal reaction time for the synthesis of compound **58h** using the GICH-UN methodology.¹² Source: This investigation.

| CI O S OCH ₂ CH ₃ | Reaction time | | | | | |
|---|---------------|------|------|------|--|--|
| Compound 58h | 20 h | 22 h | 24 h | 26 h | | |
| Yield (%) | 86% | 92% | 96% | 95% | | |

The characterization of the carbamate **58h** is described below.

Mass spectrometric analysis of compound **58h** was performed using high resolution DART+ mass spectrometry (Figure 14) showing the peak of the molecular ion M+1 at a m/z ratio of 277.98014 corresponding to the formula $C_{10}H_{10}Cl_2NO_2S$, which agrees with the molecular formula of the protonated compound. The peaks at m/z 280 and 282 correspond to the [MH+2]+ and [MH+4]+ ions that are explained by the presence of two chlorine atoms. Chlorine has the ^{35}Cl and ^{37}Cl isotopes in approximate 1:3 ratios. 57

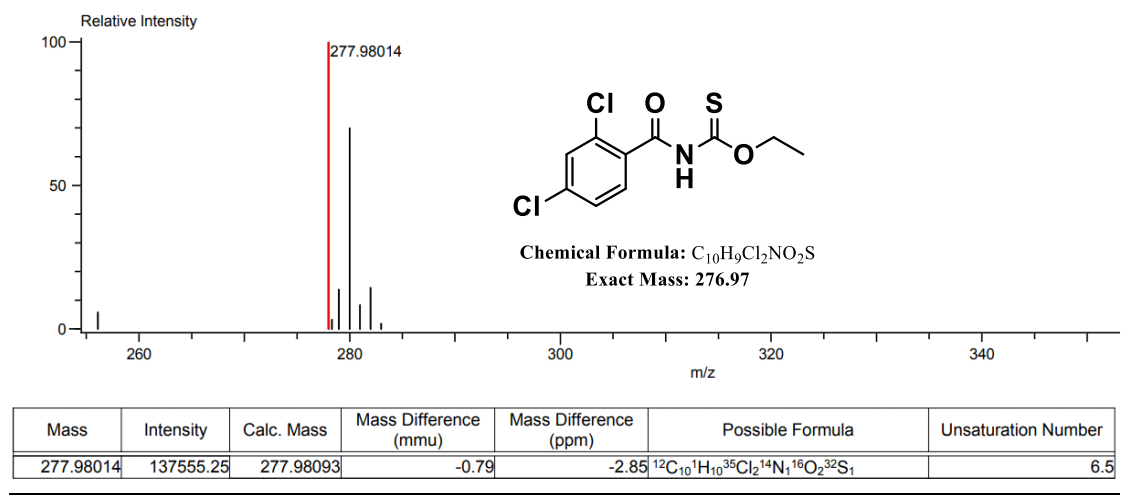


Figure 14. High-resolution DART+ mass spectrum of compound **58h**. Source: This investigation.

The infrared spectrum of compound **58h** (Figure 15) shows the characteristic bands of the carbamate.⁵⁸ The N-H stretching of the amide group is observed at 3244 cm⁻¹; the stretching of the different C-H groups (aromatic, methyl, and methylene) appears as a low intensity bands around 3050 cm⁻¹ and the aromatic C-H out of

⁵⁷ NIWA, Toshimitsu. Basic theory of mass spectrometry. *Clin Chim Acta*. 1995; **241-242**: 15-71.

⁵⁸ SILVERSTEIN, Robert M., et al. Spectrometric Identification of Organic Compounds. 8th ed. Wiley; 2014.

plane bending as a doublet at 823 and 834 cm⁻¹. The carbonyl amidic group (C=O) stretching is found within the range reported for aromatic amides, so, a high intensity band at 1668 cm⁻¹ is assigned to this vibration^{58,59}, also, de C=C aromatic bond stretching is observed at 1590.48 cm⁻¹. The <u>C=S</u> stretch is assigned to the band at 1277.50 cm⁻¹, while, the H-N-C=S stretching at 1484 cm⁻¹ and the <u>H-N</u>-C=S bending at 1397.76 cm⁻¹. These are found within the characteristic range associated with said specific bonds in other carbamates recently reported⁶⁰. The C-CI stretching is assigned¹² to the low intensity band at 742 cm⁻¹ and, finally, the C-O-C bond asymmetric stretching is assigned to the band at 1205 cm⁻¹ and symmetric stretching at 1036.98 cm⁻¹.

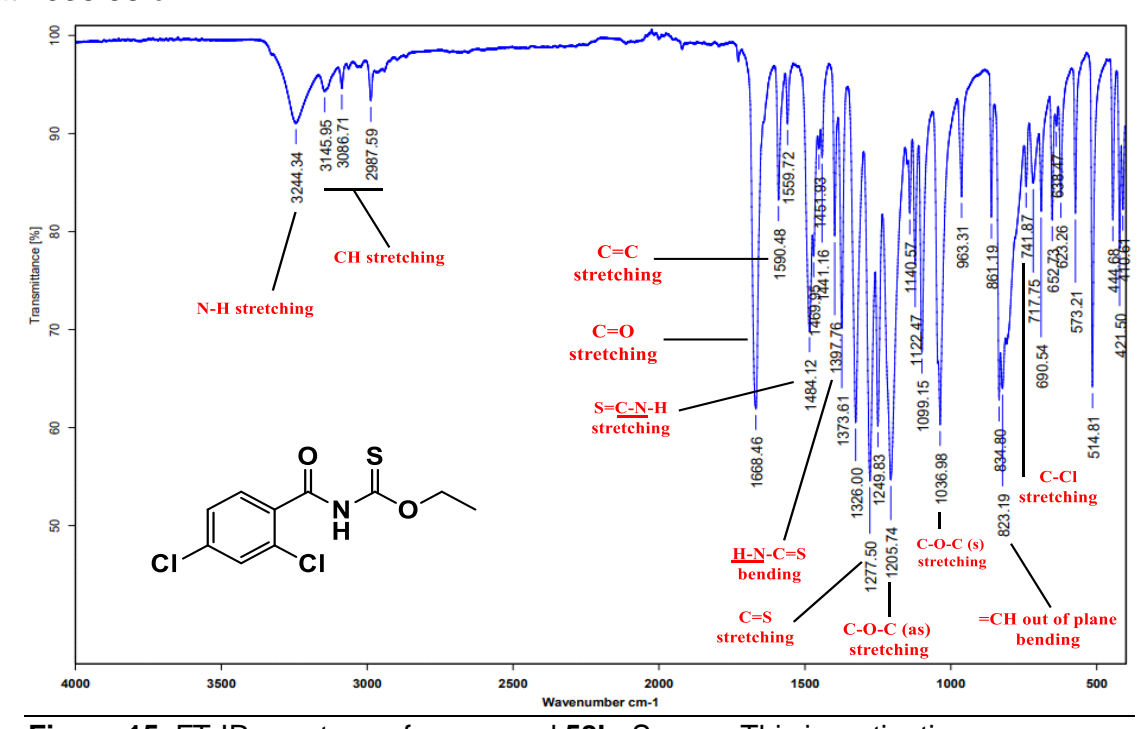


Figure 15. FT-IR spectrum of compound 58h. Source: This investigation.

The 300 MHz ¹H NMR spectrum (Figure 16) of compound **58h** shows a triplet at 1.26 ppm integrating for three protons that is assigned to the hydrogen atoms of the methyl group (**CH**₃), and at 4.51 ppm a quartet that integrates for two protons is assigned to the methylene group (**CH**₂), both are part of the ethyl group. The protons of the aromatic ring are found between 7.31 and 7.54 ppm, these were assigned in relation to the multiplicity of the signals and the coupling constants⁵⁸: hydrogen **5** shows a doublet of doublets around 7.34 ppm with coupling constants J = 1.8 Hz and J = 8.1 Hz indicating a coupling with proton **6** in the *ortho*-position and proton **3**

⁵⁹ MORRISON, Robert; BOYD, Robert. *Organic Chemistry*. 6th ed. Pearson Education; 1992.

⁶⁰ TORRES, Viviana. Síntesis de un nuevo 1,4-bis(3-etoxi-1,2,4-triazolil)benceno por reacción del tereftaloiltiocarbamato de O-etilo o del tereftaloiltimidotiocarbonato de O,S-dietilo con hidrazina. Trabajo de grado en Química, Universidad de Nariño, 2018.

in the *meta*-position; the doublet around 7.45 ppm with J = 1.8 Hz can be assigned to proton 3 due to its *meta*-coupling with proton 5; and proton 6 is observed around 7.51 ppm as a doublet with J = 8.4 Hz due to its coupling with proton 5 in the *ortho*-position. Between protons 6 and 5 and protons 3 and 5 the roof effect can be observed. Finally, the singlet at 9.05 ppm which integrates for one proton can be assigned to the hydrogen N-H of the amidic group.

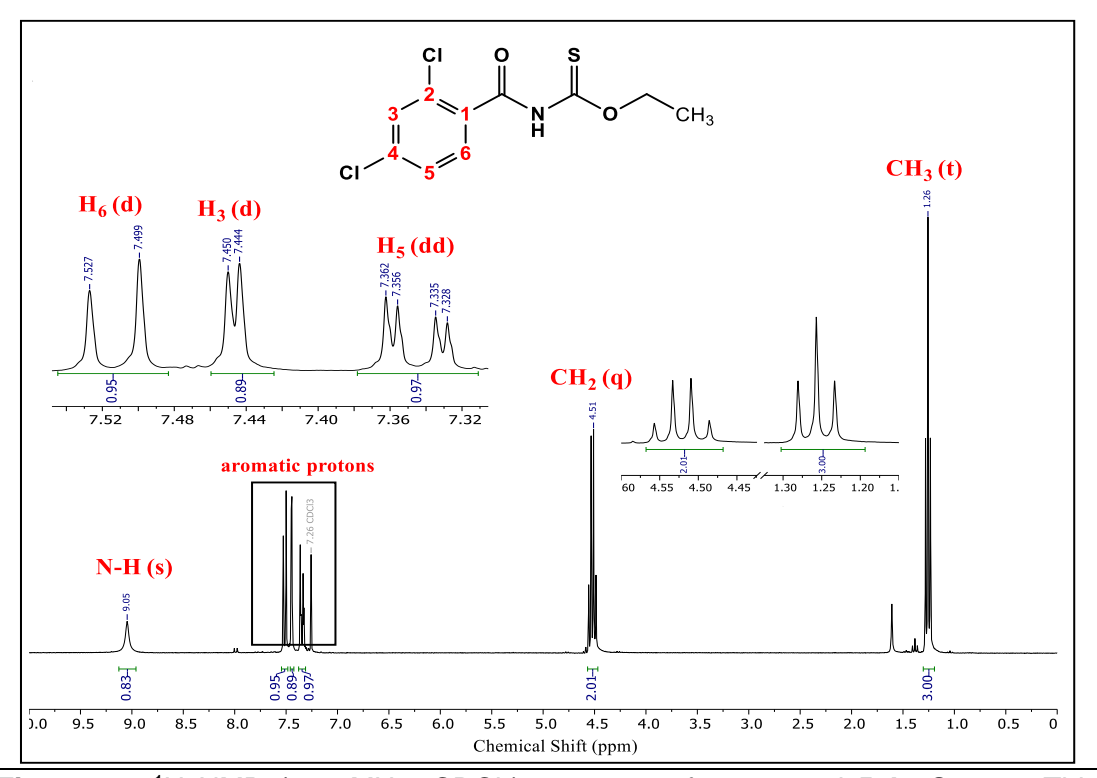


Figure 16. ¹H NMR (300 MHz, CDCl₃) spectrum of compound **58h**. Source: This investigation.

The 75 MHz ¹³C NMR spectrum (Figure 17) shows ten signals which correspond to the ten carbon atoms present in molecule **58h**, as there is not plane of symmetry, each signal corresponds to 1 carbon. The peak at 13.5 ppm corresponds to the carbon of the methyl group (CH₃) and the one at 69.6 ppm to the methylene group (CH₂), in both cases the chemical shifts are within the expected range⁵⁸. The carbon of the thioester group (C=S) is observed at 187.9 ppm and the carbon of amide group (C=O) at 162.4 ppm. These two carbon atoms were differentiated by comparison with the literature of the GICH-UN^{12,42}: the downfield field signal is assigned to the carbon of the thioester group because it is deshielded and, therefore, should appear at lower fields. The aromatic carbons are observed between 127 and 138 ppm. Because there are not 2D NMR experiments for this compound, the signals were assigned based on other similar compounds which have been reported in the literature such as pyrazolotriazines with the 2,4-dichlorobenzoyl substituent,⁶¹

likewise, it was verified with the theoretically predicted spectrum using the software *MestreNova*. The C-H carbons of the benzene ring observed at 127.7, 130.1, and 130.81 ppm correspond to carbons **5**, **3**, and **6**, respectively. This based on the literature⁶¹ as these follow the same order of chemical shift as their corresponding protons. The three quaternary carbons are observed as low intensity signals and shifted downfield at 131.8, 132.9, and 137.9 ppm, which are assigned, respectively, to carbons: **1**, **2**, and **4** by comparison with the analogous compound mentioned. Carbon atoms **2** and **4** should be found downfield due to the deshielding effect of their halogenated substituents; however, the carbon atom in the *para*-position has shown a larger chemical shift in the aforementioned studies and therefore, carbon **4** is assigned to signal shifted to the lowest field.

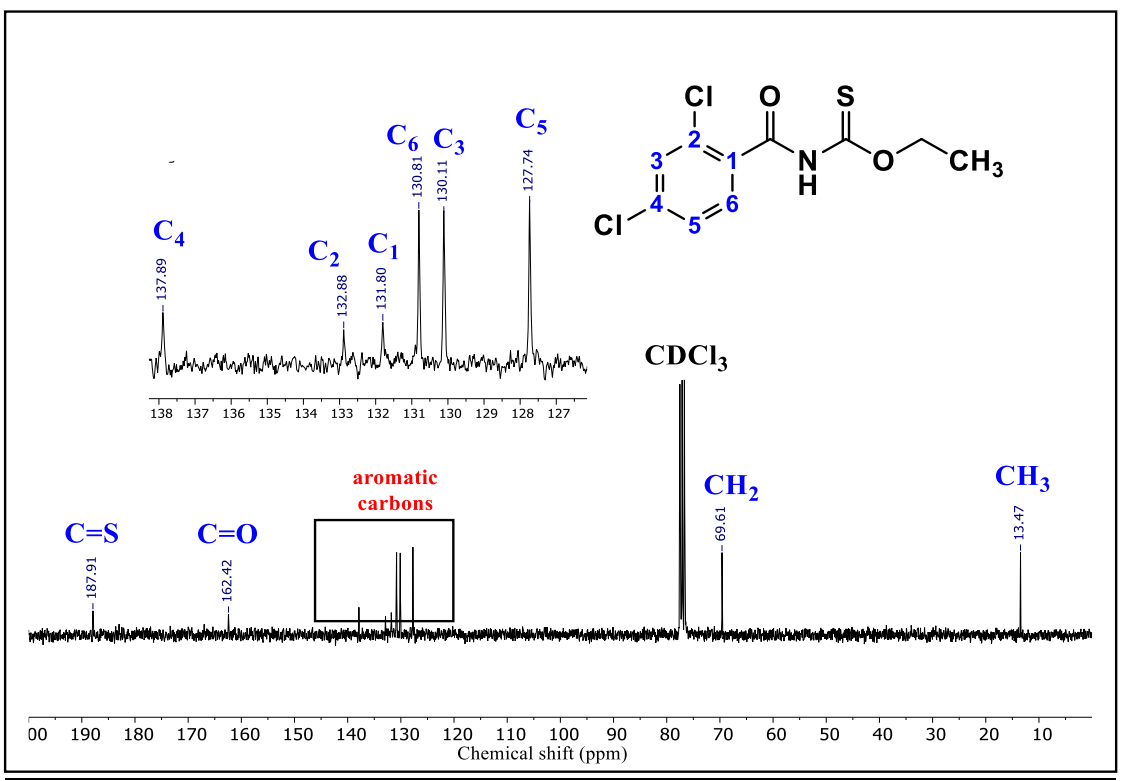
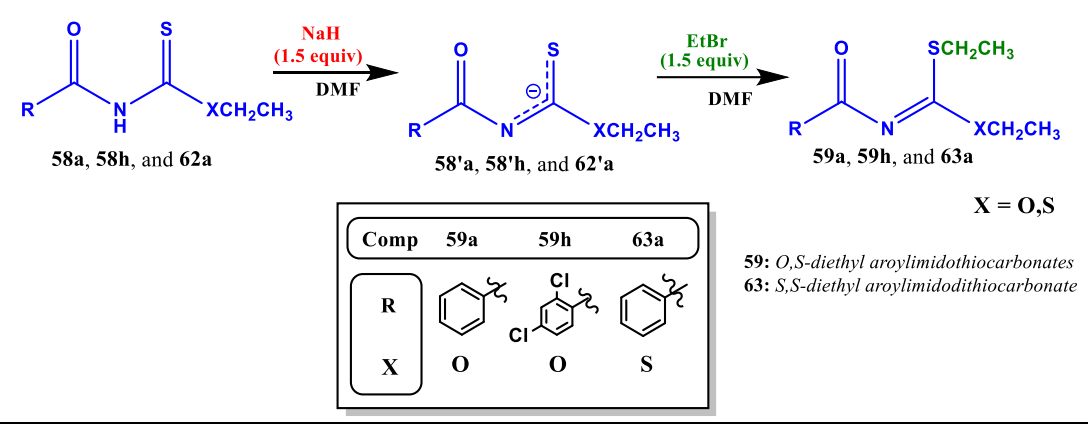


Figure 17. ¹³C NMR (75 MHz, CDCl₃) spectrum of compound **58h**. Source: This investigation.

⁶¹ MIER, Paola; SUAREZ, Gina. Sintesis de nuevas pirazolo[1,5-α]-1,3,5-triazinas por reacción de aroiliminoditiocarbonatos de S,S-dietilo con 5-amino-3-arilpirazoles usando irradiación con microondas. Trabajo de grado en Química, Universidad de Nariño, 2007.

4.1.2 Synthesis and characterization of X,S-diethyl aroylimidothiocarbonates

The second step of the synthetic procedure is the ethylation of the aroylimidotiocarbamates **58a**, **58h**, and **62a** (Scheme 15). For this, sodium hydride is added to dissolution of carbamate in DMF, which acts as a strong base (a typical use of this reactive)⁶² to eliminate the N-H proton and generate the respective sodium salt (**58'a**, **58'h**, and **62'a**) and then, ethyl bromide is added⁶³ to produce the *O*,*S*-diethyl aroylimidothiocarbonates **59a** and **59h** and the *S*,*S*-diethyl aroylimidodithiocarbonate **63a** by nucleophilic substitution.



Scheme 15. Step 2: Synthesis of the X,S-diethyl aroylimidothiocarbonates of this work. Source: This investigation.

Carbonates **59a** and **63a**, which are liquids at room temperature, have been previously synthetized by the GICH-UN. ^{12,42} The physicochemical properties of the obtained products are compared with the reported standards in Table 4. The compound **59h**, which is the reaction product of the carbamate **58h**, is a new O,S-diethyl aroylimidothiocarbonate, for this reason, it is important to report its physical properties and the conditions for its synthesis.

⁶² FONES, William. The use of sodium hydride in the alkylation of *N*-substituted amides. *J Org Chem.* 1949; **14**(6): 1099-1102.

⁶³ HESEK, Dusan *et al.* Complications from Dual Roles of Sodium Hydride as a Base and as a Reducing Agent. *J Org Chem.* 2009; **74**(6): 2567-2570

Table 4. Physicochemical parameters of the synthesized X,S-diethyl aroylimidothiocarbonates and comparison with the reported compounds by the GICH-UN.^{12,42} Source: This investigation.

| Compound | 59a | 63a | 59h | |
|--|-----------------------|---------------|------------|--|
| TLC plates 1. Product obtained in this investigation 2. Reported standard by the GICH-UN Mobile phase Hexane:ethyl acetate (6:4) | 1 2 | 1 2 | 1 | |
| Obtained melting point (°C) | | | | |
| Reported melting point (°C) | | | | |
| Physical appearance | transparent liquid | yellow liquid | yellow oil | |
| Yield (%) | 82 | 95 | 84 | |
| Reaction time (h) | 1.0 | 2.5 | 1.5 | |

The conditions used to synthesize compound **59h** were similar to those stablished by the GICH-UN¹² for the synthesis of analogous carbonates **59a** and **63a**. However, the reaction time was evaluated within the time range recommended by the methodology. In this way, four different assays were performed using reaction times of 1.0, 1.5, 2.0, and 2.5 h (Table 5). It was observed that after 1.5 h the reaction yield does not change appreciably and, therefore, this is considered as the minimal and optimal reaction time for obtaining the carbonate **59h**.

Table 5. Determination of the optimal reaction time for the synthesis of compound **59h** using the GICH-UN methodology.¹² Source: This investigation.

| CI O SCH ₂ CH ₃ | Reaction time | | | | | |
|---------------------------------------|---------------|-------|-------|-------|--|--|
| Compound 59h | 1.0 h | 1.5 h | 2.0 h | 2.5 h | | |
| Yield (%) | 76% | 84% | 85% | 85% | | |

The spectroscopic and spectrometric characterization of the new compound **59h** is described in this investigation.

The high-resolution DART+ mass spectrum in Figure 18 shows a peak of the molecular ion M+H at 306.01290 m/z which correspond to the molecular formula $C_{12}H_{14}Cl_2NO_2S$. As in the carbamate **58h** (Figure 14), the peaks at M-H+2 and M-H+4 m/z are observed too, indicating the presence of two chlorine atoms.

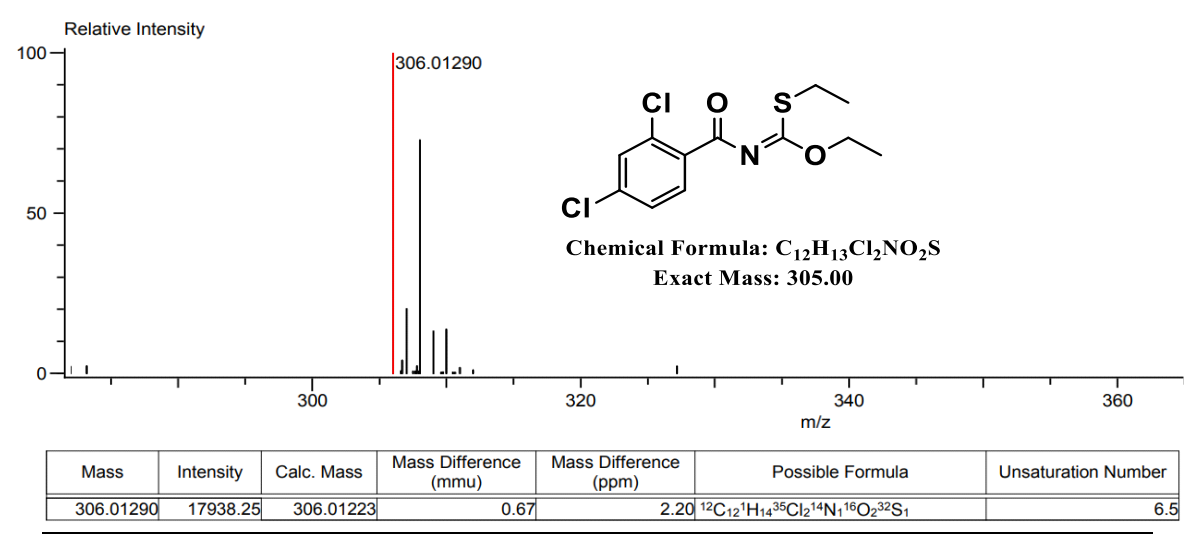


Figure 18. High-resolution DART+ mass spectrum of compound **59h**. Source: This investigation.

The IR spectrum of compound **59h** in Figure 19 also shows the characteristic bands of a carbonate. In comparison with the carbamate precursor **58h** (Figure 15), the high-energy band for the N-H stretching disappeared in the carbonate which serves as evidence of a successful reaction, which is also supported by the occurrence of a strong band at 1636.32 cm⁻¹ that is assigned to the S-<u>C=N</u> bond stretching and a weak band around of 1700 cm⁻¹ for the O-<u>C=N</u> stretch⁶⁰, which, in turn, possibly influences the C=O stretching,⁵⁹ now observed at lower wavenumber (overlapped with S-<u>C=N</u> band at 1636 cm⁻¹). Other characteristic bands are also observed in the same region of the carbamate **58h**, as the C=C stretching at 1503.69 cm⁻¹, C-O-C asymmetric and symmetric stretching⁶⁰ at 1206 and 1012.67 cm⁻¹, respectively. C-Cl stretching at 763 cm⁻¹, and C-H stretching (aromatic, methyl, and methylene) as low-intensity bands between 2800 and 3100 cm⁻¹. The band at 1311 cm⁻¹ is assigned to the C-S stretching.¹²

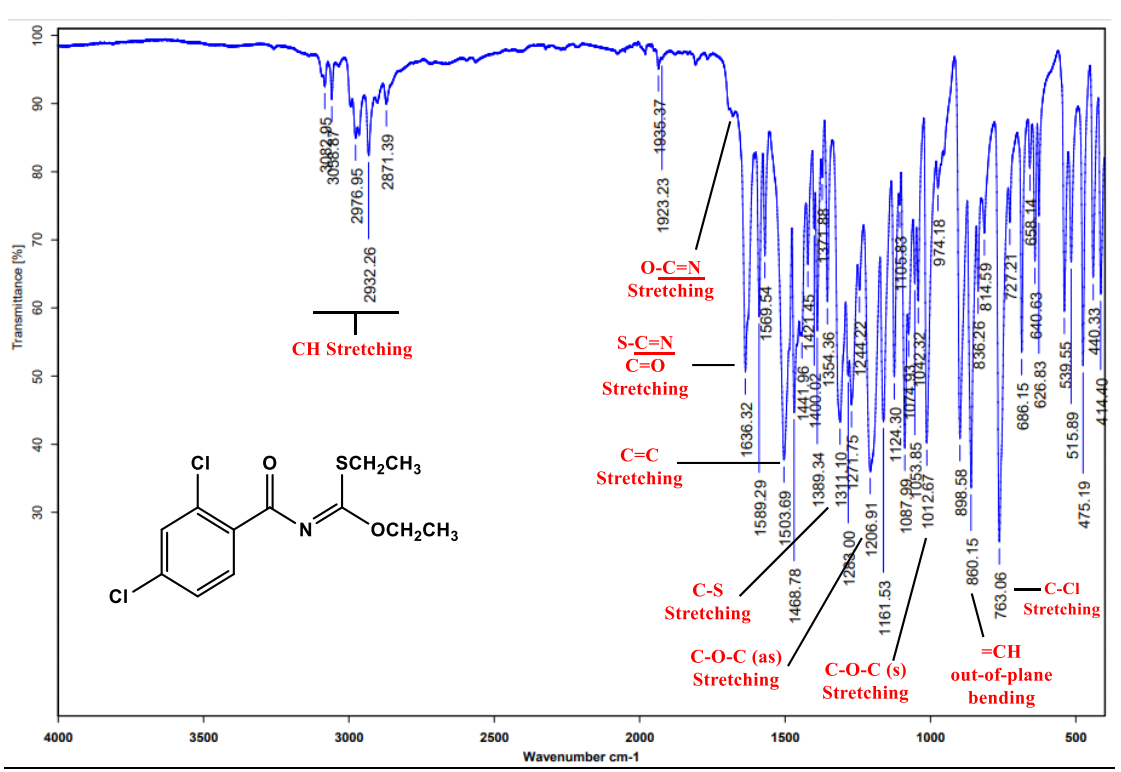


Figure 19. FT-IR spectrum of compound 59h. Source: This investigation.

The ¹H NMR spectrum of compound **59h** in Figure 20 shows seven different signals which correspond to the seven groups of protons in the molecule. The triplet centered at 1.33 ppm that integrates for three hydrogens is assigned to the methyl hydrogens of the group thioethyl (CH₃ for S-ethyl), while the triplet centered at 1.40 ppm integrating for three protons is assigned to the methyl of the ethoxy group (CH₃ for O-ethyl). Also, two quartets are observed integrating for two protons each centered at 2.96 ppm and 4.50 ppm which are assigned to methylene protons of the S-ethyl (CH₂ for S-ethyl) and the O-ethyl (CH₂ for O-ethyl) groups, respectively. It is observed that, in both cases, the protons of the ethoxy group are displaced to lower field than thioethyl protons due to the larger deshielding effect of oxygen compared to sulfur, which is also supported by literature on other carbonates⁴². In the aromatic region, the chemical shift trend is like its respective carbamate 58h: proton 5 appears between 7.24 and 7.29 ppm as a doublet of doublets with coupling constants J = 1.8 Hz and J = 8.1 Hz, hydrogen 3 as a doublet with J = 1.8 Hz at 7.43 ppm, and finally, hydrogen 6 as a doublet at 7.89 ppm with coupling constant J = 8.4Hz.

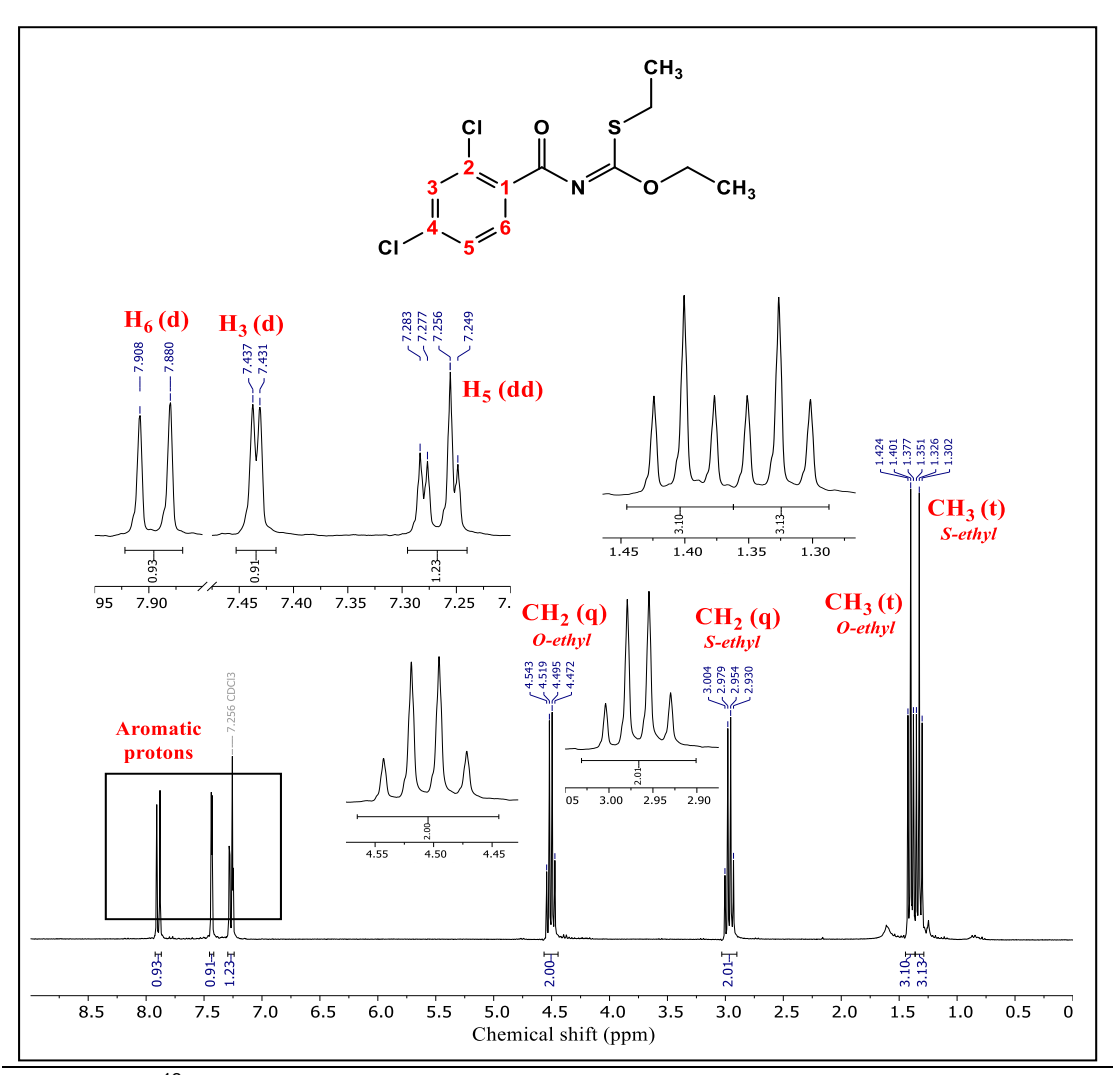


Figure 20. ¹³H NMR (300 MHz, CDCl₃) spectrum of compound **59h**. Source: This investigation.

The 75 MHz ¹³C NMR spectrum of compound **59h** in Figure 21 shows twelve signals corresponding to the twelve carbons present in the molecule. Two signals at 14.2 and 14.5 ppm are assigned to the methyl belonging to the S-ethyl group (CH₃ for S-ethyl) and the O-ethyl (CH₃ for O-ethyl), respectively. The methylene carbons are observed at 25.4 ppm for the thioethyl group (CH₂ for S-ethyl) and at 67.0 ppm for the ethoxy group (CH₂ for O-ethyl). The DEPT-135 experiment (Figure 21, bottom) corroborates the methylene character of the carbons because these signals are inverted. It is observed that the carbon atoms of methyl and methylene in the ethoxy group are observed at lower fields, as it is reported in similar compounds⁴² and as it is observed in the ¹H NMR spectrum; this is due to the larger deshielding effect of the oxygen with respect to the sulfur atom. The quaternary carbons of the iminoester (C=N) and the amide group (C=O) are observed as low intensity signals shifted downfield at exactly 172.4 and 174.3 ppm, respectively; the higher chemical shift of

the amide group might be due to the stronger deshielding effect in the C=O as compared to the C=N⁴². The aromatic carbons follow the same chemical shift trend observed in the carbamate based on the literature^{12,61} and corroborated with the theoretical spectrum predicted using the software *MestreNova*. The DEPT-135 experiment indicates that the lowest field aromatic peaks at 133.6, 134.7, and 137.5 ppm correspond to the quaternary carbons 1, 2, and 4, respectively, because they are not observed in the spectrum; while the peaks at 126.8, 130.9, and 132.9 ppm are assigned to tertiary carbons 5, 3, and 6, respectively.

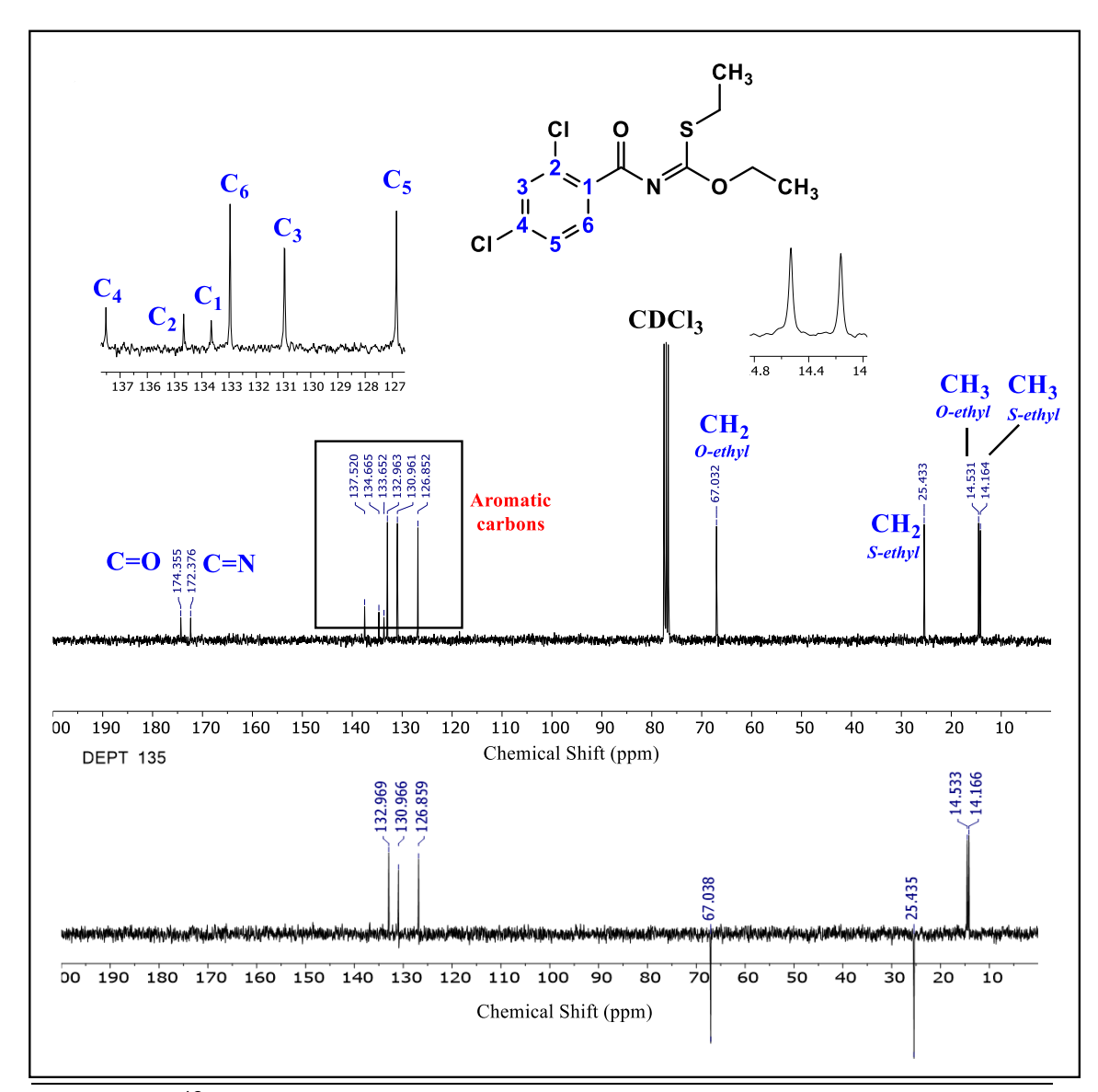


Figure 21. ¹³C NMR (top) and DEPT-135 (bottom) spectra (75 MHz, CDCl₃) of compound **59h**. Source: This investigation.

4.1.3 Synthesis and characterization of 1,2,4-triazoles

Finally, the third step in the methodology is the cyclization process between the X,Saroylimidothiocarbonates and hidrazines. This methodology was previously standardized by the GICH-UN13 under microwave and reflux conditions, with the latter allowing to obtain products with higher purity; therefore, in this investigation reflux conditions were used and the reaction time was determined for the new systems.

The reaction between the aroylimidothiocarbonates **59a**, **59e**, **59h**, and **63a** and the hydrazines 49 (a-b) occurs by a mechanism of substitution-condensation, which, will be studied in the next section. The cyclization reaction results in the eight 1,2,4triazoles substituted in positions 1, 3, and 5 shown in Scheme 16 named as T-RR₁-XC₂ (check nomenclature in Figure 11). This process is thermodynamically favorable because an aromatic system is generated.⁶⁴

Scheme 16. Step 3: Synthesis of the 1,2,4-triazole derivatives of this work. Source: This investigation.

The 1,2,4-triazoles T-1a-OC₂, T-1b-OC₂, T-1a-SC₂, and T-1b-SC₂ were previously synthetized, 13 thus, the obtained products in this investigation were confirmed through the physicochemical parameters indicated in Table 6 and through spectroscopic and spectrometric techniques (see Materials and Methods chapter). The importance of obtaining new 1,2,4-triazoles rely on the exploration of the versatility of the used methodology with different starting compounds and in the

⁶⁴ MILLER, James. Kinetic and Thermodynamic Issues in the Formation of Aromatic Compounds in Flames of Aliphatic Fuels. Combust Flame. 1992; 91: 21-39

potential biological activity that these types of compounds have. The compounds **T-3a-OC₂**, **T-3b-OC₂**, **T-4a-OC₂**, and **T-4b-OC₂** are new 1,2,4-triazoles reported in this investigation and their physical properties are summarized in Table 6. This table shows the experimental reaction time obtained in this work for all products, which was determined by TLC monitoring up to 40 minutes (Figure 22 for compound **T-3b-OC₂**), and, in the case of the compounds previously synthetized, the reported reaction time¹³ is shown too. It is worth to mention that for the triazoles **T-4a-OC₂** and **T-4b-OC₂**, unlike the other triazoles of which precursors were also synthetized in this work, only the cyclization reaction was performed on the carbonate **59e** since it was already available at the GICH-UN laboratory.

Table 6. Physicochemical parameters of the synthesized 1,2,4-triazoles and comparison with the reported compounds by the GICH-UN¹³. Source: This investigation.

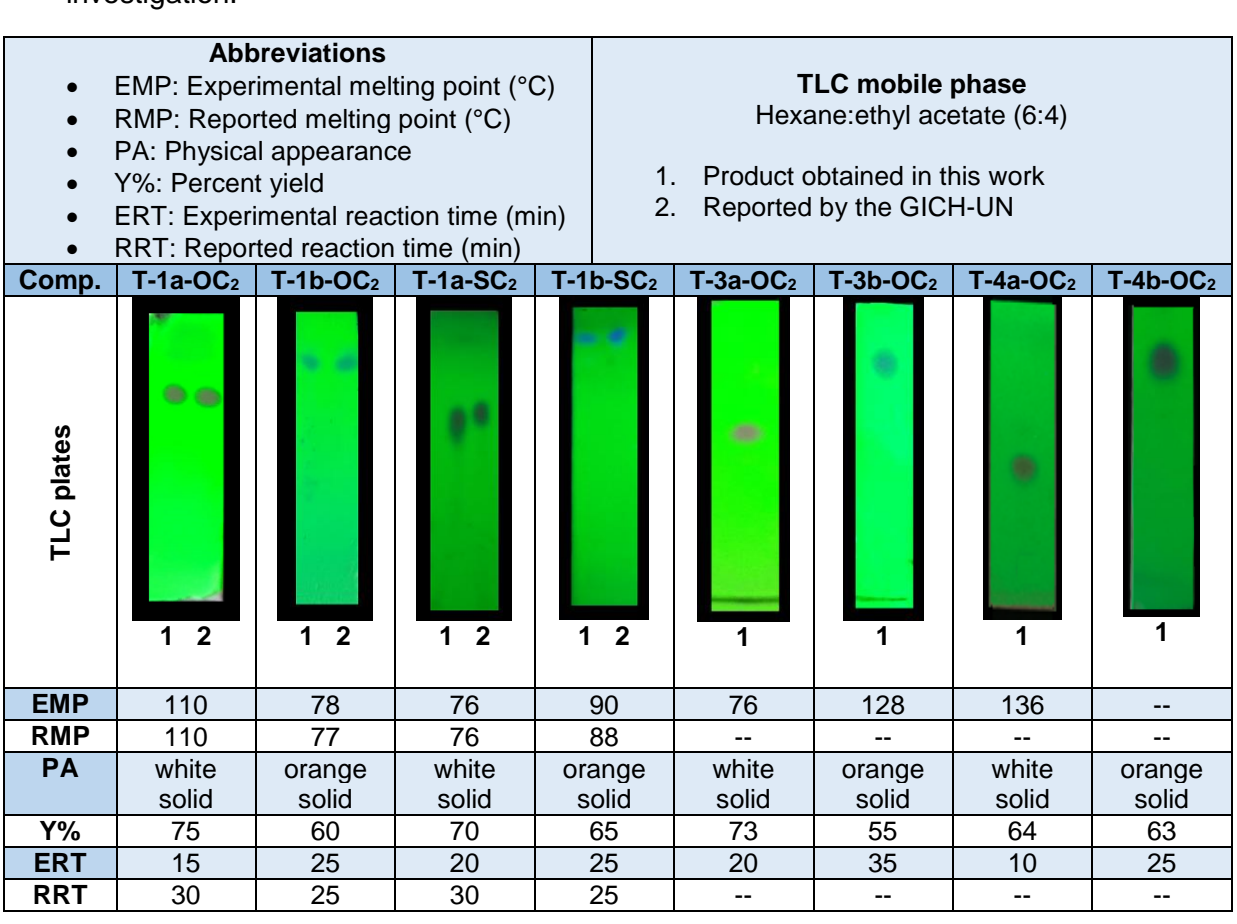


Table 6 shows that the 1,2,4-triazoles synthetized in this investigation have the same properties than those reported previously by the GICH-UN¹³. However, some differences are observed with relation to the reaction time of the 1,2,4-triazoles **T-1a-OC**₂ and **T-1a-SC**₂ which are lower than reported.¹³ Examination of the ERT row

in Table 6 indicates that lower reaction times are required when using hydrazine as precursor (**a** compounds) as compared to the case when phenylhydrazine is used as reactive (**b** compounds), which can be explained by the fact that the phenyl group in the phenylhydrazine reduce the nucleophilic character of the nitrogen as compared to the non-substituted hydrazine⁵⁹.

Regarding to the four novel triazole derivatives obtained in this work, the versatility of the synthetic methodology allowed to obtain two compounds with a substituted benzene in the R-position, while the other two have a heterocyclic (furyl) substituent, which can have a promising biological activity based on the activity shown by other furyl-containing systems¹⁷ (Figure 4). The spectroscopic and spectrometric properties of the new compounds are described with detail in this work (see Materials and Methods chapter). Below, it is described the synthesis and characterization of compound **T-3b-OC**₂ (5-(2,4-dichlorophenyl)-3-ethoxy-1-phenyl-1,2,4-triazole) as a particular example.

Figure 22 shows the monitoring by TLC of the cyclization reaction resulting in compound **T-3b-OC**₂. The 1,2,4-triazole was observed as a fluorescent signal under the 254 nm light after one minute of reaction. This signal is typical for the triazoles synthetized with phenylhidrazine as shown in Table 6, which can be attributed to the π -conjugated system resulting in a small energy gap between the HOMO and LUMO orbitals⁶⁵. The signal of the precursor disappears only 35 minutes after starting the reaction and at this time, a very pronounced signal is observed. An important common aspect among all triazoles synthetized with phenylhidrazine is the appearance of an unknown impurity with RF similar to the target compound that cannot be characterized, but it is a by-product that decrease the reaction yield of these compounds in comparison with the triazoles cyclized with hydrazine for which this signal is not found.

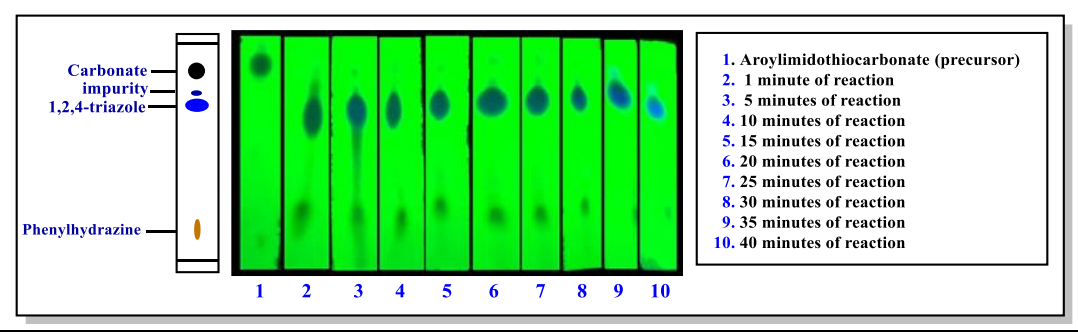


Figure 22. TLC monitoring of the reaction resulting in compound **T-3b-OC**₂. Source: This investigation.

 $^{^{65}}$ YAMAGUCHI, Yoshihiro *et al.* How the π Conjugation Length Affects the Fluorescence Emission Efficiency. *J Am Chem Soc.* 2008; 130 (42): 13867-13869.

In the DART+ mass spectrum of compound **T-3b-OC₂** in Figure 23, it is observed that the peak at 334.05107 m/z corresponds to the protonated 1,2,4-triazole with molecular formula $C_{16}H_{14}Cl_2N_3O$. It is also found that the formula predicted by the mass spectrum does not involve any sulfur atom, which shows that the generated triazole corresponds to the product O-ethyl and not S-ethyl. Again, peaks at 336 m/z and 338 m/z appear, related to the two chlorine atoms in the molecule and their two most abundant isotopes.

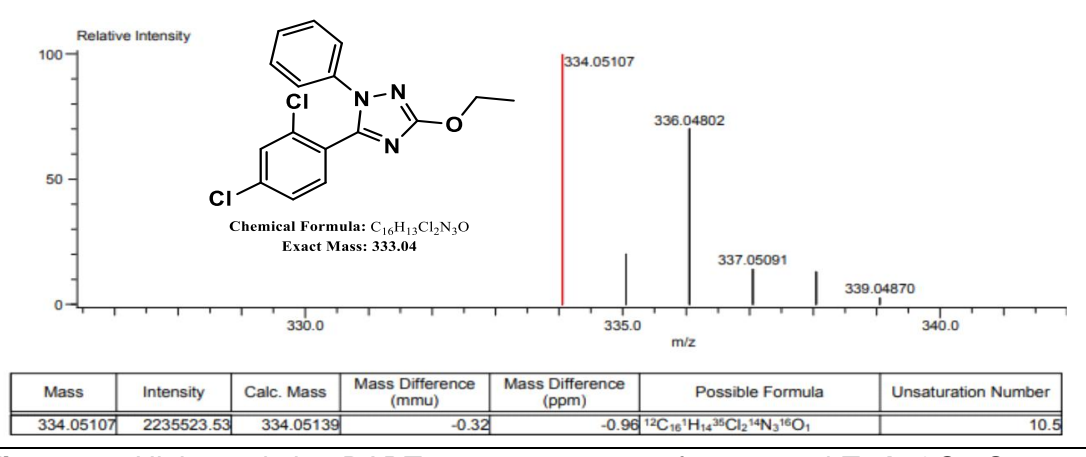


Figure 23. High-resolution DART+ mass spectrum of compound T-3b-OC₂. Source: This investigation.

The characterization of compound **T-3b-OC**₂ by IR spectroscopy (Figure 24) allows to differentiate the functional groups present in the molecule. The CH stretching of the aromatic rings, methylene, and methyl groups appear in the region between 2849 and 3094 cm⁻¹. The characteristic C=N stretch of 1,2,4-triazoles is shown as a band at 1596.51 cm⁻¹ that is within the range reported in the literature^{60,66,67}, likewise, this band is probably overlapped with the C=C stretch, which also shows other typical high intensity band⁶⁰ at 1530.48 cm⁻¹. The stretch of the C-N bond is assigned to the high intensity band at 1340.15 cm⁻¹, which agrees to what is expected for aromatic amines⁵⁸. The band at 774 cm⁻¹ is assigned to the C-Cl stretching⁶⁸, the C-O-C symmetric and asymmetric stretching is assigned to the bands at 1066.01 cm⁻¹ and 1172.45 cm⁻¹, respectively⁶⁰, and finally, the out-of-plane bending of the CH group appears at 753.44 cm⁻¹. Additionally, the aromatic overtones are observed around 1737.17 cm⁻¹ as expected for 1,2,4-substituted phenyl systems. An interesting observation in the spectrum is the disappearance of the band around 1300 cm⁻¹ related to the C-S stretching and the strong band around 1630 cm⁻¹ corresponding

⁶⁶ SHARBA, Hussain *et al.* Synthesis of Oxadiazoles, Thiadiazoles and Triazoles Derived from Benzo[b]thiophene. *Molecules*. 2005; **10**: 1161-1168.

⁶⁷ TRIVEDI, Mahendra *et al.* Characterization of Physical, Spectral and Thermal Properties of Biofield Treated 1,2,4-Triazole. *J Mol Pharm Org Process Res.* 2015; **3**(2): 128-133.

⁶⁸ BARBUSEANU, Stefania *et al.* Synthesis and Antioxidant Activity Evaluation of New Compounds from Hydrazinecarbothioamide and 1,2,4-Triazole Class Containing Diarylsulfone and 2,4-Difluorophenyl Moieties. *Int J Mol Sci.* 2014; **15**: 10908-10925.

to the C=O stretching, which together constitute an additional evidence of substitution of the thioethyl group and the condensation during the reaction.

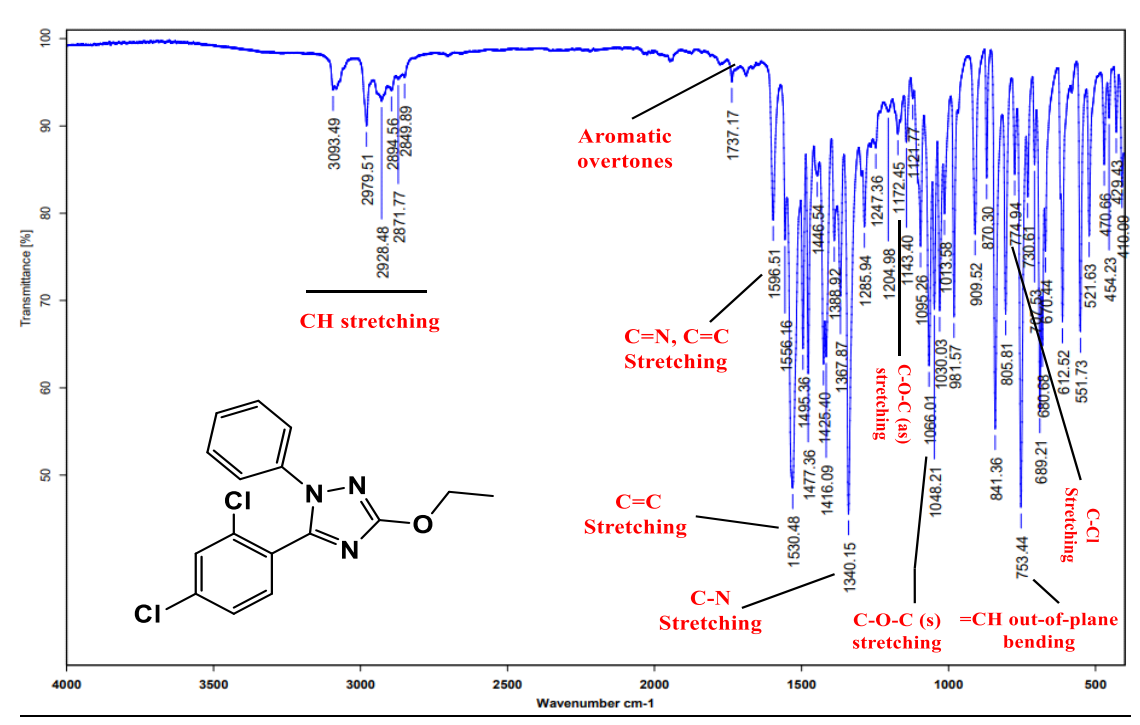


Figure 24. FT-IR spectrum of compound T-3b-OC₂. Source: This investigation.

The ¹H NMR spectrum of compound **T-3b-OC**₂ in Figure 25 shows that the integrals of the signals are consistent with the number of hydrogens in the molecule. The triplet at 1.48 ppm integrating for three protons can be assigned to the hydrogens of the methyl (CH₃) group, while the quartet at 4.44 ppm integrating for two protons is assigned to the methylene (CH₂) group. The aromatic protons of the two benzene rings are found between 7.22 and 7.43 ppm consisting of several overlapping signals that integrate for eight hydrogens in total. Despite their overlapping, it is possible to assign some signals: between 7.23 and 7.25 ppm a doublet of doublets is observed with coupling constants J = 8.2 Hz and J = 1.4 Hz that integrates for two protons, which can be assigned to the *ortho*-hydrogens (Ho) of the phenyl group (ring B) due to this multiplicity. This assignment is corroborated later with the analysis of the twodimensional experiments. Downfield a four-peak multiplet is observed which integrates for two protons that, based on observations on the precursors, reports in the literature⁶¹, and the multiplicity of the signals, are consistent with two doublets, which are assigned to hydrogens 6' and 3' overlapped. The signals at 7.4051 and 7.4168 ppm (external peaks) with J = 8.2 Hz correspond to hydrogen 6' that couples proton 5' in ortho-position while the peaks at 7.41 and 7.41 ppm (internal peaks) with J = 2.2 Hz correspond to hydrogen 3' that couples with proton 5' in *meta*-position. Two-dimensional experiments verify this assignment too. Finally, a multiplet integrating for four protons is observed; this signal can be assigned to the overlapping of the hydrogens Hm (two protons), 5, and Hp.

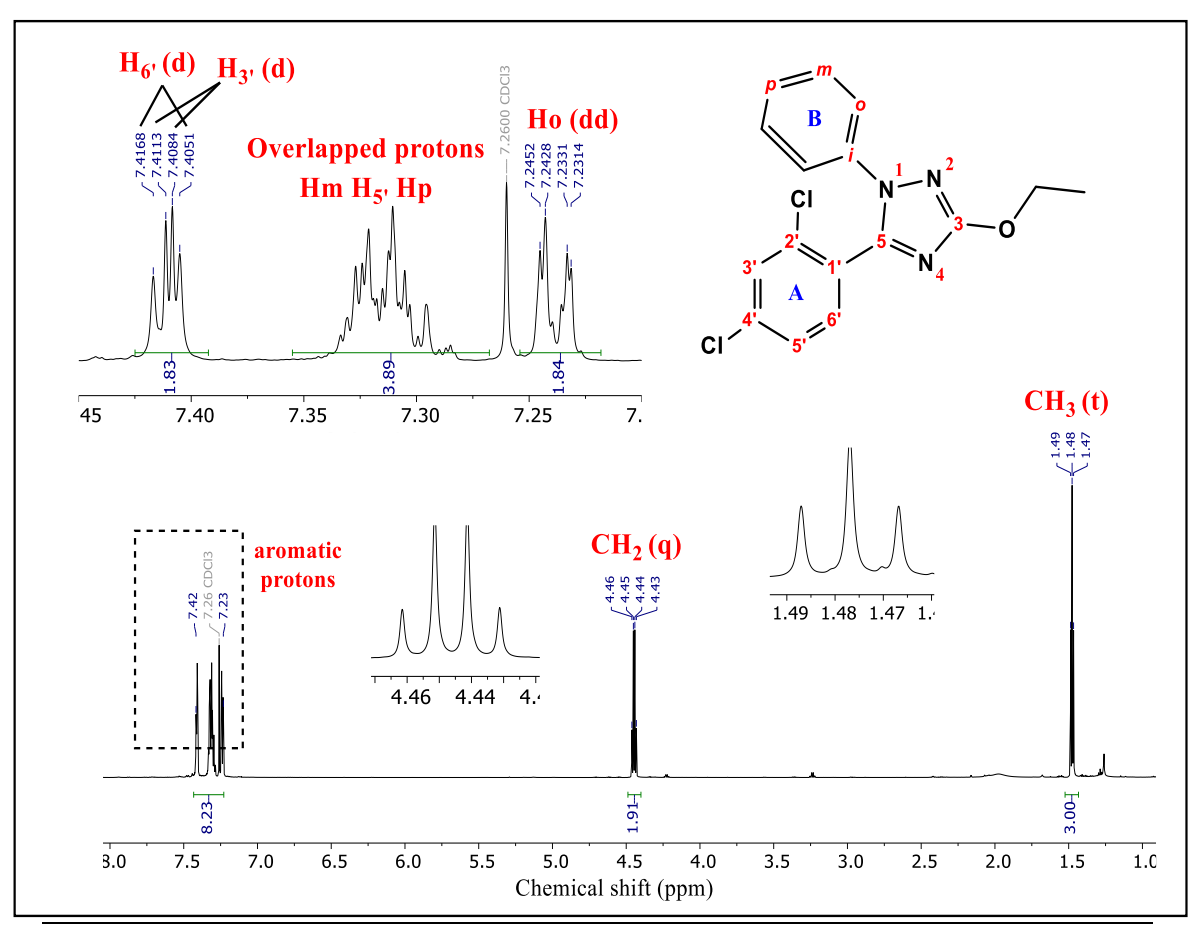


Figure 25. ¹H NMR spectrum (700 MHz, CDCl₃) of compound **T-3b-OC₂**. Source: This investigation.

The ¹³C NMR spectrum of compound **T-3b-OC**₂ in Figure 26 shows the fourteen expected signals, considering that the *ortho*- and *meta*-carbons of ring B are equivalent. The peaks at 14.7 and 65.8 ppm correspond to the methyl (**CH**₃) and methylene (**CH**₂) carbons of the ethoxy group, respectively. The signals found at 149.6 ppm and 167.9 ppm, corresponding to two quaternary carbons as indicated by the DEPT-190 spectrum, are assigned to carbons **5** and **3**, respectively. Their differentiation is verified later by the two-dimensional HMBC experiment. The carbon atoms of the aromatic rings are found between 123.4 and 137.7 ppm; the distinction of the CH carbons from the quaternary carbons is possible using the DEPT-190 experiment, which eliminates the last. The assignment was made by comparison with the literature, ^{61,68} chemical shift trends observed in precursors, and verified with the theoretical NMR spectrum predicted by the *MestreNova* software. The theoretical prediction is consistent with the trend observed in the experimental spectrum. Thus,

starting with the quaternary carbons, carbon 1' of the halogen-substituted aromatic ring (ring A) is assigned to the peak at 127.01 ppm, while the ipso-carbon (Ci in ring B) is assigned to the most displaced quaternary carbon at 137.7 ppm; the reason for this is the strong deshielding effect caused by the nitrogen in the triazole. On the other hand, the signal at 137.1 ppm is assigned to carbon 4' and the one at 134.7 ppm to carbon 2', the former is shifted downfield as has been observed in the precursors. These signals were assigned with the help of two-dimensional HMBC experiment. Regarding to the CH carbons, the strongest signals are observed at 123.4 ppm, that is assigned to the *ortho*-carbons (Co), and at 129.2 ppm, assigned to the meta-carbons (Cm); these peaks are more intense than the other C-H signals because they correspond to two equivalent carbons. The discernment of these signals was possible by the HSQC experiment. Tertiary carbons 3' and 6' appear at 130.1 ppm and 132.6 ppm, respectively. Both were assigned and differentiated from other signals by the HSQC experiment and were differentiated from each other by the chemical shift trend previously observed in the precursors. Finally, carbons 5' and Cp are assigned to the peaks at 128.1 ppm and 127.5 ppm, respectively. Despite the fact that there is not experimental certainty of their differentiation due to their similar chemical shifts, it is still possible to intuit that carbon 5' should appear downfield due to its proximity to the chlorine atoms in ring A.

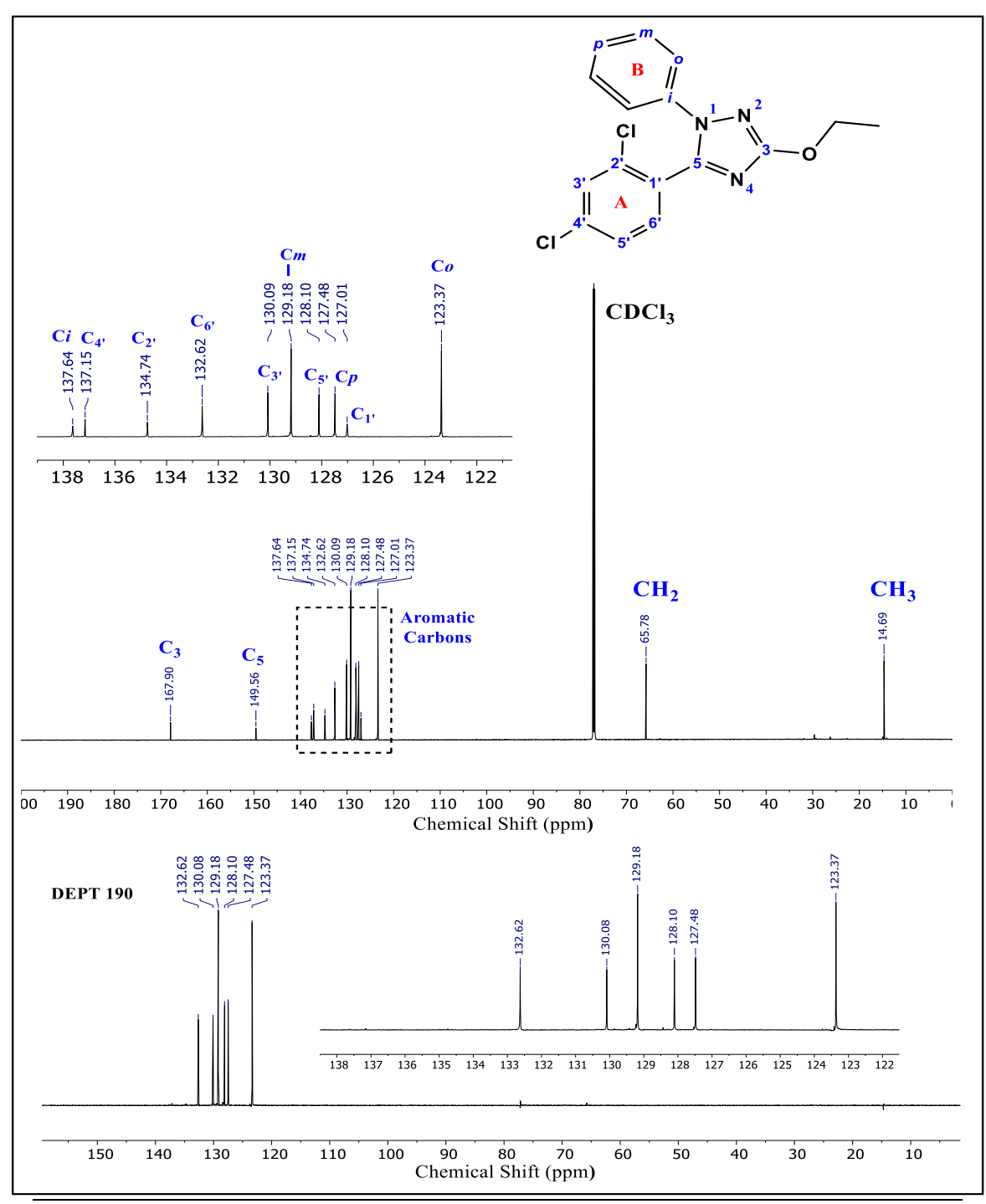


Figure 26. ¹³C NMR (top) and DEPT-190 (bottom) spectra (175 MHz, CDCl₃) of compound **T-3b-OC₂**. Source: This investigation.

Interactions at ${}^{1}J$ of the hydrogens with their respective carbons can be observed in the two-dimensional HSQC spectrum of the analyzed compound shown in Figure

27. Thus, a coupling between the protons and the carbon of the methyl group is observed as well as for the methylene group. In the aromatic region (inset), a coupling of the double of doublets of the *ortho*-hydrogens of ring B (Ho) with their respective carbons (Co) can be observed. This allows to corroborate the assignment of said signal in the ¹³C NMR spectrum and to differentiate it from the *meta*-carbons (Cm) because the multiplicity of the signal observed in the ¹H NMR spectrum coincides with the expected double of doublets of the ortho-hydrogens and not with the triplet for the *meta*-hydrogens. It is also observed that the overlapping signals of the hydrogens 3' and 6' in the ¹H NMR spectrum are correlated to the peaks assigned to their respective carbons (3' and 6') but, due to the overlap of these protons, the coupling observed does not allow to distinguish the carbons from each other; for this reason, these were assigned based on the trend observed in the carbonate precursor which shows the carbon 6' downfield. Finally, a large coupling in the intermediate aromatic region of the spectrum is observed, which is assigned to a ¹J interaction between the hydrogens Hm, 5', and Hp with their corresponding carbons.

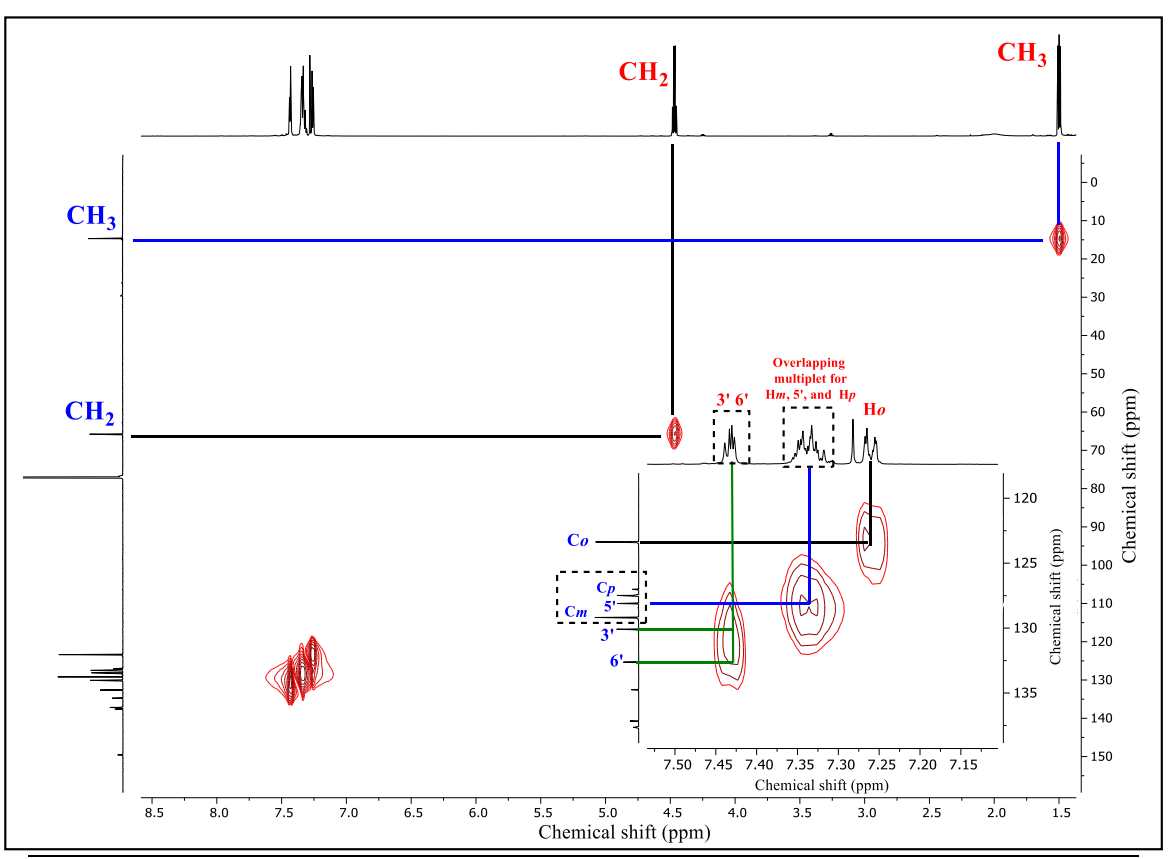


Figure 27. Two-dimensional HSQC spectrum (CDCl₃) of compound T-3b-OC₂. Source: This investigation.

In the HMBC spectrum shown in Figure 28, the coupling of hydrogens to carbons at two and three bonds (2J and 3J) are observed. For clarity, the spectrum is divided into two regions, the aliphatic (Figure 28 top) and the aromatic (Figure 28 bottom). Within the aliphatic region, a 2J coupling of the methyl protons (${\rm CH_3}$) with the methylene carbon (${\rm CH_2}$) is observed, also, the methylene protons (${\rm CH_2}$) have a coupling with the methyl carbon (${\rm CH_3}$) at 2J and with the carbon 3 at 3J , which allowed to differentiate the carbons 3 and 5.

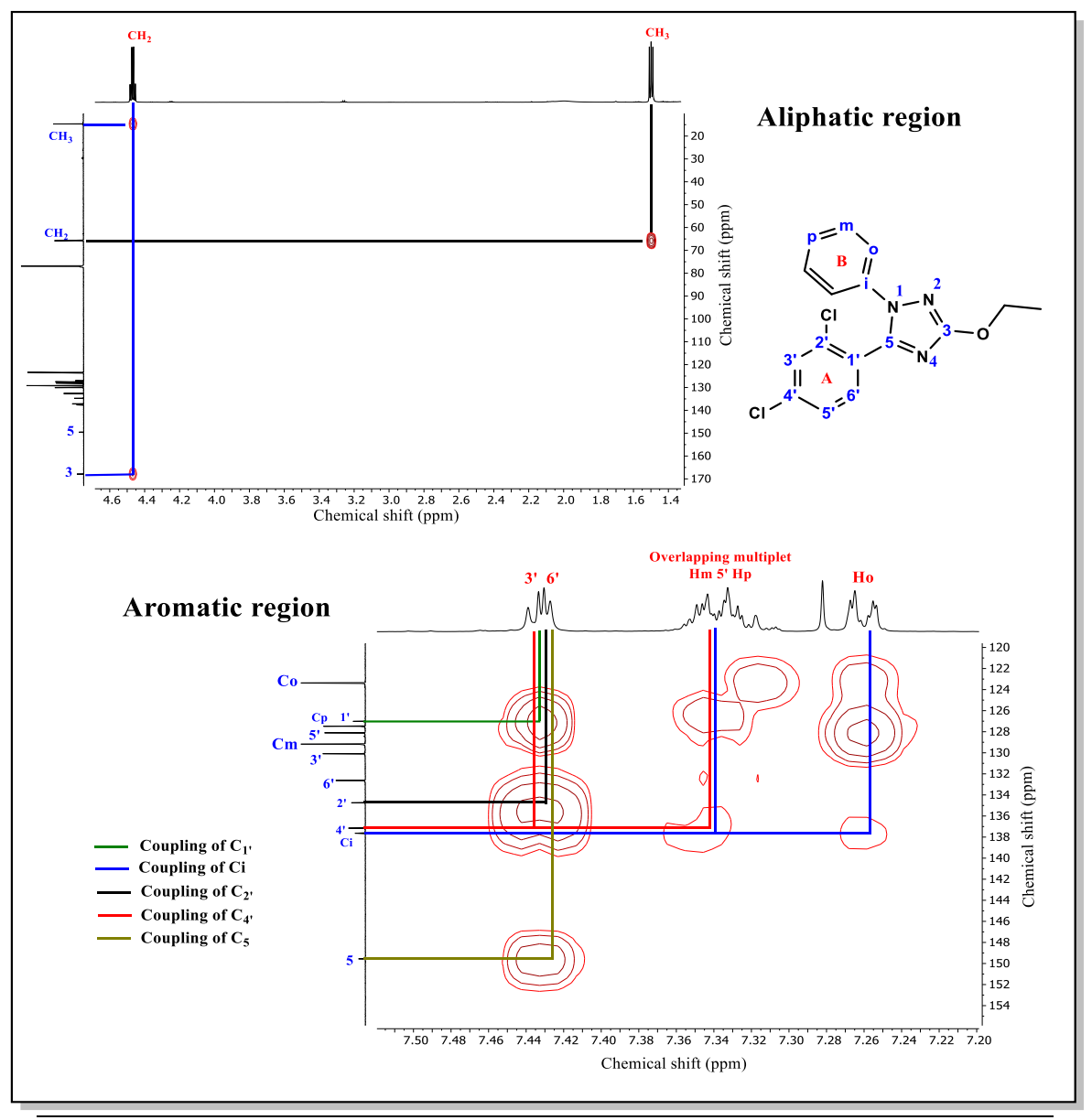


Figure 28. HMBC spectrum (CDCl $_3$) of compound **T-3b-OC_2**. Source: This investigation.

Despite the fact that in the aromatic region some signals appear overlapped, it is still possible to observe several couplings, therefore, this two-dimensional experiment is used to distinguish the guaternary carbons. Carbon 1' shows a coupling with the multiplet of hydrogens 6' and 3' due to ²J and ³J interactions, respectively. The ipsocarbon (Ci) has a coupling (to ²J) with the Ho protons and also shows an interaction with the multiplet where the meta-hydrogens (Hm) are found, corresponding to a ³J coupling. Carbon 2' presents only an interaction with the signal of the protons 3' and 6' due to ${}^{2}J$ and ${}^{3}J$ coupling, respectively; while carbon 4', with a similar chemical environment since it is also bonded to a chlorine atom, shows, in addition to the ²J and ${}^{3}J$ interactions with the protons 3' and 6', respectively, an interaction with the multiplet in the intermediate region due to 2J coupling with proton 5'. Additionally, the carbon 5 of the triazole ring shows a coupling to ³J with the proton 6'. Besides, the spectrum also shows some interactions of the CH carbons. The *ortho*-carbons (Co) have a unique interaction with the multiplet where the Hm and Hp are found, which correspond to interactions at two and three bonds, respectively. The *meta*-carbons (Cm) show a ${}^{2}J$ coupling with the *ortho*-hydrogens (Ho), but the interaction with the para-hydrogens (Hp) is not clearly observed in the spectrum. The para-carbon (Cp) shows a ³J coupling with the protons Ho and an interaction with the multiplet in the central region, which correspond to a ²J coupling with protons Hm. In the ring A, the carbon 6' shows a ²J coupling with the hydrogen 5', however, the interaction of this proton with carbon 3' is not clearly observed. Finally, carbon 5' shows an interaction with the multiplet of hydrogens 6' and 3' which correspond to a 2J and 3J coupling, respectively. For simplicity, the HMBC spectrum in Figure 28 only shows the interaction of the quaternary carbons in the aromatic region, additional interactions are shown in the Appendix (Figure A26).

The important conclusion of this section is that the methodology stablished by the GICH-UN to obtain 1,3,5-substituted-1,2,4-triazoles is versatile and allows the synthesis of different compounds with alternative substitutions in the positions: R, R₁, X, and R₂. Figure 29 summarizes the different combinations of substituents that are currently being synthetized at the GICH-UN laboratory using this methodology and commercially available reagents. In order explore the chemical space spanned by this synthetic methodology, different substitutions are suggested such as a large number of substituted benzene and heterocyclic aromatic systems coming from the carbonate (*R*-position); three different options in the R₁-position: hydrogen, phenyl, and methyl coming from hydrazines; and the **X**-atom being sulfur or oxygen. Some of these compounds have been synthetized in this investigation or in concurrent works; however, others such as the *N*-methyl-substituted triazoles, have not been synthetized yet but are synthetically viable due to the versatility of the methodology.

Figure 29. 1,3,5-substituted-1,2,4-triazole derivatives that are synthetically viable using the GICH-UN methodology. Source: This investigation.

4.1.3.1 Computational study of the cyclization reaction

The third step of the synthetic methodology is the cyclization reaction between aroylimidothiocarbonates and hydrazines to obtain the 1,3,5-substituted-1,2,4-triazoles. This reaction is believed to proceed by a mechanism in three sub-steps:

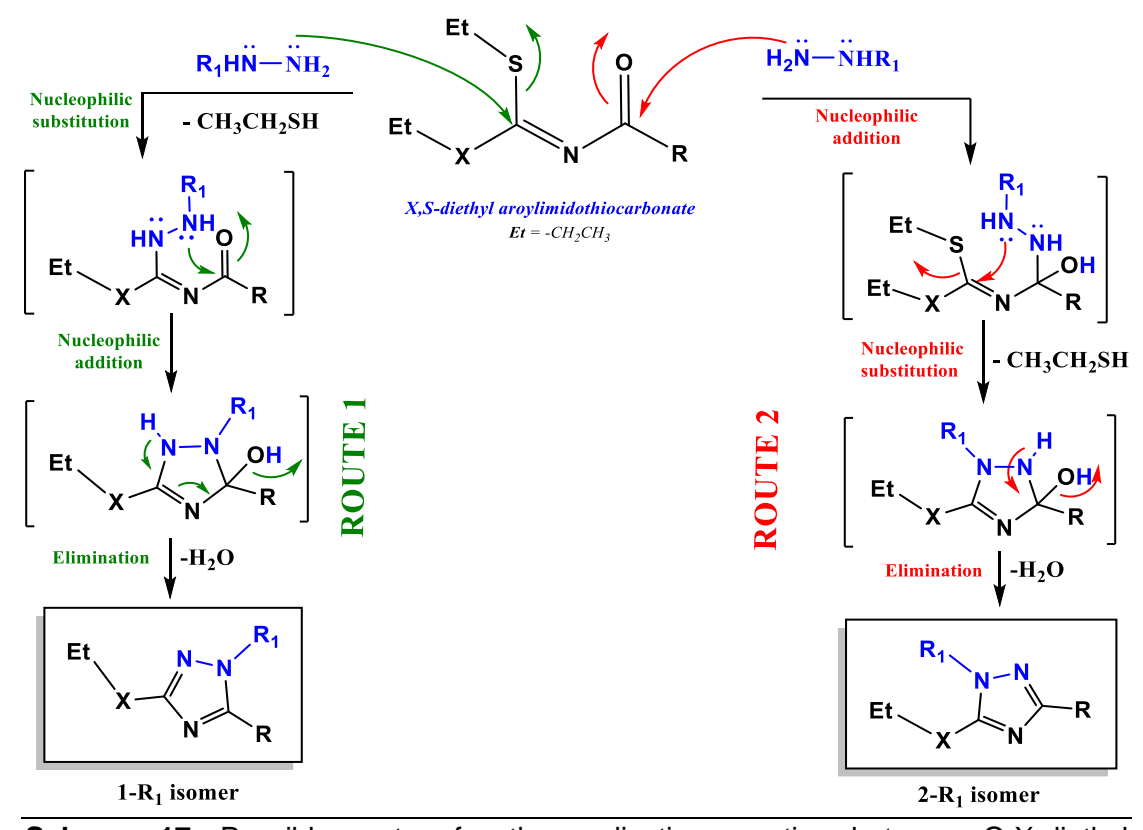
- ❖ Nucleophilic substitution: in this step, the carbon of the imino-ester group from the carbonate undergoes a nucleophilic attack by a nitrogen from the hydrazine leading to the elimination of ethanethiol as outgoing group.
- ❖ Nucleophilic addition: This step consists in a nucleophilic attack from a nitrogen of the hydrazine to the carbon of the amide group to generate a hydroxi-substituted intermediate.
- ❖ Elimination: In this step, the elimination of a water molecule occurs to generate the triazole ring.

In this way, the two mechanisms shown in Scheme 17 can be proposed considering that the carbonates have two electrophilic centers resulting in different products. The **route 1** proposes that the sub-steps are carried out in the following consecutive order: 1st) nucleophilic substitution, 2nd) nucleophilic addition, and 3rd) elimination; this generates the isomer with the R_1 -substituent in the N-position near to the aromatic group, which has been named **1-R1 isomer**. On the other hand, the **route 2** proposes that the sub-steps have the following order: 1st) nucleophilic addition, 2nd) nucleophilic substitution, and 3rd) elimination; resulting in the isomer with the R_1 -substituent in the N-position near to the X-ethyl group, which has been named **2-R1 isomer**.

The first reports in the literature date from early 1900s, where it was observed that the cyclization of the S,S-dimethyl benzoilimidodithiocarbonate with phenylhydrazine

(see scheme 12) resulted in the isomer 3-methylthio-1,5-diphenyl-1,2,4-triazole **73** (analogous to the **1-R**₁ **isomer**), while the isomer 5-methylthio-1,3-dyphenyl-1,2,4-triazole **74** (analogous to the **2-R**₁ **isomer**) was not obtained. These observations were verified through analysis of the NOESY spectrum by Hidalgo¹³ but using O,S-diethyl and S,S-diethyl aroylimidothiocarbonates.

Based on these antecedents, in this work computational calculations were carried out to determinate the relative thermodynamic stability of the two different triazole isomers that can be synthetized using this versatile synthetic methodology and different commercially available reagents (see Figure 29). The calculations were carried out using the hybrid DFT functional $\omega B97XD^{69}$ and the 6-311++G(d,p) basis set as implemented in Gaussian 16⁷⁰. Results for the Gibbs energy, which is the thermodynamic quantity related with the stability, are summarized in Table 7. It is important to clarify that in the R₁-position only the substituents phenyl (R₁ = Ph) and methyl (R₁ = CH₃) were evaluated, because the H-isomers (R₁ = H) can exist in three tautomeric forms.



Scheme 17. Possible routes for the cyclization reaction between O,X-diethyl aroylimidothiocarbonates with hydrazines. Source: This investigation.

75

_

⁶⁹ CHAI, Jeng-Da; HEAD-GORDON, Martin. Long-range corrected hybrid density functionals with damped atomatom dispersion corrections. *Phys. Chem. Chem. Phys.* 2008; **10**(44): 6615-20.

⁷⁰ FRISCH, Michael et al. Gaussian 16, Revision B.01, Gaussian, Inc., Wallingford CT, 2016.

The Gibbs energies summarized in Table 7 indicate that the 2-R₁ isomer (bold numbers) is thermodynamically more stable than 1-R₁ isomer, by approximately 12.1 kJ/mol in N-phenyl triazoles and 18.2 kJ/mol in N-methyl triazoles, in average; however, only in the system $R/R_1/X = 2.4-Cl_2Ph/Ph/S$, the 1-R₁ isomer (bold-italic number) T-3b-SC₂ is more stable by 2.7 kJ/mol with respect to its 2-R₁ isomer T-3B-SC₂. The common pattern found indicates that the thermodynamic preference of most compounds is the 2-R₁ isomer, which allows to conclude that the product obtained. purified. and characterized by the reaction between aroylimidothiocarbonates and hydrazines using the experimental conditions stablished in the methodology of the GICH-UN correspond to the kinetic product and not the thermodynamic product. The stabilization energies given above correspond to a temperature of 1455 K in N-phenyl triazoles and 2189 K in N-methyl triazoles, which indicates that it is not possible to thermally interconvert the 1-R₁ and 2-R₁ isomers. In principle, it was considered that the explanation of this observation was related to the greater electrophilic character of the iminoster carbon in comparison with the amidic carbon, but a Natural Population Analysis⁷¹ study of both isomers in terms of NBO charges, in which, through formulating a series of hybrid orbitals at each atom and description of the molecule by a series of localized bonding orbitals corresponding to a Lewis structure permits the assignment of atomic charges⁷², revealed that the amidic carbons have a higher NBO charge meaning that they are more electrophilic (see Table A1 in the Appendix for the NBO values). Therefore, two possible explanations are proposed: first, the route 2 mechanism presents a competitive reaction in the first sub-stage, in which the nucleophilic attack of the hydrazine on the amidic group can generate the addition reaction necessary for the obtaining triazoles or a substitution reaction resulting in a substitutedbenzohydrazide derivative 78 (Scheme 18). Products 78 have been observed by Hidalgo¹³ indicating that the substitution product can effectively compete with the addition product, despite that the latter results in an aromatic system. Second, it is expected that the activation energy in the rate-determining step of route 2 will be larger than that of route 1. Currently, the computational modeling of the different steps is being carried out by the GIFBA research group.

_

⁷¹ REED, Alan; WEINSTOCK, Robert; WEINHOLD, Frank. Natural population analysis. *J. Chem. Phys.* 1985; **83**(2): 735-46.

⁷² CAREY, Francis; SUNDBERG, Richard. *Advanced Organic Chemistry, Part A: Structure and Mechanisms*. 4th ed. Springer; 2007

Table 7. Thermodynamic stability of $1-R_1$ and $2-R_1$ isomers of 1,2,4-triazoles. Source: This investigation.

| | <i>N</i> -p | henyl-1,2,4-tri | iazoles | <i>N</i> -m | ethyl-1,2,4-tria | azoles |
|---|--------------------------|-----------------|------------|-----------------------------|------------------|------------|
| R | Isomer (R ₁) | | G mol) | Isomer (R ₁) | (kJ/i | |
| | (111) | X=O | X=S | (111) | X=O | X=S |
| 2,4-Cl ₂ Ph | 1-Ph | -4665849.4 | -5513848.9 | 1-CH ₃ | -4162633.1 | -5010629.3 |
| 2,4-012F11 | 2-Ph | -4665857.4 | -5513846.3 | 2-CH ₃ | -4162644.6 | -5010637.6 |
| 2 furyl | 1-Ph | -2246656.5 | -3094652.8 | 1-CH ₃ | -1743449.1 | -2591440.9 |
| 2-furyl | 2-Ph | -2246670.2 | -3094658.5 | 2-CH₃ | -1743456.7 | -2591448.8 |
| 2 thionyl | 1-Ph | -3094675.2 | -3942670.5 | 1-CH ₃ | -2591457.9 | -3439455.8 |
| 2-thienyl | 2-Ph | -3094691.8 | -3942678.7 | 2-CH₃ | -2591478.0 | -3439470.1 |
| 2 4 5 (OCU) Db | 1-Ph | -3154167.3 | -4002162.0 | 1-CH ₃ | -2650946.0 | -3498941.7 |
| 3,4,5-(OCH ₃) ₃ Ph | 2-Ph | -3154178.6 | -4002167.6 | 2-CH₃ | -2650967.5 | -3498957.6 |
| 2 E (CU) Dh | 1-Ph | -2458723.0 | -3306724.1 | 1-CH ₃ | -1955509.3 | -2803502.8 |
| 3,5-(CH ₃) ₂ Ph | 2-Ph | -2458744.6 | -3306727.6 | 2-CH₃ | -1955527.7 | -2803518.0 |
| 2.5 (NO.) Ph | 1-Ph | -3326203.1 | -4174197.2 | 1-CH ₃ | -2822982.4 | -3670975.7 |
| 3,5-(NO ₂) ₂ Ph | 2-Ph | -3326226.2 | -4174216.3 | 2-CH₃ | -2823015.5 | -3671005.8 |
| 4-CH₃Ph | 1-Ph | -2355566.2 | -3203561.7 | 1-CH ₃ | -1852345.9 | -2700341.4 |
| 4-CH3FII | 2-Ph | -2355578.2 | -3203567.7 | 2-CH₃ | -1852365.3 | -2700355.2 |
| 4-CIPh | 1-Ph | -3459130.8 | -4307125.8 | 1-CH ₃ | -2955913.7 | -3803909.2 |
| 4-CIPII | 2-Ph | -3459148.3 | -4307137.1 | 2-CH₃ | -2955936.9 | -3803927.3 |
| 4-FPh | 1-Ph | -2512986.7 | -3360981.1 | 1-CH ₃ | -2009768.4 | -2857764.7 |
| 4-FFII | 2-Ph | -2513003.7 | -3360991.6 | 2-CH₃ | -2009791.0 | -2857781.4 |
| 4-NO ₂ Ph | 1-Ph | -2789308.5 | -3637303.7 | 1-CH ₃ | -2286090.0 | -3134085.6 |
| 4-NO2F11 | 2-Ph | -2789330.6 | -3637317.5 | 2-CH₃ | -2286118.0 | -3134108.8 |
| 4-OCH₃Ph | 1-Ph | -2552999.5 | -3400996.9 | 1-CH ₃ | -2049782.7 | -2897780.7 |
| 4-00H3FH | 2-Ph | -2553015.6 | -3401002.3 | 2-CH₃ | -2049801.5 | -2897793.4 |
| Ph | 1-Ph | -2252401.1 | -3100398.7 | 1-CH₃ | -1749183.9 | -2597180.2 |
| Pn | 2-Ph | -2252417.7 | -3100405.9 | 2-CH₃ | -1749204.3 | -2597195.7 |

Apart from the observations related to the relative stability of the isomers, some additional aspects can be analyzed about of the effect of substituents in the thermodynamic stability. When comparing the Gibbs energy of sulfur-containing compounds and oxygen-containing compounds, it is found that the former are more stable than the latter, for both *N*-phenyl and *N*-methyl systems. Besides, the *N*-phenyl triazoles are more stable than the *N*-methyl triazoles, which can be related to the fact that *N*-phenyl compounds have a resonant aromatic system with 18 π electrons while the *N*-methyl compounds only have 12 π electrons. In conclusion, the *N*-phenyl sulfur-containing triazoles are the most stable systems being the isomers **T-3B-SC**₂ (2-Ph isomer) and **T-3b-SC**₂ (1-Ph isomer) the most stable among all evaluated compounds. This aspect will be relevant when discussing the results of antifungal activity in the next section.

Scheme 18. Competitive reactions involved in the route 2 mechanism of Scheme 17. Source: This investigation.

Other important information derived from the calculated Gibbs energies allows to evaluate the effect of the substituents on the stability of an isomer with respect to another, for which, the Gibbs energy difference between 2-R_1 and 1-R_1 isomers is shown in Figure 30. In general, the largest energy difference among the isomers is observed for the *N*-methyl oxygen-containing compounds as indicated by the red bars in Figure 30. With respect to the effect of the R-substituent, the $4\text{-NO}_2\text{Ph}$ and $3,5\text{-}(\text{NO}_2)_2\text{Ph}$ are the systems exhibiting the most important effect in the energy difference between the 2-R_1 and 1-R_1 isomers. This indicates that the nitro-group, either strongly stabilize the 2-R_1 isomer, or strongly destabilize the 1-R_1 isomer. The combination of a *N*-methyl substituent and an oxygen atom in the X-position are the structural factors that causes the largest energy difference between the isomers **T-11c-OC**₂ with $\Delta G = -33.1$ kJ/mol.

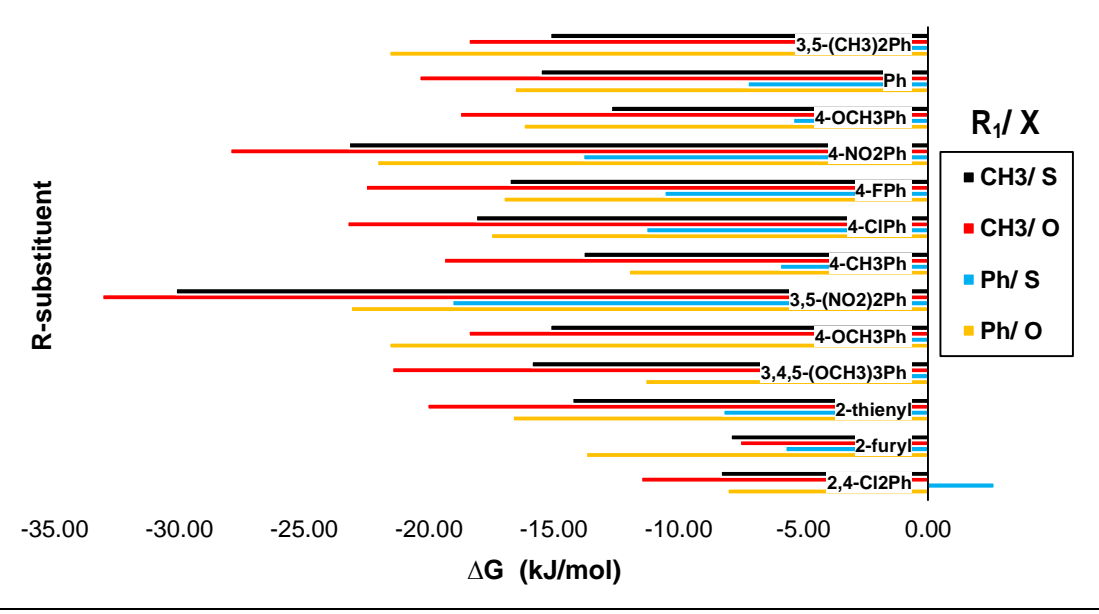


Figure 30. Gibbs energy differences between $2-R_1$ and $1-R_1$ isomers of 1,2,4-triazoles. Source: This investigation.

4.2 QSAR study of the antifungal activity of 1,2,4-triazoles

As it was mentioned previously, the biological activity of a series of compounds can be rationalized in terms of their molecular properties, so, in this work, a QSAR study was carried out with the purpose of identify the most important properties that affect the antifungal activity of the triazole derivatives synthesized (Scheme 16) and proposed (Figure 29) in this work.

Linear models as in Equation [1] express the fungal activity FA as a linear combination of several molecular descriptors X_k , and therefore, by determining these descriptors for novel molecules, it is possible to predict their fungal activity.

$$FA = a_0 + a_1 X_1 + a_2 X_2 + a_3 X_3 \dots$$
 [1]

These models will allow a quantitative understanding of the importance of the different substituents in the triazoles, such as, substituents in the benzene, halogen atoms, aliphatic chain lengths, among others, that will provide a molecular structure exhibiting an optimal interaction with the target enzyme of the azoles, the CYP51, and therefore, the best antifungal activity.

4.2.1 Building the QSAR models

QSAR models were constructed using the reported antifungal activity of a series of novel 1,2,4-triazoles with a 4-(4-substituted-phenyl) piperazine side chain **35 (a-y)** based on the structure of commercial antifungals as Fluconazole and Itraconazole synthetized by Xu *et al*¹⁵ (Figure 31).

| Comp | R | R' | Comp | R | R' | Comp | R | R' | Comp | R | R' | Comp | R | R' |
|------|---|---|------|---|---|------|---|--|------|---|---|------|---|---|
| 35a | Н | CH ₂ Cl | 35f | Н | CH(CH ₃) ₂ | 35k | Н | CH ₂ (CH ₂) ₅ CH ₃ | 35p | F | CH ₂ Cl | 35u | F | C(CH ₂) ₃ |
| 35b | Н | CF ₂ Cl | 35g | Н | CH ₂ (CH ₂) ₂ CH ₃ | 351 | Н | CH ₂ (CH ₂) ₇ CH ₃ | 35q | F | CH₂CH₃ | 35v | F | CH ₂ (CH ₂) ₃ CH ₃ |
| 35c | Н | CF ₃ | 35h | Н | CH ₂ (CH ₂) ₃ CH ₃ | 35m | Н | CH ₂ (CH ₂) ₉ CH ₃ | 35r | F | CH ₂ CH ₂ CH ₃ | 35w | F | CH ₂ (CH ₂) ₄ CH ₃ |
| 35d | н | CH ₂ CH ₃ | 35i | Н | C(CH ₂) ₃ | 35n | Н | CH ₂ (CH ₂) ₁₃ CH ₃ | 35s | F | CH(CH ₃) ₂ | 35x | F | CH ₂ (CH ₂) ₅ CH ₃ |
| 35e | Н | CH ₂ CH ₂ CH ₃ | 35j | Н | CH ₂ (CH ₂) ₄ CH ₃ | 350 | F | CH ₃ | 35t | F | CH ₂ (CH ₂) ₂ CH ₃ | 35y | F | CH ₂ Ph |

Figure 31. 1,2,4-triazole derivatives with a 4-(4-substituted-phenyl) piperazine side chain used for the QSAR study. Adapted from reference 15.

The twenty-five compounds exhibit broad antifungal activity against several fungi as measured in terms of the IC₈₀ (Table 8), which express the 80% to minimal inhibitory concentration⁷³. Specifically, the compounds are active against three species of the genus *Candida: Candida albicans* (C. ALB), *Candida parapsilosis* (C. PAR), and *Candida tropicalis* (C. TRO); a fungus of genus *Cryptococcus: Cryptococcus neoformans* (C. NEO); a fungus of genus *Trichophyton: Trichophyton rubrum* (T. RUB); a fungus of genus *Fonsecaea: Fonsecaea compacta* (F. COM); and finally, a fungus of genus *Microsporum: Microsporum gypseum* (M. GYP).

-

⁷³ BONEV, Boyen *et al.* Principles of assessing bacterial susceptibility to antibiotics using the agar diffusion method. *J Antimicrob Chemother.* 2008; **61**: 1295-1301

Table 8. *In vitro* antifungal activity in terms of IC₈₀ (μg/mL) for 1,2,4-triazole derivatives with a 4-(4-substituted-phenyl) piperazine side chain. Taken from Reference 15.

| Comp | C. ALB | C. PAR | C. TRO | C. NEO | T. RUB | F. COM | M. GYP |
|------------|---------|---------|---------|---------|---------|--------|--------|
| 35a | 0.00390 | 0.01560 | 0.01560 | 0.25000 | 0.06250 | 0.0625 | 0.0625 |
| 35b | 0.00097 | 0.00390 | 0.00390 | 0.06250 | 0.01560 | 0.0625 | 0.0039 |
| 35c | 0.00097 | 0.00390 | 0.00097 | 0.01560 | 0.01560 | 0.0156 | 0.0039 |
| 35d | 0.01560 | 0.01560 | 0.01560 | 1.00000 | 0.06250 | 0.2500 | 0.2500 |
| 35e | 0.00097 | 0.01560 | 0.06250 | 0.25000 | 0.06250 | 0.2500 | 0.0625 |
| 35f | 0.00390 | 0.01560 | 0.01560 | 1.00000 | 0.25000 | 0.2500 | 0.0625 |
| 35g | 0.01560 | 0.06250 | 0.06250 | 0.25000 | 0.06250 | 0.2500 | 0.2500 |
| 35h | 0.01560 | 0.25000 | 0.25000 | 1.00000 | 0.06250 | 1.0000 | 0.0625 |
| 35i | 0.01560 | 0.01560 | 0.01560 | 0.25000 | 0.00390 | 1.0000 | 0.0156 |
| 35j | 0.00097 | 0.01560 | 0.01560 | 0.06250 | 0.00390 | 0.0625 | 0.0039 |
| 35k | 0.01560 | 0.06250 | 0.06250 | 0.06250 | 0.06250 | 1.0000 | 0.0156 |
| 35I | 0.01560 | 1.00000 | 0.25000 | 0.06250 | 0.06250 | 1.0000 | 0.0156 |
| 35m | 0.06250 | 0.25000 | 1.00000 | 0.06250 | 0.06250 | 0.2500 | 0.0156 |
| 35n | 0.25000 | 1.00000 | 1.00000 | 16.0000 | 0.25000 | 4.0000 | 0.2500 |
| 35o | 0.06250 | 0.06250 | 0.06250 | 1.00000 | 0.25000 | 0.2500 | 1.0000 |
| 35p | 0.00390 | 0.01560 | 0.01560 | 0.06250 | 0.06250 | 0.0625 | 0.0156 |
| 35q | 0.06250 | 0.06250 | 0.06250 | 1.00000 | 0.06250 | 1.0000 | 0.2500 |
| 35r | 0.01560 | 0.01560 | 0.01560 | 0.25000 | 0.01560 | 0.2500 | 0.0156 |
| 35s | 0.06250 | 0.25000 | 4.00000 | 16.0000 | 0.06250 | 1.0000 | 0.0625 |
| 35t | 0.01560 | 0.25000 | 0.25000 | 1.00000 | 0.25000 | 1.0000 | 0.2500 |
| 35u | 0.01560 | 0.01560 | 0.01560 | 0.25000 | 0.01560 | 0.0625 | 0.0156 |
| 35v | 0.00390 | 0.25000 | 0.06250 | 0.06250 | 0.01560 | 0.2500 | 0.2500 |
| 35w | 0.00097 | 0.06250 | 0.06250 | 0.06250 | 0.01560 | 0.2500 | 0.0625 |
| 35x | 0.06250 | 0.0625 | 0.06250 | 0.25000 | 0.00390 | 0.2500 | 0.0625 |
| 35y | 0.01560 | 0.0625 | 0.06250 | 1.00000 | 0.00390 | 0.0625 | 0.0156 |

The fungi species which show inhibition by these compounds have relevant impact on the health of people and animals. The yeast of genus *Candida* have been studied in the last decades by their development of drug resistance against many traditional antifungals as Flucytosine (a fluorinated pyrimidine) and Ketoconazole, likewise, they are involved in different diseases as acquired immunodeficiency syndrome which has favored the appearance of mycoses⁷⁴ or the candidiasis, which affects genial organs in humans. Dermatophytosis or cutaneous mycoses are among the most prevalent infections in the world, they are rarely debilitating or life-threatening but billions of dollars are expended annually in their treatment. Dermatophytosis is caused by fungi that infect only the keratinized tissue (skin, hair, and nails) and the most important of these are the dermatophytes of genera *Microsporum* and

⁷⁴ DE BEDOUT, Catalina *et al.* Evaluación de la susceptibilidad de especies de Candida al fluconazol por el método de difusión de disco. *Biomédica*. 2003; **23**: 31-7.

Trichophyton, which are inhibited by the mentioned compounds, Epydermophyton. The genus Microsporum mainly affects hair and skin, for example, M. gypseum, which is most prevalent in warm, humid tropical, and subtropical environments, infects dogs and cats. 75 Trichophyton can affect skin and nails and T. rubrum is the most common superficial fungus, accounting for at least 60% of all superficial fungal infections in humans. 76 In relation to genus *Fonsacaea*, they have been linked to an infection named chromoblastomycosis (also known as chromomycosis), which is a chronic disease caused by saprophagous dematiaceous fungi, when it enters through an open wound and infects both skin and subcutaneous tissue⁷⁷. The genus Cryptococcus, such as C. neoformans, show a most complicated medical condition because many studies have demonstrated that cryptococcal diseases are associated with self-limiting cutaneous infections but they can lead to fatal systemic infections too, for example, primary pulmonary infection by inhalation of desiccated yeast and spores or cryptococcal meningitis, affecting the central nervous system, that can have a mortality between 10 and 30% when it is associated to HIV.78

Several molecular descriptors were used to rationalize the biological activity. Three groups of descriptors were taken into account related to structural, thermodynamic, and electronic properties; the latter related with the reactivity of the molecules. The descriptors used were entropy (S), Gibbs energy (G), hydration energy (ΔH_{hidrat}), thermal energy (E_{therm}), superficial area (A_{super}), molar mass (M), refractivity (R), dipolar moment (D), volume (V), logarithm of the partition coefficient n-octanol—water (LogP), polarizability (α) (this descriptor was calculated with two different softwares: α_{hyper} with Hyperchem⁷⁹ and α_{gauss} with Gaussian⁷⁰), electronic affinity (EA), ionization energy (IP), electronic potential (μ), hardness (η), softness (δ), and electrophilicity index (ω).

The electronic affinity and the ionization potential are related directly with the energy of the LUMO and HOMO orbitals as shown in Equations [2] and [3], respectively. This approximation is defined by the Koopmans theorem⁸⁰ and renders a practical alternative to calculate these parameters without the need to determinate the energy of respective cationic and anionic forms⁸¹, which requires two additional calculations

⁷⁵ SANABRIA, Rosa *et al.* Dermatofitos y hongos levaduriformes productores de micosis superficiales. *Mem Inst Investia Cienc Salud.* 2001: **1**(1): 63-68.

⁷⁶ WANG, Lingling *et al.* Analysis of the dermatophyte *Trichophyton rubrum* expressed sequence tags. *BMC Genomics*. 2006; **6**: 255-67.

⁷⁷ KIM, Dong Min *et al.* Chromoblastomycosis caused by *Fonsecaea pedrosoi. Ann Dermato.* 2011. **23**(3): 369-73.

⁷⁸ SRIKANTA, Deepa *et al. Cryptococcus neoformans*: Historical curiosity to modern pathogen. *Yeast.* 2014; **31**: 47-60.

⁷⁹ HYPERCUBE, Inc. HyperChem, Release 8.0.8, 2009

⁸⁰ LEVINE, Ira. Quantum Chemistry. 7th ed. Pearson Education; 2014.

⁸¹ SUN, Haitao *et al.* Ionization Energies, Electron Affinities, and Polarization Energies of Organic Molecular Crystals: Quantitative Estimations from a Polarizable Continuum Model (PCM)-Tuned Range-Separated Density Functional Approach. *J Chem Theory Comput.* 2016; **12**: 2906-16.

and, therefore, longer computational time. These quantum-chemical electronic descriptors are widely used because the frontier molecular orbitals are involved in the formation of many charge-transfer complexes⁸² as it is the case of the coordinate bond formed between the triazole and the iron atom of the heme-group in the CYP51 enzyme inhibited by the triazoles. The descriptors EA and IP allow the calculation of the other electronic parameters^{83,84} shown in Equations [4], [5], [6], and [7], which provide information on the chemical reactivity of the compounds. For example, the hardness can be interpreted as the resistance of a molecule to give up its electronic density, while large softness values indicate a greater reactivity. The electrophilicity index provides information on the electrophilic character of a molecule, thus, small values of ω are characteristic of highly nucleophilic species⁸⁵. On the other hand, the polarizability of a molecule, an important physical property relating the induced dipole moment to an applied electric field, is currently attracting attention in the area of QSAR for chemical-biological interactions⁸⁶, for example, some authors have studied the polarizability effects on ligand-substrate interactions⁸⁷. Another very important property is the n-octanol-water partition coefficient (LogP) which is directly related to the hydrophilic-hydrophobic character of the compound and is relevant in this QSAR study because antifungal medications must interact with amphipathic cell membranes. The hydration energy is a thermodynamic descriptor related to the energy released during the solvation process in water, a solvent omnipresent in living organism. Structural descriptors, as superficial area, are chosen because are common in 2D-QSAR studies⁵² and are related to the space occupied by the compounds, an important aspect for the compounds that enter the active site of the enzyme. Finally, thermodynamic properties as entropy and Gibbs energy are a measure of the stability of compounds when they exert their biochemical action⁸⁸.

-

⁸² KARELSON, Mati; LOVANOV, Victor. Quantum-chemical descriptors in QSAR/QSPR studies. *Chem Rev.* 1996; **96**: 1027-43.

⁸³ SARKAR, Nilmoni *et al.* Toxicity analysis of polychlorinated dibenzofurans through global and local electrophilicities. *J Mol Struct.* 2006; **758**: 119-25.

⁸⁴ BLANCO, Edgard *et al.* Estudio computacional conformacional, espectroscópico, ONL, HOMO–LUMO y reactividad de 1,3,5-trifenilpirazol. *Rev Ion.* 2018; **31**(2): 51-6.

⁸⁵ GUERRA, Cristian *et al.* Análisis QSAR-2D de los derivados de 1,4-di-*N*-oxidos de quinoxalina con actividad contra la enfermedad de chagas. *Quim Nova.* 2016; 39(6): 647-54.

⁸⁶ HANSCH, Corwin *et al.* On the Role of Polarizability in Chemical-Biological Interactions. *J Chem Inf Comput Sci.* 2003; **43**: 120-25.

⁸⁷ VERMA, Rajeshwar et al. On the role of polarizability in QSAR. Bioorg Med Chem. 2005; 13: 237-55.

⁸⁸ FLORES, Maryury *et al.* Molecular modeling studies of bromopyrrole alkaloids as potential antimalarial compounds: a DFT approach. *Med Chem Res.* 2018; **27**: 844-856.

$$EA = -E_{LUMO}$$
 [2]

$$IP = -E_{HOMO}$$
 [3]

$$\mu = \frac{-(EA + IP)}{2} \tag{4}$$

$$\eta = \frac{IP - EA}{2} \tag{5}$$

$$\delta = \frac{1}{2\eta}$$
 [6]

$$\omega = \frac{\mu^2}{2\eta} \tag{7}$$

Since molecular descriptors are determined computationally, their numerical value depends on the particular level of theory used. A specific level of theory consists in the combination of a method and a basis set. Each method constitutes a particular approximation to solve the time-independent Schrödinger equation, while a basis sets is used to expand the molecular wave function as a linear combination of atomic orbitals, with expansion coefficients determined by the Variational method⁸⁰. Quantum-chemical methods can be classified as semiempirical and *ab initio*, with the latter including the Hartree-Fock and post-Hartree-Fock methods and the methods based on the density functional theory (DFT). In this work, molecular descriptors were calculated using three different levels of theory. The first one is the semiempirical method Austin Model 1 (AM1)⁸⁹, the second one is DFT employing the hybrid exchange-correlation functional using the Coulomb-attenuating method⁹⁰ CAM-B3LYP with the 6-31++G(d,p) basis set, and finally, the third one is a two-layer ONIOM⁹¹ scheme with CAM-B3LYP/6-31++G(d,p) for the high layer and AM1 for the low layer.

The AM1 method, like other semiempirical methods, considers a minimum basis set in the form of Slater orbitals. The eigenvalues ε_i and expansion coefficients C_{si} of the eigenfunctions are determined by solving the Fock-Roothaan secular Equation [8], where several approximations are made in order to reduce calculation costs. The most important is related to the construction of the Fock matrix, in which some of its elements

⁸⁹ DEWAR, Michael J; ZOEBISCH, Eve G; HEALY, Eamonn. AM1: A New General Purpose Quantum Mechanical Molecular Model. *J. Am. Chem. Soc.* 1985; **107**(13): 3902-3909

⁹⁰ YANAI, Takeshi; TEW, David P; HANDY, Nicholas C. A new hybrid exchange-correlation functional using the Coulomb-attenuating method (CAM-B3LYP). *Chem. Phys. Lett.* 2004; **393**(1): 51-7.

⁹¹ LUNG WA, Chung, et al. The ONIOM method and its applications. Chem. Rev. 2015; 115(12): 5678-5796.

 $F_{rs} = \langle \chi_r | \hat{F} | \chi_s \rangle$ are taken from experimental data⁹².

$$\sum_{s=1}^{b} C_{si} \left(F_{rs} - \varepsilon_i S_{rs} \right) = 0$$
 [8]

DFT methods are based on the Hohenberg-Kohn theorem proving that the ground state total energy of a system E_o is an unique functional of the electron density $\rho(r)$, so $E_o = E(\rho)^{85,86}$, as in Equation [9]. Since the purely electronic Hamiltonian operator is the sum of the kinetic energy $T(\rho)$, the electron-nucleus energy $V_{ne}(\rho)$, and the electron-electron repulsion energy $V_{ee}(\rho)$, the total energy depends on the electron density⁹².

$$E(\rho) = T(\rho) + V_{ne}(\rho) + V_{ee}(\rho)$$
 [9]

Kohn and Sham proposed a method to determine the electron density and hence the energy of a system from the Kohn-Sham orbitals θ^{KS} as in Equation [10]. These orbitals are the orbitals of a fictitious non-interacting electron reference calculated in such a way that the molecular energy is minimized using the Variational theorem. The results show that the $V_{ee}(\rho)$ functional can be considered as the sum of an electronic repulsion functional and an exchange and correlation energy functional $E_{xc}(\rho)$ [11] which is calculated differently according to the DFT method in particular 92,93,94 .

$$\rho = \sum_{i=1}^{n} [\theta_i^{ks}]^2$$
 [10]

$$V_{ee}(\rho) = \frac{1}{2} \iint \frac{\rho(r_1)\rho(r_2)}{r_{12}} dr_1 dr_2 + E_{xc}(\rho)$$
 [11]

Ab-initio methods, like DFT, do not use any simplification to save computational time as semiempirical methods do. In fact, the resulting equations are written based on the information of the molecular system under study, i.e., the number of electrons and the nature and number of nuclei, and therefore are computationally intensive. A middle point between semiempirical and *ab initio* methods is the ONIOM method⁹¹, in which, the whole molecular system is divided in the so-called layers. Each layer can be treated by a different method according to the studied properties. Usually, the part of the molecule that determine the properties of interest are described by *ab*

⁹² CUEVAS, Gabriel; CORTES; Fernando. Introducción a la Química Computacional. Fondo de Cultura Económica; 2003

⁹³ SHARMA, Indrajit; THAPA, Ranjit. Basic concepts of Density Functional Theory: Electronic structure calculation. *J Phys: Conf Ser.* 2016; **765**(1): 1-4.

⁹⁴ KRYACHKO, Eugene; LUDEÑA, Eduardo. Density functional theory: Foundations reviewed. *Phys Rep.* 2014; **544**: 123-239.

initio methods, and any other part, by computationally cheaper methodologies, like semiempirical methods. In this way, *ab initio* quality results can be obtained with a reduced computational time as compared to the case where the whole molecule is treated by *ab initio* methods. For the purpose of this work, the aliphatic chain in the R' position of the compounds shown in Figure 31 was chosen as the low layer due to the fact that this chain has less relevance in the electronic structure. Besides, based on the enzymatic action of these compounds, this aliphatic chain does not play an essential role in inhibition due to its distance from the triazole active center. The numerical values of the molecular descriptors obtained by the different levels of theory used are shown in the Appendix (Tables A3, A4, and A5).

Using these data, linear models as in Equation [1] were built by mans of the statistical software Statgraphics Centurion XVI. Roughly, the construction of the models was done through an iterative process, in which different combinations of descriptors were used, always choosing those that improve the statistical parameter R^2 ; then, the less statistically significant parameters were progressively eliminated until the pvalue of the ANOVA table is reduced to values lower than 0.05, which means that there is a statistical dependence between the antifungal activity and the molecular descriptors with a confidence level of 95%. This methodology provided better results than the typical methodology based on Pearson's correlation matrix, because the least contributory parameters can be eliminated without significantly affecting the multilinear fit. Table 9 summarizes the molecular descriptors included in the best models obtained with the three different levels of theory for the seven fungi. The models indicated that some compounds exhibited an atypical antifungal activity, which were consequently removed resulting in a model with an improved R^2 value. Therefore, in the different rows of Table 9, the molecular descriptors used in the models are shown considering the whole set of (n =) 25 compounds, but also for 24, 23, and, in some cases, even 22 compounds.

The results in Table 9 show that the R^2 (and R^2_{adj}) value of the corresponding model increases when some molecules are removed from the set. In the case of C. ALB, C. PAR, C. NEO, T. RUB, and M. GYP up to three molecules were removed which corresponds to 12% of the total set, while in C. TRO and F. COM up to two molecules were removed which correspond to 8%. In all cases, the removed data were those for which the predicted activity value differs from the real value by more than 2.5 standard deviations. The percentage of molecules removed can be considered low and the number of molecules that are preserved is adequate. For this reason, the models with the best statistical parameter R^2_{adj} were chosen, which correspond to models with the maximum number of compounds removed (two or three) from the original set of 25.

The total computing time varies widely when comparing the three different levels of theory used: AM1 calculations take between 30 and 180 seconds; calculations using ONIOM take between 6 and 8 hours; while calculations using full DFT require a time-

range between 14 and 20 hours. This clearly shows that the computational cost of the DFT method is significantly larger in comparison to the semiempirical method used, being in average about 600 times larger; while the calculations using ONIOM take up to 250 times longer than AM1, but this technique reduce the computational time around 40% compared to full DFT.

In order to compare the different models obtained, the statistical parameter R_{adj}^2 has been used. This parameter explains the percentage of variation of the dependent variable that collectively accounts for all the independent variables and it is useful to compare models with a different number of independent variables⁵¹. The information about the statistical parameters for model comparison for the different computational methods is summarized in Figure 32.

Table 9. Molecular descriptors included in the QSAR models designed for the seven different fungi using the three different computational methods. Source: This investigation.

| Fungus | | | Candida all | bicans (C. ALB) | | |
|-----------------|-----------|---|-------------|---------------------------------------|-----------|--|
| Method | Semi | empirical | 10 | MOIN | | DFT |
| | Parameter | Descriptors | Parameter | Descriptors | Parameter | Descriptors |
| n | 25 | $V \Delta H_{hidrat}$ | 25 | S V LogP R | 25 | $A_{super} \Delta H_{hidrat}$ |
| R^2 | 60.9322 % | LogP α_{Hypher} | 60.2607 % | M D E $_{therm}$ η | 55.6831 % | LogP R α _{Gauss} |
| R_{adj}^2 | 37.4916 % | M G D Etherm | 40.3911 % | | 29.0929 % | M D E _{therm} μ |
| P-value | 0.0492 | η | 0.0281 | | 0.0989 | |
| n | 24 | ΔH_{hidrat} LogP | 24 | S V LogP M | 24 | $A_{super} \Delta H_{hidrat}$ |
| R^2 | 67.9769 % | $\alpha_{Hypher}\ M\ G\ D$ | 72.5712 % | D E _{therm} η | 73.3801 % | $LogP\ R\ \alpha_{Gauss}$ |
| R_{adj}^2 | 53.9669 % | Etherm | 60.5711 % | | 56.2674 % | M D E $_{therm}$ μ |
| <i>p</i> -value | 0.0043 | Removed: 35w | 0.0014 | Removed: 35w | 0.0077 | Removed: 35w |
| n | 23 | ΔH _{hidrat} LogP | 23 | α _{Gauss} V M | 23 | A _{super} ΔH _{hidrat} |
| R^2 | 73.7658 % | $\alpha_{Hypher}\ M\ G\ D$ | 78.2189 % | D E _{therm} η | 83.0212 % | $LogP\ R\ \alpha_{Gauss}$ |
| R_{adj}^2 | 61.5232 % | Etherm | 70.051 % | | 71.2667 % | M D E $_{therm}$ μ |
| <i>p</i> -value | 0.0018 | Removed: 35j and 35w | 0.0001 | Removed: 35j and 35w | 0.0009 | Removed: 35j and 35w |
| n | 22 | ΔH _{hidrat} LogP | 22 | α _{Gauss} V M | 22 | A _{super} ΔH _{hidrat} |
| R^2 | 80.1799 % | $\alpha_{Hypher}\ M\ G\ D$ | 85.6518 % | D E _{therm} η | 88.3376 % | LogP R α _{Gauss} |
| R_{adj}^2 | 70.2698 % | Etherm | 79.9125 % | | 79.5908 % | M D E _{therm} μ |
| <i>p</i> -value | 0.0005 | Removed: 35e , 35j , and 35w | 0.0000 | Removed: 35j, 35v, and 35w | 0.0002 | Removed: 35j , 35v , and 35w |

| Fungus | Candida parapsilosis (C. PAR) | | | | | | |
|-----------------|-------------------------------|---|-----------|---------------------------------------|-----------|--|--|
| Method | Semi | empirical | OI | MOIN | | DFT | |
| | Parameter | Descriptors | Parameter | | Parameter | Descriptors | |
| n | 25 | A _{super} V | 25 | LogP R | 25 | G A _{super} V | |
| R^2 | 76.3331 % | ΔH _{hidrat} LogP | 74.109 % | α _{Gauss} D | 75.1957 % | ΔH _{hidrat} LogP R | |
| R_{adj}^2 | 64.4997 % | R α_{Hypher} G μ | 65.4787 % | $E_{therm}\;\omega$ | 60.3131 % | $lpha$ Hypher E therm ω | |
| <i>p</i> -value | 0.0008 | | 0.0002 | | 0.0030 | | |
| n | 24 | V LogP R | 24 | LogP R | 24 | G A _{super} V | |
| R^2 | 75.4552 % | $lpha$ Hypher G μ | 79.9109 % | α_{Gauss} D | 81.0507 % | ΔH _{hidrat} LogP R | |
| R_{adj}^2 | 66.7923 % | Removed: 35t | 72.8207 % | $E_{therm}\;\omega$ | 68.8691 % | $lpha$ Hypher $E_{therm}\;\omega$ | |
| <i>p</i> -value | 0.0002 | | 0.0000 | Removed: 35r | 0.0009 | Removed: 35j | |
| n | 23 | V LogP R | 23 | LogP R | 23 | G A _{super} V | |
| R^2 | 79.7785 % | $lpha$ Hypher G μ | 85.3117 % | α _{Gauss} D | 85.3315 % | ΔH _{hidrat} LogP R | |
| R_{adj}^2 | 72.1954 % | Removed: 35t | 79.8037 % | $E_{therm}\;\omega$ | 75.1764 % | α Hypher E therm ω | |
| <i>p</i> -value | 0.0001 | and 35v | 0.0000 | Removed: 35h and 35r | 0.0004 | Removed: 35j and 35t | |
| n | 22 | V LogP R | 22 | LogP R D | 22 | G A _{super} V | |
| R^2 | 84.5457 % | α _{Hypher} G μ | 85.2997 % | ω | 91.0663 % | ΔH _{hidrat} LogP R | |
| R_{adj}^2 | 78.364 % | | 81.8408% | | 84.366 % | $lpha$ Hypher $E_{	ext{therm}}$ ω | |
| <i>p</i> -value | 0.0000 | Removed: 35j , 35t , and 35v | 0.0000 | Removed: 35h, 35r, and 35y | 0.0001 | Removed: 35j , 35t , and 35v | |
| Fungus | | | | picalis (C. TRO |) | | |
| Method | | empirical | | MOIN | | DFT | |
| | Parameter | Descriptors | Parameter | <u> </u> | Parameter | Descriptors | |
| n | 25 | A _{super} V | 25 | A _{super} LogP | 25 | G A _{super} V | |
| R ² | 88.0409 % | $\Delta H_{hidrat} R$ | 72.1714 % | R α _{Gauss} M | 75.8961 % | ΔH _{hidrat} LogP R | |
| R_{adj}^2 | 80.8655 % | α _{Hypher} M E _{therm} EA IP | 58.2571 % | D E _{therm} δ | 61.4338 % | $lpha$ Hypher $E_{therm}\;\omega$ | |
| <i>p</i> -value | 0.0000 | Ltherm LA IF | 0.0025 | | 0.0025 | | |
| n | 24 | A _{super} V | 24 | A _{super} α _{Gauss} | 24 | G A _{super} ΔH _{hidrat} | |
| R^2 | 92.8023 % | ΔH_{hidrat} R | 80.0594 % | M D E_{therm} | 78.4471 % | $lpha$ Hypher $E_{therm}\ \omega$ | |
| R_{adj}^2 | 88.1752 % | α _{Hypher} M | 74.5204 % | | 70.8401 % | Pomovod: 250 | |
| <i>p</i> -value | 0.0000 | E _{therm} EA IP Removed: 35t | 0.0000 | Removed: 35s | 0.0001 | Removed: 35s | |
| n | 23 | A _{super} V | 23 | A _{super} α _{Gauss} | 23 | G A_{super} ΔH_{hidrat} | |
| R^2 | 93.739 % | ΔH_{hidrat} R | 84.3389 % | M D Etherm | 85.7139 % | $lpha$ Hypher $E_{therm}\;\omega$ | |
| R_{adj}^2 | 90.1613 % | α _{Hypher} M | 79.7326 % | Domesia | 80.3566 % | Domoved: 25: | |
| <i>p</i> -value | 0.0000 | E _{therm} μ Removed: 35j and 35t | 0.0000 | Removed: 35h and 35s | 0.0000 | Removed: 35j and 35s | |

| Method Parameter Parameter S Asuper LogP MD M D Etherm ω M D Eth | Fungus | | Cr | yptococus ne | eoformans (C. N | IEO) | |
|---|---|--|---|--|--|--|---|
| R | | Semi | | | | | DFT |
| R ² 66.1994 % Δ-Hudrat LogP R α Gauss D Ehrerm μ | | Parameter | Descriptors | Parameter | | Parameter | Descriptors |
| R ² adj | | 25 | S A _{super} V | 25 | S A _{super} | 25 | |
| Devalue 0.0416 | | | _ | | | | M D E $_{therm}$ ω |
| R | | | | | E _{therm} α _{Hypher} | | |
| R ² 73,303 % R Gauss D Einerm 51,7638 % Einerm Chypher 59,2267 % Removed: 35n | <i>p</i> -value | | · | | | | |
| Removed: 35n Salary Sal | | | | | | | |
| P-value 0.0012 Removed: 35n 0.0059 Removed: 35n 0.0018 Removed: 35n 0.0018 Removed: 35n Re | | | | 66.4444 % | | 71.6359 % | M D E _{therm} ω |
| P-value | R_{adj}^2 | 61.6235 % | Etherm | 51.7638 % | Etherm αHypher | 59.2267 % | Domovodi 25 n |
| R | <i>p</i> -value | 0.0012 | Removed: 35n | 0.0059 | | 0.0018 | Removed. 3311 |
| P-value | n | 23 | S A _{super} LogP | 23 | S A _{super} | 23 | V ΔH _{hidrat} LogP |
| P-value 0.0004 Removed: 35h and 35n 0.0039 and 35s Removed: 35n and 35s Rem | R^2 | 78.8474 % | R α _{Gauss} D | 70.4301 % | LogP M D | 71.2326 % | M D E _{therm} ω |
| P-value 0.0004 Removed: 35h and 35n 0.0039 Removed: 35n and 35s 0.0033 Sn and 35s 0.0033 Sn and 35s 0.0033 Sn and 35s Sn an | R_{adi}^2 | 68.9762 % | Etherm | 56.6308 % | Etherm αHypher | 57.8078 % | |
| R² 83.1988 % R² adauss D R² adauss D R αGauss D Etherm 77.175 % 65.7626 % LogP M D Etherm αHypher 75.9391 % 63.9086 % M D Etherm α Hypher M D Etherm α Hypher Assper ΔHhidrat Assper ΔHhidrat Assper ΔHhidrat Assper ΔHoldrat Assp | | 0.0004 | | 0.0039 | | 0.0033 | |
| P-value | n | 22 | S A _{super} LogP | 22 | S A _{super} | 22 | V ΔH _{hidrat} LogP |
| Removed: 35h, 35n, and 35s Removed: 35h, 35n, and 35s | R^2 | 83.1988 % | | 77.175 % | LogP M D | 75.9391 % | M D E _{therm} ω |
| Removed: 35h, 35n, and 35s Removed: 35h, 35n, and 35s | R_{adi}^2 | 74.7982 % | Etherm | 65.7626 % | E _{therm} α _{Hypher} | 63.9086 % | |
| Method Semiempirical ONIOM DFT n 25 54.5836 % R^2_{adj} Asuper ΔHnidrat LogP α _{sauss} M D Etherm 25 54.3461 % 35.5475 % S V M Etherm EA IP αHypher 25 49.2795 % 28.3946 % S Asuper ΔHnidrat 49.2795 % 28.3946 % M D Etherm ω R² adj 64.2902 % 54.3708 % ΔHnidrat LogP αGauss M Etherm 24 66.1946 % 54.2632 % Removed: 35j S V M Etherm μ αΗγpher 24 63.5101 % 47.5458 % S Asuper ΔHnidrat M D Etherm ω R² P-value 78.4809 % 0.000 Removed: 35j and 35t 35.398 % S LogP M αHypher 23 66.5134 % S Asuper ΔHnidrat M D Etherm ω P-value 0.000 Removed: 35j and 35t 0.0004 Removed: 35j and 35t 35 Asuper ΔHnidrat 77.1682 % M D Etherm ω P-value 0.000 AHnidrat LogP α _{Gauss} M Etherm 22 0.0004 S V M Etherm 65.398 % 23 αHypher S Asuper ΔHnidrat 77.1682 % N D Etherm ω P-value 0.000 AHnidrat LogP α _{Gauss} M Etherm 22 82.3568 % S V M Etherm αHypher 22 84.2416 % S Asuper ΔHnidrat Μ D Etherm ω P-value 0.000 | <i>p</i> -value | 0.0002 | 35h , 35n , and | 0.0013 | 35n, 35s, | 0.0018 | |
| $\begin{array}{c ccccccccccccccccccccccccccccccccccc$ | | | | | | | |
| n 25 Asuper ΔHhidrat R² 25 S V M Etherm EA IP αHypher 25 S Asuper ΔHhidrat A9.2795 % 28.3946 % 28.3 | | | | | | 3) | |
| R² 54.5836 % R²adj LogP αGauss M D Etherm 54.3461 % 35.5475 % 35.5475 % EA IP αHypher (28.3946 % 28.3946 % 28.3946 % 28.3946 % 28.3946 % 28.3946 % 28.3946 % 28.3946 % 28.3946 % 28.3946 % 28.3946 % 28.3946 % 28.3946 % 28.3946 % 28.3946 % 28.3946 % 28.3946 % 28.3946 % 29.0003 M D Etherm ω (24.35) (24.3708 % Etherm (24.35) (25.4632 % Etherm (25.4632 | | | • | OI | | | |
| R ² _{adj} 35.8828 % M D Etherm 35.5475 % 28.3946 % 28.3946 % 20.0703 n 24 ΔHhidrat LogP αGauss M R ² 64.2902 % ΔHhidrat LogP αGauss M Etherm 24 S V M Etherm μ α Hypher 24 S Asuper ΔHhidrat A Go.5101 % M D Etherm ω p-value 0.0013 Removed: 35j 0.0024 Removed: 35j 0.0105 Removed: 35j n 23 ΔHhidrat LogP αGauss M Etherm 74.8349 % Etherm δ Etherm δ 77.1682 % M D Etherm ω p-value 0.000 Removed: 35j and 35t Removed: 3 | Method | Parameter | Descriptors | Of Parameter | MOIM | Parameter | Descriptors |
| p-value 0.0337 0.0349 0.0703 n 24 ΔHhidrat LogP αGauss M Etherm 24 S V M Etherm μ αHypher 24 S Asuper ΔHhidrat M D Etherm ω (47.5458 %) R²adj 54.3708 % Etherm 54.2632 % Removed: 35j Removed: 35j Removed: 35j Removed: 35j S LogP M (23) 23 S Asuper ΔHhidrat M D Etherm ω (47.5458 %) Removed: 35j Removed: | Method n | Parameter 25 | Descriptors A _{super} ΔH _{hidrat} | Of Parameter 25 | S V M E _{therm} | Parameter 25 | Descriptors S A _{super} ΔH _{hidrat} |
| n 24 ΔHhidrat LogP R^2 24 S V M Etherm μ αHypher 24 S Asuper ΔHhidrat M D Etherm μ αHypher 24 S Asuper ΔHhidrat M D Etherm μ αHypher 24 S Asuper ΔHhidrat M D Etherm μ αHypher 24 S Asuper ΔHhidrat M D Etherm μ αHypher 24 S Asuper ΔHhidrat M D Etherm μ αHypher 24 S Asuper ΔHhidrat M D Etherm μ αHypher 24 S Asuper ΔHhidrat M D Etherm μ αHypher 24 S Asuper ΔHhidrat M D Etherm μ αHypher 24 S Asuper ΔHhidrat M D Etherm μ αHypher 24 S Asuper ΔHhidrat M D Etherm μ αHypher 24 S Asuper ΔHhidrat M D Etherm μ αHypher 24 S Asuper ΔHhidrat M D Etherm μ αHypher 24 S Asuper ΔHhidrat M D Etherm μ αHypher 24 S Asuper ΔHhidrat M D Etherm μ αHypher 23 S Asuper ΔHhidrat M D Etherm μ αHypher 23 S Asuper ΔHhidrat M D Etherm μ αHypher 24 S Asuper ΔHhidrat M D Etherm μ αHypher 25 S Asuper ΔHhidrat M D Etherm μ αHypher 24 S Asuper ΔHhidrat M D Etherm μ αHypher 24 S Asuper ΔHhidrat M D Etherm μ αHypher 24 S Asuper ΔHhidrat M D Etherm μ αHypher 25 S Asuper ΔHhidrat M D S S Asuper ΔHidrat M D S S Asuper μ αHypher 25 S Asuper μ αHypher 25 S Asuper μ αHypher 25 S As | n R ² | 25 54.5836 % | Descriptors A _{super} ΔH _{hidrat} LogP α _{Gauss} | Of Parameter 25 54.3461 % | S V M E _{therm} | Parameter 25 49.2795 % | Descriptors S A _{super} ΔH _{hidrat} |
| R^2 64.2902 % αGauss M 66.1946 % μ α Hypher 63.5101 % M D Etherm ω R^2_{adj} 54.3708 % Etherm 54.2632 % Removed: 47.5458 % Removed: 35j ρ -value 0.0013 Removed: 35j 0.0024 35t 0.0105 Removed: 35j R^2 78.4809 % αGauss M 74.8349 % Etherm δ 77.1682 % M D Etherm ω R^2_{adj} 72.1518 % Removed: 35j Removed: 35j and 35t Removed: 35j and 35t Removed: 35j and 35t ρ -value 0.000 AHhidrat LogP αGauss M Etherm 22 S V M Etherm δ αHypher 22 S Asuper ΔHhidrat M D Etherm ω R^2 83.0324 % αGauss M Etherm 82.3568 % δ αHypher 84.2416 % M D Etherm ω R^2 83.0324 % Removed: 35j, | n R ² R _{adj} | Parameter 25 54.5836 % 35.8828 % | Descriptors A _{super} ΔH _{hidrat} LogP α _{Gauss} | Of Parameter 25 54.3461 % 35.5475 % | S V M E _{therm} | Parameter 25 49.2795 % 28.3946 % | Descriptors S A _{super} ΔH _{hidrat} |
| R_{adj}^2 54.3708 % Etherm 54.2632 % Removed: 35j 47.5458 % Removed: 35j p -value 0.0013 Removed: 35j 0.0024 35t 0.0105 Removed: 35j R^2 78.4809 % α_{Gauss} M 74.8349 % Etherm δ 77.1682 % M D Etherm ω R_{adj}^2 72.1518 % Removed: 35j | Method n R^2 R_{adj}^2 p -value | 25 54.5836 % 35.8828 % 0.0337 | Descriptors A _{super} ΔH _{hidrat} LogP α _{Gauss} M D E _{therm} | Of Parameter 25 54.3461 % 35.5475 % 0.0349 | S V M E _{therm} EA IP α _{Hypher} | Parameter 25 49.2795 % 28.3946 % 0.0703 | Descriptors S A _{super} ΔH _{hidrat} M D E _{therm} ω |
| p-value 0.0013 Removed: 35j 0.0024 Removed: 35t Removed: 35j Removed: 35j <t< th=""><th>Method n R^2 R_{adj}^2 p-value n</th><th>25 54.5836 % 35.8828 % 0.0337 24</th><th>Descriptors Asuper ΔHhidrat LOGP αGauss M D Etherm ΔHhidrat LOGP</th><th>Ol Parameter 25 54.3461 % 35.5475 % 0.0349 24</th><th>S V M Etherm EA IP αHypher</th><th>Parameter 25 49.2795 % 28.3946 % 0.0703 24</th><th>Descriptors S A_{super} ΔH_{hidrat} M D E_{therm} ω S A_{super} ΔH_{hidrat}</th></t<> | Method n R^2 R_{adj}^2 p -value n | 25 54.5836 % 35.8828 % 0.0337 24 | Descriptors Asuper ΔHhidrat LOGP αGauss M D Etherm ΔHhidrat LOGP | Ol Parameter 25 54.3461 % 35.5475 % 0.0349 24 | S V M Etherm EA IP αHypher | Parameter 25 49.2795 % 28.3946 % 0.0703 24 | Descriptors S A _{super} ΔH _{hidrat} M D E _{therm} ω S A _{super} ΔH _{hidrat} |
| p-value 0.0013 Removed: 35j 0.0024 35t 0.0105 n 23 ΔH _{hidrat} LogP α_{Gauss} M $Etherm$ 23 S LogP M $Etherm$ 23 S Asuper ΔH _{hidrat} M D Etherm ω R^2_{adj} 72.1518 % Etherm 65.398 % αHypher 66.5134 % Removed: 35j and 35t p-value 0.000 AH _{hidrat} LogP and 35t 22 S V M Etherm ω S Asuper ΔH _{hidrat} AH _{hidrat} M D Etherm ω R ² 83.0324 % AH _{hidrat} LogP ω 22 S V M Etherm ω S Asuper ΔH _{hidrat} M D Etherm ω R ² R ² _{adj} 77.7300 % Removed: 35j, T.2996 % Removed: 35j, 35t, and Removed: 35j, 35t, and Removed: 35j, 35t, and | | 25 54.5836 % 35.8828 % 0.0337 24 64.2902 % | Descriptors Asuper ΔHhidrat LOGP αGauss M D Etherm ΔHhidrat LOGP αGauss M | Ol Parameter 25 54.3461 % 35.5475 % 0.0349 24 66.1946 % | S V M Etherm EA IP αHypher | Parameter 25 49.2795 % 28.3946 % 0.0703 24 63.5101 % | Descriptors S A _{super} ΔH _{hidrat} M D E _{therm} ω S A _{super} ΔH _{hidrat} |
| n 23 ΔH _{hidrat} LogP α_{Gauss} M α_{Gauss} M α_{Gauss} M α_{Gauss} M α_{Hidrat} α_{Gauss} M α_{Hidrat} α_{Gauss} M α_{Hidrat} α_{Hidrat | $\begin{array}{c} \textbf{Method} \\ \textbf{n} \\ R^2 \\ R^2_{adj} \\ \textbf{p-value} \\ \textbf{n} \\ R^2 \\ R^2_{adj} \end{array}$ | 25 54.5836 % 35.8828 % 0.0337 24 64.2902 % 54.3708 % | Descriptors Asuper ΔHhidrat LOGP αGauss M D Etherm ΔHhidrat LOGP αGauss M | Ol Parameter 25 54.3461 % 35.5475 % 0.0349 24 66.1946 % 54.2632 % | S V M Etherm EA IP αHypher S V M Etherm μ αHypher | Parameter 25 49.2795 % 28.3946 % 0.0703 24 63.5101 % 47.5458 % | Descriptors S A _{Super} ΔH _{hidrat} M D E _{therm} ω S A _{Super} ΔH _{hidrat} M D E _{therm} ω |
| R ² _{adj} 72.1518 % Etherm 65.398 % α Hypher 66.5134 % Removed: 35j and 35t S V M Etherm δ α α μγρher 22 S Asuper ΔΗ hidrat M D Etherm ω Μ D Etherm ω Μ D Etherm ω 76.3624 % Removed: 35j, 35t, and 35t, and 35t, and 35t, and 35t, and 35t | $\begin{array}{c} \textbf{Method} \\ \textbf{n} \\ R^2 \\ R^2_{adj} \\ \textbf{p-value} \\ \textbf{n} \\ R^2 \\ R^2_{adj} \end{array}$ | 25 54.5836 % 35.8828 % 0.0337 24 64.2902 % 54.3708 % | Descriptors Asuper ΔHhidrat LogP αGauss M D Etherm ΔHhidrat LogP αGauss M Etherm | Ol Parameter 25 54.3461 % 35.5475 % 0.0349 24 66.1946 % 54.2632 % | S V M Etherm EA IP αHypher S V M Etherm μ αHypher Removed: | Parameter 25 49.2795 % 28.3946 % 0.0703 24 63.5101 % 47.5458 % | Descriptors S A _{Super} ΔH _{hidrat} M D E _{therm} ω S A _{Super} ΔH _{hidrat} M D E _{therm} ω |
| p-value 0.000 Removed: 35j and 35t 0.0004 Removed: 35j and 35t 0.0007 Removed: 35j and 35t Removed: 35j and 35t 0.0007 Removed: 35j and 35t Removed: 35j and 35t 0.0007 Removed: 35j and 35t S V M Etherm 22 S Asuper ΔHhidrat M D Etherm ω R^2 83.0324 % 82.3568 % 5 α Hypher 84.2416 % M D Etherm ω R^2 77.7300 % Removed: 35j, Removed: 35j, Removed: 35j, 35t, and 35x | $\begin{array}{c} \textbf{Method} \\ \textbf{n} \\ R^2 \\ R^2_{adj} \\ \textbf{\textit{p-value}} \\ \textbf{n} \\ R^2 \\ R^2_{adj} \\ \textbf{\textit{p-value}} \\ \textbf{\textit{p-value}} \\ \textbf{\textit{n}} \\ \end{array}$ | 25 54.5836 % 35.8828 % 0.0337 24 64.2902 % 54.3708 % 0.0013 | Descriptors Asuper ΔHhidrat LOGP αGauss M D Etherm ΔHhidrat LOGP αGauss M Etherm Removed: 35j ΔHhidrat LOGP | Ol Parameter 25 54.3461 % 35.5475 % 0.0349 24 66.1946 % 54.2632 % 0.0024 | S V M Etherm EA IP αHypher S V M Etherm μ αHypher Removed: 35t S LogP M | Parameter 25 49.2795 % 28.3946 % 0.0703 24 63.5101 % 47.5458 % 0.0105 | Descriptors S A _{Super} ΔH _{hidrat} M D E _{therm} ω S A _{Super} ΔH _{hidrat} M D E _{therm} ω Removed: 35 j |
| p-value 0.000 Removed: 35j and 35t 0.0004 Removed: 35j and 35t 0.0007 Removed: 35j and 35t Removed: 35j and 35t 0.0007 Removed: 35j and 35t Removed: 35j and 35t 0.0007 Removed: 35j and 35t S V M Etherm 22 S Asuper ΔHhidrat M D Etherm ω R^2 83.0324 % 82.3568 % 5 α Hypher 84.2416 % M D Etherm ω R^2 77.7300 % Removed: 35j, Removed: 35j, Removed: 35j, 35t, and 35x | $\begin{array}{c} \textbf{Method} \\ \textbf{n} \\ R^2 \\ R^2_{adj} \\ \textbf{p-value} \\ \textbf{n} \\ R^2 \\ R^2_{adj} \\ \textbf{p-value} \\ \textbf{n} \\ \textbf{n} \\ R^2 \end{array}$ | 25 54.5836 % 35.8828 % 0.0337 24 64.2902 % 54.3708 % 0.0013 23 | Descriptors Asuper ΔHhidrat LOGP αGauss M D Etherm ΔHhidrat LOGP αGauss M Etherm Removed: 35j ΔHhidrat LogP αGauss M | Ol Parameter 25 54.3461 % 35.5475 % 0.0349 24 66.1946 % 54.2632 % 0.0024 23 | S V M Etherm EA IP αHypher S V M Etherm μ αHypher Removed: 35t S LogP M | Parameter 25 49.2795 % 28.3946 % 0.0703 24 63.5101 % 47.5458 % 0.0105 23 | Descriptors S A _{super} ΔH _{hidrat} M D E _{therm} ω S A _{super} ΔH _{hidrat} M D E _{therm} ω Removed: 35j |
| R² 83.0324 % α _{Gauss} M 82.3568 % δ α _{Hypher} 84.2416 % M D E _{therm} ω 75.2996 % 76.3624 % Removed: 35j, Removed: 35j, and 35x | $\begin{array}{c} \textbf{Method} \\ \textbf{n} \\ R^2 \\ R^2_{adj} \\ \textbf{p-value} \\ \textbf{n} \\ R^2 \\ R^2_{adj} \\ \textbf{p-value} \\ \textbf{n} \\ \textbf{n} \\ R^2 \end{array}$ | 25 54.5836 % 35.8828 % 0.0337 24 64.2902 % 54.3708 % 0.0013 23 78.4809 % | Descriptors Asuper ΔHhidrat LOGP αGauss M D Etherm ΔHhidrat LOGP αGauss M Etherm Removed: 35j ΔHhidrat LogP αGauss M | Ol Parameter 25 54.3461 % 35.5475 % 0.0349 24 66.1946 % 54.2632 % 0.0024 23 74.8349 % | S V M Etherm EA IP αHypher S V M Etherm μ αHypher Removed: 35t S LogP M Etherm δ | Parameter 25 49.2795 % 28.3946 % 0.0703 24 63.5101 % 47.5458 % 0.0105 23 77.1682 % | Descriptors S A _{super} ΔH _{hidrat} M D E _{therm} ω S A _{super} ΔH _{hidrat} M D E _{therm} ω Removed: 35j S A _{super} ΔH _{hidrat} M D E _{therm} ω |
| R² adj 83.0324 % T7.7300 % α _{Gauss} M E _{therm} 82.3568 % T5.2996 % δ α _{Hypher} 84.2416 % T6.3624 % M D E _{therm} ω T6.3624 % Removed: 35j, and Table 1 Removed: 35j, and 35x 35t, and 35x | $\begin{array}{c} \textbf{Method} \\ \textbf{n} \\ R^2 \\ R^2_{adj} \\ \textbf{p-value} \\ \textbf{n} \\ R^2 \\ R^2_{adj} \\ \textbf{p-value} \\ \textbf{n} \\ \textbf{n} \\ R^2 \\ R^2_{adj} \end{array}$ | 25 54.5836 % 35.8828 % 0.0337 24 64.2902 % 54.3708 % 0.0013 23 78.4809 % 72.1518 % | Descriptors Asuper ΔHhidrat LogP αGauss M D Etherm ΔHhidrat LogP αGauss M Etherm Removed: 35j ΔHhidrat LogP αGauss M Etherm Removed: 35j | Ol Parameter 25 54.3461 % 35.5475 % 0.0349 24 66.1946 % 54.2632 % 0.0024 23 74.8349 % 65.398 % | S V M Etherm EA IP αHypher S V M Etherm μ αHypher Removed: 35t S LogP M Etherm δ αHypher Removed: | Parameter 25 49.2795 % 28.3946 % 0.0703 24 63.5101 % 47.5458 % 0.0105 23 77.1682 % 66.5134 % | Descriptors S A _{Super} ΔH _{hidrat} M D E _{therm} ω S A _{Super} ΔH _{hidrat} M D E _{therm} ω Removed: 35j S A _{Super} ΔH _{hidrat} M D E _{therm} ω Removed: 35j |
| Removed: 35j, 35t, and 35x 35t, and 35x | $\begin{array}{c} \textbf{Method} \\ \textbf{n} \\ R^2 \\ R^2_{adj} \\ \textbf{\textit{p-}value} \\ \\ \textbf{n} \\ \textbf{\textit{n}} \\ \\ \\ \\ \textbf{\textit{n}} \\ \\ \\ \\ \textbf{\textit{n}} \\ \\ \\ \\ \\ \textbf{\textit{n}} \\ \\ \\ \\ \\ \\ \\ \\ \\ \\ \\ \\ \\ \\ \\ \\ \\ \\ $ | 25 54.5836 % 35.8828 % 0.0337 24 64.2902 % 54.3708 % 0.0013 23 78.4809 % 72.1518 % | Descriptors Asuper ΔHhidrat LogP αGauss M D Etherm ΔHhidrat LogP αGauss M Etherm Removed: 35j ΔHhidrat LogP αGauss M Etherm Removed: 35j and 35t | Ol Parameter 25 54.3461 % 35.5475 % 0.0349 24 66.1946 % 54.2632 % 0.0024 23 74.8349 % 65.398 % | S V M Etherm EA IP αHypher S V M Etherm μ αHypher Removed: 35t S LogP M Etherm δ αHypher Removed: 35j and 35t | Parameter 25 49.2795 % 28.3946 % 0.0703 24 63.5101 % 47.5458 % 0.0105 23 77.1682 % 66.5134 % | S A _{super} ΔH _{hidrat} M D E _{therm} ω S A _{super} ΔH _{hidrat} M D E _{therm} ω Removed: 35j S A _{super} ΔH _{hidrat} M D E _{therm} ω Removed: 35j and 35t |
| Removed: 35j, 35t, and 35x 35t, and 35x | $\begin{array}{c} \textbf{Method} \\ \textbf{n} \\ R^2 \\ R^2_{adj} \\ \textbf{\textit{p-}value} \\ \\ \textbf{n} \\ \textbf{\textit{n}} \\ \\ \\ \\ \textbf{\textit{n}} \\ \\ \\ \\ \textbf{\textit{n}} \\ \\ \\ \\ \\ \textbf{\textit{n}} \\ \\ \\ \\ \\ \\ \\ \\ \\ \\ \\ \\ \\ \\ \\ \\ \\ \\ $ | 25 54.5836 % 35.8828 % 0.0337 24 64.2902 % 54.3708 % 0.0013 23 78.4809 % 72.1518 % | Descriptors Asuper ΔHhidrat LOGP αGauss M D Etherm ΔHhidrat LOGP αGauss M Etherm Removed: 35j ΔHhidrat LOGP αGauss M Etherm Removed: 35j and 35t ΔHhidrat LOGP αGauss M Etherm | Ol Parameter 25 54.3461 % 35.5475 % 0.0349 24 66.1946 % 54.2632 % 0.0024 23 74.8349 % 65.398 % | S V M Etherm EA IP αHypher S V M Etherm μ αHypher Removed: 35t S LogP M Etherm δ αHypher Removed: 35j and 35t | Parameter 25 49.2795 % 28.3946 % 0.0703 24 63.5101 % 47.5458 % 0.0105 23 77.1682 % 66.5134 % | Descriptors S Asuper ΔHhidrat M D Etherm ω S Asuper ΔHhidrat M D Etherm ω Removed: 35j S Asuper ΔHhidrat M D Etherm ω Removed: 35j and 35t |
| | $\begin{array}{c} \textbf{Method} \\ \textbf{n} \\ R^2 \\ R^2_{adj} \\ \textbf{\textit{p-value}} \\ \textbf{\textit{p-value}} \\ \textbf{\textit{n}} \\ R^2 \\ R^2_{adj} \\ \textbf{\textit{p-value}} \\ \textbf{\textit{n}} \\ R^2 \\ \textbf{\textit{m}} \\ R^2 \\ \textbf{\textit{m}} \\ $ | Parameter | Descriptors Asuper ΔHhidrat LOGP αGauss M D Etherm ΔHhidrat LOGP αGauss M Etherm Removed: 35j ΔHhidrat LOGP αGauss M Etherm Removed: 35j and 35t ΔHhidrat LOGP αGauss M Etherm | Ol Parameter 25 54.3461 % 35.5475 % 0.0349 24 66.1946 % 54.2632 % 0.0024 23 74.8349 % 65.398 % 0.0004 | S V M Etherm EA IP αHypher S V M Etherm μ αHypher Removed: 35t S LogP M Etherm δ αHypher Removed: 35j and 35t S V M Etherm δ αHypher | Parameter 25 49.2795 % 28.3946 % 0.0703 24 63.5101 % 47.5458 % 0.0105 23 77.1682 % 66.5134 % 0.0007 | Descriptors S A _{Super} ΔH _{hidrat} M D E _{therm} ω S A _{Super} ΔH _{hidrat} M D E _{therm} ω Removed: 35j S A _{Super} ΔH _{hidrat} M D E _{therm} ω Removed: 35j and 35t S A _{Super} ΔH _{hidrat} M D E _{therm} ω |

| Fungus | Fonsecaea compacta (F. COM) | | | | | | |
|---------------------|-----------------------------|--|-----------|---|-----------|--|--|
| Method | Semi | empirical | | MOIN | | DFT | |
| | Parameter | Descriptors | Parameter | | Parameter | Descriptors | |
| n | 25 | S A _{super} | 25 | A _{super} LogP | 25 | S V ΔH _{hidrat} | |
| R^2 | 74.5204 % | ΔH_{hidrat} R | 57.2561 % | $R \alpha_{Gauss} M$ | 74.6618 % | LogP R M D | |
| R_{adj}^2 | 59.2327 % | $\alpha_{Hypher}\;M\;\;D$ | 39.6556 % | E_{therm} δ | 56.5631 % | Etherm ω α Hypher | |
| <i>p</i> -value | 0.0035 | E _{therm} EA | 0.0222 | | 0.0082 | | |
| n | 24 | S A _{super} V | 24 | A _{super} LogP | 24 | S V ΔH _{hidrat} | |
| R^2 | 83.9653 % | ΔH_{hidrat} R | 61.4335 % | Μδ | 81.5756 % | LogP R M D | |
| R_{adj}^2 | 71.631 % | $\alpha_{\text{Hypher}} M D$ | 53.3143 % | | 67.4029 % | Etherm ω α Hypher | |
| <i>p</i> -value | 0.0010 | E _{therm} η Removed: 35 j | 0.0008 | Removed: 35 u | 0.0022 | Removed: 35 j | |
| n | 23 | S A _{super} | 23 | A _{super} LogP | 23 | S V ΔH _{hidrat} | |
| R^2 | 88.7538 % | $\Delta H_{hidrat} R$ | 68.1498 % | Μδ | 87.3281 % | LogP R M D | |
| R_{adj}^2 | 80.968 % | α _{Hypher} M D | 61.072 % | Removed: | 76.7681 % | Etherm ω α Hypher | |
| <i>p</i> -value | 0.0001 | E _{therm} EA Removed: 35j and 35m | 0.0002 | 35j and 35u | 0.0005 | Removed: 35j and 35m | |
| Fungus | | | | ypseum (M. GYP) | | | |
| Method | | empirical | _ | MOIN | DFT | | |
| | Parameter | Descriptors | Parameter | 0 4 1/ 14 | Parameter | Descriptors | |
| n n ² | 25 | ΔH _{hidrat} LogP | 25 | S A _{super} V M | 25 | A _{super} R α _{Gauss} | |
| R^2 | 53.3967 % | α _{Hypher} M G D | 67.0062 % | E _{therm} α _{Hypher} | 52.7059 % | M D E _{therm} | |
| R_{adj}^2 | 34.2071 % | E _{therm} | 56.0083 % | | 36.9411 % | | |
| <i>p</i> -value | 0.0401 | | 0.0013 | | 0.0216 | | |
| n n | 24 | ΔH _{hidrat} LogP | 24 | S A _{super} V M | 24 | A _{super} R α _{Gauss} | |
| R^2 | 65.1781 % | α _{Hypher} M G D | 73.5802 % | E _{therm} α _{Hypher} | 71.0009 % | M D Etherm | |
| R_{adj}^2 | 49.9435 % | Etherm | 64.2556 % | Removed: | 60.766 % | Removed: 35n | |
| <i>p</i> -value | 0.0076 | Removed: 35n | 0.0004 | 35g | 0.0007 | | |
| n n² | 23 | ΔH _{hidrat} LogP | 23 | S A _{super} V M | 23 | A _{super} R α _{Gauss} | |
| R^2 | 71.7962 % | α _{Hypher} M G | 77.0163 % | E _{therm} α _{Hypher} | 79.4566 % | M D E _{therm} | |
| R_{adj}^2 | 61.2197 % | E _{therm} | 68.3974 % | Removed: | 71.7528 % | Removed: 35j | |
| <i>p</i> -value | 0.0010 | Removed: 35j and 35n | 0.0002 | 35g and 35t | 0.0001 | and 35n | |
| n | 22 | ΔH _{hidrat} LogP | 22 | S_A _{super} V M | 22 | Asuper R αGauss | |
| R^2 | 81.6653 % | α _{Hypher} M G | 81.8534 % | $E_{therm} \; \alpha_{Hypher}$ | 89.845 % | M D Etherm | |
| R_{adj}^2 | 74.3314 % | Etherm | 74.5947 % | Dama | 85.783 % | Damaya da 05' | |
| <i>p</i> -value | 0.0001 | Removed: 35j , 35n , and 35r | 0.0001 | Removed: 35g , 35p , and 35t | 0.0000 | Removed: 35j , 35n , and 35r | |

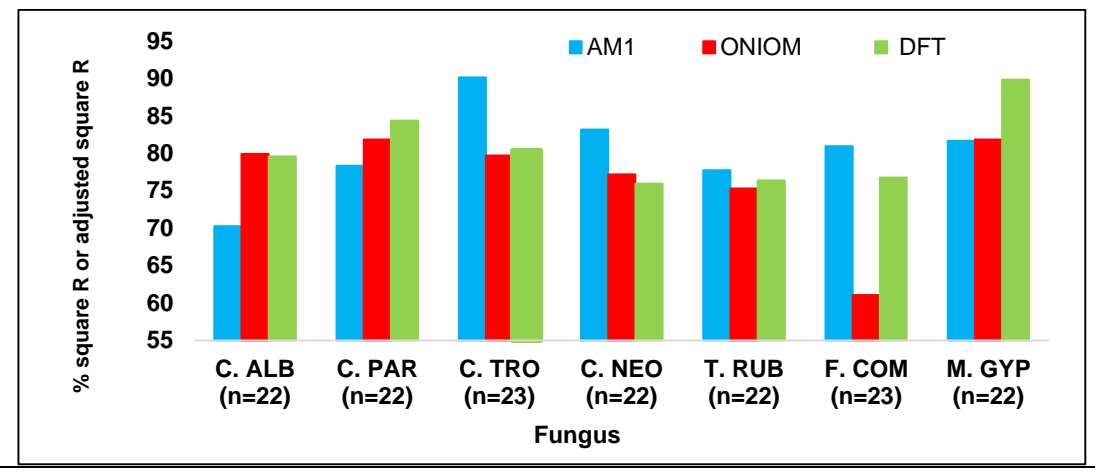


Figure 32. Comparison of R^2_{adj} (C. ALB, C. PAR, C. TRO, T. RUB, and F. $\overline{\text{COM}}$) and R^2 (C. NEO and M. GYP) for the different computational methods. Source: This investigation.

The model designed to C. ALB with full DFT shows an increase of 9% of its R_{adi}^2 value with respect to the one found with AM1, and it is comparable with the one obtained using ONIOM. In C. PAR, the DFT based-model has a 6% improvement with respect to the AM1 based-model, while the ONIOM based-model only has a 3.5% improvement. Also, in M. GYP, the DFT based-model shows outstanding results with values of R_{adi}^2 11% and R^2 9% better than AM1, but ONIOM has statistical parameters similar to the semiempirical model. For M. GYP and C. NEO the R^2 is the parameter used for comparison because all models have the same number of independent variables. For the other four fungi, the model obtained with the AM1 method has the best statistical performance. In the case of C. TRO, the AM1 based-model shows a R_{adi}^2 value about 10% better than the ONIOM and DFT based-models; for C. NEO, the model with AM1 shows an increase in the value of R² of 6% and 7% with respect to ONIOM and DFT, respectively. On another hand, for T. RUB the three models obtained have similar values of R^2 and R^2_{adi} . Finally, for F. COM, the AM1 based-model shows better results too, with an improvement of 4% versus DFT and almost 20% versus ONIOM. Together, these results indicate that, when considering the relationship statistical quality/computational cost, models obtained with the AM1 semiempirical method are the preferred ones. We also propose that, despite the computational cost, models obtained at DFT or ONIOM level which improve the R_{adi}^2 value by, at least, 10% over the AM1 model can be used as working models. According to these, the ONIOM and DFT based-models designed for C. PAR, although show better R_{adj}^2 , do not exceed the proposed 10%; while the DFT based-model for C. ALB and M. GYP satisfies the suggest condition. Considering the results shown, it is concluded that molecular descriptors obtained by means of the semiempirical AM1 method renders satisfactory models to study the antifungal activity of these fungal species. The AM1 method drastically reduces the

computational cost and the statistical performance of the obtained models is comparable and even better than models obtained using higher theoretical levels. It is worth to mention that similar results were obtained by Netzeva *et al*⁹⁵ studing the toxicity of a heterogeneous set of 568 compounds to the fish fathead minnow, concluding that a high level of theory does not contribute noticeably to the quality of the derived QSAR models. The explicit models obtained (and their statistical parameters) are given by Equations [12] to [18].

$$FA (C.ALB) = 93.2903 + 3.81602 \Delta H_{hidrat} + 3.6191 \log P + 9.99023 \alpha_{Hypher}$$

$$- 0.690569 M - 129.274 G - 0.372433 D - 0.508553 E_{Therm}$$

$$n = 22 R^2 = 80.18\% R_{adj}^2 = 70.27\% SD = 0.33 F = 8.09$$

$$FA(C.PAR) = 68.7941 - 0.0447836 V + 1.6055 LogP - 0.75944 R + 2.9113 \alpha_{Hypher}$$
 [13]
- 14.0354 G + 366.05 μ
 $n = 22 R^2 = 84.55\% R_{adj}^2 = 78.36\% SD = 0.31 F = 13.68$

$$FA (C.TRO) = 88.6177 + 0.0376289 A_{Super} - 0.160267 V - 1.82846 \Delta H_{hidrat}$$

$$- 1.71038 R + 4.28647 \alpha_{Hypher} + 0.245038 M + 0.231886 E_{Therm}$$

$$+ 730.669 \mu$$

$$n = 23 R^2 = 93.74\% R_{adi}^2 = 90.16\% SD = 0.25 F = 26.20$$

$$FA (C.NEO) = 14.9618 - 0.220851 S + 0.0494583 A_{Super} + 2.22492 LogP$$

$$- 0.235412 R + 0.140722 \alpha_{Gauss} + 0.428902 D - 0.0429904 E_{Therm}$$

$$n = 22 R^2 = 83.20\% R_{adj}^2 = 74.80\% SD = 0.34 F = 9.90$$

$$FA (T.RUB) = 24.783 + 1.26492 \Delta H_{hidrat} + 3.68804 LogP + 0.274779 \alpha_{Gauss} - 0.0940484 M - 0.152097 E_{Therm}$$

$$n = 22 R^2 = 83.03\% R_{adj}^2 = 77.73\% SD = 0.24 F = 15.66$$

$$FA (F.COM) = 1.96606 - 0.587858 \, S + 0.0400735 \, A_{Super} - 1.38585 \, \Delta H_{hidrat}$$
 [17]
- 1.65637 R + 2.61133 $\alpha_{Hypher} + 0.211958 \, M + 0.251922 \, D$
+ 0.189147 $E_{Therm} - 462.171 \, EA$
 $n = 23 \, R^2 = 88.75\% \, R_{adj}^2 = 80.97\% \, SD = 0.25 \, F = 11.40$

$$FA (M.GYP) = 33.4849 - 38.3951 \, G + 1.10379 \, \Delta H_{hidrat} + 2.96793 \, LogP$$
 [18]
 $+ 3.12171 \, \alpha_{Hypher} - 0.222482 \, M - 0.184206 \, E_{Therm}$
 $n = 22 \, R^2 = 81.67\% \, R_{adj}^2 = 74.33\% \, SD = 0.32 \, F = 11.14$

In these models some common descriptors are found that explain the antifungal activity against different species. For example, the *n*-octane–water partition

92

⁹⁵ NETZEVA, Tatiana I *et al.* Description of the Electronic Structure of Organic Chemicals Using Semiempirical and Ab Initio Methods for Development of Toxicological QSARs. *J. Chem. Inf. Model.* 2005; **45**(1): 106-114

coefficient (LogP) indicates the importance of the amphipathic character of these compounds as a determinant factor in the antifungal activity. The hydration energy, another common descriptor, reveals the relationship of the antifungal activity with the thermodynamic factors involved in the solvation process. Also, the polarizability is present in all models, in this case, many QSAR studies have demonstrated the influence of this property in biological activities where the mechanism of action is related with enzymatic inhibition through a ligand-metal coordination bond such as in the cytomegalovirus DNA polymerase, farnesyltransferase, or the metalloproteinase-13⁸⁶, therefore, the polarizability value has an important influence on inhibition of the CYP51 enzyme because the mechanism involves a coordinate bond.

4.2.2 Antifungal activity of the 1,2,4-triazole derivatives obtained in this work

Once the QSAR models of Equations [12] to [18] were designed, they were used to predict the antifungal activity of 1,2,4-triazoles synthesized by cyclization of X,S-diethyl aroylimidothiocarbonates and hydrazines. Due to the large number of synthetically viable substitutions that triazole derivatives could have by different combination of precursors (Figure 29), not only the activity of the eight compounds synthesized in this work was evaluated, but also the activity of other analogous compounds which could be synthetized using the same methodology. This theoretical study allows to find the most active compounds from a large set of synthetic alternatives which will save reactants and experimental time. Table 10 summarizes the antifungal activities predicted for different 1,2,4-triazole derivatives expressed as pIC₈₀, where higher pIC₈₀ values correspond to better antifungal activities. It should be noted that the numerical values obtained are not comparable with the reference compounds shown in Figure 31 because their structures are different, but these results allow to identify the best antifungal compounds among the synthetically viable study set.

Table 10. Predicted antifungal activity (as pIC₈₀) of the 1,2,4-triazoles derivatives that could be synthetized by means of the methodology used in this work. Source: This investigation.

| F | Х | | 0 | | | S | |
|--------|---|---------|---------|-----------------|---------|---------|-----------------|
| Fungus | R/R₁ | Н | Ph | CH ₃ | Н | Ph | CH₃ |
| | 2,4-Cl ₂ Ph | 55.317 | 68.280 | 63.159 | 70.903 | 84.029 | 78.907 |
| | 2-furyl | 24.231 | 44.687 | 35.672 | 39.736 | 60.344 | 52.565 |
| | 2-thienyl | 14.732 | 30.777 | 23.941 | 30.237 | 46.331 | 39.798 |
| | 3,4,5-(OCH ₃) ₃ Ph | 22.477 | 35.741 | 30.345 | 37.991 | 51.398 | 46.051 |
| | 3,5-(CH ₃) ₂ Ph | 54.262 | 67.053 | 61.672 | 69.728 | 82.672 | 77.394 |
| C. ALB | 3,5-(NO ₂) ₂ Ph | -51.365 | -34.187 | -42.465 | -35.876 | -18.615 | -25.579 |
| C. ALB | 4-CH₃Ph | 50.540 | 64.018 | 58.538 | 65.997 | 79.602 | 74.296 |
| | 4-CIPh | 50.185 | 64.816 | 59.313 | 65.756 | 80.527 | 75.107 |
| | 4-FPh | 46.861 | 61.601 | 56.147 | 62.366 | 77.267 | 71.861 |
| | 4-NO₂Ph | -4.248 | 11.493 | 6.061 | 11.304 | 27.044 | 21.755 |
| | 4-OCH₃Ph | 36.031 | 49.290 | 43.697 | 51.496 | 64.861 | 59.545 |
| | Ph | 46.469 | 60.396 | 54.735 | 62.010 | 76.008 | 70.495 |
| Fungus | R/R₁ | Н | Ph | CH₃ | Н | Ph | CH₃ |
| | 2,4-Cl₂Ph | 8.924 | 8.215 | 5.054 | 12.974 | 15.346 | 13.173 |
| | 2-furyl | 6.367 | 2.337 | 2.651 | 7.695 | 7.951 | 7.315 |
| | 2-thienyl | -2.097 | -4.427 | -6.590 | 0.706 | 1.573 | -0.206 |
| | 3,4,5-(OCH ₃) ₃ Ph | 7.219 | 4.421 | 2.197 | 9.306 | 10.955 | 9.185 |
| | 3,5-(CH ₃)₂Ph | 11.146 | 8.818 | 6.948 | 13.390 | 15.043 | 14.219 |
| C. PAR | 3,5-(NO ₂) ₂ Ph | -24.954 | -25.451 | -25.828 | -18.743 | -15.814 | -18.424 |
| C. PAR | 4-CH₃Ph | 11.489 | 8.735 | 6.793 | 13.855 | 14.954 | 13.895 |
| | 4-CIPh | 9.681 | 7.623 | 5.199 | 12.817 | 14.228 | 12.622 |
| | 4-FPh | 9.266 | 6.967 | 4.605 | 12.355 | 13.472 | 11.975 |
| | 4-NO₂Ph | -10.536 | -10.150 | -13.299 | -5.406 | -2.941 | -5.120 |
| | 4-OCH₃Ph | 12.187 | 8.357 | 6.742 | 13.664 | 14.277 | 13.406 |
| | Ph | 10.705 | 8.579 | 6.570 | 13.587 | 14.984 | 13.995 |
| Fungus | R/R₁ | Н | Ph | CH₃ | Н | Ph | CH₃ |
| | 2,4-Cl ₂ Ph | -15.927 | -23.214 | -26.986 | -13.302 | -14.453 | -16.214 |
| | 2-furyl | -6.535 | -24.431 | -18.224 | -9.302 | -18.723 | -15.916 |
| | 2-thienyl | -27.014 | -39.218 | -39.951 | -26.906 | -32.667 | -32.710 |
| | 3,4,5-(OCH ₃) ₃ Ph | 0.269 | -11.316 | -13.096 | -1.003 | -3.444 | -4.543 |
| | 3,5-(CH₃)₂Ph | -11.457 | -22.191 | -23.238 | -12.341 | -15.354 | -14.174 |
| C. TRO | 3,5-(NO ₂) ₂ Ph | -26.444 | -37.419 | -30.332 | -19.473 | -21.042 | -22.407 |
| o. mo | 4-CH₃Ph | -9.079 | -20.971 | -22.140 | -9.658 | -13.988 | -13.454 |
| | 4-CIPh | -12.410 | -23.063 | -25.085 | -11.588 | -15.277 | -15.772 |
| | 4-FPh | -11.951 | -23.031 | -24.944 | -11.101 | -15.534 | -15.660 |
| | 4-NO₂Ph | -24.083 | -29.650 | -33.224 | -19.300 | -20.742 | -22.379 |
| | 4-OCH₃Ph | 1.104 | -12.979 | -13.484 | -1.211 | -6.471 | -5.648 |
| | Ph | -9.133 | -19.996 | -21.177 | -8.718 | -12.673 | -11.785 |
| Fungus | R/R₁ | Н | Ph | CH ₃ | Н | Ph | CH ₃ |
| | 2,4-Cl₂Ph | 18.360 | 19.155 | 16.350 | 19.125 | 19.656 | 17.107 |
| | 2-furyl | 9.867 | 11.502 | 9.262 | 10.605 | 12.251 | 10.005 |
| C. NEO | 2-thienyl | 11.694 | 13.890 | 11.458 | 12.564 | 14.676 | 12.063 |
| | 3,4,5-(OCH ₃) ₃ Ph | 10.992 | 11.888 | 10.104 | 11.802 | 12.777 | 10.808 |
| | 3,5-(CH ₃) ₂ Ph | 14.881 | 16.675 | 14.925 | 15.647 | 17.518 | 15.578 |

| | 3,5-(NO ₂) ₂ Ph | 0.533 | -1.167 | -2.545 | 1.310 | -0.307 | -1.607 |
|----------|---|---------|---------|-----------------|---------|---------|-----------------|
| | 4-CH₃Ph | 15.226 | 17.349 | 15.469 | 16.009 | 18.153 | 16.145 |
| | 4-CIPh | 17.414 | 18.121 | 16.222 | 18.186 | 18.955 | 16.923 |
| | 4-FPh | 16.247 | 16.758 | 14.874 | 17.033 | 17.591 | 15.546 |
| | 4-NO₂Ph | 9.437 | 8.499 | 6.564 | 10.231 | 9.442 | 7.360 |
| | 4-OCH₃Ph | 14.239 | 16.661 | 14.758 | 15.036 | 17.479 | 15.455 |
| | Ph | 15.052 | 16.699 | 14.939 | 15.833 | 17.506 | 15.588 |
| Fungus | R/R₁ | Н | Ph | CH ₃ | Н | Ph | CH ₃ |
| - angar | 2,4-Cl ₂ Ph | 24.136 | 33.419 | 26.580 | 29.372 | 38.682 | 31.618 |
| | 2-furyl | 8.401 | 21.078 | 11.843 | 13.553 | 26.226 | 17.914 |
| | 2-thienyl | 16.061 | 27.463 | 19.708 | 21.280 | 32.628 | 24.666 |
| | 3,4,5-(OCH ₃) ₃ Ph | 8.395 | 17.657 | 11.013 | 13.701 | 22.993 | 16.031 |
| | 3,5-(CH ₃) ₂ Ph | 23.315 | 32.830 | 26.012 | 28.488 | 38.134 | 30.959 |
| | 3,5-(NO ₂) ₂ Ph | -21.151 | -11.178 | -19.243 | -15.765 | -5.845 | -12.973 |
| T. RUB | 4-CH₃Ph | 22.023 | 31.846 | 24.851 | 27.215 | 37.115 | 29.847 |
| | 4-CIPh | 22.265 | 32.137 | 25.138 | 27.502 | 37.449 | 30.184 |
| | 4-FPh | 20.475 | 30.370 | 23.393 | 25.719 | 35.651 | 28.369 |
| | 4-NO₂Ph | -0.220 | 9.437 | 2.629 | 5.176 | 14.811 | 7.722 |
| | 4-OCH₃Ph | 15.668 | 25.380 | 18.457 | 20.897 | 30.665 | 23.479 |
| | Ph | 19.731 | 29.708 | 22.682 | 24.947 | 34.985 | 27.640 |
| Fungus | R/R₁ | Н | Ph | CH ₃ | Н | Ph | CH ₃ |
| | 2,4-Cl ₂ Ph | 2.900 | -6.624 | -9.219 | -2.590 | -11.870 | -14.253 |
| | 2-furyl | 7.245 | -9.867 | -2.554 | -0.443 | -14.725 | -11.288 |
| | 2-thienyl | -9.963 | -21.706 | -22.191 | -15.056 | -26.607 | -27.194 |
| | 3,4,5-(OCH ₃) ₃ Ph | 9.259 | -0.769 | -0.184 | 3.791 | -5.783 | -5.225 |
| | 3,5-(CH ₃) ₂ Ph | 2.517 | -8.503 | -6.223 | -5.063 | -13.763 | -11.221 |
| F. COM | 3,5-(NO ₂) ₂ Ph | -9.595 | -21.843 | -17.507 | -15.307 | -27.146 | -26.659 |
| F. COIVI | 4-CH₃Ph | 4.861 | -5.980 | -3.905 | -1.549 | -11.144 | -8.914 |
| | 4-CIPh | 4.340 | -6.584 | -5.548 | -1.052 | -11.586 | -10.564 |
| | 4-FPh | 4.279 | -6.944 | -5.859 | -1.117 | -11.914 | -10.859 |
| | 4-NO₂Ph | -5.680 | -16.434 | -16.616 | -11.232 | -21.475 | -21.701 |
| | 4-OCH₃Ph | 11.902 | 1.106 | 3.546 | 4.996 | -4.132 | -1.422 |
| | Ph | 8.798 | -2.903 | -0.564 | 1.877 | -8.106 | -5.570 |
| Fungus | R/R₁ | Н | Ph | CH ₃ | Н | Ph | CH ₃ |
| | 2,4-Cl₂Ph | 26.831 | 31.610 | 27.958 | 32.217 | 37.040 | 33.412 |
| | 2-furyl | 11.914 | 19.033 | 13.674 | 17.275 | 24.437 | 20.029 |
| | 2-thienyl | 10.560 | 16.475 | 12.328 | 15.938 | 21.853 | 17.795 |
| | 3,4,5-(OCH ₃) ₃ Ph | 11.349 | 16.329 | 12.604 | 16.729 | 21.747 | 18.031 |
| | 3,5-(CH₃)₂Ph | 25.239 | 30.226 | 26.514 | 30.585 | 35.641 | 31.938 |
| M. GYP | 3,5-(NO ₂) ₂ Ph | -21.851 | -16.285 | -21.485 | -16.489 | -10.880 | -15.102 |
| 311 | 4-CH₃Ph | 23.844 | 29.064 | 25.303 | 29.191 | 34.448 | 30.758 |
| | 4-CIPh | 24.483 | 29.689 | 25.912 | 29.864 | 35.117 | 31.379 |
| | 4-FPh | 22.746 | 27.931 | 24.185 | 28.125 | 33.348 | 29.611 |
| | 4-NO₂Ph | 0.063 | 5.198 | 1.429 | 5.460 | 10.597 | 6.869 |
| | 4-OCH₃Ph | 17.922 | 23.136 | 19.339 | 23.268 | 28.520 | 24.825 |
| | Ph | 22.389 | 27.669 | 23.872 | 27.778 | 33.062 | 29.308 |

The results indicate that the predicted antifungal activity of the 1,2,4-triazole derivatives exhibits large pIC $_{80}$ values for most fungi, being particularly remarkable

the activity against C. ALB and M. GYP, followed by T. RUB, C. NEO, and C. PAR, while the predicted activity for C. TRO and F. COM is smaller. On the other hand, an important dependence of the antifungal activity is observed as function of the aromatic substituent R. In fact, the most active compounds have the same substituent in the R-position. This characteristic is common to all fungi with the exception of C. PAR that shows a more irregular behavior. Then, the analysis will be focused on finding the best combination of substituents R/R₁/X that optimizes the activity against each fungus and stablish a comparison between the antifungal potential of these compounds against the different species.

The compounds with the R-substituent **2,4-dichlorophenyl** exhibit better antifungal activity in comparison with the other derivatives evaluated based on the designed models. These compounds are the most active against the five fungi: C. ALB, C. PAR, C. NEO, T. RUB, and M. GYP. Figure 33 shows the predicted antifungal activity for compounds with R = 2,4-dichlorophenyl and different substitutions in the R₁position and X-atom against the five fungal species mentioned. In general, the results indicate that these compounds have a remarkably large antifungal activity against Candida albicans. The compound T-3b-SC₂ (R₁/X = Ph/S) exhibits the best activity against all fungal species. The activity of compounds T-3c-SC₂ (R₁/X = CH₃/S), **T-3b-OC₂** (R₁/X = Ph/O), and **T-3a-SC₂** (R₁/X = H/S) against T. RUB and M. GYP is comparable, while compounds $T-3c-OC_2$ (R₁/X = CH₃/O) and $T-3a-OC_2$ (R₁/X = H/O) are the least active, mainly against C. PAR. These results also indicate that there is a preference toward sulfur-substituted systems as the most active since the activity of the thioethyl-substituted compounds is better than the ethoxy-substituted ones for the same R₁. In general, the better antifungal activity of 2,4-dichlorophenyl systems in comparison with other compounds can be precisely attributed to these halogenated substituents which are characteristic of traditional ergosterol inhibitor drugs that block the active site of CYP51. In fact, the first- and second-generation triazoles shown in Figure 7 have a common 2,4-dihalogenphenyl substituent, and the 2,4-dichlorophenyl is found specifically in **Itrazonazole 15**.

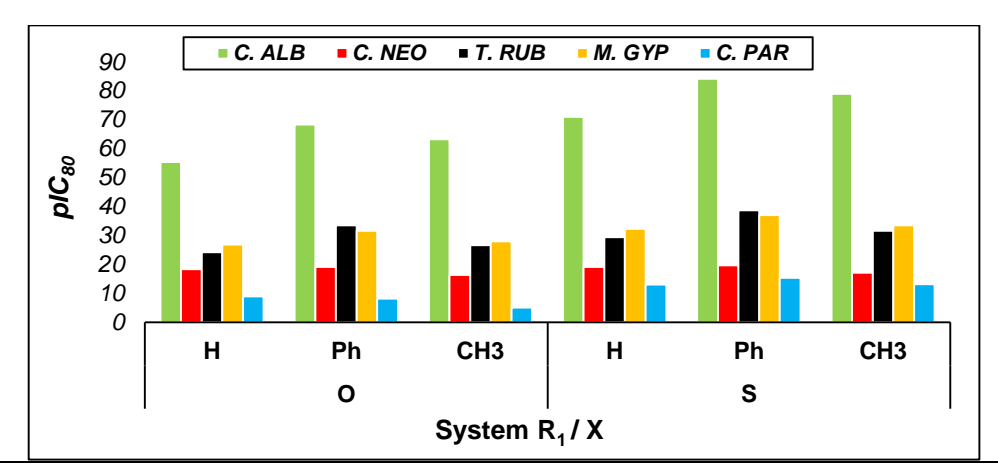


Figure 33. Antifungal activity of R = 2,4-dichlorophenyl triazoles. Source: This investigation.

The substituent **3,5-dimethylphenyl** also shows a large antifungal activity against C. ALB, C. PAR, T. RUB, and M. GYP, even larger than the 2,4-dichlorophenyl for C. PAR. In particular, the compound **T-10b-SC**₂ (R₁/X =Ph/S) exhibits the best activity overall (Figure 34), interestingly, the substituents R₁ and X are the same as the most active 2,4-dichlorophenyl compound $T-3b-SC_2$ ($R_1/X = Ph/S$). As in the previous case, the compound T-10b-SC2 is more active against C. ALB and less active against C. PAR. For the specific case of C. NEO, the second most active substituent is **4-chlorophenyl**, being the compound **T-6b-SC₂** (R₁/X= Ph/S) the best antifungal (Figure 34). Again, the best antifungal molecule has the phenyl substituent in R_1 -position and the thioethyl group (X = S). The analysis of these two systems supports the aforementioned conclusion about the improved activity of thioethylsubstituted molecules in comparison with ethoxy-substituted ones for the same R₁substituent. Also, a common pattern can be identified for the R₁ position because the phenyl group improves the activity against all fungi, which indicates the importance of hydrophobic and bulky substituents for an effective enzymatic inhibition.

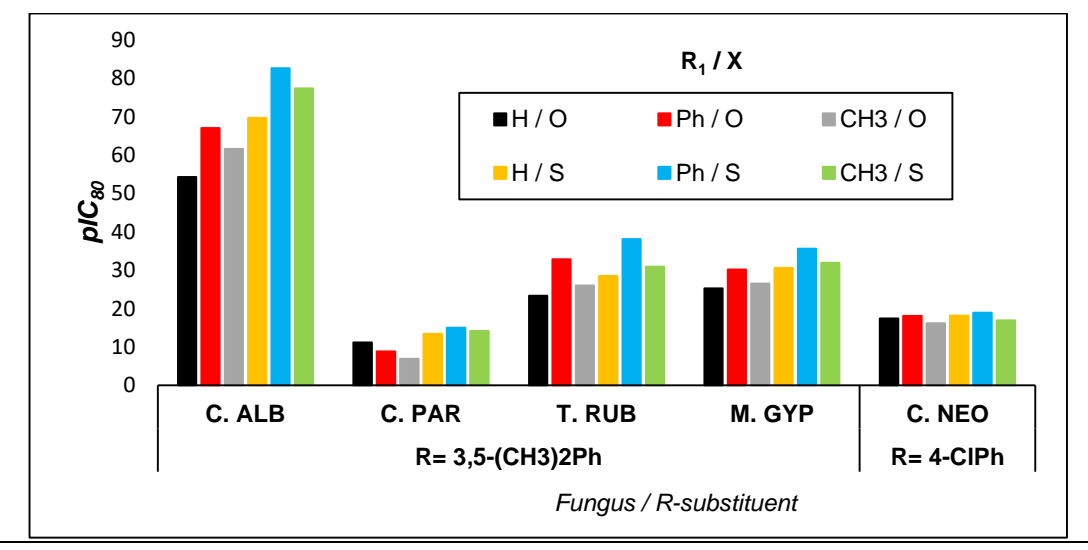


Figure 34. Antifungal activity of 3,5-dimethylphenyl- and 4-chlorophenyl-substituted triazoles. Source: This investigation.

The results in Table 10 also show that the 1,2,4-triazole derivatives are not very active against the two fungal species C. TRO and F. COM. Despite this, both methoxyphenyl-substituted systems, **4-methoxyphenyl** and **3,4,5-trimethoxyphenyl** derivatives, are the best antifungals. The plC₈₀ values of these compounds against the mentioned fungi are shown in Figure 35. In general, the activities reported for F. COM are better than for C. TRO since the plC₈₀ values of C. TRO are mostly negative, indicating high minimal inhibitory concentrations. The results evidence a better antifungal activity of 4-methoxyphenyl-substituted triazoles against F. COM in comparison to 3,4,5-trimethoxyphenyl triazoles, specifically, the compound **T-9a-OC**₂ (R₁/X = H/O, black bars in Figure 35), which also has the best

activity against C. TRO being the only with positive pIC₈₀. Some authors have reported the positive effect of the methoxy-substituent in the antifungal activity such as Gładkowski $et \, al^{96}$ who report the activity of methoxy-substituted γ -oxa- ϵ -lactones against fungi of genera *Fusarium*, *Aspergillus*, and *Candida*. Although the only way to know exactly the mechanism of action of this substituent is through molecular docking, it is possible to predict that the effect is similar to the halogenated derivatives by generating intermolecular interactions of hydrogen bond type in the active site of CYP51.

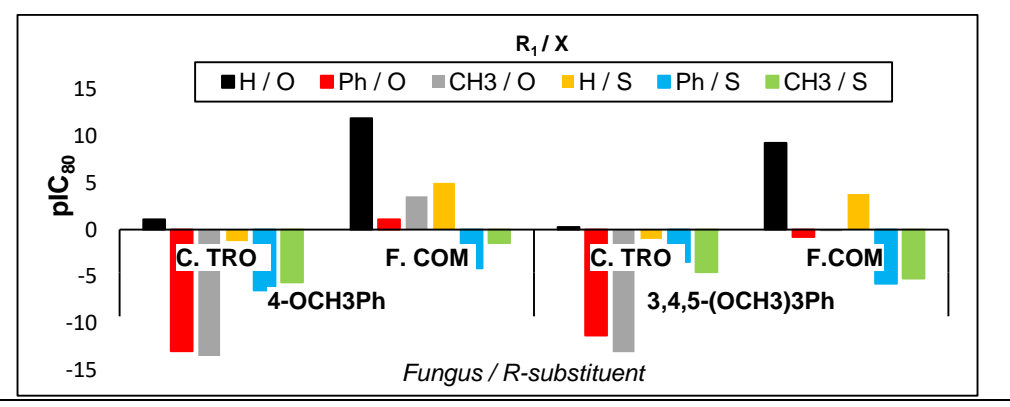


Figure 35. Antifungal activity of methoxyphenyl triazoles against C. TRO and F. COM. Source: This investigation.

In Table 10, it is also evident that both nitrophenyl-substituted systems, 4-NO₂Ph and 3,5-(NO₂)₂Ph, have negative pIC₈₀ values against all fungi indicating that these compounds are particularly ineffective as antifungals. These results correlate with the fact that aromatic nitro groups belong to a series of *Structural Alerts*⁹⁷ that are molecular substructures or reactive groups that are related to the carcinogenic and mutagenic properties of the compounds containing them, and therefore, the use of this group in biological agents is not widespread since drugs containing nitro groups have been extensively associated with mutagenicity and genotoxicity.⁹⁸ However, it is worth to mention that despite the unlikely use of nitro-containing 1,2,4-triazoles as antifungal agents, a recent investigation by the GIFBA⁹⁹ has found that precisely these nitro compounds exhibit the largest nonlinear optical response among all synthetically viable substituents which makes them feasible materials for nonlinear optical applications.

⁹⁶ GŁADKOWSKI, Witold *et al.* Synthesis and Antimicrobial Activity of Methoxy Substituted γ-Oxa-ε-lactones Derived from Flavanones. *Molecules*. 2019; **24**: 4151-4166

⁹⁷ BENIGNI, Romualdo; BOSSA, Cecilia. Structural Alerts of Mutagens and Carcinogens. *Curr Comput Aided Drug* Des. 2006; **2**(2): 169-176.

⁹⁸ NEPALI, Kunal et al. Nitro-Group-Containing Drugs. J. Med. Chem. 2019; 62(6): 2851-2893.

⁹⁹ ORTEGA MUÑOZ, Christian Camilo. Estudio computacional de las propiedades ópticas no-lineales de derivados de 1,2,4-triazoles. Trabajo de grado en Física, Universidad de Nariño, 2021

On other hand, Figure 36 shows the predicted antifungal activity of the triazole derivatives specifically synthesized in this investigation. These compounds show the highest activity against *C. albicans*, followed by *M. gypseum* and *T. rubrum*, and then C. neoformans and C. paralsiolosis. The antifungal potential of these compounds against C. tropicalis and F. compacta is considerably lower in comparison to the other species, in particular, against the former, where all triazoles have negative pIC₈₀ values. The results show that the compound with the best activity is **T-1b-SC₂** $(R/R_1/X = Ph/Ph/S, brown bars in Figure 36)$ which exhibits the best result against the four fungi species: C. ALB, C. PAR, T. RUB, and M. GYP, while the triazole T-**4a-OC**₂ (R/R₁/X = 2-furyl/H/O, blue bars in Figure 36) shows an adequate activity against C. TRO and F. COM; however, for this last fungus, the compound **T-1a-OC**₂ $(R/R_1/X = Ph/H/O)$ has the best activity. Against C. NEO, the triazole **T-3b-OC₂** $(R/R_1/X = 2,4-Cl_2Ph/Ph/O)$ exhibits the best antifungal activity; interestingly, this triazole also exhibits the second-best activity against C. ALB, T. RUB, and M. GYP. Finally, the activities of two additional compounds are important to highlight, these are the compounds **T-1a-SC₂** (R/R₁/X = Ph/H/S, purple bars) and **T-3a-OC₂** (R/R₁/X = 2,4-Cl₂Ph/H/O, gray bars) which are the second best against C. PAR and C. NEO, respectively. A general observation from the results in Figure 36 indicates that compounds with R_1 = Ph have better activities than compounds with R_1 = H for the same R/X, with exception of the activity against C. TRO, F. COM, and the 2-furyl system in C. PAR which exhibits an opposite behavior. All of this support the hypothesis about the improved antifungal activity in more hydrophobic and polarizable systems, as occurs when a sulfur atom occupies the X-position instead of an oxygen atom, in particular, for the fungi C. ALB, C. PAR, T. RUB, and M. GYP.

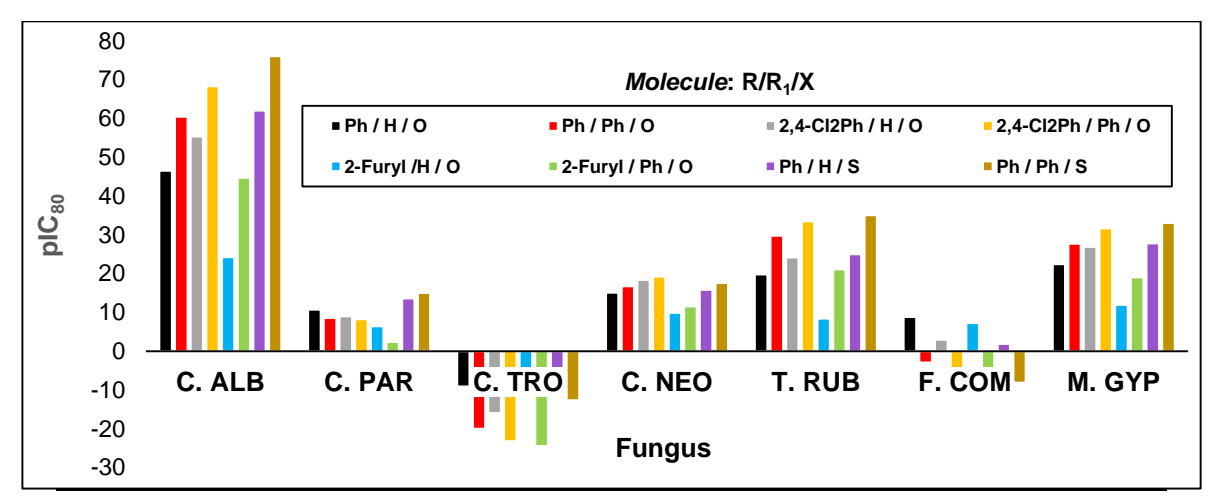


Figure 36. Predicted antifungal activity for the triazoles synthesized in this investigation. Source: This investigation.

4.2.3 Aliphatic chain effect on the antifungal activity of 1,2,4-triazoles

According to the known mechanism of action of azoles inhibiting the CYP51 enzyme (Section 3.1.3.2 Enzymatic action of azoles), the nitrogen atoms of the triazole have the function of bonding to the heme-group, while the substituted benzene blocks the substrate binding site. This interaction site is accessible through a long channel where there are also hydrophobic amino acids with which intermolecular interactions are expected to occur by means of the lateral chains. Although these lateral chains are not determinant for the antifungal activity, they play an important role in conditioning the physicochemical properties of the molecule, helping to reduce side effects, and improving the pharmacological properties, which also conditions the inhibitory effect of drug. In this section, the influence of the lateral chains is analyzed for the triazoles shown in Figure 31 and for the synthetically viable triazole derivatives shown in Figure 29.

Results for the antifungal activity of the piperazine-substituted 1,2,4-triazole derivatives (Figure 31) shown in Table 8 indicate that there is not a continuous change in the biological activity as a function of the number of carbons in the linear chain in R' position, and therefore, its effect on the antifungal activity is evaluated for R = H. With the purpose of determine an optimal size for the linear carbon chain length in R' position, a simple quadratic model of the antifungal activity as function of the number of carbon atoms was proposed. The results in Figure 37 show regression values R^2 greater than 0.5 for all studied fungi.

In order to ascertain the number of carbons in the aliphatic chain R' that optimizes the antifungal activity, the minimum of the function is calculated by means of $d(IC_{80})/dn=0$. The obtained results indicate that the optimal number of carbons is six for *C. neoformans* and *T. rubrum*, five for *C. albicans* and *F. compacta*, and eight for *M. gypseum*. These results allow to conclude that, for these fungi, very large or very short alkyl chains decrease the biological activity possibly because very long aliphatic chains fail to enter the active site of the enzyme and very short aliphatic chains are not competitive to the substrate. On the other hand, for *C. parapsiolosis* and *C. tropicalis* the activity is optimized if there are not alkyl chains in the R' position because the minimum of the function is negative for these two species of fungi.

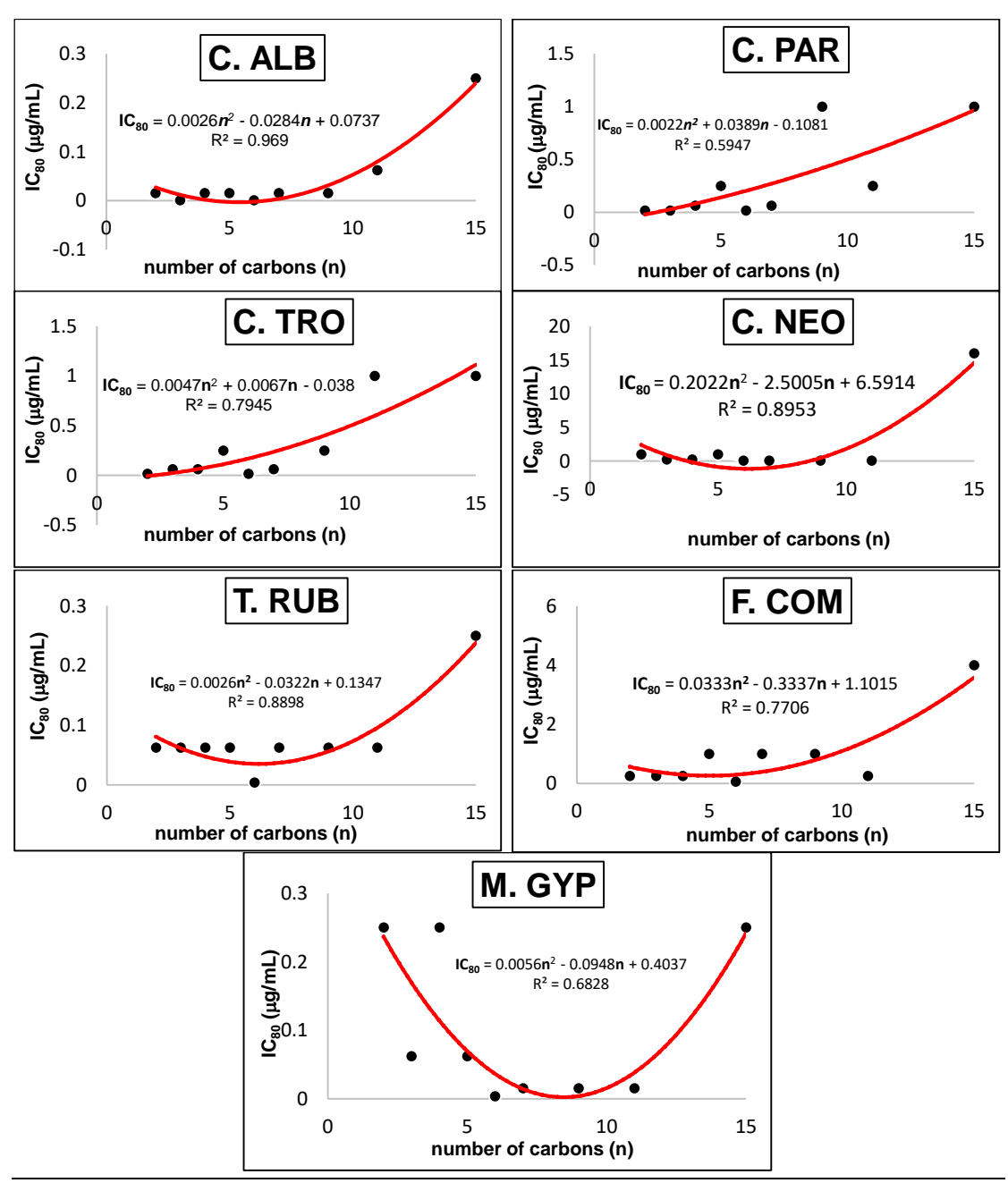


Figure 37. Effect of the alkyl chain length (R') on the antifungal activity of piperazine-substituted 1,2,4-triazoles. Source: This investigation.

On the other hand, the effect of the alkyl chains on the antifungal activity can be also analyzed for the case of the 1,2,4-triazole derivatives obtained using the synthetic methodology of this investigation, since these derivatives have an O-ethyl or S-ethyl group as a substituent on the triazole ring. This substituent R₂ can be easily modified

in the first stage of the synthetic methodology, which consists on the generation of the aroylimidothiocarbamate (see Scheme 14), where ethanol for X=O (or ethanethiol for X=S) can be substituted by other linear (thio-)alcohols as alkylation reagents. In this way, once the most active antifungals were found in the previous section, the next step is to find the number of carbons in the alkyl chain that improves the activity of the mentioned compounds for each fungus through prediction of the activities of the corresponding derivatives shown in Figure 38. An alkyl chain up to 14 carbon atoms was chosen because 1-tetradecanol is the last linear alcohol in liquid form; the next one, the 1-pentadecanol, is a white solid.

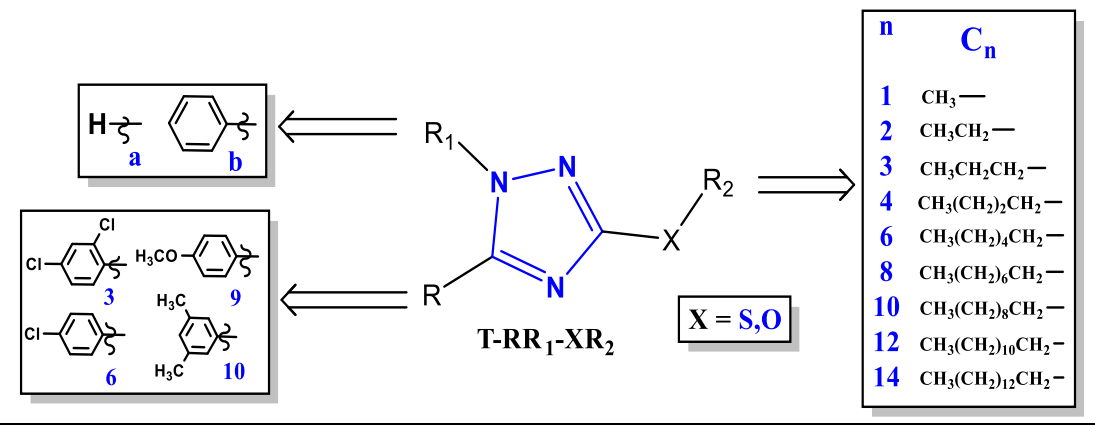


Figure 38. 1,3,5-substituted-1,2,4-triazoles with different X-alkyl chains. Source: This investigation.

The predicted antifungal activities are summarized in Figure 39 for C. ALB, C. PAR, T. RUB, M. GYP, and C. NEO which have the system $R/R_1/X = 2.4-Cl_2Ph/Ph/S$ as the most active and the system $R/R_1/X = 3.5-(CH_3)_2Ph/Ph/S$ as the second most active for the first four fungi while the system $R/R_1/X = 4$ -ClPh/ Ph/S is the second most active for C. NEO. In general, it is observed that the effect of the aliphatic chain does not significantly change the antifungal activity as compared to the effect generated by a modification of the substituents in positions R, R₁, or X. Despite this, particular trends for each fungus can be drawn. In the case of C. ALB, which continue to show remarkable activity as compared to other species, the biological activity shows a peak of optimal activity when the alkyl chain has 4 carbons (which can be achieved using butane-1-thiol as alkylating agent) for both molecules: T-3b-SC4 (R = 2,4-Cl₂Ph) and **T-10b-SC**₄ (R = 3,5-(CH₃)₂Ph). For T. RUB, the behavior is similar, but for this fungus the optimal activity is obtained with alkyl chains of 6 to 8 carbons, therefore, T-3b-SC₆ and T-10b-SC₈ are the most active; in fact, an average optimal chain of 7 carbons can be stablished for this fungus. Interestingly, for C. PAR the activity decreases almost linearly with the increase of the length of the carbon chain, and therefore the most active compounds are T-3b-SC₁ and T-10b-SC₁, which can be synthesized by using methanethiol as alkylating agent in the mentioned step.

Finally, for C. NEO and M. GYP, the behavior is the opposite to C. PAR, being the triazole with a chain of 14 carbons **T-3b-SC**₁₄ (R = 2,4-Cl₂Ph) the best antifungal, while the second most active is **T-6b-SC**₁₄ (R = 4-ClPh) for C. NEO and **T-10b-SC**₁₄ (R = 3,5-(CH₃)₂Ph) for M. GYP.

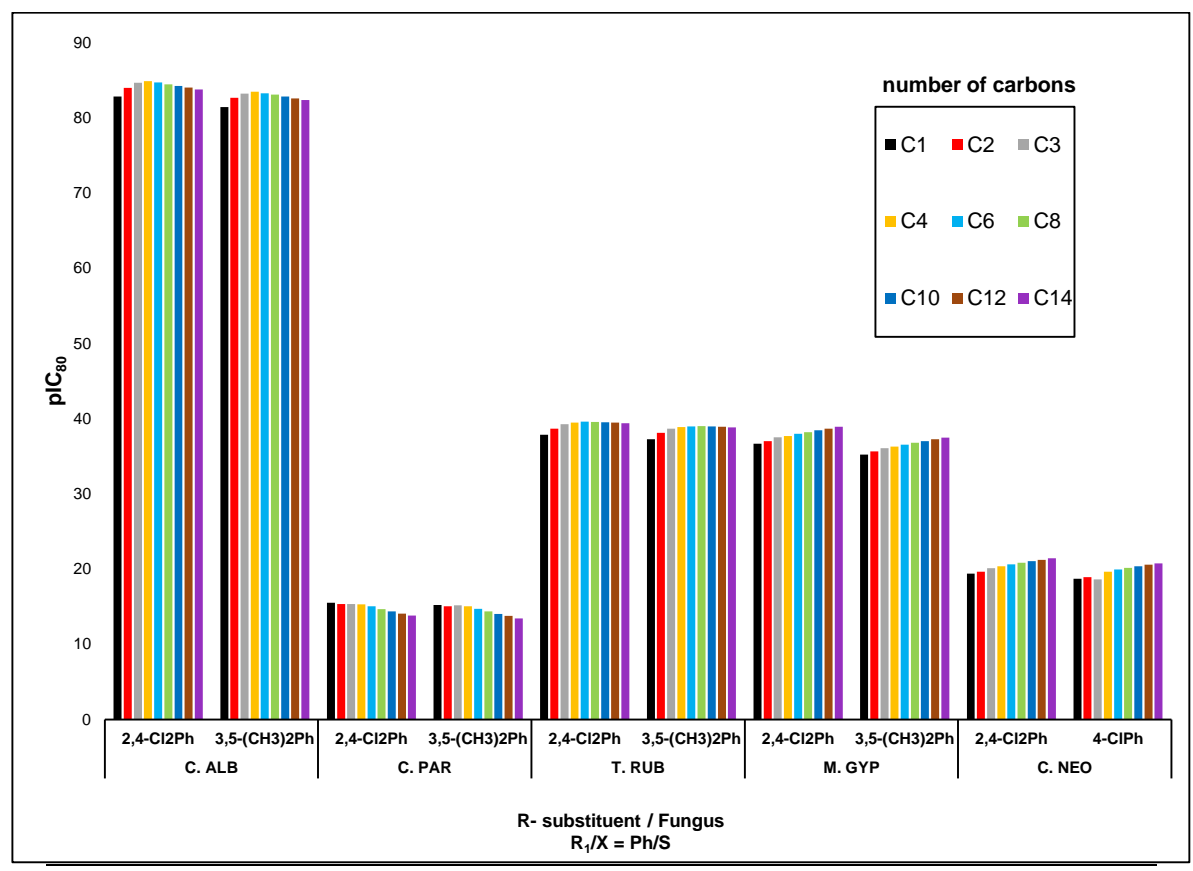


Figure 39. Effect of X-alkyl chains of 1,3,5-substituted-1,2,4-triazoles on the antifungal activity against C. ALB, C. PAR. C. NEO, T. RUB, and M. GYP. Source: This investigation.

Finally, for the fungi C. TRO and F. COM, the best antifungal is the system R/R₁/X = 4-OCH₃Ph/H/O, therefore, the predicted antifungal activity due to variations in the O-alkyl chain is shown in Figure 40. It is observed that the effect of aliphatic chain for both fungi is similar to the observed in C. PAR where the methoxy-group, which correspond the triazole **T-9a-OC**₁, exhibits the best antifungal potential. In these two cases the effect of the alkyl chains is more evident when compared to the fungi in Figure 39, in particular, for F. COM the most active compound has a comparable activity as the most active system against C. PAR.

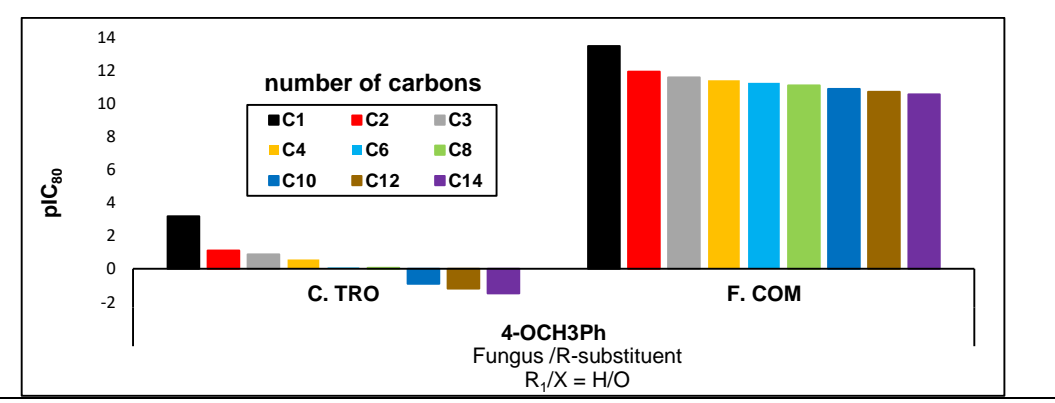


Figure 40. Effect of X-alkyl chains of 1,3,5-substituted-1,2,4-triazoles on the antifungal activity against C. TRO and F. COM. Source: This investigation.

4.2.4 Effect of additional modifications on the antifungal activity of 1,2,4-triazoles

An important part of the process of developing potential drugs is to build different systems with a large amount different substitutions in order to explore a wide chemical space, and then, evaluate, either theoretically or experimentally, their *in vitro* activity. According to this and the structure of commercial antifungal drugs (Figure 7), in this section, the effect of the substitution by fluorine atoms in different positions of the previously obtained molecules is evaluated due to the importance of this halogen in the antifungal activity. The evaluated compounds are summarized in Figure 41. In fact, many drugs and drug candidates in clinical development have halogenated structures. Initially, the insertion of halogen atoms was predominantly performed to exploit their steric effects, however, halogens influence several processes rather than steric aspects alone. The majority of halogenated drugs are fluorine drugs (57%), followed by chlorine ones (38%), while bromine is rare (4%), and the only iodine drug is the thyroid hormone thyroxine 100.

.

¹⁰⁰ HERNANDES, Marcelo *et al.* Halogen atoms in the modern medicinal chemistry: Hints for the drug design. *Curr. Drug Targets*, 2010; **11**(3): 303-314.

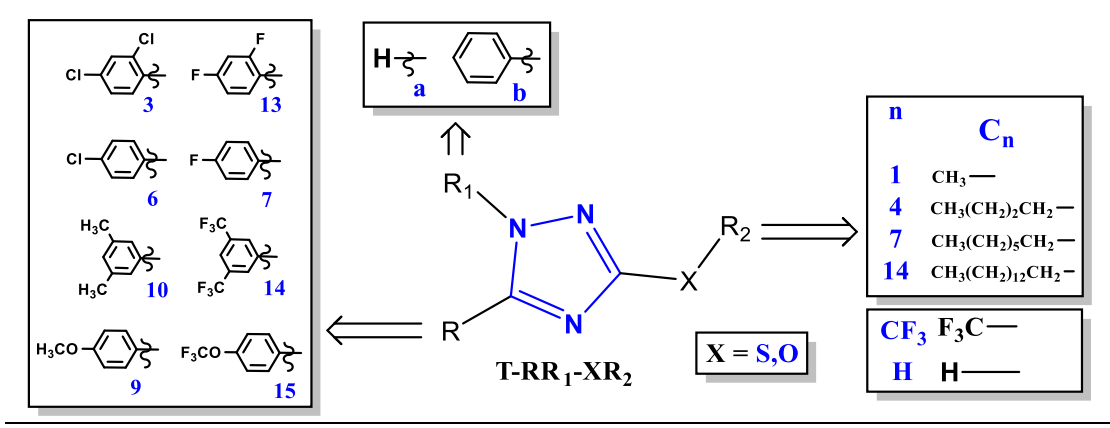


Figure 41. 1,3,5-substituted-1,2,4-triazoles with different halogenated substituents in R and R₂ position. Source: This investigation.

The substitutions proposed in Figure 41 apply for the most active systems found after optimizing the alkyl chain length for each fungus (previous section). Instead of the X- C_n systems ($R_2 = C_n$) two additional variations are evaluated, which are the trifluoromethyl substituent ($R_2 = CF_3$) and the hydroxy or thiol (sulfhydryl) substituents ($R_2 = H$). In the R-position, the substitutions consist in exchanging the chlorine atoms by fluorine in the case of 2,4- Cl_2Ph and 4-ClPh systems and the hydrogen atoms by fluorine in the compounds with 3,5- $(CH_3)_2Ph$ and 4- OCH_3Ph substituents.

The obtained results for the activity of the proposed derivatives against C. ALB, C. PAR, C. NEO, T. RUB and M. GYP are shown in Figure 42. The first conclusion that can be extracted from these results is that the presence of fluorine atoms in the phenyl-substituted ring is negative for the antifungal activity in all cases since, when systems with the same R₁/S-R₂ are compared, the 2,4-Cl₂Ph, 3,5-(CH₃)₂Ph, and 4-CIPh original substituents result always better than their fluorinated analogous. It is also important to highlight that the 2,4-(Cl)₂Ph-substituted compounds continue to exhibit the best activity. On the other hand, the substituent S-CF₃ in the thio-alkyl position (blue bars in Figure 42) improves the antifungal potential of all compounds against C. ALB, T. RUB, M. GYP, and C. NEO; in fact, the activity of the S-CF3 system is even better than the one reported for the compounds with an optimal aliphatic chain in the S-alkyl position. These results indicate that fluorine atoms in the R₂ position are more important than a long alkyl chain by stablishing better interactions with the amino acids in the entrance channel of CYP51, possibility hydrogen bond-like interactions which are stronger than the hydrophobic interactions of an aliphatic chain. In conclusion, for the fungi C. ALB, T. RUB, M. GYP, and C. NEO, the most active compound is **T-3b-SCF**₃ (R/R₁/X-R₂ = 2,4-Cl₂Ph/Ph/S-CF₃). In C. PAR the effect shown by the S-CF₃ substituent is negative, similar to the effect of fluorine atoms in the R position, therefore, in this case, **T-3a-SC**₁ (R/R₁/X-R₂ = 2,4-Cl₂Ph/Ph/S-C₁) is the best compound against this fungus. Finally, the substituent S-

H (yellow bars in Figure 42) instead of an alkyl chain does not improve the activity; indeed, it results in the worst activity for all evaluated fungi, with exception of C. PAR.

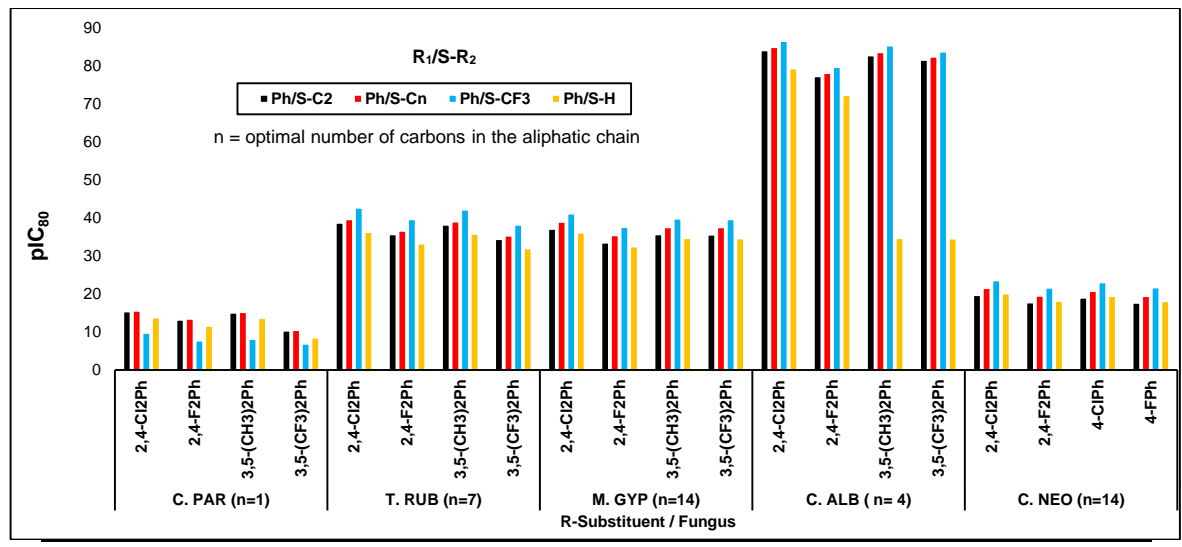


Figure 42. Effect of additional R_2 and R substitutions in 1,3,5-substituted-1,2,4-triazoles on the antifungal activity against C. ALB, C. PAR, C. NEO, T. RUB. and M. GYP. Source: This investigation.

For C. TRO and F. COM, the most active compound is **T-9a-OC**₁ (R/R₁/X-C_n = **4-OCH**₃**Ph/H/O-C**₁) and the results for additional R₂ and R modifications are shown in Figure 43. It is found that the presence of fluorine atoms decreases appreciably the antifungal activity, either in the R or R₂ position, with plC₈₀ values always lower than the corresponding hydrogenated systems. On the other hand, an interesting result is obtained for the O-R₂ substituent, where the antifungal potential of the compound improves when there are not carbon atoms in this position. In other words, the best antifungal against both fungi is the compound **T-9a-OH**, which has a hydroxyl group as substituent in XR₂ (yellow bars in Figure 43). As a matter of fact, the hydroxyl group improve considerably the antifungal activity against C. TRO, with plC₈₀ values now comparable to the best antifungal against C. PAR.

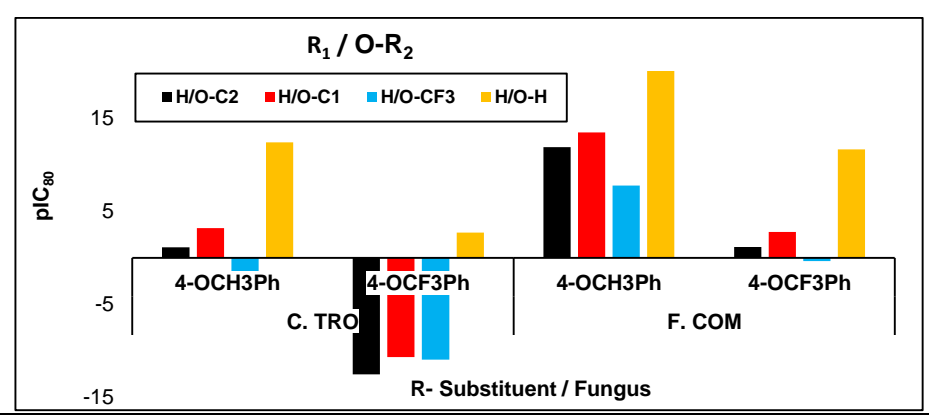


Figure 43. Effect of additional R_2 and R substitutions in 1,3,5-substituted-1,2,4-triazoles on the antifungal activity against C. TRO and F. COM. Source: This investigation.

Once the effect of halogens was evaluated and the best compounds were chosen a final structural modification was made on the most active systems. A detailed analysis of the structure of commercial antifungals (Figure 7) reveals that the heterocyclic moiety is separated by two bonds from the substituted-benzene group. For the triazoles studied in this work, this requires having a benzyl substituent (Bz) in the R position instead of a benzene. This substitution is synthetically viable if substituted-phenyl acetyl chlorides are used as precursors to obtain the respective carbamates, carbonates, and finally, the triazoles. The effect of a substituted-benzyl instead of a substituted-benzene on the antifungal activity of the most active systems is shown in Figure 44. The new modification on the compound **T-3b-SCF**₃, which is the most active against C. ALB, C. NEO, T. RUB, and M. GYP impairs its antifungal activity; while against C. PAR, the 2,4-dichlorobenzyl substituent ($R = 2,4-Cl_2Bz$, 16) in the triazole T-16b-SC₁ improves the antifungal activity in comparison to T-3b-SC₁ (green text in Figure 44). Finally, the compound **T-17a-OH**, with the R = 4-OCH₃Bz substituent (17), also exhibits a considerable improvement of the activity against C. TRO and F. COM with respect to the compound **T-9a-OH** with R = 4-OCH₃Ph.

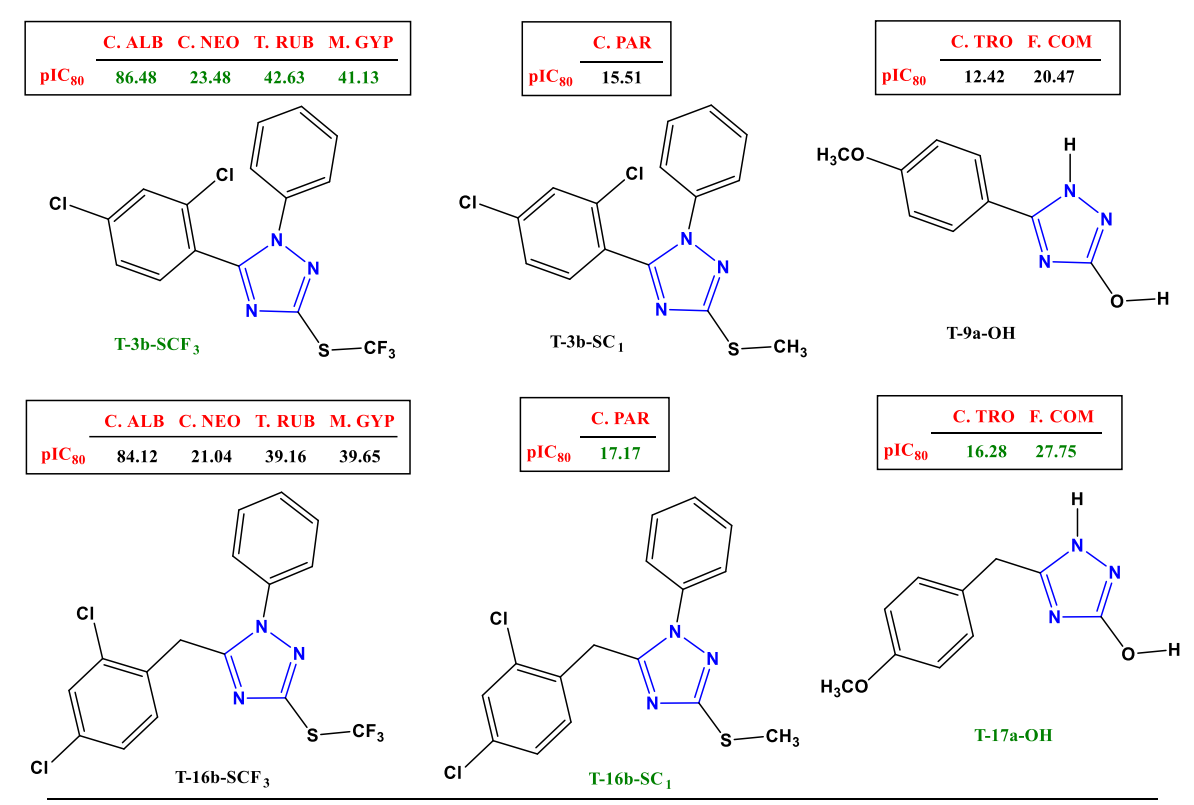


Figure 44. Effect of the distance between the triazole and the substituted-benzene on the antifungal activity of the best 1,3,5-substituted-1,2,4-triazoles found. Source: This investigation.

Finally, despite that the precise geometry of the interaction between the triazoles and the active site of the CYP51 enzyme can be found through molecular docking, an approximation was designed in this work. The NBO charges were calculated to identify the nitrogen atom with the largest electron density which will be the atom involved in the coordinate bond with the iron of the heme-group in the CYP51 enzyme (see Table A2 in the Appendix for numerical values). For the three most active compounds identified (green labels in Figure 44), it is found that the nitrogen four has the most negative charge, and therefore, the proposed geometry of the triazole-CYP51 interaction is shown in Figure 45. Further studies in this direction are being carried out by the GIFBA research group.

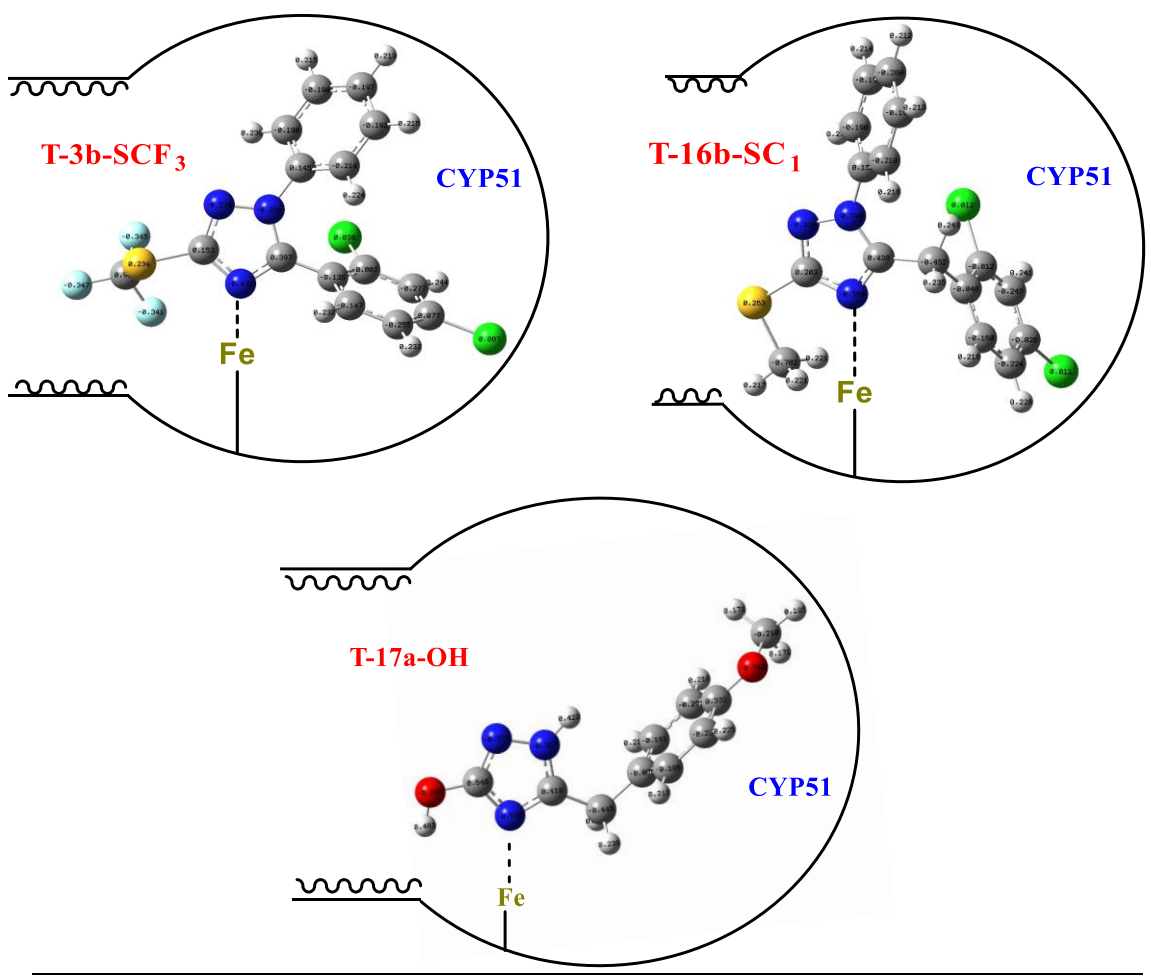


Figure 45. Proposed geometry for the interaction between the most active 1,3,5-substituted-1,2,4-triazoles with the active site of the CYP51 enzyme. Source: This investigation.

The results of this chapter indicate that the used methodology is very versatile to obtain a wide variety of 1,3,5-substituted-1,2,4-triazoles with potential antifungal activity. An exhaustive QSAR study of synthetically viable structural modifications suggests that the compound **T-3b-SCF**₃ (R/R₁/X-R₂ = 2,4-Cl₂Ph/Ph/S-CF₃) is the most active against *Candida albicans*, *Cryptococcus neoformans*, *Trichophyton rubrum*, and *Microsporum gypseum*; the compound **T-16b-SC**₁ (R/R₁/X-R₂ = 2,4-Cl₂Bz/Ph/S-CH₃) is the most active against *Candida parapsilosis*; and finally, the compound **T-17a-OH** (R/R₁/X-R₂ = 4-OCH₃Bz/H/O-H) is the most active against *Candida tropicalis* and *Fonsecaea compacta*.

5 MATERIALS AND METHODS

5.1 Synthesis of intermediates and products

The characterization of the compound was carried out by NMR spectroscopy, IR spectroscopy, MS-DART+ spectrometry, and melting point. The ¹H and ¹³C NMR spectra were measured in Varian Unity (300 MHz) and Varian Unity Inova (700 MHz) spectrometers. The software *MestreNova* was used to process the spectra. The infrared characterization was performed in a Bruker Tensor 27 spectrophotometer. High-resolution mass spectra were measured in a Jeol SX 102 A and the melting point was determined in a fusiometer C-LMP 1. The progress of the reactions was monitored using thin layer chromatography in the case of the third step (synthesis of 1,2,4-triazoles) and revealed with an UV lamp (254 nm). The products and intermediates were purified by column chromatography using silica gel as stationary phase. Reagents and solvents were acquired from Sigma-Aldrich and used as received.

5.1.1 General process for the synthesis of the X-ethyl aroylimidothiocarbamates

The synthesis was carried out using the methodology standardized by the GICH-UN¹². A reaction mixture consisting of the acid chloride **56a** or **56h** and KSCN (1:1 molar ratio) in acetonitrile was brought to reflux and then, the mixture was allowed to cool to room temperature. Excess ethanol was added and the mixture is left stirring at room temperature for a time range between 20 and 26 h.¹² The optimal time of the synthesis of intermediate **58h** was determined because it is a new compound reported in this investigation, for this, assays at different reaction times were made within the time range mentioned¹² and the time with the major yield was reported. The products were purified by recrystallization in hexane.

The compounds **58a** and **62a** are compound synthetized previously by the GICH-UN⁴² for this reason the product obtained was verified by comparison of melting point and RF using hexane:ethyl acetate (6:4) as mobile phase.

O-ethyl (2,4-dichlorobenzoyl)carbamothioate (58h)

The optimal reaction time was 24 hours and was recrystallized of hexane. The compound was obtained with 96% yield as a while crystalline solid

(MP: 88 °C). ¹H NMR (300 MHz, CDCl₃) δ (ppm): 9.05 (s, 1H); 7.51 (d, J= 8.4 Hz, 1H); 7.45 (d, J= 1.8 Hz, 1H); 7.34 (dd, J= 1.8 Hz J= 8.1 Hz, 1H); 4.51 (q, J= 7.1 Hz, 2H); 1.26 (t, J= 7.1 Hz, 3H). ¹³C NMR (75 MHz, CDCl₃) δ (ppm): 187.9; 162.4; 132.9; 131.8; 130.8; 130.1; 127.7; 69.6; 13.5. ATR-FT-IR λ (cm⁻¹): 3244 (N-H); 3066 (=CH); 2987 (CH₂, CH₃); 1668 (C=O); 1590 (C=C); 1484 (S=<u>C-N</u>-H); 1277 (S=C); 1205 (C-O); 741 (C-Cl). HRMS (DART+): Calculated for C₁₀H₁₀Cl₂NO₂S [M+1] 277.9809; Found: 277.9801.

5.1.2 General process for the synthesis of the X,S-diethyl aroylimidothiocarbonates

The synthesis was carried out using the conditions standardized by GICH-UN¹². A mixture of the X-ethyl aroyliminothiocarbamate **58a**, **58h**, or **62a** and NaH in molar ratio 1:1.5 was dissolved in DMF. Then, 2 equivalents of ethyl bromide were added and the mixture was left stirring at room temperature for a time range between 1 and 2.5 h. The optimal reaction time for the new compound **59h** was determined the same way as was done with the aroylimidothiocarbamate. The products were purified by column chromatography using hexane:ethyl acetate (8:2).

The compounds **59a** and **63a** were previously synthetized by the GICH-UN⁴² for this reason the verification of the obtained product was made by comparison of appearance and RF using hexane:ethyl acetate (6:4) as mobile phase.

O,S-diethyl-(2,4-dichlorobenzoyl)carbonimidothioate (59h)

The optimal reaction time was 1.5 hours and was purified by column chromatography using hexane:ethyl acetate (8:2). The compound was obtained with 84% yield as a yellow oil. 1 H NMR (300 MHz, CDCl₃) δ (ppm): 7.89 (d,

J= 8.4 Hz, 1H); 7.43 (d, *J*= 1.8 Hz, 1H); 7.26 (dd, *J*= 1.8 Hz *J*= 8.1 Hz, 1H); 4.50 (q, *J*= 7.1 Hz, 2H); 2.29 (q, *J*= 7.4 Hz, 2H); 1.40 (t, *J*= 7.0 Hz, 3H) 1.33 (t, *J*= 7.2 Hz, 3H). ¹³**C NMR** (75 MHz, CDCl₃) δ (ppm): 174.4; 172.4; 137.5; 134.7; 133.6; 132.9; 130.9; 126.8; 67.0; 25.4; 14.5; 14.2. **ATR-FT-IR** λ (cm⁻¹): 3082 (=CH); 2932 (CH₂, CH₃); 1700 (O-<u>C=N</u>); 1636 (C=O, S-<u>C=N</u>); 1503 (C=C); 1311 (C-S); 1206 (C-O) 763

(C-CI) **HRMS** (DART+): Calculated for $C_{12}H_{14}Cl_2NO_2S$ [M+1] 306.0122; Found: 306.0129.

5.1.3 General process for the synthesis of the 1,2,4-triazole derivatives

A reaction mixture of the X,S-diethyl aroylimidodithiocarbonate synthetized **59h** or the carbonate available at the GICH-UN **59e** (1 equivalent) and the hydrazine **49** (a-b) (1.1 equivalent) was heated to reflux using ethanol as solvent¹³. The formation of the product was followed by TLC between 0 to 40 minutes to determine the optimal reaction time of the compounds **T-3a-OC₂**, **T-3b-OC₂**, **T-4a-OC₂**, and **T-4b-OC₂** which are new products obtained in this investigation.

The compounds **T-1a-OC**₂, **T-1b-OC**₂, **T-1a-SC**₂, and **T-1b-SC**₂ were previously synthetized by the GICH-UN, for this reason the verification of the obtained product was made by comparison of melting point and RF using hexane:ethyl acetate (6:4) as mobile phase. Also, some spectra as NMR, IR, and MS were measured in order to ascertain the obtained products.

• 1,2,4-triazoles previously reported¹³

3-Ethoxy-5-phenyl-1*H*-1,2,4-triazole (T-1a-OC₂)

The optimal reaction time was 15 minutes and was purified by column chromatography using hexane:ethyl acetate (6:4) or by recrystallization of acetone-water (3:1) mixture. The compound was obtained with 75% yield by both purification methods as a while crystalline

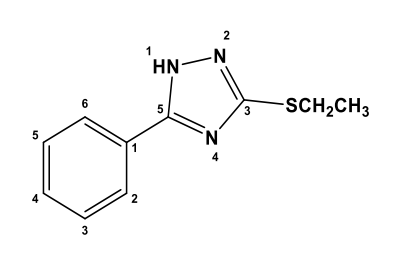
solid (**MP**: 110 °C) ¹**H NMR** (300 MHz, CDCl₃) δ (ppm): 10.02 (s, 1H); 7.95 (dd, J= 3 Hz J= 7.0 Hz, 2H); 7.36 – 7.39 (m, 3H); 4.2 (q, J= 7.0 Hz, 2H) 1.40 (t, J= 7.0 Hz, 3H). ¹³**C NMR** (75 MHz, CDCl₃) δ (ppm): 165.4; 156.7; 130.12; 128.8; 128.6; 126.4; 66.5; 14.7. **ATR-FT-IR** λ (cm⁻¹): 3134 (N-H); 3003 (=CH); 2977 (CH₂, CH₃); 1529 (C=C, C=N); 1148 (C-O). **HRMS** (DART+): Calculated for C₁₀H₁₂N₃O [M+1] 190.0980; Found: 190.0981.

3-Ethoxy-1,5-diphenyl-1*H*-1,2,4-triazole (T-1b-OC₂)

The optimal reaction time was 25 minutes and was purified by column chromatography using hexane:ethyl acetate (6:4) or, alternatively, by recrystallization of acetone-water (3:1) mixture. The compound was obtained with 60% yield using column chromatography and 75% yield with recrystallization as a light-orange solid. (**MP:** 78 °C) 1 **H NMR** (300 MHz, CDCl₃) δ (ppm):

7.47 (dd, J= 1.7 Hz J= 8.2, 2H); 7.30 – 7.40 (m, 8H); 4.41 (q, J= 7.1 Hz, 2H); 1.46 (t, J= 7.1 Hz, 3H). **ATR-FT-IR** λ (cm⁻¹): 3064 (=CH); 2974 (CH₂, CH₃); 1593 (C=N, C=C); 1536 (C=C); 1350 (C-N); 1167 (C-O). **HRMS** (DART+): Calculated for C₁₆H₁₆N₃O [M+1] 266.1293; Found: 266.1290.

3-(Ethylthio)-5-phenyl-1H-1,2,4-triazole (T-1a-SC₂)



The optimal reaction time was 20 minutes and was purified by column chromatography using hexane:ethyl acetate (6:4) or by recrystallization of acetone-water (3:1) mixture. The compound was obtained with 70% yield using column chromatography and 61 % yield with

recrystallization as a while crystalline solid (**MP:** 76 °C) ¹**H NMR** (400 MHz, DMSO-d₆) δ (ppm): 4.28 (s, 1H); 7.96 (dd, J= 1.6 Hz J= 8.4 Hz, 2H); 7.46 - 7.52 (m, 3H); 3.15 (q, J= 7.2 Hz, 2H); 1.34 (t, J= 7.2 Hz Hz). **ATR-FT-IR** λ (cm⁻¹): 3156 (N-H); 2983 (=CH); 2938 (CH₂, CH₃); 1503 (C=C, C=N); 1464 (C-S).

3-(Ethylthio)-1,5-diphenyl-1*H*-1,2,4-triazole (T-1b-SC₂)

The optimal reaction time was 25 minutes and was purified by column chromatography using hexane:ethyl acetate (8:2) or, alternatively, by recrystallization of acetone-water (3:1) mixture. The compound was obtained with 65% yield using column chromatography and 68% yield with recrystallization as a light-orange

solid. (**MP**: 90 °C) ¹**H NMR** (700 MHz, CDCl₃) δ (ppm): 7.54 (d, J= 8.4 Hz, 2H); 7.43 - 7.46 (m, 4H); 7.36 - 7.38 (m, 4H); 3.28 (q, J= 7.5 Hz, 2H); 1.50 (t, J= 7.4 Hz, 3H). ¹³**C NMR** (175 MHz, CDCl₃) δ (ppm): 160.4; 154.3; 137.7; 130.6; 129.5; 129.1; 129.0; 128.7; 126.5; 125.3; 26.3; 14.9. **ATR-FT-IR** λ (cm⁻¹): 3063 (=CH); 2964 (CH₂, CH₃); 1592 (C=C, C=N); 1494 (C=C); 1361 (C-N); 1465 (C-S). **HRMS** (DART+): Calculated for C₁₆H₁₆N₃S [M+1] 282.1065; Found: 282.1067.

New 1,2,4-triazoles reported in this investigation.

$$\begin{array}{c|c}
CI & 1 & 1 & 2 \\
& & 1 & 1 & 1 \\
& & & 5 & 1 \\
& & & & 4
\end{array}$$

$$\begin{array}{c|c}
CI & 4 & 5 & 6 \\
& & & & 4
\end{array}$$

$$\begin{array}{c|c}
CI & 4 & 5 & 6 \\
& & & & 4
\end{array}$$

5-(2,4-dichlorophenyl)-3-ethoxy-1*H*-1,2,4-triazole (T-3a-OC₂)

The optimal reaction time was 20 minutes and was purified by column chromatography using hexane:ethyl acetate (6:4) or by recrystallization of acetone-water mixture (3:1). The compound was obtained with 73%

yield using column chromatography and 65 % with recrystallization as a while crystalline solid (**MP**: 76 °C) ¹**H NMR** (300 MHz, CDCl₃) δ (ppm): 9.58 (s, 1H); 8.07 (d, J= 8.4 Hz, 1H); 7.46 (d, J= 2.1 Hz, 1H); 7.34 (dd, J= 2.1 Hz J= 8.4 Hz, 1H); 4.42 (q, J= 7.2 Hz, 2H); 1.44 (t, J= 7.0 Hz, 3H). ¹³**C NMR** (75 MHz, CDCl₃) δ (ppm): 166.1; 152.4; 136.5; 132.3; 132.1; 130.5; 127.9; 125.1; 66.4; 14.7. **ATR-FT-IR** λ (cm⁻¹): 3336 (N-H); 3087 (=CH); 2983 (CH₂, CH₃); 1592 (C=N, C=C); 1523 (C=C); 1130 – 1072 (C-O); 760 (C-Cl). **HRMS** (DART+): Calculated for C₁₀H₁₀Cl₂N₃O [M+1] 258.0201; Found: 258.0199.

5-(2,4-dichlorophenyl)-3-ethoxy-1-phenyl-1*H*-1,2,4-triazole (T-3b-OC₂)

The optimal reaction time was 35 minutes and was purified by column chromatography using hexane:ethyl acetate (6:4). The compound was obtained with 55% yield as a light-orange crystalline solid (**MP:** 128 °C) ¹**H NMR** (700 MHz, CDCl₃) δ (ppm): 7.41 (d, J= 8.2 Hz, 1H); 7.40

(d, J= 2.0 Hz, 1H); 7.28-7.34 (m, 4H); 7.24 (dd, J= 1.4 Hz J= 8.2 Hz, 2H); 4.44 (q, J= 7.0 Hz, 2H); 1.48 (t, J= 7.0 Hz, 3H). ¹³**C NMR** (175 MHz, CDCl₃) δ (ppm): 167.9; 149.6; 137.6; 137.1; 134.7; 132.6; 130.1; 129.2; 128.1; 127.5; 127.0; 123.4; 65.8; 14.7. **ATR-FT-IR** λ (cm⁻¹): 3093 (=CH); 2928 (CH₂, CH₃); 1596 (C=N,C=C); 1530 (C=C); 1340 (C-N); 1172 – 1066 (C-O); 774 (C-Cl). **HRMS** (DART+): Calculated for C₁₆H₁₄Cl₂N₃O [M+1] 334.0514; Found: 334.0511.

3-Ethoxy-5-(furan-2-yl)-1H-1,2,4-triazole (T-4a-OC₂)

The optimal reaction time was 10 minutes and was purified by column chromatography using hexane:ethyl acetate (6:4). The compound was obtained with 64% yield as a white solid. (**MP:** 136 °C), 1 **H NMR** (300 MHz, CDCl₃) δ (ppm): 8.03 (s, 1H); 7.45 (d, J= 1.0 Hz, 1H); 7.00 (d, J= 3.3 Hz, 1H); 7.48 (dd, J= 1.8 Hz J= 3.3 Hz, 1H); 4.46 (q,

J=7.0 Hz, 2H); 1.42 (t, J=7.1 Hz, 3H). ¹³**C NMR** (175 MHz, CDCl₃) δ (ppm): 164.7;

149.5; 144.3; 143.6; 111.7; 110.4; 66.8; 14.6. **ATR-FT-IR** λ (cm⁻¹): 3111 (N-H); 3029 (=CH); 2866 (CH₂, CH₃); 1523 (C=C, C=N); 1140 (C-O) **LRMS** (DART+): 180 m/z.

3-Ethoxy-5-(furan-2-yl)-1-phenyl-1H-1,2,4-triazole (T-4b-OC₂)

The optimal reaction time was 25 minutes and was purified by column chromatography using hexane:ethyl acetate (6:4). The compound was obtained with 63% yield as an orange solid. ^{1}H NMR (700 MHz, CDCl₃) δ (ppm): 7.49 - 7.46 (m, 3H); 7.44 - 7.43 (m, 2H); 7.40 (dd,

J= 1.8 Hz J= 1.0 Hz, 1H); 6.61 (dd, J= 3.5 Hz J= 0.7 Hz, 1H); 6.40 (dd, J= 3.5 Hz J= 2.1 Hz, 1H); 4.42 (q, J= 7.0 Hz, 2H); 1.45 (t, J= 7.0 Hz, 3H). ¹³**C NMR** (175 MHz, CDCl₃) δ (ppm): 167.8; 144.8; 144.3; 142.2; 138.0; 129.2; 129.2; 126.0; 113.3; 111.6; 65.8; 14.7. **ATR-FT-IR** λ (cm⁻¹): 3110 (=CH); 2987 (CH₂, CH₃); 1593 (C=N, C=C) 1528 (C=C); 1340 (C-N); 1143 (C-O). **HRMS** (DART+): Calculated for C₁₄H₁₄N₃O₂ [M+1] 256.1082; Found: 256.1082.

Additionally, the study of cyclization reaction required computational calculations of the different 1,2,4-triazole isomers, for this, the *Gaussian 16*⁷⁰ software was used and the Gibbs energies of compounds were obtained at DFT level using the hybrid functional wB97XD⁶⁹ and the 6-311++G(d,p) basis set.

5.2 QSAR study of the antifungal activity

The QSAR study was performed on the compounds reported by Xu et al¹⁵ and their activities against the fungi: *C. albicans, C. parapsilosis, C. tropicalis, C. neoformans, T. rubrum, F. compacta*, and *M. gypseum*. The molecular descriptors were calculated in Gaussian 16⁷⁰ and Hyperchem 8⁷⁹ with three different levels of theory: the semiempirical AM1⁸⁹ method, the DFT hybrid functional CAM-B3LYP⁹⁰ with the basis set 6-31++G(d,p), and the two-layer ONIOM⁹¹ method, using AM1 for the low-layer and CAM-B3LYP/6-31++G(d,p) for the high-layer. The multiple lineal regression for building the models was made using the software *Statgraphic Centurion XVI* and the models with best R² and lowest P-values were selected. The activities of 1,3,5-substituted-1,2,4-triazoles (**T-RR**₁-**XR**₂) were predicted with the obtained models using the best computational method and different structural modifications on the most active compounds were evaluated to find the best molecules against the mentioned fungi.

6 CONCLUSIONS

The cyclization reaction between aroylimidothiocarbonates and hydrazines 49 (a-b) allowed the synthesis of eight 1,2,4-triazoles derivatives, of which four are new compounds reported in this work: T-3a-OC2 and T-3b-OC2 from the synthetized precursor 59h and T-4a-OC₂, and T-4b-OC₂ from the carbonate 59e available in the The synthesis of the **GICH** laboratory. intermediates X-ethyl aroylimidthiocarbamates (58a. 58h. and and X.S-diethyl 62a) aroylimidothiocarbonates (59a, 59h, and 63a) was carried out using the conditions stablished by the GICH-UN. The precursors synthetized and already reported (58a, 59a, 62a and 63a) were verified by comparison of RF and melting point. The carbamate **58h** is a new compound reported in this investigation. It was synthetized with 96% yield and an optimal reaction time of 24 h. Also, the carbonate 59h, which is the ethylation product of the corresponding carbamate, was synthetized with 84% yield finding an optimal time of 1.5 h. In both cases the precursors were characterized by means of spectroscopic techniques ¹³C NMR, ¹H NMR, and FT-IR and spectrometric analysis. The novel 1,2,4-triazoles have the 2,4-dichlorophenyl substituent, which was chosen by its promising biological activity because this substituent is found in commercial antifungals, and the 2-furyl substituent which is also found in several drugs. The new triazoles were obtained with yields above 55%. In general, it was observed that the 1,2,4-triazoles cyclized with hydrazine require lower reaction times than those cyclized with phenylhydrazine due to the higher nucleophilic character of the nitrogen atom in the former hydrazine. According to the obtained results and those from other ongoing investigations, it has been demonstrated that the synthetic methodology is very versatile to generate a huge chemical space of 1,3,5-substituted-1,2,4-triazoles. Additionally, preliminary results from a computational study of the cyclization reaction mechanism revealed that this methodology generate compounds corresponding to kinetic products and not thermodynamic products.

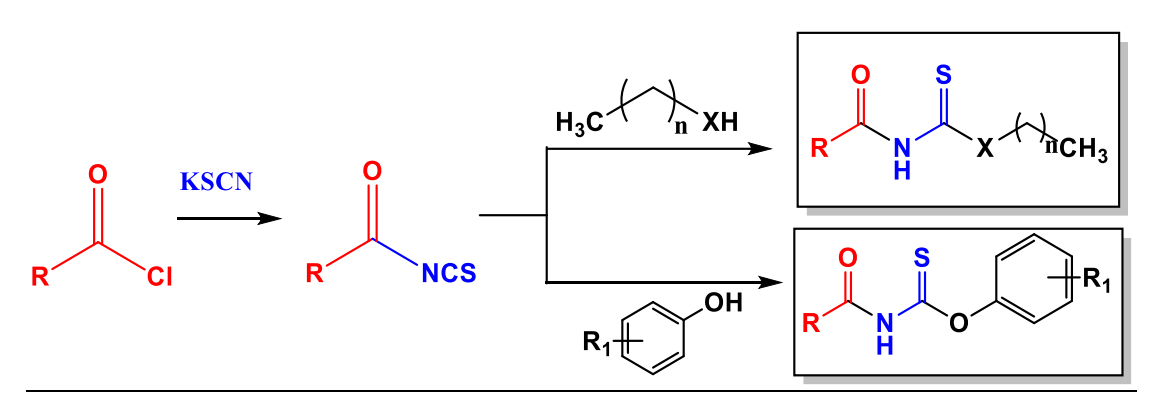
A QSAR study was performed on the reported antifungal activities of a series of piperazine-substituted 1,2,4-triazoles against *C. albicans, C. parapsilosis, C. tropicalis, C. neoformans, T. rubrum, F. compacta*, and *M. gypseum*. The results indicated that the best mathematical models relating the biological activity and molecular descriptors are obtained using the semiempirical AM1 method, with statistical parameters comparable or even better than those models obtained using higher levels of theory like DFT or ONIOM, at a fraction of the computational time. The obtained QSAR models were used to predict the antifungal potential against the aforementioned fungi of several 1,3,5-substituted-1,2,4-triazoles synthetically viable. The results show a general preference for *N*-phenyl and sulfur-containing

compounds with exception of F. COM and C. TRO, where the less hydrophobic and polarizable compounds are preferred. After several systematic structural modifications, it was found that the compound **T-3b-SCF**₃ is the most active against *C. albicans*, *C. neoformans*, *T. rubrum*, and *M. gypseum*; the compound **T-16b-SC**₁ is the most active against *C. parapsilosis*; and finally, the compound **T-17a-OH** is the most active against *C. tropicalis* and *F. compacta*.

7 RECOMMENDATIONS

In order to determine the antifungal potential of the 1,2,4-triazole derivatives synthesized, it is recommendable to determine the minimal inhibitory concentration against several fungi and even bacteria, since these systems also have antibacterial activity.

The QSAR study revealed that diverse structural modifications can lead to 1,3,5-substituted-1,2,4-triazoles with improved antifungal activity, which allows to propose several recommendations. It is suggested to evaluate different alcohols in the first step of the methodology to obtain additional aroylimidotiocarbamates with X-alkyl, from alkyl alcohols (X=O) or thiols (X=S) and X-aryl, from phenol-derivatives as shown in Scheme 19. These compounds can be useful to generate triazole derivatives with different substituents (length chain and type) in their ramifications, which, as it was demonstrated in this work, these have an effect on the antifungal activity due to the hydrophobic interactions with the amino acids at the entrance channel in the CYP51 enzyme.



Scheme 19. Proposed X-alkyl and X-aryl aroylimidotiocarbamates. Source: This investigation.

Considering the structure of commercial antifungals (Figure 7) and the results shown in Figure 44, it is recommended to use 2-(2,4-dichlorophenyl)acetyl chloride as precursor using the same synthetic methodology in order to obtain the corresponding 5-(2,4-dichlorobenzyl)-3-ethoxy-1-substitued-1,2,4-triazoles depending on the hydrazine used (Scheme 20). The synthetic conditions should be also optimized. The results obtained in this work indicate that benzyl-substituted 1,2,4-triazoles might have an improved antifungal activity (Figure 44).

CI GICH-UN methodology
$$O$$
, S-diethyl-(2-(2,4-dichlorophenyl)acetyl) carbonimidothioate O , S-diethyl-(2-(2,4-dichlorophenyl)acetyl) O , S-diethyl-(2-(2,4-di

Scheme 20. Proposed synthesis of 5-(2,4-dichlorobenzyl)-3-ethoxy-1-substituted-1,2,4-triazoles using the 2-(2,4-dichlorophenyl)acetyl chloride as precursor. Source: This investigation.

It is also recommended to evaluate the cyclization reaction of X,S-diethyl aroylimidothiocarbonates with hydroxylamine instead of hydrazine, as shown in Scheme 21, as an alternative method to obtain 1,2,4-oxadiazole derivatives. The syntheses of these systems are based mostly on the use of primary amidoximes and acylating agents as the initial reactants or via 1,3-dipolar cycloadditions, with primary amidoximes¹⁰¹. 1,2,4-oxadiazole-based compounds exhibit immense bioactivities and may have significant importance in the synthesis of novel agents potentially useful in the treatment of cancer, inflammation, insomnia, Alzheimer's disease, among others¹⁰².

Scheme 21. Proposed synthesis of 1,2,4-oxadiazole derivatives by cyclization of X,S-diethyl aroylimidothiocarbonates and hydroxylamine. Source: This investigation.

On the other hand, considering the wide range of biological activities exhibited by 1,2,4-triazoles derivatives, in particular, antiviral activity¹⁰³, it is recommended to evaluate the antiviral potential of the 1,2,4-triazole derivatives synthesized in this work and those synthetically viable, since new alternatives are sought to face the public health problem caused by the SARS-CoV-2 virus¹⁰⁴.

119

 ¹⁰¹ KAYUKOVA, Lyudmila. Synthesis of 1,2,4-oxadiazoles (a review). *Pharm Chem J.* 2005; **39**(10), 539-547
 102 BIERNACKI, Karol *et al.* Novel 1,2,4-oxadiazole derivatives in drug discovery. *Pharmaceuticals*. 2020, **13**(6): 111-156

¹⁰³ EL-SEBAEY, Samiha. Recent advances in 1,2,4-triazole scaffolds as antiviral agents. *ChemistrySelect.* 2020; **5**(37): 11654-80.

¹⁰⁴ BEN, Hu, et al. Characteristics of SARS-CoV-2 and COVID-19. Nat. Rev. Microbiol. 2021; 19(3): 141-154.

8 PRODUCTS

Results derived from this work were presented in the following academic events:

Regional event

V Jornada de Actualización Científica en Química. November 7th-9th 2018, Pasto
 Colombia.

National event

- VII Encuentro Nacional de Químicos Teóricos y Computacionales and IV Escuela Colombiana de Teoría y Computación en Ciencias Moleculares. September 9th-12th 2018, Barranquilla – Colombia.
- XVIII Congreso Colombiano de Química. November 6th-8th 2019, Popayán Colombia.

International event

 IX Simposio de Química Aplicada and I Congreso Internacional de Nanoquímica, Nanofísica y Nanomedicina. August 21st-23rd 2019, Armenia – Colombia.

9 REFERENCES

AL-MASOUDI, Najim et al. synthesis of 1,2,4-triazole c-nucleosides from hydrazonyl chlorides and nitriles, *Nucleos Nucleot Nucl.* 2007; **26**: 37-43.

AL-SOUD, Yassen *et al.* Synthesis, antitumor and antiviral properties of some 1,2,4-triazole derivatives, *Il Farmaco.* 2004; **59**(10): 775-83.

ALVARES, Rosa *et al.* 1,2,3-Triazole-[2,5-Bis-O-(tert-butyldimethylsilyl)-beta-D-ribofuranosyl]-3'-spiro-5"-(4"-amino-1",2"-oxathiole 2",2"-dioxide) (TSAO) Analogs: Synthesis and Anti-HIV-1 Activity. *J Med Chem.* 1994; **37**(24): 4185-94. ARAGON, Martin *et al.* Antimicóticos dermatológicos. *Farmacia Profesional.* 2014; **18**(7), 38-48.

BAGIHALLI, Gangadhar *at al.* Synthesis, spectral characterization, in vitro antibacterial, antifungal and cytotoxic activities of Co(II), Ni(II) and Cu(II) complexes with 1,2,4-triazole Schiff bases. *Eur J Med Chem.* 2008; **43**: 2639-2649.

BARBUSEANU, Stefania *et al.* Synthesis and Antioxidant Activity Evaluation of New Compounds from Hydrazinecarbothioamide and 1,2,4-Triazole Class Containing Diarylsulfone and 2,4-Difluorophenyl Moieties. *Int J Mol Sci.* 2014; **15**: 10908-10925.

BARRATT, Gillian et al. Optimizing efficacy of Amphotericin B through nanomodification, *Int J Nanomedicine*. 2007; **2**(3): 301-13. BAUMANN, Marcos *et al*. An overview of the key routes to the best-selling 5-membered ring heterocyclic pharmaceuticals, *Beilstein J Org Chem*. 2011; **7**: 442–495.

BEN, Hu, et al. Characteristics of SARS-CoV-2 and COVID-19. Nat. Rev. Microbiol. 2021; **19**(3): 141-154.

BENIGNI, Romualdo; BOSSA, Cecilia. Structural Alerts of Mutagens and Carcinogens. *Curr Comput Aided Drug* Des. 2006; **2**(2): 169-176. BENSON, Frederic; SAVELL, Walter. The Chemistry of the Vicinal Triazoles. *Chem Rev.* 1950; **46**(1): 1-68.

BIERNACKI, Karol *et al.* Novel 1,2,4-oxadiazole derivatives in drug discovery. *Pharmaceuticals*. 2020, **13**(6): 111-156.

BLANCO, Edgard *et al.* Estudio computacional conformacional, espectroscópico, ONL, HOMO–LUMO y reactividad de 1,3,5-trifenilpirazol. *Rev Ion.* 2018; **31**(2): 51-6.

BONEV, Boyen *et al.* Principles of assessing bacterial susceptibility to antibiotics using the agar diffusion method. *J Antimicrob Chemother.* 2008; **61**: 1295-1301.

CALDWELL, Gary et al. The IC₅₀ Concept Revisited. Curr Top Med Chem. 2012; **12**(11): 1282-1290.

CAREY, Francis; SUNDBERG, Richard. *Advanced Organic Chemistry, Part A:* Structure and Mechanisms. 4th ed. Springer; 2007.

CASTANEDO, Georette et al. Rapid Synthesis of 1,3,5-Substituted 1,2,4-Triazoles from Carboxylic Acids, Amidines, and Hydrazines. *J Org Chem.* 2011; **76**: 1177-1179.

CASTRO, Edison; SANCHEZ, Edison. Evaluación de las interacciones entre las 4,5-diamino-6-pirimidonas y los aroil y heteroiliminotiocarbonatos de O,S-dietilo. Trabajo de grado en Química, Universidad de Nariño, 2008.

CHAI, Jeng-Da; HEAD-GORDON, Martin. Long-range corrected hybrid density functionals with damped atom-atom dispersion corrections. *Phys. Chem. Chem. Phys.* 2008; **10**(44): 6615-20.

CORRADO, Girmenia *et al.* New-generation triazole antifungal drugs: review of the Phase II and III trials. *Clin Invest.* 2011; **1**(11): 1577-1594. COWEN, Leah et al. Mechanisms of Antifungal Drug Resistance, *Cold Spring Harb Perspect Med.* 2017; **5**(7): 1-22.

CUEVAS, Gabriel; CORTES; Fernando. *Introducción a la Química Computacional*. Fondo de Cultura Económica; 2003.

DALLOUL, Hany. Heterocyclic synthesis using nitrilimines: Part 19. Synthesis of novel 1,3,5-trisubstituted-1,2,4-triazoles. *Arab J Chem.* 2014; **7**(5): 604-608.

DE BEDOUT, Catalina *et al.* Evaluación de la susceptibilidad de especies de Candida al fluconazol por el método de difusión de disco. *Biomédica.* 2003; **23**: 31-7.

DEWAR, Michael J; ZOEBISCH, Eve G; HEALY, Eamonn. AM1: A New General Purpose Quantum Mechanical Molecular Model. *J. Am. Chem. Soc.* 1985; **107**(13): 3902-3909.

DIAZ, Emilio *et al.* Industrialization of the screening process. *Eur Pharm Reviews*. 2004; **9**: 74-77.

DIMOVA, Vesna; PERIŠIĆ-JANJIĆ, Nada. QSAR study by 1,2,4-triazoles using several physicochemical descriptors. *Maced J Chem Chem Eng.* 2009; **28**(1): 79-89.

DUDEK, Arkadiusz *et al.* Computational methods in developing Quantitative Structure-Activity Relationships (QSAR): A Review. *Comb Chem & High Through Scree*. 2006; **9**(3): 213-228.

EGBUTA, Chinaza *et al.* Mechanism of Inhibition of Estrogen Biosynthesis by Azole Fungicides. *Endocrinology*. 2014;**155**(2): 4622-4628.

EL-SEBAEY, Samiha. Recent advances in 1,2,4-triazole scaffolds as antiviral agents. *ChemistrySelect*. 2020; **5**(37): 11654-80.

ESTRADA, Sandra. Síntesis de nuevas 4-heteroarilpirazolo $[1,5-\alpha]$ -1,3,5-triazinas por reacción entre heteroaroiliminotiocarbonatos de O,S-dietilo y 5-amino-3-aril-1*H*-pirazoles. Trabajo de grado en Química, Universidad de Nariño, 2009.

FLORES, Maryury *et al.* Molecular modeling studies of bromopyrrole alkaloids as potential antimalarial compounds: a DFT approach. *Med Chem Res.* 2018; **27**: 844-856.

FONES, William. The use of sodium hydride in the alkylation of *N*-substituted amides. *J Org Chem.* 1949; **14**(6): 1099-1102.

FRISCH, Michael *et al.* Gaussian 16, Revision B.01, Gaussian, Inc., Wallingford CT, 2016.

GHANNOUM, Mahmoud; RICE, Louis. Antifungal Agents: Mode of Action, Mechanisms of Resistance, and Correlation of These Mechanisms with Bacterial Resistance, *Clin Microbiol Rev.* 1999; **12**(4): 501-517.

GŁADKOWSKI, Witold *et al.* Synthesis and Antimicrobial Activity of Methoxy Substituted γ-Oxa-ε-lactones Derived from Flavanones. *Molecules.* 2019; **24**: 4151-4166.

GOPALRAO, Vikas *et al.* Green synthesis and evaluation of 5-(4-aminophenyl)-4-aryl-4*H*-1,2,4-triazole-3-thiol derivatives. *Iran J Pharm Sci.* 2017; **13**(2): 37-50.

GRAMATICA, Paola *et al.* QSAR Modeling is not "Push a Button and Find a Correlation": A Case Study of Toxicity of (Benzo-)triazoles on Algae. *Mol. Inf.* 2012; **31**: 817-835.

GUERRA, Cristian *et al.* Análisis QSAR-2D de los derivados de 1,4-di-*N*-oxidos de quinoxalina con actividad contra la enfermedad de chagas. *Quim Nova.* 2016; 39(6): 647-54.

HANSCH, Corwin *et al.* On the Role of Polarizability in Chemical-Biological Interactions. *J Chem Inf Comput Sci.* 2003; **43**: 120-25.

HERBRECHT, Raoul. Voriconazole: Therapeutic review of a new azole antifungal. *Expert Rev Anti-infect Ther.* 2004; **2**(4): 485-497.

HERNANDES, Marcelo *et al.* Halogen atoms in the modern medicinal chemistry: Hints for the drug design. *Curr. Drug Targets*, 2010; **11**(3): 303-314.

HESEK, Dusan *et al.* Complications from Dual Roles of Sodium Hydride as a Base and as a Reducing Agent. *J Org Chem.* 2009; **74**(6): 2567-2570

HIDALGO, Andres. Síntesis de nuevos 1,2,4-triazoles por reacción de aroilimidotiocarbonatos de O, S-dietilo o aroilimidoditiocarbonatos de S,S-dietilo con hidrazinas. Trabajo de grado en Química, Universidad de Nariño, 2017. HYPERCUBE, Inc. HyperChem, Release 8.0.8, 2009.

INSUASTY, Henry *et al.* Regioselective synthesis of novel 4-aryl-2-ethylthio-7-methylpyrazolo[1,5-α]-1,3,5-triazinas. *Tetrahedron Lett.* 2006; **47**: 5441-5443.

INSUASTY, Henry *et al.* Solvent-free microwave-assisted synthesis of novel 4-hetarylpyrazolo[1,5- α][1,3,5] triazines. *J Heterocyclic Chem.* 2012; **49**; 1339-1345.

INSUASTY, Henry *et al.* Three practical approaches for the synthesis of 4,7-dihetarylpyrazolo[1,5- α]-1,3,5-triazinas. *Tetrahedron.* 2012; **68:** 9384-9390.

KARELSON, Mati; LOVANOV, Victor. Quantum-chemical descriptors in QSAR/QSPR studies. *Chem Rev.* 1996; **96**: 1027-43.

KAUSHIK, Manu; MOHIUDDIN, Syed. Clinical utility of valsartan in treatment of children and adolescents with high blood pressure. *Adol Heal Med and Therap.* 2011; **2**: 97-103.

KAYUKOVA, Lyudmila. Synthesis of 1,2,4-oxadiazoles (a review). *Pharm Chem J.* 2005; **39**(10), 539-547.

KHAM, Iram *et al.* 1,4-Benzodiazepine: an overview of biological properties. *Sci Rev Chem Commun.* 2015; **5**(1): 13-20.

KIM, Dong Min *et al.* Chromoblastomycosis caused by *Fonsecaea pedrosoi*. *Ann Dermato*. 2011. **23**(3): 369-73.

KRYACHKO, Eugene; LUDEÑA, Eduardo. Density functional theory: Foundations reviewed. *Phys Rep.* 2014; **544**: 123-239.

LAGOS, Yolanda; CHECA, Camilo. Evaluación de las interacciones del 5-amino-1-fenil-3-metilpirazol con los isotiocianatos de aroilo con los aroiliminoditiocarbonatos de S,S-dietilo. Trabajo de grado en Química, Universidad de Nariño, 2005.

LEVINE, Ira. Quantum Chemistry. 7th ed. Pearson Education; 2014.

LUNG WA, Chung, et al. The ONIOM method and its applications. Chem. Rev. 2015; **115**(12): 5678-5796.

MAERTENS, Jan. History of the development of azole derivative. *Clin Microbiol Infect.* 2004; **10**(1): 1-10.

MAKARA, Gergely. Solid-phase synthesis of 3-alkylamino-1,2,4-triazoles. *Org Lett.* 2002; **4**(10): 1751-1754.

MARTINS, Pedro *et al.* Heterocyclic Anticancer Compounds: Recent Advances and the Paradigm Shift towards the Use of Nanomedicine's Tool Box, *Molecules*. 2015; **20(9)**: 16852-16891.

MIER, Paola; SUAREZ, Gina. Sintesis de nuevas pirazolo $[1,5-\alpha]$ -1,3,5-triazinas por reacción de aroiliminoditiocarbonatos de S,S-dietilo con 5-amino-3-arilpirazoles usando irradiación con microondas. Trabajo de grado en Química, Universidad de Nariño, 2007.

MILLER, James. Kinetic and Thermodynamic Issues in the Formation of Aromatic Compounds in Flames of Aliphatic Fuels. *Combust Flame*. 1992; **91**: 21-39.

MORRISON, Robert; BOYD, Robert. *Organic Chemistry*. 6th ed. Pearson Education; 1992.

MYINT, Kyaw; XIE, Xiang. Recent Advances in Fragment-Based QSAR and Multi-Dimensional QSAR Methods. *Int J Mol Sci.* 2010; **11**(10): 3846-3866. NEPALI, Kunal *et al.* Nitro-Group-Containing Drugs. *J. Med. Chem.* 2019; **62**(6): 2851-2893.

NETH, Jeniel *et al.* Antifungal agents: Spectrum of activity, pharmacology, and clinical indications. *Infect Dis Clin North Am.* 2016; **30**(1): 51-83.

NETZEVA, Tatiana I *et al.* Description of the Electronic Structure of Organic Chemicals Using Semiempirical and Ab Initio Methods for Development of Toxicological QSARs. *J. Chem. Inf. Model.* 2005; **45**(1): 106-114.

NIWA, Toshimitsu. Basic theory of mass spectrometry. *Clin Chim Acta*. 1995; **241-242**: 15-71.

NOWACZYK, Alicja; MODZELEWSKA-BANACHIEWICZ, Bożena. QSAR studies of a number of triazoles antifungal alcohols. *Cent Eur J Chem.* 2010; 8(2): 440-447.

ORTEGA MUÑOZ, Christian Camilo. Estudio computacional de las propiedades ópticas no-lineales de derivados de 1,2,4-triazoles. Trabajo de grado en Física, Universidad de Nariño, 2021

PEYTON, Lee *et al.* Triazole antifungal: A review. *Drugs Today.* 2015; **51**(12): 705-718.

PFALLER, Michael. Antifungal Drug Resistance: Mechanisms, Epidemiology, and Consequences for Treatment. *Am J Med*, 2012; **125**(1): 3-13.

POKHODYLO, Nazariy *et al.* Synthesis of 1,2,3-Triazole Derivatives and Evaluation of their Anticancer Activity. *Sci Pharm.* 2013; **81**(3): 663-76.

POKURI, Sateesh *et al.* Insights on the Antioxidant Potential of 1, 2, 4-Triazoles: Synthesis, Screening & QSAR Studies. *Current Drug Metabolism.* 2014; **15**(4): 389-397.

PUZYN, Tomasz; LESZCZYNSKI, Jerzy; CRONIN, Mark. Recent Advances in QSAR Studies: Methods and Applications. Vol. 8. Springer; 2010.

REED, Alan; WEINSTOCK, Robert; WEINHOLD, Frank. Natural population analysis. *J. Chem. Phys.* 1985; **83**(2): 735-46.

RESTREPO, Vanessa. Evaluación de la interacción entre los heteroilimidotiocarbonatos de O,S-dietilo y el 5-amino-3-fenil-1H-1,2,4-triazol como método de obtención de nuevas triazolotriazinas. Trabajo de grado en Química, Universidad de Nariño, 2012.

SAAG, Michael *et al.* Azole antifungal agents: emphasis on new triazoles. *Antimicrob Agents Chemother.* 1988; **32**(1): 1-8.

SADABA, Belen *et al.* Relación entre estructura y función de los azoles. *Rev Esp Quimioterap.* 2014; **17**(1): 71-78.

SANABRIA, Rosa *et al.* Dermatofitos y hongos levaduriformes productores de micosis superficiales. *Mem Inst Investig Cienc Salud.* 2001; **1**(1): 63-68.

SARKAR, Nilmoni *et al.* Toxicity analysis of polychlorinated dibenzofurans through global and local electrophilicities. *J Mol Struct.* 2006; **758**: 119-25.

SCHDFER-KORTING, Monika. Pharmacokinetic Optimization of Oral Antifungal Therapy. *Clin Pharmacokinet*. 1993; **25** (4): 329-341.

SHARBA, Hussain *et al.* Synthesis of Oxadiazoles, Thiadiazoles and Triazoles Derived from Benzo[b]thiophene. *Molecules.* 2005; 10: 1161-1168.

SHARMA, Indrajit; THAPA, Ranjit. Basic concepts of Density Functional Theory: Electronic structure calculation. *J Phys: Conf Ser.* 2016; **765**(1): 1-4.

SILVERSTEIN, Robert M., et al. Spectrometric Identification of Organic Compounds. 8th ed. Wiley; 2014.

SMITH, Edgar. History of antifungal, *J Am Acad Dermatol.* 1990; **23(**4): 776-78. SRIKANTA, Deepa *et al. Cryptococcus neoformans*: Historical curiosity to modern pathogen. *Yeast.* 2014; **31**: 47-60.

SUN, Haitao *et al.* Ionization Energies, Electron Affinities, and Polarization Energies of Organic Molecular Crystals: Quantitative Estimations from a Polarizable Continuum Model (PCM)-Tuned Range-Separated Density Functional Approach. *J Chem Theory Comput.* 2016; **12**: 2906-16.

TORRES, Viviana. Síntesis de un nuevo 1,4-bis(3-etoxi-1,2,4-triazolil)benceno por reacción del tereftaloiltiocarbamato de O-etilo o del

tereftaloilimidotiocarbonato de O,S-dietilo con hidrazina. Trabajo de grado en Química, Universidad de Nariño, 2018.

TRIVEDI, Mahendra *et al.* Characterization of Physical, Spectral and Thermal Properties of Biofield Treated 1,2,4-Triazole. *J Mol Pharm Org Process Res.* 2015; **3**(2): 128-133.

VEERASAMY, Ravichandran *et al.* Validation of QSAR Models - Strategies and Importance. *Int J Drug Discov.* 2011; **2**(3): 511-519.

VERMA, Rajeshwar *et al.* On the role of polarizability in QSAR. *Bioorg Med Chem.* 2005; **13**: 237-55.

WANG, Lingling *et al.* Analysis of the dermatophyte *Trichophyton rubrum* expressed sequence tags. *BMC Genomics*. 2006; **6**: 255-67.

WEETE, John. Mechanism of Fungal Growth Suppression by Inhibitors of Ergosterol Biosynthesis. En: *Ecology and Metabolism of Plant Lipids*. FULLER, G.; NES W. D. Eds, Chapter 17, 1987: 268-265.

WEI, Quing-Li *at al.* Synthesis and QSAR studies of novel triazole compounds containing thioamide as potential antifungal agents. *Bio Med Chem.* 2006; **14**(21): 7146-7153.

WHEAT, Joe *et al*, Hypothesis on the Mechanism of Resistance to Fluconazole in Histoplasma capsulatum, *Antimicrob agents chemother*. 1997; **41**(2): 410-414.

WHELESS, James; VASQUEZ, Blanca. Rufinamide: A novel broad-spectrum antiepileptic drug. *Epilepsy Curr.* 2010; **10**(1): 1-6.

WU, Junqi *et al.* Molecular docking, design, synthesis and antifungal activity study of novel triazole derivatives. *Eur J Med Chem.* 2018; **143**: 1840-1846.

XU, Jianming et al. Design, synthesis and antifungal activities of novel 1,2,4-triazole derivatives. Eur J Med Chem. 2011; **46**: 3142-3148.

YAMAGUCHI, Yoshihiro *et al.* How the π Conjugation Length Affects the Fluorescence Emission Efficiency. *J Am Chem Soc.* 2008; 130 (42): 13867-13869.

YANAI, Takeshi; TEW, David P; HANDY, Nicholas C. A new hybrid exchange-correlation functional using the Coulomb-attenuating method (CAM-B3LYP). *Chem. Phys. Lett.* 2004; **393**(1): 51-7.

YOUNG, David. Computational Drug Design. Jhon Wiley & Sons; 2009. YU, Shichong *et al.* Triazole derivatives with improved in vitro antifungal activity over azole drugs. *Drug Des Devel Ther.* 2014; **8**: 383-390.

ZHOU, Loughu *at al.* Synthesis and antiviral activities of 1,2,3-triazole functionalized thymidines: 1,3-dipolar cycloaddition for efficient regioselective diversity generation. *Antivir Chem Chemother*. 2005; **16**(6): 375-83.

10 APPENDIX

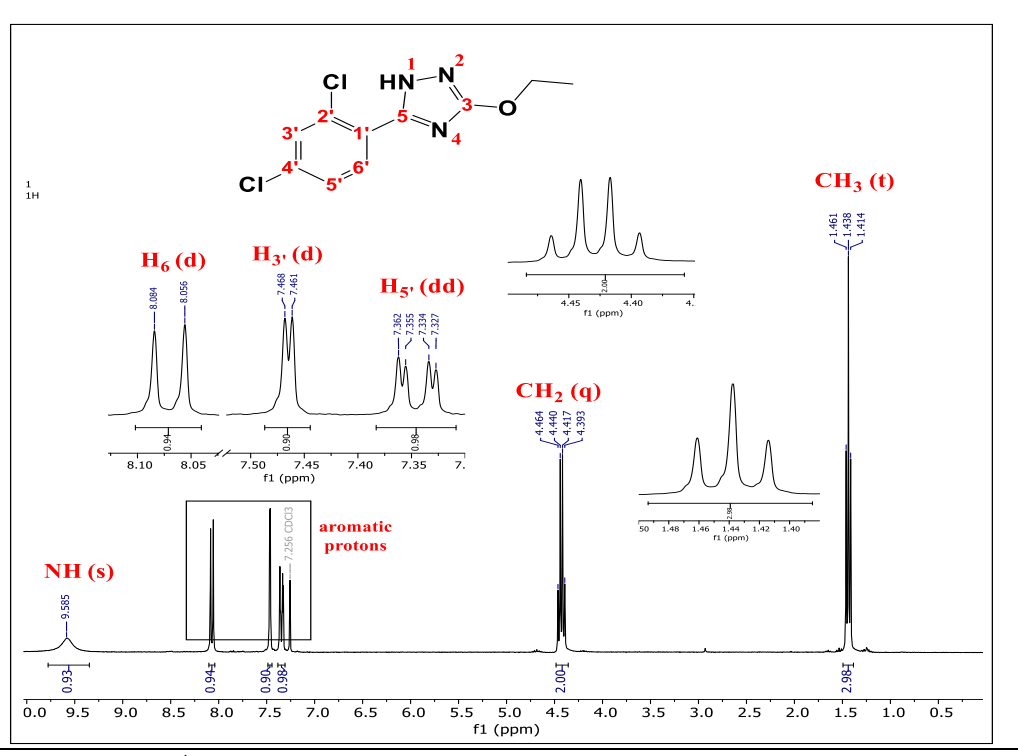


Figure A1. ¹H NMR (300 MHz, CDCl₃) spectrum of compound T-3a-OC₂.

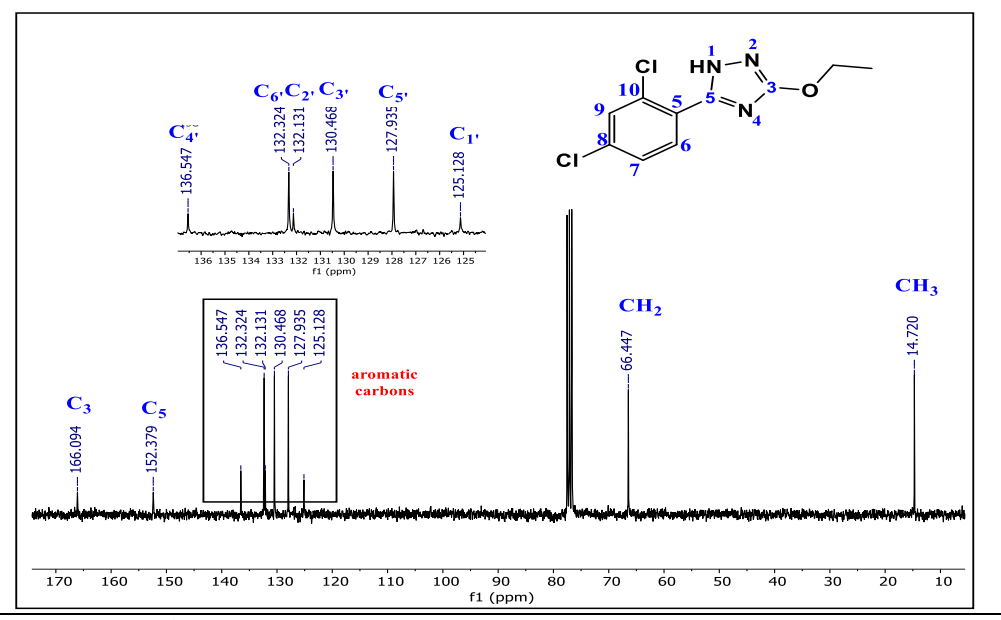


Figure A2. ¹³C NMR (75 MHz, CDCl₃) spectrum of compound T-3a-OC₂.

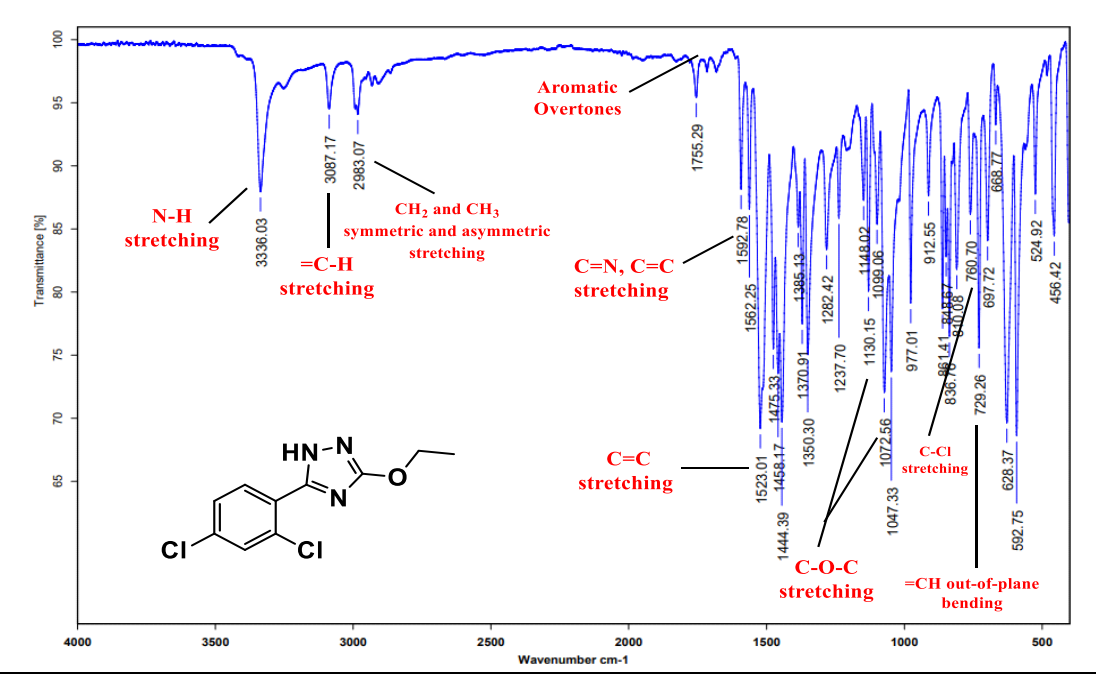


Figure A3. FT-IR spectrum of compound T-3a-OC₂.

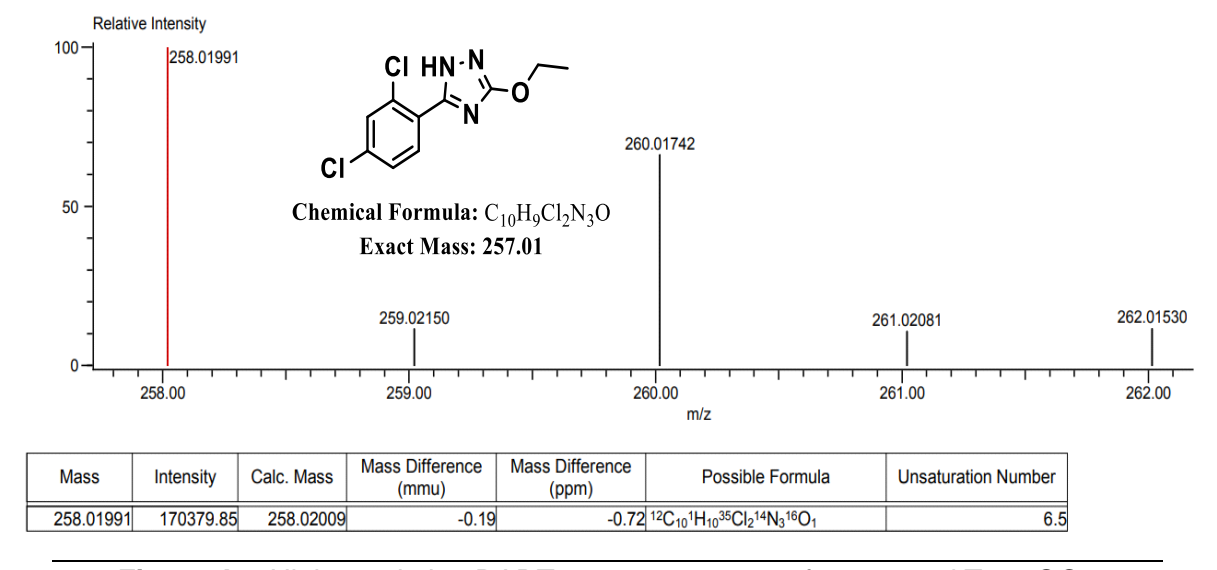


Figure A4. High-resolution DART+ mass spectrum of compound T-3a-OC₂.

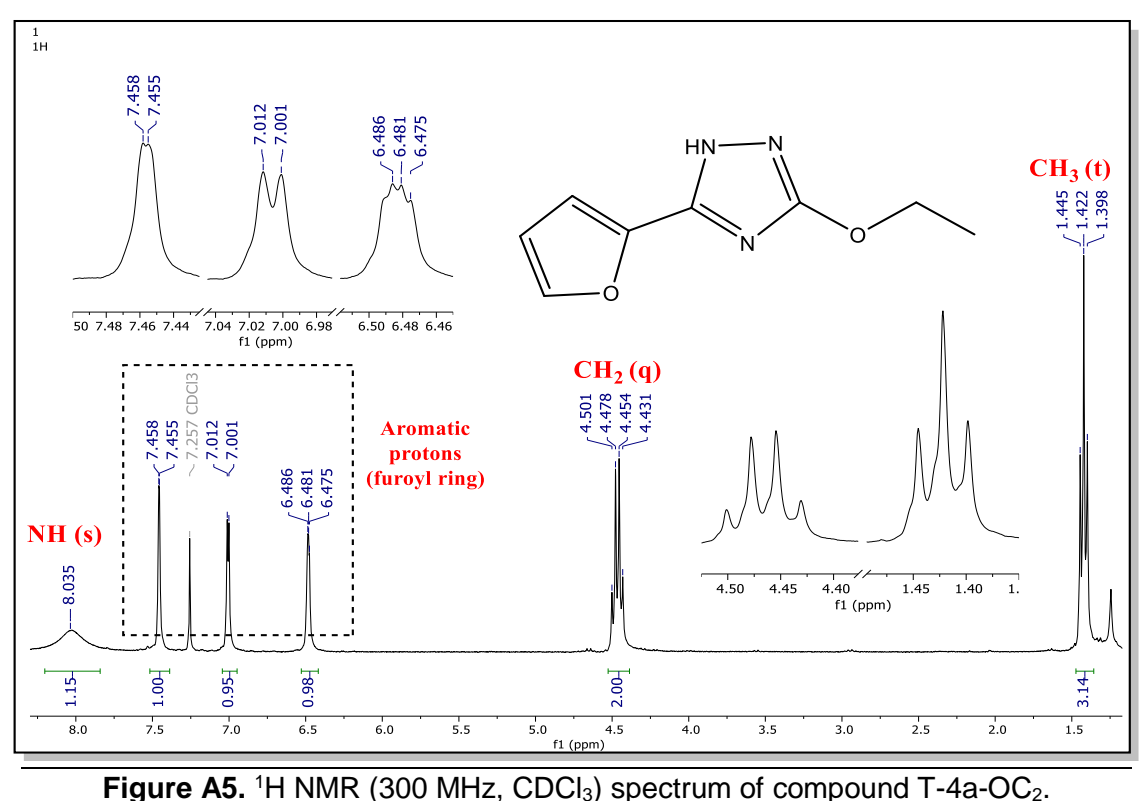


Figure A5. ¹H NMR (300 MHz, CDCl₃) spectrum of compound T-4a-OC₂.

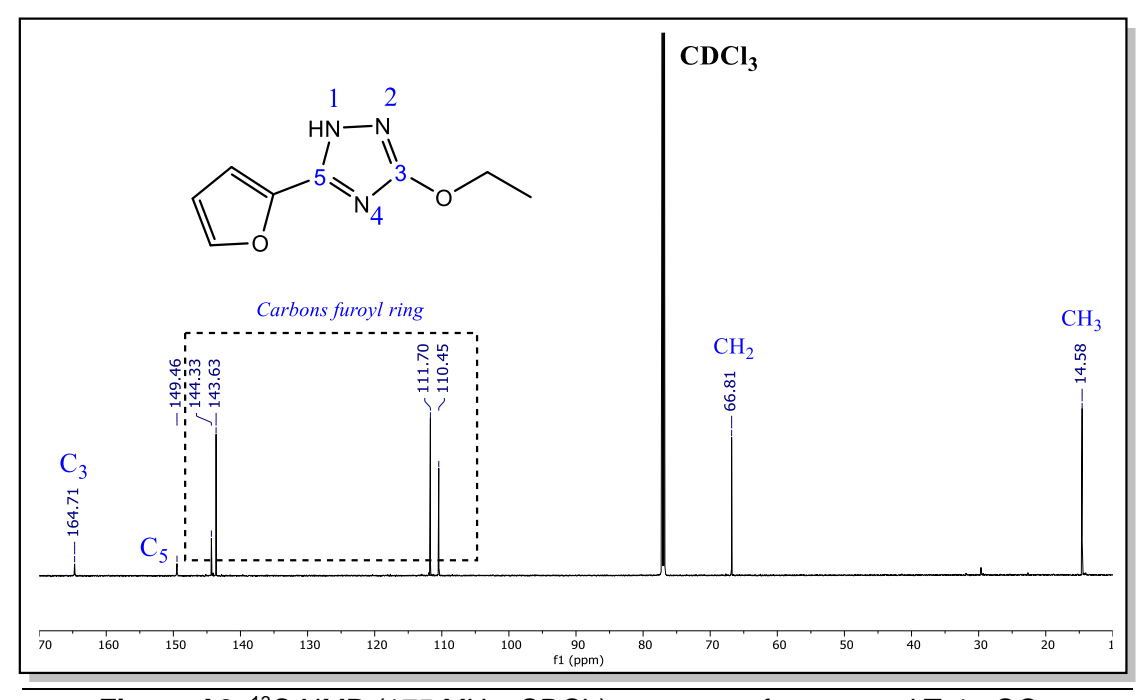


Figure A6. ¹³C NMR (175 MHz, CDCl₃) spectrum of compound T-4a-OC₂.

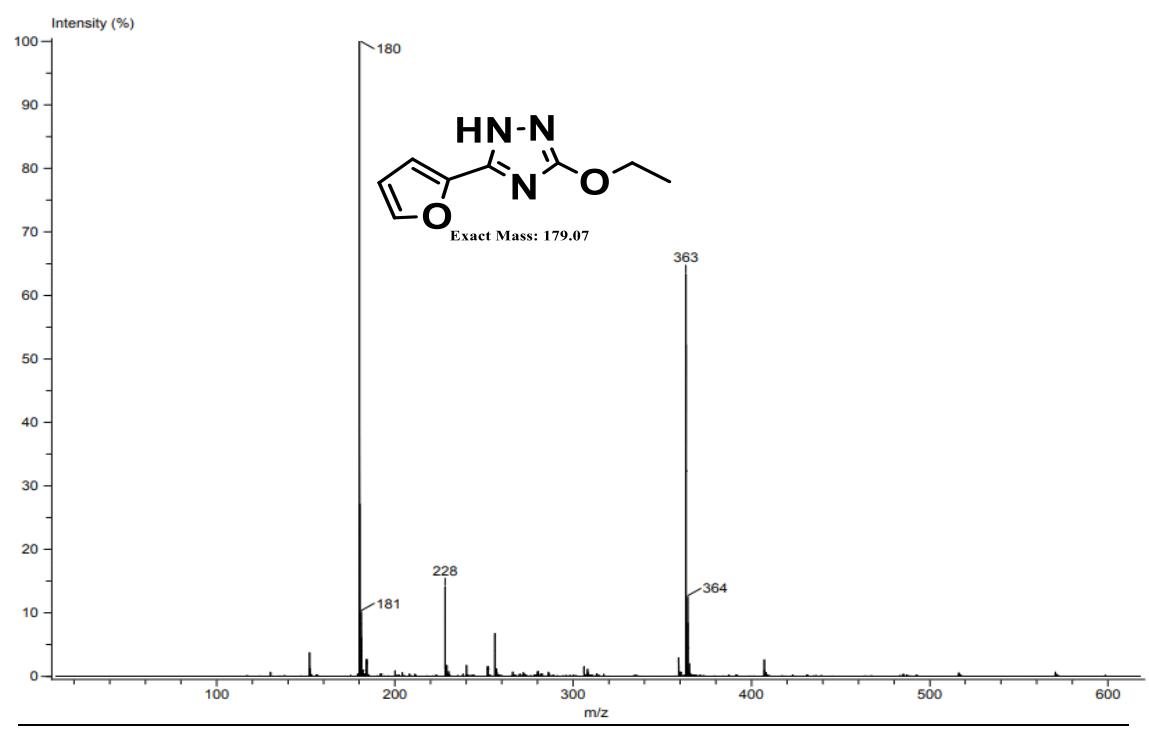


Figure A7. Low-resolution DART+ mass spectrum of compound T-4a-OC₂.

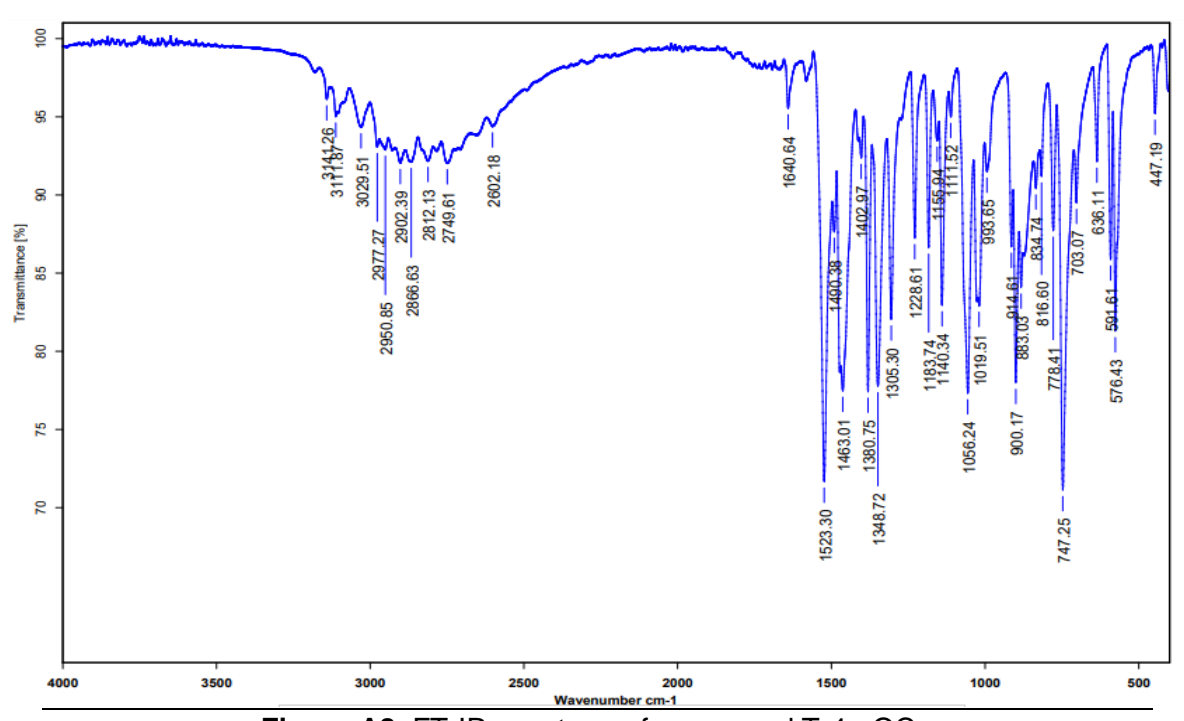


Figure A8. FT-IR spectrum of compound T-4a-OC₂.

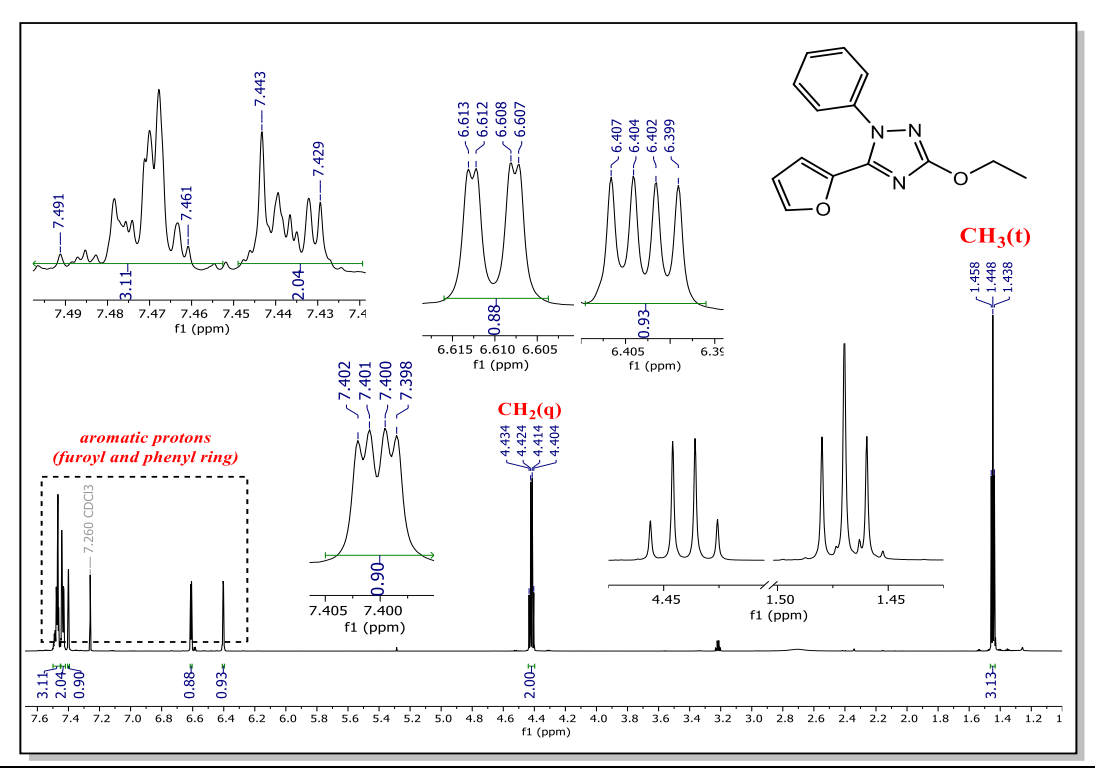


Figure A9. ¹H NMR (700 MHz, CDCl₃) spectrum of compound T-4b-OC₂.

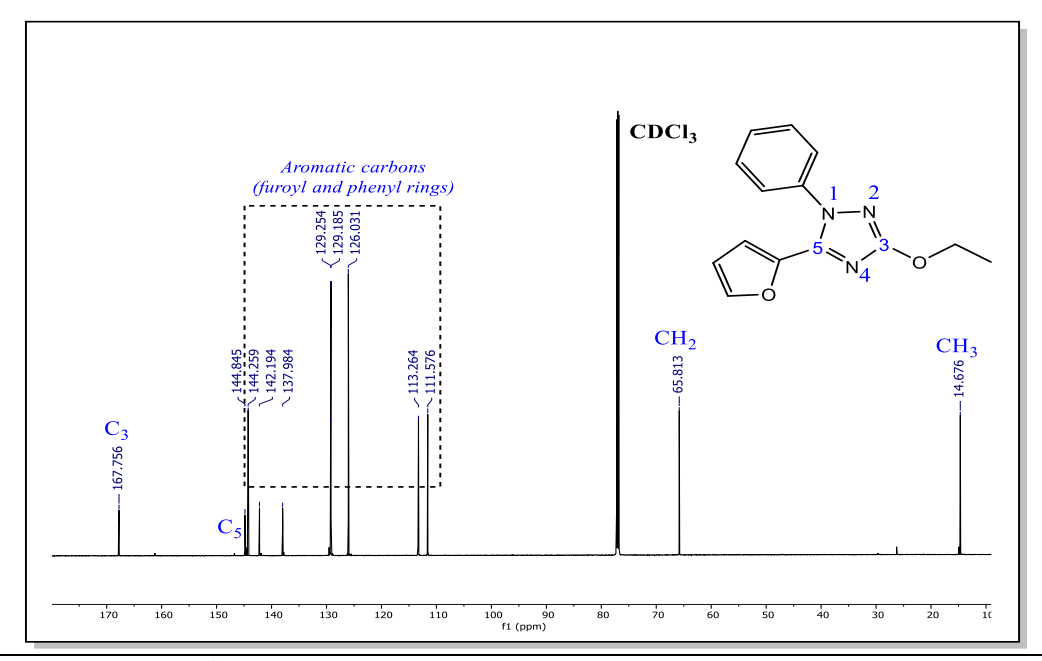


Figure A10. ¹³C NMR (175 MHz, CDCl₃) spectrum of compound T-4b-OC₂.

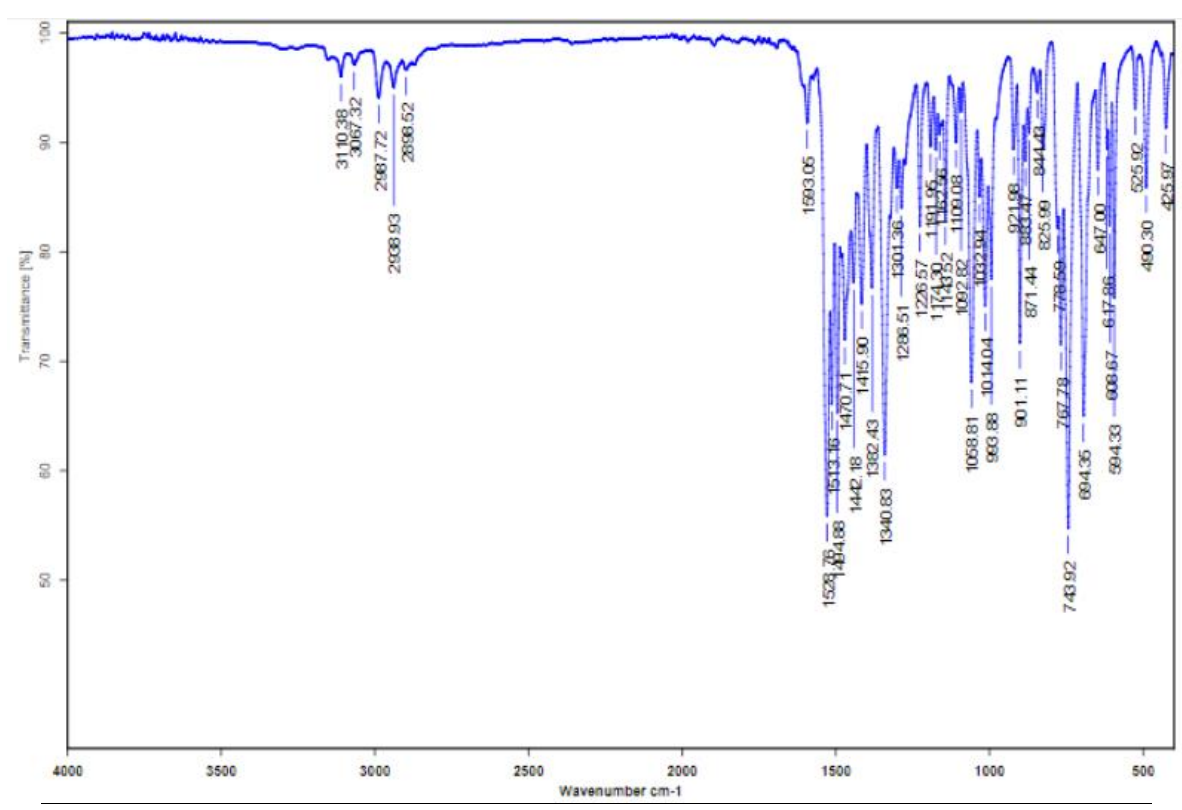


Figure A11. FT-IR spectrum of compound T-4b-OC₂.

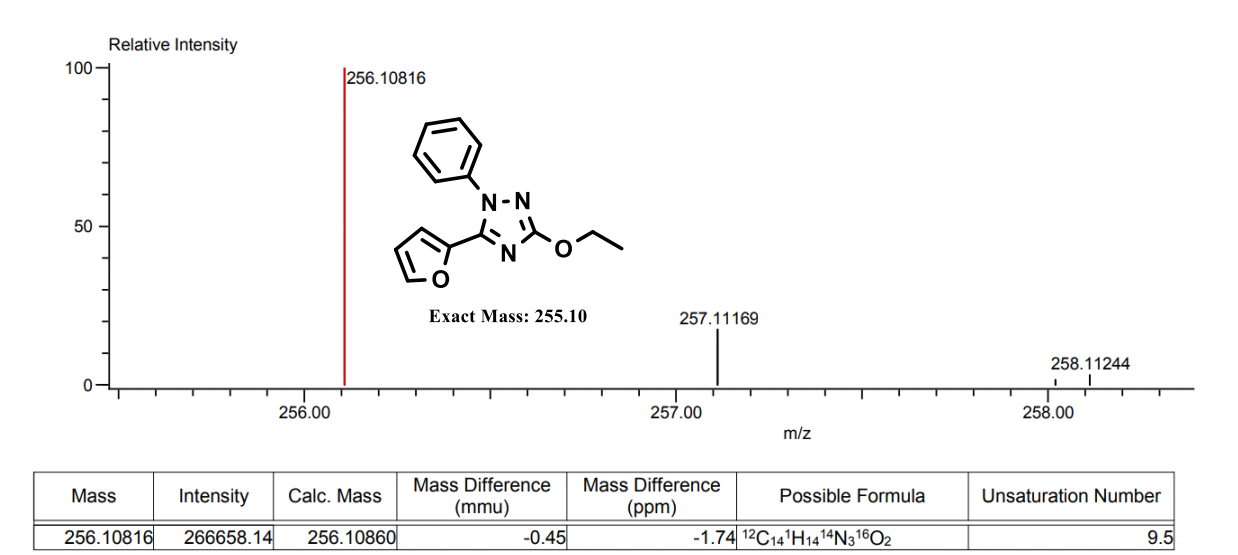


Figure A12. High-resolution DART+ mass spectrum of compound T-4b-OC₂.

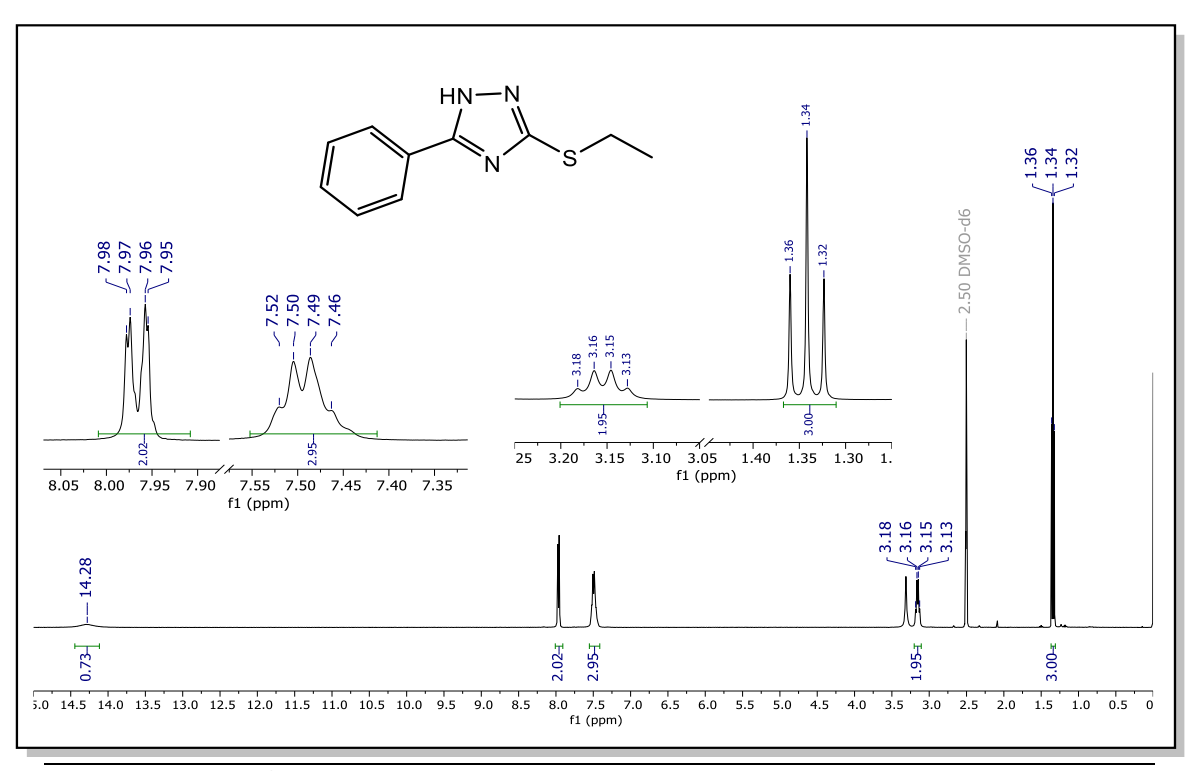


Figure A13. ¹H NMR (400 MHz, DMSO-d₆) spectrum of compound T-1a-SC₂.

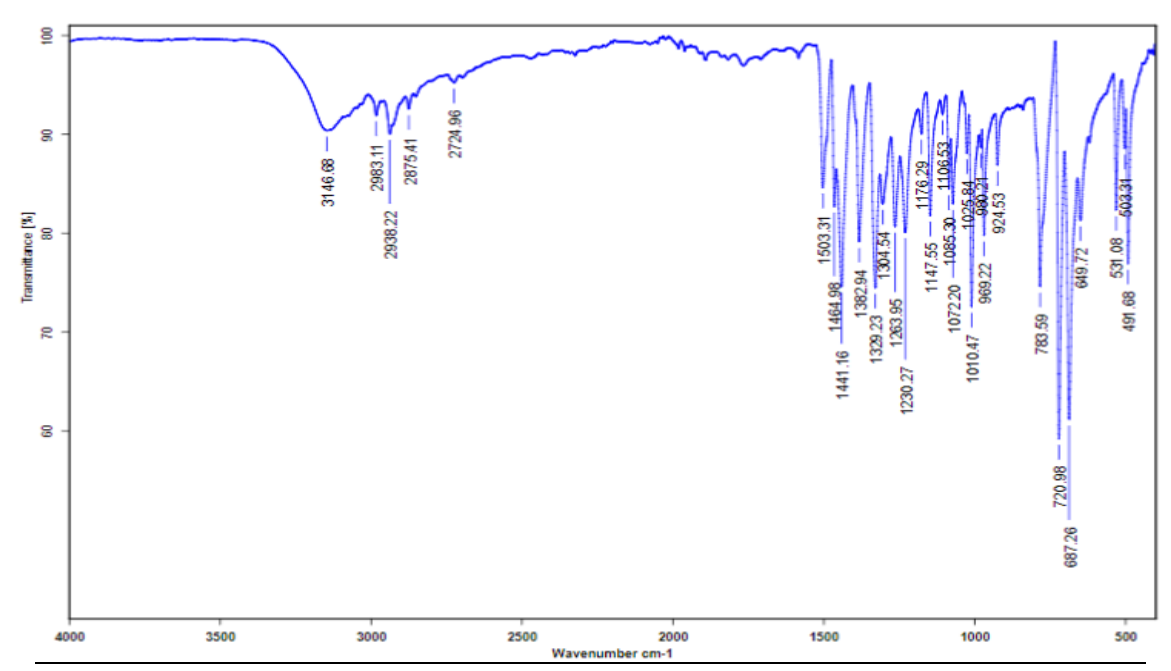


Figure A14. FT-IR spectrum of compound T-1a-SC₂.

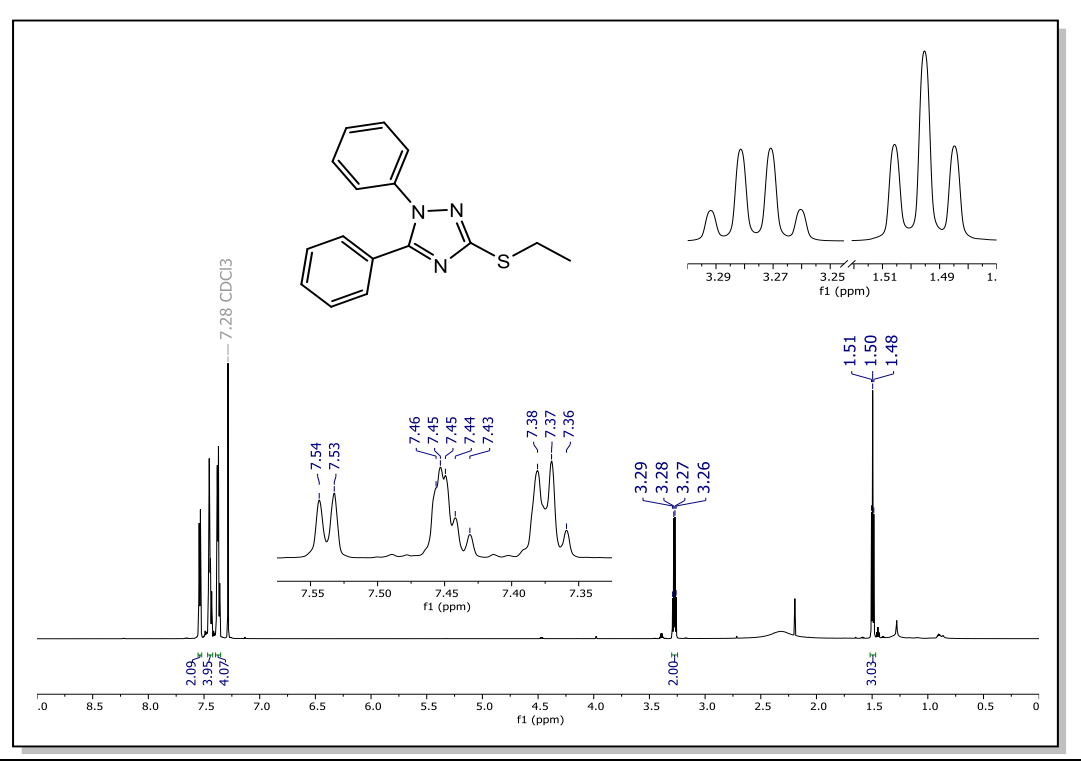


Figure A15. ¹H NMR (700 MHz, CDCl₃) spectrum of compound T-1b-SC₂.

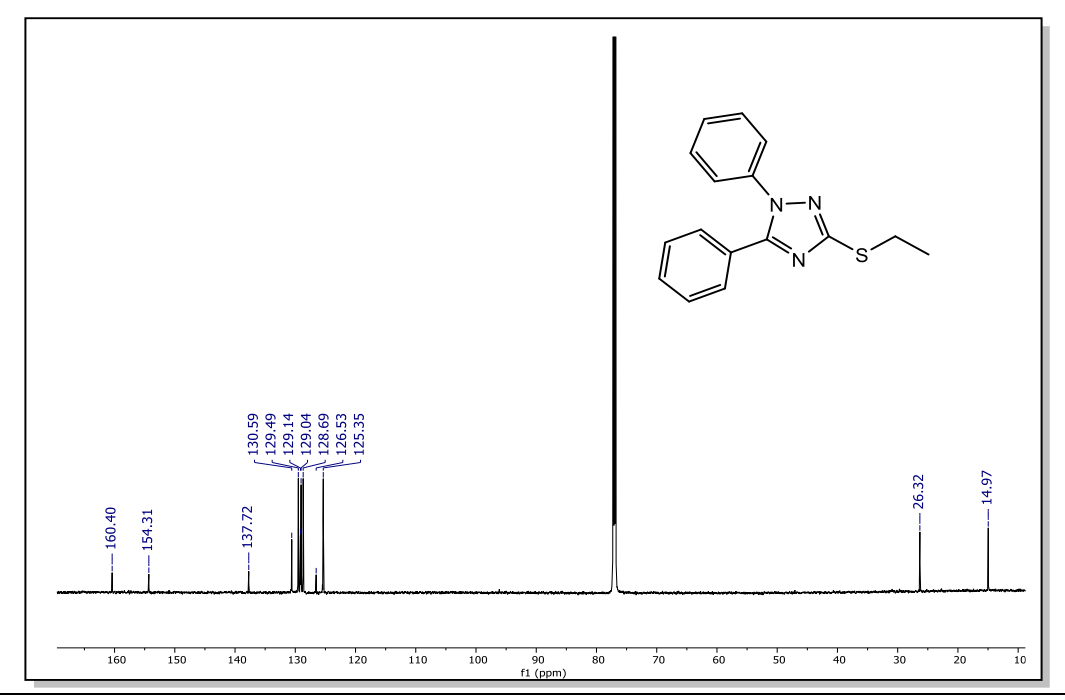


Figure A16. ¹³C NMR (175 MHz, CDCl₃) spectrum of compound T-1b-SC₂.

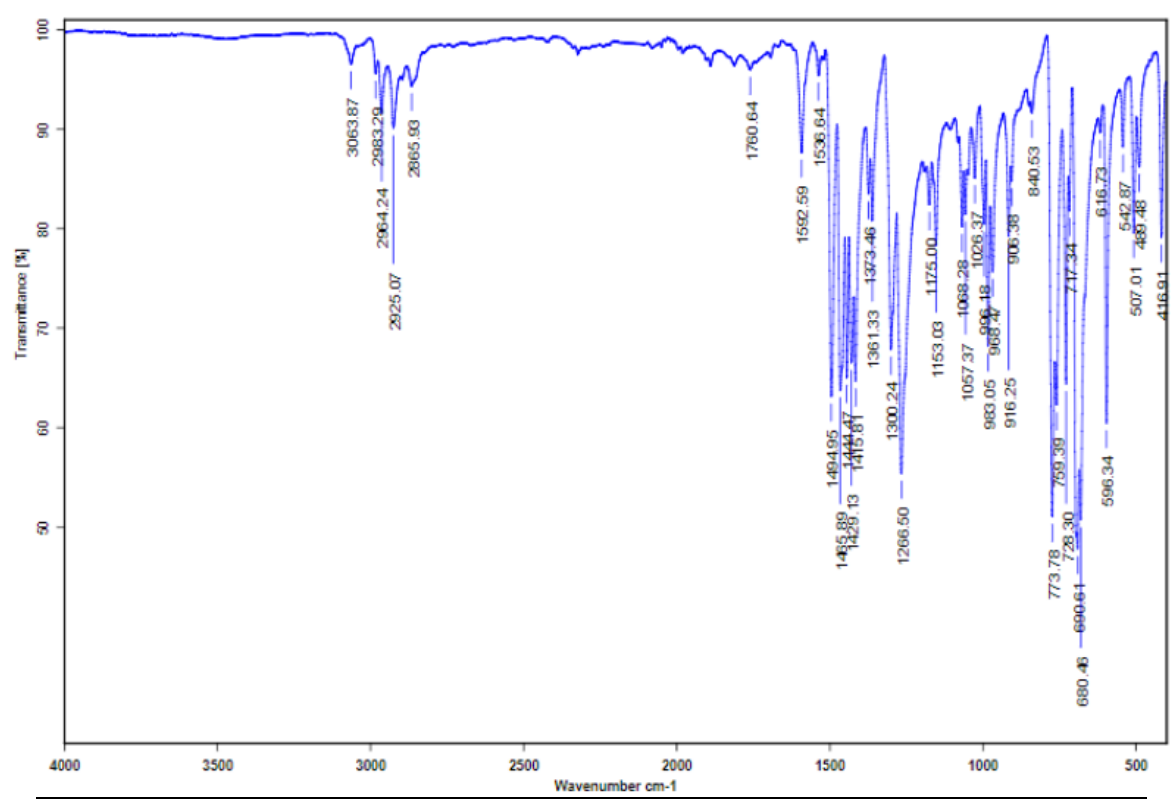


Figure A17. FT-IR spectrum of compound T-1b-SC₂.

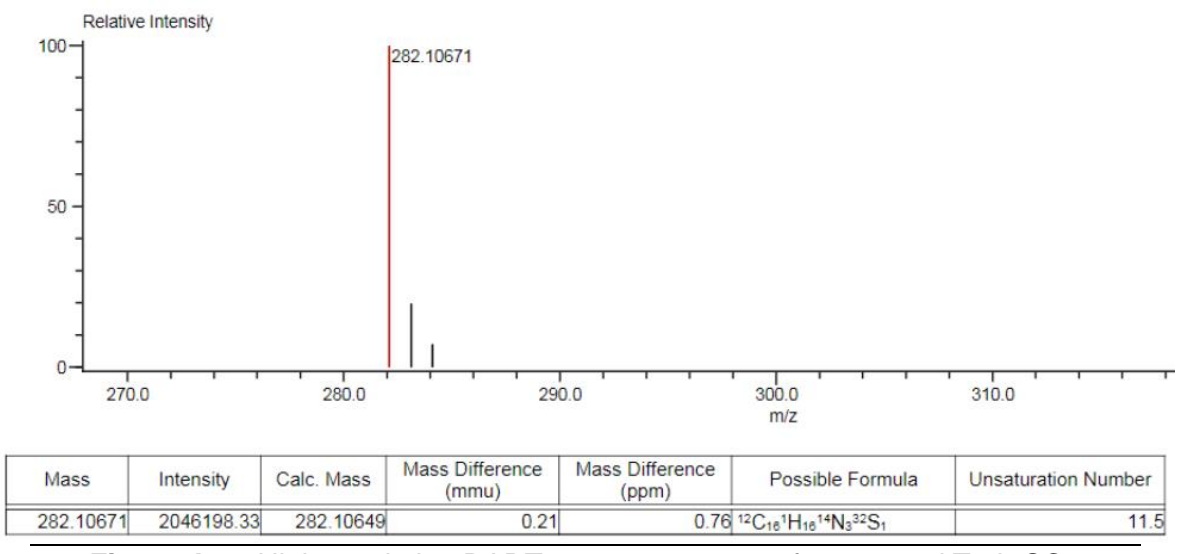


Figure A18. High-resolution DART+ mass spectrum of compound T-1b-SC₂.

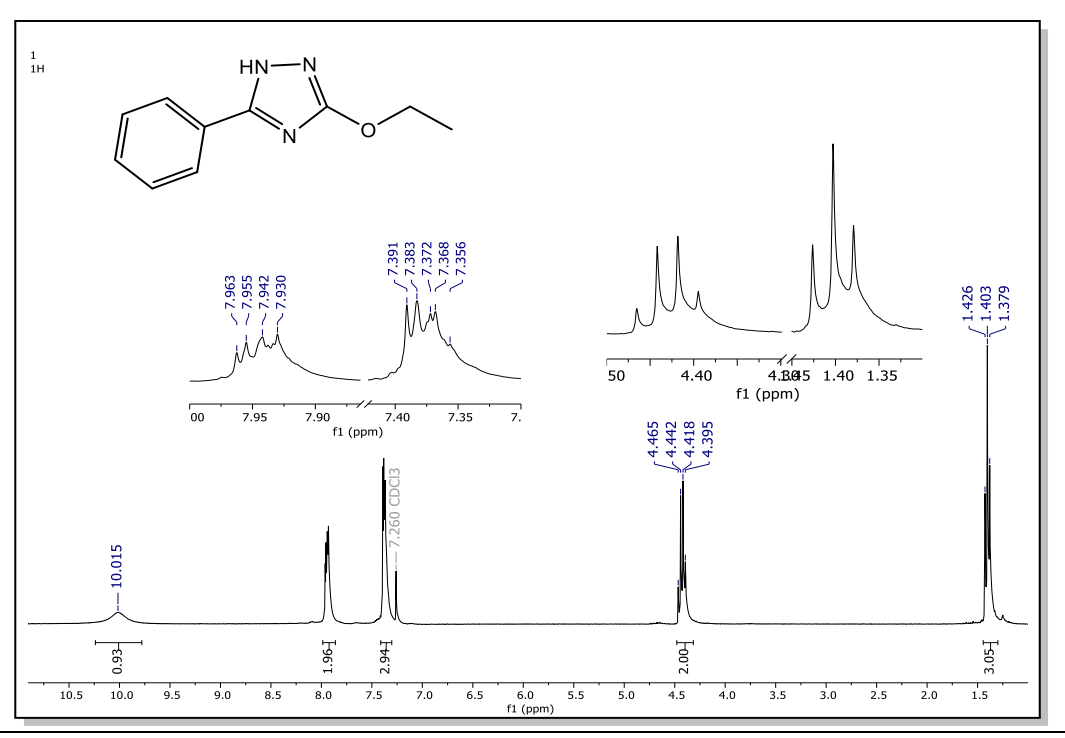


Figure A19. ¹H NMR (300 MHz, CDCl₃) spectrum of compound T-1a-OC₂.

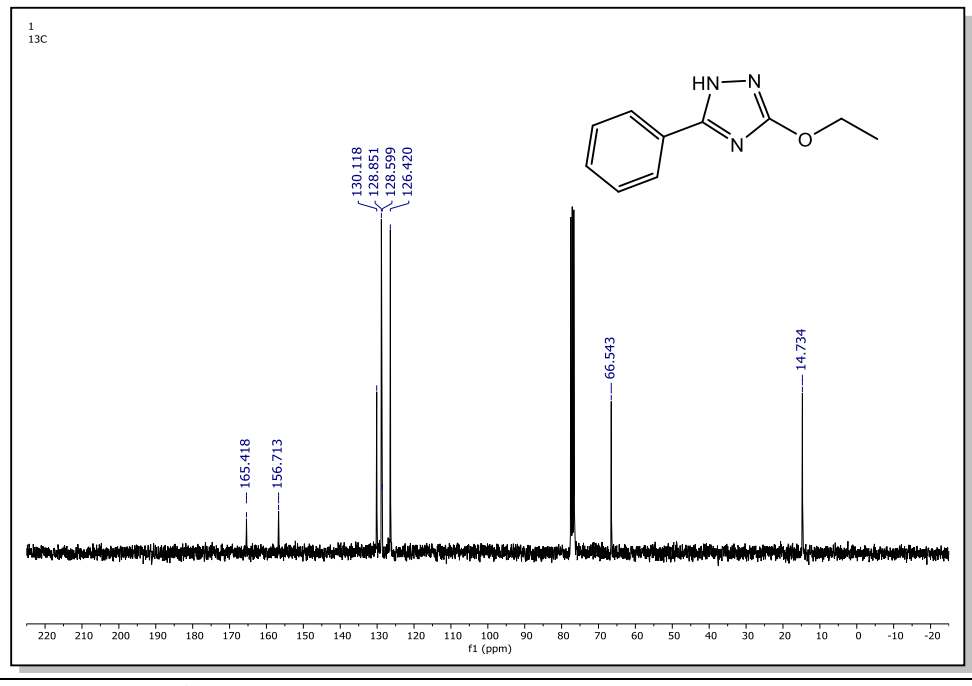


Figure A20. ¹³C NMR (75 MHz, CDCl₃) spectrum of compound T-1a-OC₂.

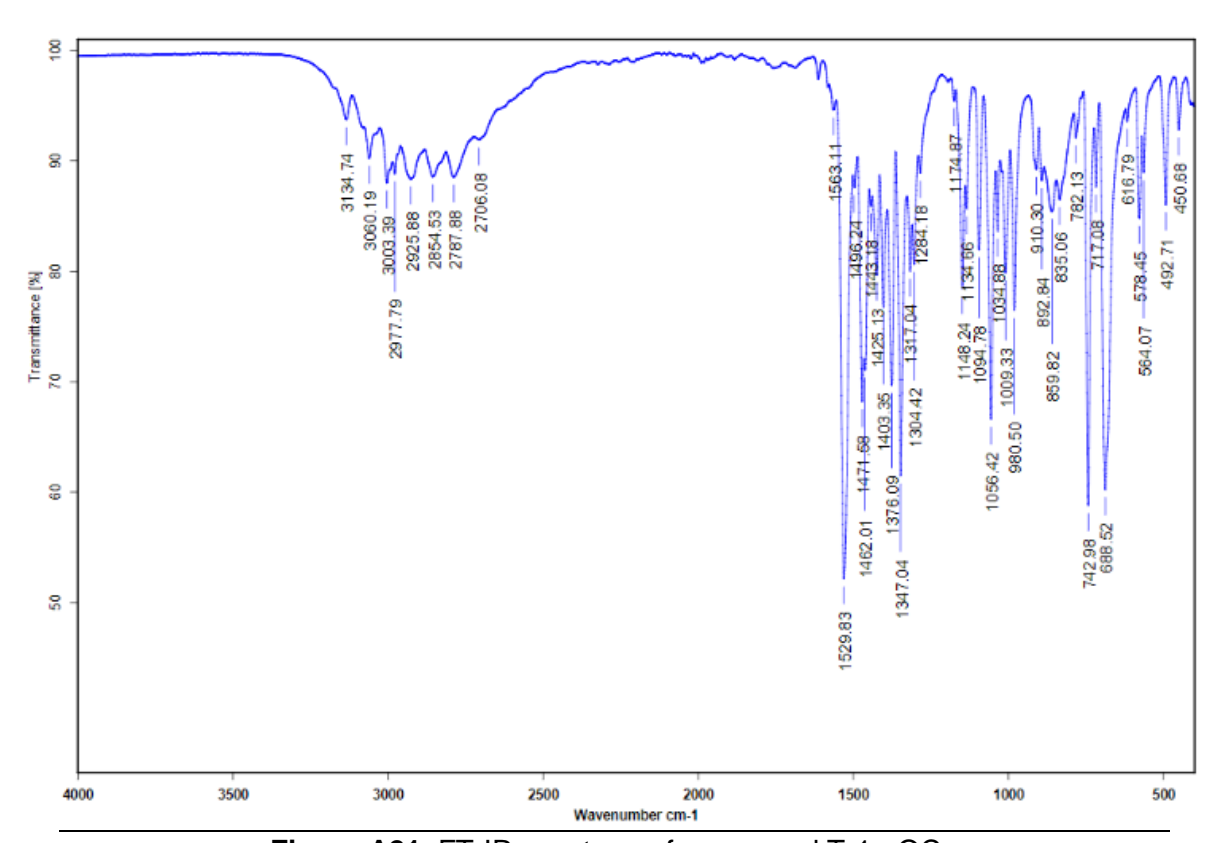


Figure A21. FT-IR spectrum of compound T-1a-OC₂.

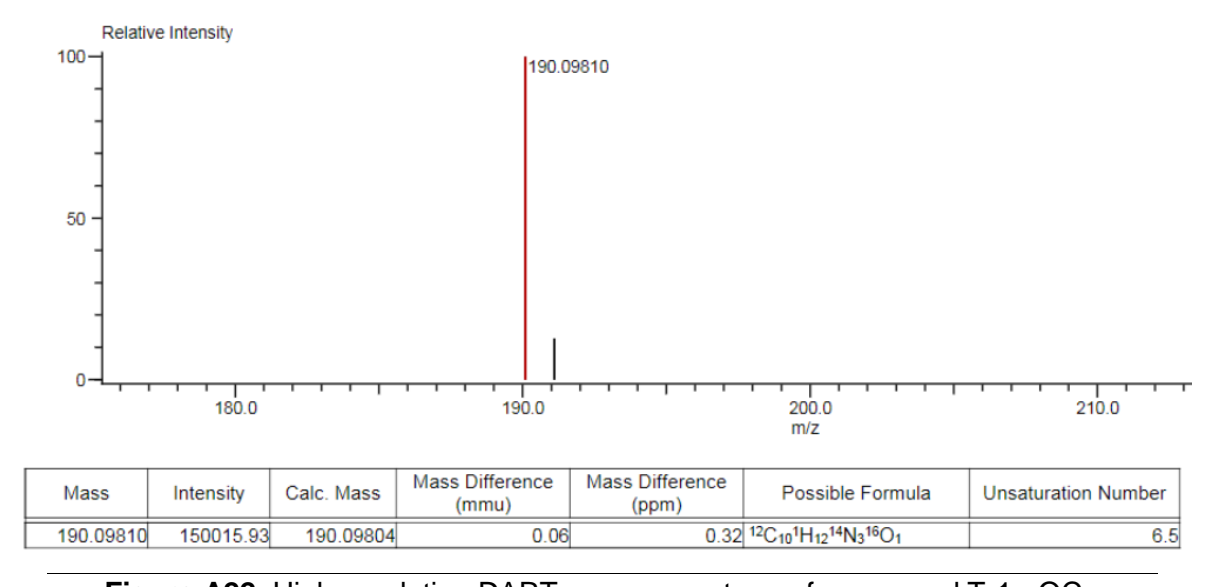


Figure A22. High-resolution DART+ mass spectrum of compound T-1a-OC₂.

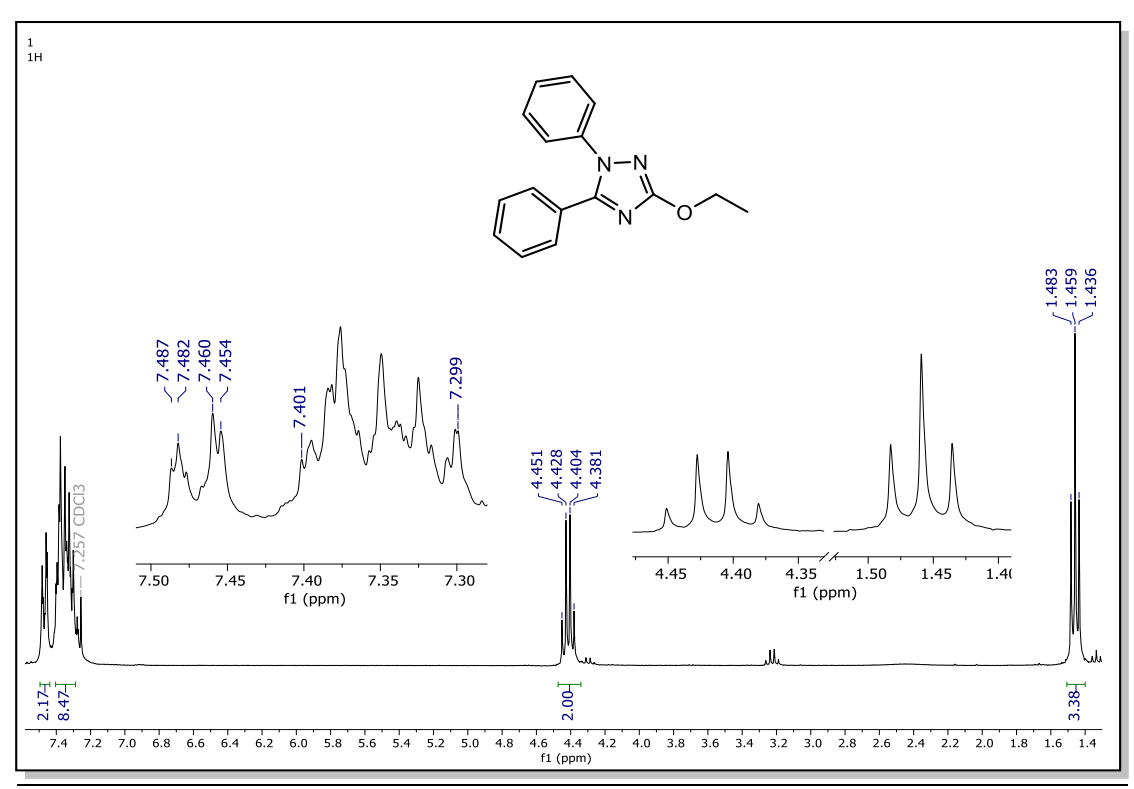


Figure A23. ¹H NMR (300 MHz, CDCl₃) spectrum of compound T-1b-OC₂.

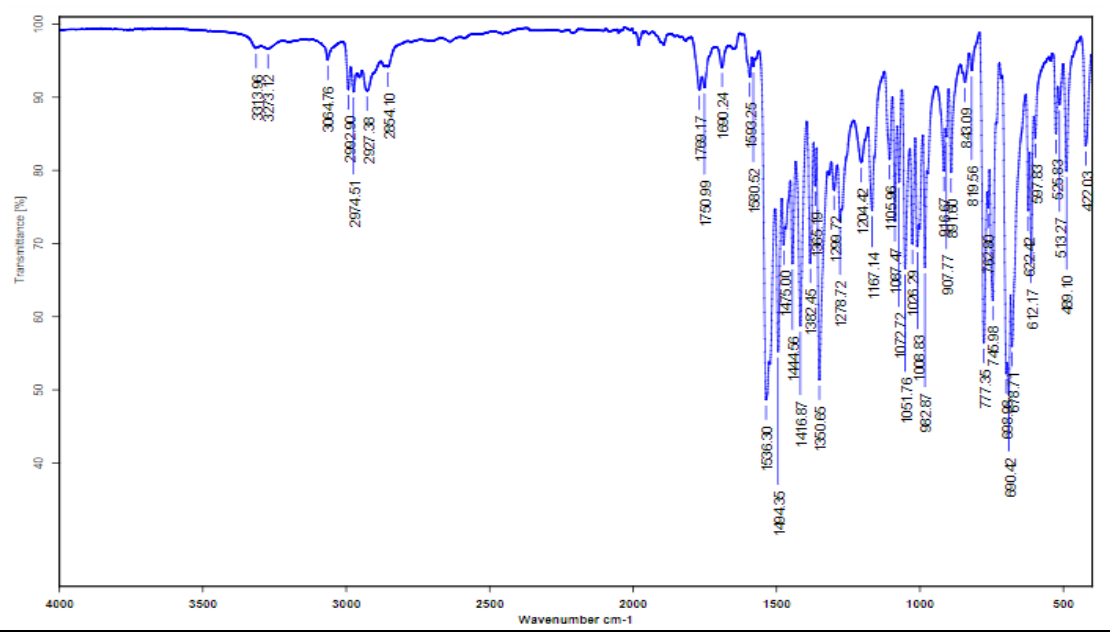


Figure A24. FT-IR spectrum of compound T-1b-OC₂.

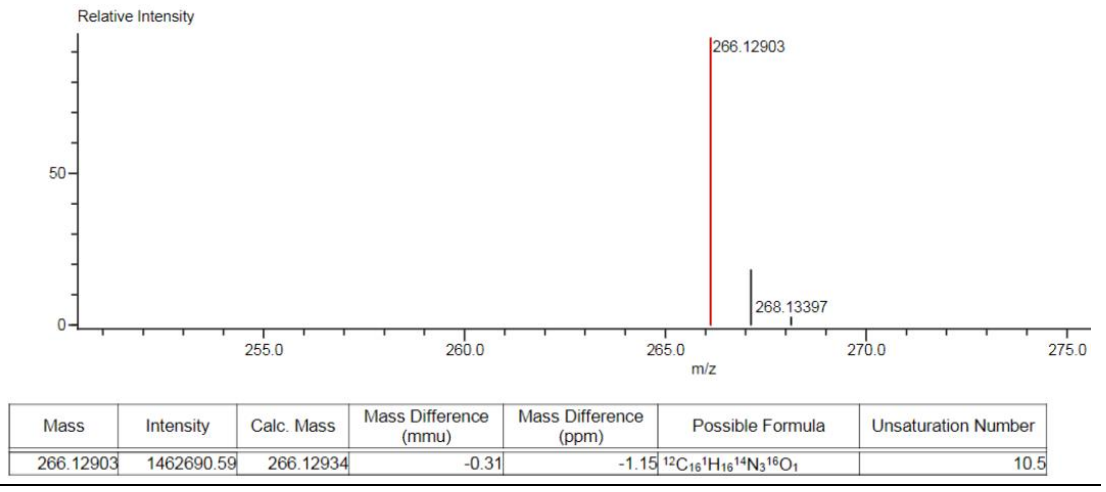


Figure A25. High-resolution DART+ mass spectrum of compound T-1b-OC₂.

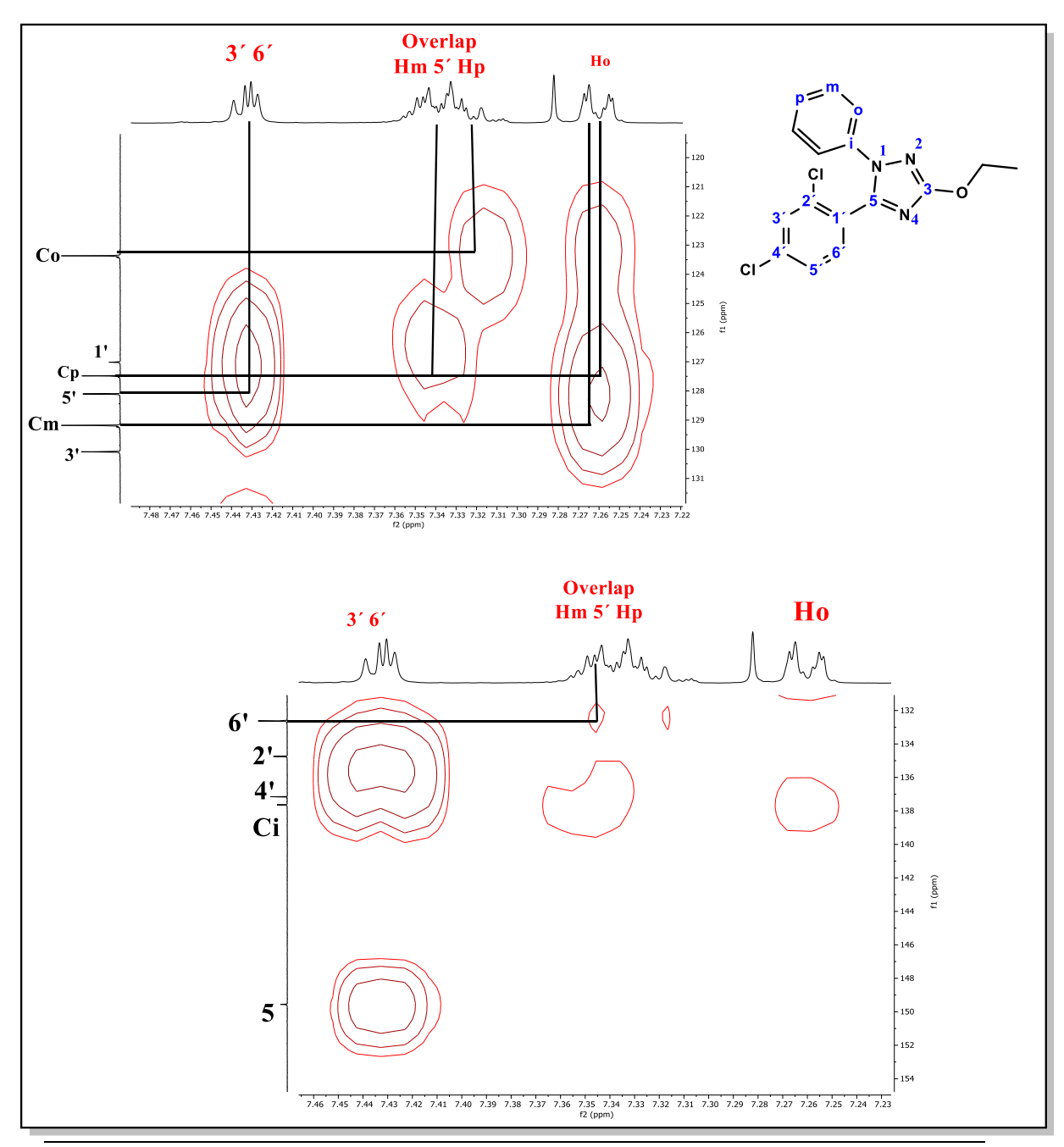


Figure A26. HMBC spectrum of compound T-3b-OC₂, couplings of CH carbons in the aromatic region.

Table A1. Carbon NBO charges of O,S-diethyl aroylimidothiocarbonates.

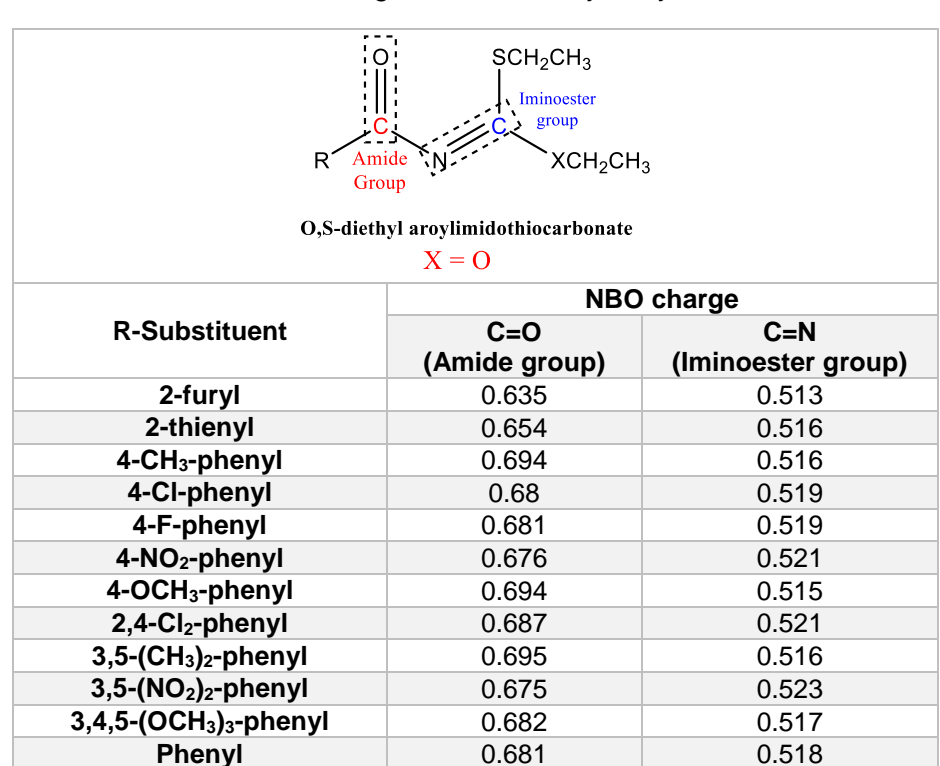


Table A2. Nitrogen NBO charges for the most active 1,3,5-substituted-1,2,4-triazoles.

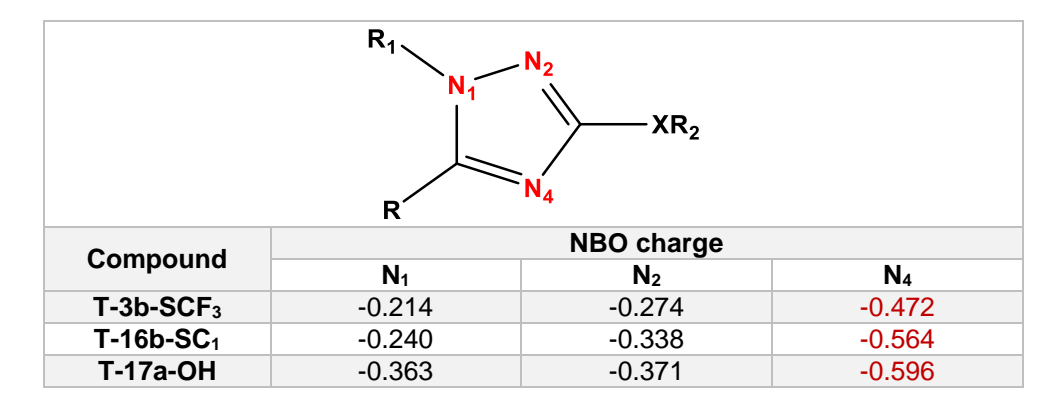


 Table A3.
 Molecular descriptors of piperazine-substituted-1,2,4-triazoles with the AM1 semiempirical method.

| | S (cal/molK) | A _{super} (Å ²) | V (Å ³) | ΔH _{Hydrat} (kcal/mol) | logP | R (A ³) | α _{Gauss} (a.u.) | M (amu) | G (a.u.) | D (Debyes) | E _{thermal} (kcal/mol) | EA (a.u.) | IP (a.u.) | α _{Hyper} (Å ³) |
|-----|-----------------|--------------------------------------|-------------------------------|---------------------------------|------|------------------------|------------------------------|------------|-------------|---------------|---------------------------------|--------------|--------------|--------------------------------------|
| 35a | 206.612 | 569.12 | 1254.02 | -8.78 | 2.96 | 118.16 | 258.767 | 490.94 | 0.381918 | 4.45369 | 319.186 | 0.02296 | 0.31479 | 48.47 |
| 35b | 215.223 | 572.30 | 1268.54 | -8.89 | 3.64 | 118.38 | 261.329 | 526.92 | 0.233536 | 3.89841 | 310.468 | 0.02425 | 0.32248 | 48.42 |
| 35c | 214.506 | 553.81 | 1242.60 | -8.79 | 3.46 | 113.55 | 256.503 | 510.47 | 0.147265 | 7.59043 | 311.532 | 0.02288 | 0.32059 | 46.4 |
| 35d | 207.386 | 577.29 | 1263.54 | -8.11 | 3.00 | 118.04 | 262.307 | 470.52 | 0.417762 | 3.60854 | 342.980 | 0.02218 | 0.30999 | 48.38 |
| 35e | 215.279 | 611.48 | 1318.45 | -7.66 | 3.39 | 122.64 | 270.375 | 484.55 | 0.433036 | 3.60634 | 361.844 | 0.02214 | 0.30987 | 50.21 |
| 35f | 216.078 | 577.48 | 1301.37 | -7.59 | 3.54 | 121.74 | 266.374 | 484.55 | 0.441736 | 5.82049 | 361.504 | 0.02245 | 0.31688 | 50.34 |
| 35g | 223.308 | 650.12 | 1371.03 | -7.27 | 3.79 | 127.24 | 278.521 | 498.58 | 0.448441 | 3.59047 | 380.721 | 0.02214 | 0.30988 | 52.05 |
| 35h | 231.288 | 687.30 | 1425.28 | -6.89 | 4.18 | 131.84 | 286.592 | 512.60 | 0.463779 | 3.59400 | 399.595 | 0.02213 | 0.30988 | 53.88 |
| 35i | 222.206 | 620.18 | 1342.39 | -7.08 | 4.22 | 127.11 | 274.341 | 498.58 | 0.466044 | 5.59222 | 380.004 | 0.02231 | 0.31644 | 52.05 |
| 35j | 239.286 | 722.73 | 1477.77 | -6.53 | 4.58 | 136.44 | 294.709 | 526.63 | 0.479129 | 3.58590 | 418.470 | 0.02213 | 0.30989 | 55.72 |
| 35k | 247.276 | 757.89 | 1531.21 | -6.16 | 4.98 | 141.04 | 302.794 | 540.66 | 0.494469 | 3.58976 | 437.345 | 0.02213 | 0.3099 | 57.55 |
| 16I | 263.260 | 827.87 | 1641.76 | -5.43 | 5.77 | 150.24 | 318.996 | 568.71 | 0.525154 | 3.58732 | 475.095 | 0.02214 | 0.30992 | 61.22 |
| 35m | 279.260 | 897.85 | 1749.46 | -4.71 | 6.56 | 159.45 | 335.201 | 596.76 | 0.555831 | 3.58571 | 512.845 | 0.02214 | 0.30993 | 64.89 |
| 35n | 311.273 | 1037.81 | 1958.62 | -3.25 | 8.15 | 177.85 | 367.621 | 652.87 | 0.617175 | 3.58382 | 588.344 | 0.02214 | 0.30994 | 72.23 |
| 35o | 204.350 | 550.13 | 1220.22 | -8.18 | 2.51 | 113.63 | 255.532 | 474.49 | 0.325272 | 4.69106 | 319.840 | 0.02163 | 0.31355 | 46.45 |
| 35p | 211.205 | 572.34 | 1262.75 | -8.42 | 3.10 | 118.38 | 260.566 | 508.93 | 0.306817 | 4.96505 | 314.894 | 0.02219 | 0.31747 | 48.38 |
| 35q | 211.864 | 574.71 | 1271.17 | -7.77 | 3.14 | 118.25 | 263.572 | 488.51 | 0.342807 | 4.60329 | 338.722 | 0.02159 | 0.31384 | 48.29 |
| 35r | 218.414 | 601.19 | 1318.47 | -7.34 | 3.53 | 122.85 | 271.858 | 502.54 | 0.360089 | 4.58158 | 357.661 | 0.02152 | 0.31348 | 50.12 |
| 35s | 219.300 | 582.16 | 1308.22 | -7.39 | 3.70 | 122.83 | 267.804 | 502.54 | 0.364334 | 5.21306 | 357.228 | 0.02045 | 0.32313 | 50.12 |
| 35t | 226.291 | 636.39 | 1371.88 | -6.92 | 3.93 | 127.46 | 280.06 | 516.57 | 0.375403 | 4.56977 | 376.531 | 0.02150 | 0.31346 | 51.96 |
| 35u | 225.410 | 625.30 | 1352.06 | -6.89 | 4.36 | 127.33 | 275.775 | 516.57 | 0.388631 | 4.98392 | 375.728 | 0.02030 | 0.32269 | 51.96 |
| 35v | 234.294 | 671.46 | 1427.03 | -6.54 | 4.32 | 132.06 | 288.305 | 530.59 | 0.390801 | 4.54776 | 395.409 | 0.02149 | 0.31346 | 53.79 |
| 35w | 242.273 | 708.81 | 1479.48 | -6.16 | 4.72 | 136.66 | 296.499 | 544.62 | 0.406138 | 4.54949 | 414.283 | 0.02149 | 0.31348 | 55.63 |
| 35x | 250.274 | 744.44 | 1532.69 | -5.79 | 5.12 | 141.26 | 304.706 | 558.65 | 0.421485 | 4.53895 | 433.158 | 0.02149 | 0.31349 | 57.46 |
| 35y | 230.806 | 614.36 | 1435.69 | -9.74 | 4.35 | 138.35 | 301.294 | 550.58 | 0.444804 | 5.31873 | 375.370 | 0.02078 | 0.31888 | 56.11 |

Table A4. Molecular descriptors of piperazine-substituted-1,2,4-triazoles with the ONIOM (CAM-B3LYP/6-31++G(d,p):AM1) method.

| | S (cal/molK) | A _{super} (Å ²) | V (ų) | ΔH _{Hydrat} (kcal/mol) | logP | R (A ³) | α _{Gauss} (a.u.) | M (amu) | G (a.u.) | D (Debyes) | E _{thermal} (kcal/mol) | EA (a.u.) | IP (a.u.) | $lpha_{	ext{Hyper}}$ (\mathring{A}^3) |
|-----|-----------------|--------------------------------------|----------|------------------------------------|------|------------------------|------------------------------|------------|--------------|---------------|---------------------------------|--------------|--------------|---|
| 35a | 204.978 | 567.15 | 1243.25 | -9.79 | 1.91 | 124.51 | 313.039 | 490.94 | -1530.394461 | 5.99568 | 316.503 | 0.01881 | 0.31719 | 48.72 |
| 35b | 213.665 | 576.67 | 1263.29 | -9.40 | 2.69 | 124.79 | 319.269 | 526.92 | -1530.534744 | 9.37287 | 307.753 | 0.02008 | 0.31563 | 48.54 |
| 35c | 211.781 | 559.54 | 1234.17 | -9.44 | 2.51 | 119.95 | 313.976 | 510.47 | -1530.622331 | 9.74739 | 308.839 | 0.02013 | 0.3158 | 46.52 |
| 35d | 206.088 | 575.15 | 1253.65 | -8.69 | 2.02 | 123.57 | 319.299 | 470.52 | -1530.347968 | 7.33851 | 340.201 | 0.01936 | 0.31319 | 48.63 |
| 35e | 212.768 | 601.6 | 1301.65 | -8.24 | 2.42 | 128.17 | 327.648 | 484.55 | -1530.330587 | 7.24166 | 359.114 | 0.01931 | 0.31265 | 50.47 |
| 35f | 213.22 | 607.59 | 1302.55 | -8.24 | 2.50 | 128.14 | 326.772 | 484.55 | -1530.32823 | 7.26427 | 358.826 | 0.01941 | 0.31368 | 50.47 |
| 35g | 220.535 | 636.85 | 1357.03 | -7.82 | 2.81 | 132.77 | 335.841 | 498.58 | -1530.315216 | 7.22973 | 377.986 | 0.01931 | 0.31261 | 52.30 |
| 35h | 228.431 | 671.90 | 1410.11 | -7.43 | 3.21 | 137.37 | 344.076 | 512.6 | -1530.299766 | 7.21535 | 396.866 | 0.01931 | 0.31259 | 54.14 |
| 35i | 218.288 | 627.07 | 1331.7 | -7.71 | 3.25 | 132.65 | 333.101 | 498.58 | -1530.300480 | 7.73464 | 377.335 | 0.01986 | 0.31786 | 52.30 |
| 35j | 236.246 | 709.27 | 1464.81 | -7.05 | 3.61 | 141.97 | 352.26 | 526.63 | -1530.284349 | 7.21904 | 415.743 | 0.01931 | 0.31259 | 55.97 |
| 35k | 244.143 | 744.90 | 1517.79 | -6.68 | 4.00 | 146.58 | 360.457 | 540.66 | -1530.268953 | 7.21401 | 434.620 | 0.01931 | 0.31259 | 57.81 |
| 16I | 260.869 | 832.70 | 1630.28 | -6.46 | 4.72 | 156.59 | 375.201 | 568.71 | -1530.249417 | 5.63200 | 472.387 | 0.01823 | 0.31314 | 61.48 |
| 35m | 276.912 | 902.63 | 1738.58 | -5.73 | 5.51 | 165.8 | 391.415 | 596.76 | -1530.218748 | 5.62883 | 510.148 | 0.01821 | 0.31308 | 65.15 |
| 35n | 308.995 | 1042.59 | 1952.15 | -4.28 | 7.10 | 184.2 | 423.828 | 652.87 | -1530.157436 | 5.62650 | 585.648 | 0.01821 | 0.31307 | 72.49 |
| 35o | 204.057 | 556.14 | 1214.9 | -8.83 | 1.53 | 119.16 | 310.402 | 474.49 | -1629.593206 | 5.88431 | 316.471 | 0.01865 | 0.31993 | 46.71 |
| 35p | 210.247 | 577.87 | 1254.55 | -9.07 | 2.12 | 123.91 | 315.471 | 508.93 | -1629.611971 | 6.77663 | 311.553 | 0.01921 | 0.31901 | 48.63 |
| 35q | 210.923 | 580.50 | 1264.05 | -8.42 | 2.16 | 123.79 | 318.622 | 488.51 | -1629.575381 | 5.91969 | 335.375 | 0.01886 | 0.31992 | 48.54 |
| 35r | 217.73 | 607.01 | 1312.29 | -7.98 | 2.56 | 128.39 | 326.9 | 502.54 | -1629.558114 | 5.76574 | 354.298 | 0.01876 | 0.31986 | 50.38 |
| 35s | 217.997 | 613.63 | 1312.34 | -7.98 | 2.72 | 128.36 | 326.191 | 502.54 | -1629.555587 | 5.85942 | 353.994 | 0.01894 | 0.32002 | 50.38 |
| 35t | 225.577 | 642.23 | 1365.86 | -7.56 | 2.95 | 132.99 | 335.088 | 516.57 | -1629.542783 | 5.75120 | 373.168 | 0.01876 | 0.31984 | 52.21 |
| 35u | 223.597 | 631.76 | 1342.48 | -7.49 | 3.39 | 132.86 | 332.276 | 516.57 | -1629.527647 | 6.74486 | 372.460 | 0.01977 | 0.32235 | 52.21 |
| 35v | 233.566 | 677.33 | 1419.53 | -7.18 | 3.35 | 137.59 | 343.319 | 530.59 | -1629.527381 | 5.73353 | 392.045 | 0.01876 | 0.31983 | 54.05 |
| 35w | 241.557 | 714.67 | 1473.02 | -6.80 | 3.75 | 142.19 | 351.499 | 544.62 | -1629.512049 | 5.73547 | 410.919 | 0.01876 | 0.31983 | 55.88 |
| 35x | 249.594 | 750.30 | 1526.98 | -6.43 | 4.14 | 146.79 | 359.692 | 558.65 | -1629.49672 | 5.72883 | 429.795 | 0.01876 | 0.31983 | 57.72 |
| 35y | 228.155 | 617.07 | 1425.66 | -10.29 | 3.38 | 143.88 | 357.658 | 550.58 | -1629.474803 | 6.96706 | 372.265 | 0.01879 | 0.32100 | 56.37 |

Table A5. Molecular descriptors of piperazine-substituted-1,2,4-triazoles with the CAM-B3LYP/6-31++G(d,p) DFT method.

| | S (cal/molK) | A _{super} (Å ²) | V (Å ³) | ΔH _{Hydrat} (kcal/mol) | logP | R (A ³) | α _{Gauss} (a.u.) | M (amu) | G (a.u.) | D (Debyes) | E _{thermal} (kcal/mol) | EA (a.u.) | IP (a.u.) | $\begin{array}{c} \alpha_{\text{Hyper}} \\ (\mathring{A}^3) \end{array}$ |
|-----|-----------------|---|-------------------------------|------------------------------------|------|------------------------|------------------------------|------------|--------------|---------------|---------------------------------|--------------|--------------|--|
| 35a | 207.777 | 571.53 | 1248.5 | -9.3 | 1.98 | 123.7 | 323.632 | 490.94 | -2029.260572 | 8.30357 | 316.806 | 0.00523 | 0.26596 | 48.72 |
| 35b | 214.426 | 576.97 | 1263.51 | -9.42 | 2.69 | 124.79 | 324.506 | 526.92 | -2227.720543 | 9.05763 | 307.214 | 0.00515 | 0.26769 | 48.54 |
| 35c | 212.864 | 554.73 | 1231.13 | -9.41 | 2.51 | 119.95 | 313.820 | 510.47 | -1867.360682 | 9.03618 | 308.088 | 0.00515 | 0.26797 | 46.52 |
| 35d | 207.83 | 584.04 | 1259.09 | -9.14 | 1.95 | 124.39 | 322.601 | 470.52 | -1608.935124 | 6.25674 | 340.368 | -0.00115 | 0.26461 | 48.63 |
| 35e | 216.007 | 619.32 | 1313.63 | -8.68 | 2.34 | 128.99 | 334.159 | 484.55 | -1648.201085 | 6.12472 | 359.203 | -0.00125 | 0.2641 | 50.47 |
| 35f | 218.594 | 608.13 | 1307.64 | -8.23 | 2.58 | 128.14 | 335.513 | 484.55 | -1648.192850 | 7.73885 | 359.048 | 0.0046 | 0.26391 | 50.47 |
| 35g | 223.791 | 658.6 | 1367.93 | -8.29 | 2.74 | 133.59 | 346.458 | 498.58 | -1687.467008 | 6.16325 | 378.050 | -0.00125 | 0.26399 | 52.30 |
| 35h | 230.932 | 696.44 | 1422.12 | -7.90 | 3.14 | 138.19 | 358.320 | 512.6 | -1726.732656 | 6.06318 | 396.899 | -0.0013 | 0.26380 | 54.14 |
| 35i | 218.907 | 630.09 | 1335.10 | -7.69 | 3.25 | 132.65 | 347.496 | 498.58 | -1687.448280 | 7.44237 | 377.482 | 0.00454 | 0.26336 | 52.30 |
| 35j | 238.57 | 732.72 | 1476.52 | -7.52 | 3.53 | 142.79 | 370.530 | 526.63 | -1765.998494 | 6.12658 | 415.748 | -0.00129 | 0.26376 | 55.97 |
| 35k | 245.75 | 768.79 | 1531.22 | -7.15 | 3.93 | 147.39 | 382.561 | 540.66 | -1805.264127 | 6.03369 | 434.602 | -0.00133 | 0.26358 | 57.81 |
| 16I | 261.041 | 840.64 | 1640.28 | -6.40 | 4.72 | 156.59 | 406.787 | 568.71 | -1883.795835 | 6.02338 | 472.297 | -0.00133 | 0.26356 | 61.48 |
| 35m | 276.439 | 912.49 | 1749.09 | -5.66 | 5.51 | 165.80 | 430.999 | 596.76 | -1962.327577 | 6.01763 | 509.988 | -0.00134 | 0.26357 | 65.15 |
| 35n | 306.845 | 1056.19 | 1966.75 | -4.16 | 7.10 | 184.20 | 479.570 | 652.87 | -2119.390908 | 6.01122 | 585.381 | -0.00134 | 0.26355 | 72.49 |
| 35o | 205.641 | 556.73 | 1217.18 | -8.80 | 1.53 | 119.16 | 313.064 | 474.49 | -1668.887413 | 6.23136 | 316.557 | 0.00342 | 0.26501 | 46.71 |
| 35p | 214.815 | 583.54 | 1263.75 | -9.09 | 2.12 | 123.91 | 323.219 | 508.93 | -2128.487248 | 9.26646 | 311.670 | 0.00565 | 0.27276 | 48.63 |
| 35q | 213.333 | 583.5 | 1268.26 | -8.40 | 2.16 | 123.79 | 324.614 | 488.51 | -1708.151809 | 6.12437 | 335.609 | 0.0034 | 0.26529 | 48.54 |
| 35r | 219.538 | 609.01 | 1316.41 | -7.96 | 2.56 | 128.39 | 336.863 | 502.54 | -1747.415475 | 6.00442 | 354.519 | 0.00328 | 0.26475 | 50.38 |
| 35s | 220.258 | 615.11 | 1315.54 | -7.96 | 2.72 | 128.36 | 335.852 | 502.54 | -1747.418383 | 6.24300 | 354.236 | 0.00352 | 0.26578 | 50.38 |
| 35t | 227.047 | 646.42 | 1370.94 | -7.54 | 2.95 | 132.99 | 349.092 | 516.57 | -1786.681376 | 5.89213 | 373.355 | 0.00321 | 0.26459 | 52.21 |
| 35u | 225.003 | 634.42 | 1343.91 | -7.47 | 3.39 | 132.86 | 346.516 | 516.57 | -1786.675868 | 6.40624 | 372.625 | 0.00387 | 0.26741 | 52.21 |
| 35v | 234.636 | 682.18 | 1425.04 | -7.15 | 3.35 | 137.59 | 361.465 | 530.59 | -1825.947155 | 5.92941 | 392.209 | 0.00321 | 0.26458 | 54.05 |
| 35w | 242.206 | 720.34 | 1479.08 | -6.76 | 3.75 | 142.19 | 373.651 | 544.62 | -1865.212998 | 5.87019 | 411.052 | 0.00319 | 0.26457 | 55.88 |
| 35x | 249.766 | 756.82 | 1533.26 | -6.38 | 4.14 | 146.79 | 385.983 | 558.65 | -1904.478805 | 5.92301 | 429.900 | 0.00319 | 0.26456 | 57.72 |
| 35y | 227.664 | 614.51 | 1417.64 | -10.35 | 3.38 | 143.88 | 377.876 | 550.58 | -1899.742049 | 7.14650 | 371.456 | 0.00370 | 0.26812 | 56.37 |